

# Nondestructive Evaluation of Iowa Pavements: Phase I

National Concrete Pavement  
Technology Center



**Final Report**  
**December 2007**

**Sponsored by**  
the Iowa Department of Transportation  
(CTRE Project 04-177)



IOWA STATE  
UNIVERSITY

## **About the National Concrete Pavement Technology Center**

The mission of the National Concrete Pavement Technology Center is to unite key transportation stakeholders around the central goal of advancing concrete pavement technology through research, tech transfer, and technology implementation.

### **Disclaimer Notice**

The contents of this report reflect the views of the authors, who are responsible for the facts and the accuracy of the information presented herein. The opinions, findings and conclusions expressed in this publication are those of the authors and not necessarily those of the sponsors.

The sponsors assume no liability for the contents or use of the information contained in this document. This report does not constitute a standard, specification, or regulation.

The sponsors do not endorse products or manufacturers. Trademarks or manufacturers' names appear in this report only because they are considered essential to the objective of the document.

### **Nondiscrimination Statement**

Iowa State University does not discriminate on the basis of race, color, age, religion, national origin, sexual orientation, gender identity, sex, marital status, disability, or status as a U.S. veteran. Inquiries can be directed to the Director of Equal Opportunity and Diversity, (515) 294-7612.

**Technical Report Documentation Page**

|   |  |  |                        |
|---|--|--|------------------------|
| <b>1. Report No.</b><br>CTRE Project 04-177   | <b>2. Government Accession No.</b>                                 | <b>3. Recipient's Catalog No.</b>                            |                        |
| <b>4. Title and Subtitle</b><br>Nondestructive Evaluation of Iowa Pavements-Phase I   |  | <b>5. Report Date</b><br>December 2007                       |                        |
|   |  | <b>6. Performing Organization Code</b>                       |                        |
| <b>7. Author(s)</b><br>Halil Ceylan, Alper Guclu, Mustafa Birkan Bayrak, and Kasthurirangan Gopalakrishnan  |  | <b>8. Performing Organization Report No.</b>                 |                        |
| <b>9. Performing Organization Name and Address</b><br>Center for Transportation Research and Education<br>Iowa State University<br>2711 South Loop Drive, Suite 4700<br>Ames, IA 50010-8664   |  | <b>10. Work Unit No. (TRAIS)</b>                             |                        |
|   |  | <b>11. Contract or Grant No.</b>                             |                        |
| <b>12. Sponsoring Organization Name and Address</b><br>Iowa Department of Transportation<br>800 Lincoln Way<br>Ames, IA 50010   |  | <b>13. Type of Report and Period Covered</b><br>Final Report |                        |
|   |  | <b>14. Sponsoring Agency Code</b>                            |                        |
| <b>15. Supplementary Notes</b><br>Visit <a href="http://www.ctre.iastate.edu">www.ctre.iastate.edu</a> for color PDF files of this and other research reports.  |  |  |                        |
| <b>16. Abstract</b><br><br>Evaluating structural conditions of existing, in-service pavements is a part of the routine maintenance and rehabilitation activities undertaken by the most departments of transportation (DOTs). In the field, the pavement deflection profiles (or basins) gathered from the nondestructive falling weight deflectometer (FWD) test data are typically used to evaluate pavement structural conditions. Over the past decade, interest has increased in a new class of computational intelligence system, known as artificial neural networks (ANNs), for use in geomechanical and pavement systems applications. This report describes the development and use of ANN models as pavement structural analysis tools for the rapid and accurate prediction of layer parameters of Iowa pavements subjected to typical highway loadings. ANN models trained with the results from the structural analysis program solutions have been found to be practical alternatives. The ILLI-PAVE, ISLAB2000, and DIPLOMAT programs were used as the structural response models for solving the deflection parameters of flexible, rigid, and composite pavements, respectively. The trained ANN models in this study were capable of predicting pavement layer moduli and critical pavement responses from FWD deflection basins with low errors.<br><br>The developed methodology was successfully verified using results from long-term pavement performance (LTPP) FWD tests, as well as Iowa DOT FWD field data. All successfully developed ANN models were incorporated into a Microsoft Excel spreadsheet-based backcalculation software toolbox with a user-friendly interface. The final outcome of this study was a field-validated, nondestructive pavement evaluation toolbox that will be used to assess pavement condition, estimate remaining pavement life, and eventually help assess pavement rehabilitation strategies by the Iowa DOT pavement management team. |  |  |                        |
| <b>17. Key Words</b><br>backcalculation—falling weight deflectometer— neural networks—nondestructive evaluation— pavements  |  | <b>18. Distribution Statement</b><br>No restrictions.        |                        |
| <b>19. Security Classification (of this report)</b><br>Unclassified.  | <b>20. Security Classification (of this page)</b><br>Unclassified. | <b>21. No. of Pages</b><br>152                               | <b>22. Price</b><br>NA |



# **NONDESTRUCTIVE EVALUATION OF IOWA PAVEMENTS: PHASE I**

**Final Report  
December 2007**

**Principal Investigator**

Halil Ceylan, Assistant Professor  
Department of Civil, Construction and Environmental Engineering, Iowa State University

**Research Assistants**

Alper Guclu (PhD Candidate)  
Mustafa Birkan Bayrak (PhD Candidate)

**Research Assistant Professor**

Kasthurirangan Gopalakrishnan

**Authors**

Halil Ceylan, Alper Guclu, Mustafa Birkan Bayrak, and Kasthurirangan Gopalakrishnan

Preparation of this report was financed in part  
through funds provided by the Iowa Department of Transportation  
through its research management agreement with the  
Center for Transportation Research and Education,  
CTRE Project 04-177

A report from  
**Center for Transportation Research and Education  
Iowa State University**

2711 South Loop Drive, Suite 4700  
Ames, IA 50010-8664  
Phone: 515-294-8103  
Fax: 515-294-0467  
[www.ctre.iastate.edu](http://www.ctre.iastate.edu)



## TABLE OF CONTENTS

|   |      |
|---|------|
| TABLE OF CONTENTS.....                                      | V    |
| LIST OF FIGURES .....                                       | IX   |
| LIST OF TABLES.....   | XIII |
| LIST OF SYMBOLS .....                                       | XV   |
| LIST OF ACRONYMS .....                                      | XVI  |
| ACKNOWLEDGMENTS .....                                       | XVII |
| EXECUTIVE SUMMARY .....                                     | XIX  |
| Research Summary .....                                      | xix  |
| Research Conclusions and Benefits .....                     | xx   |
| Recommendations.....  | xx   |
| INTRODUCTION .....  | 1    |
| LITERATURE REVIEW .....                                     | 4    |
| Backcalculation of Pavement Layer Moduli .....              | 4    |
| Application of ANNs in Pavement Structural Evaluation ..... | 5    |
| ARTIFICIAL NEURAL NETWORKS – A BRIEF REVIEW .....           | 10   |
| ANNs .....  | 10   |
| Architecture .....  | 11   |
| Learning Method.....  | 12   |
| ANN MODELS FOR CFP SYSTEMS.....                             | 13   |
| Nonlinear Geomaterial Characterization .....                | 13   |
| ILLI-PAVE Finite Element Program.....                       | 15   |
| Generating ILLI-PAVE Finite Element Solution Database ..... | 18   |
| ANN-Based CFP Backcalculation Models.....                   | 22   |
| Noise-Introduced ANN Backcalculation Models .....           | 23   |
| ANN-Based CFP Forward Calculation Models.....               | 24   |
| Performance of CFP ANN Models .....                         | 24   |
| Validation of CFP-ANN Models .....                          | 27   |

|   |     |
|---|-----|
| Case Studies of Individual Pavement Sections.....   | 30  |
| ANN Models for CFP Systems – Summary and Conclusions.....   | 40  |
| Summary .....   | 40  |
| Conclusions.....  | 41  |
| <br>  |     |
| ANN MODELS FOR FULL-DEPTH FLEXIBLE PAVEMENT SYSTEMS .....   | 43  |
| Generating ILLI-PAVE Finite Element Solution Database .....   | 43  |
| ANN-Based FD Backcalculation Models.....  | 45  |
| Noise-Introduced ANN-Based FD Backcalculation Models.....   | 46  |
| ANN-Based FD Forward Calculation Models.....  | 47  |
| Performance of FD-ANN Models.....   | 48  |
| Validation of FD-ANN Models .....   | 51  |
| Case Studies of Individual Pavement Sections – Iowa DOT Data.....                                       | 57  |
| ANN Models for Full-Depth Flexible Pavement Systems – Summary and Conclusions .....                     | 58  |
| Summary .....   | 58  |
| Conclusions.....  | 59  |
| <br>  |     |
| ANN MODELS FOR RIGID PAVEMENT (RGD) SYSTEMS.....  | 61  |
| Review of Existing RGD Layer Moduli Backcalculation Models .....  | 61  |
| ISLAB2000 Finite Element Program.....   | 63  |
| Selection of the Forward Calculation Methodology.....   | 64  |
| Generating ISLAB2000 Finite Element Solution Database .....   | 66  |
| Data Preprocessing for ANN Modeling.....  | 68  |
| Formation of Data Sets for Training and Testing Sets .....  | 68  |
| ANN-Based RGD Backcalculation Models .....  | 69  |
| Model Architecture .....  | 70  |
| Noise-Introduced RGD-ANN Backcalculation Models .....   | 75  |
| RGD-ANN Forward Calculation Models .....  | 78  |
| Performance of ANN Models .....   | 78  |
| The Significance of Layer Bonding and Thickness in Backcalculation of Rigid Pavement Layer Moduli ..... | 80  |
| The Effect of the Layer Thickness in the $E_{PCC}$ Predictions .....                                    | 82  |
| The Effect of the Pavement Layer Bonding in the $E_{PCC}$ Predictions .....                             | 82  |
| Case Study of Individual Pavement Sections .....  | 83  |
| Iowa FWD Data Analysis .....  | 91  |
| ANN Models for Rigid Pavement Systems - Summary and Conclusions.....                                    | 96  |
| Summary .....   | 96  |
| Conclusions.....  | 96  |
| <br>  |     |
| ANN MODELS FOR COMPOSITE PAVEMENT (CP) SYSTEMS.....   | 99  |
| DIPLOMAT Model .....  | 99  |
| Generating DIPLOMAT Solution Database.....  | 99  |
| ANN-Based CP Backcalculation Models .....   | 101 |
| Data Preprocessing .....  | 101 |
| ANN Network Architecture.....   | 102 |

|  |     |
|--|-----|
| Noise-Introduced CP-ANN Backcalculation Models.....  | 106 |
| CP-ANN Forward Calculation Models.....   | 107 |
| Validation of ANN Models.....  | 107 |
| Case Studies of Individual Pavement Sections.....  | 111 |
| ANN Models for Composite Pavements — Summary and Conclusions .....                         | 117 |
| Summary .....  | 117 |
| Conclusions.....   | 117 |
| <br>   |     |
| DEVELOPMENT OF A USER-FRIENDLY SPREADSHEET ANALYSIS TOOL FOR<br>DEVELOPED ANN MODELS ..... | 118 |
| Introduction.....  | 118 |
| Program Overview .....   | 118 |
| Program Menus and Pavement Analysis Menu .....   | 118 |
| Pavement Analysis Using the Excel Sheets.....  | 119 |
| <br>   |     |
| SUMMARY AND CONCLUSIONS .....  | 127 |
| Benefits .....   | 128 |
| Implementation .....   | 128 |
| <br>   |     |
| RECOMMENDATIONS .....  | 129 |
| <br>   |     |
| REFERENCES .....   | 130 |



## LIST OF FIGURES

|   |    |
|---|----|
| Figure 1. FWD test equipments, (a) Iowa DOT FWD: JILS-20, (b) DYNATEST FWD, (c) KUAB FWD, and (d) JILS FWD (Source: <a href="http://training.ce.washington.edu/WSDOT/Modules/09_pavement_evaluation/09-5_body.htm">http://training.ce.washington.edu/WSDOT/Modules/09_pavement_evaluation/09-5_body.htm</a> ) ..... | 2  |
| Figure 2. FWD bottom view with sensor locations (Source: <a href="http://training.ce.washington.edu/WSDOT/Modules/09_pavement_evaluation/09-5_body.htm">http://training.ce.washington.edu/WSDOT/Modules/09_pavement_evaluation/09-5_body.htm</a> ) .....  | 2  |
| Figure 3. A general view of the ANNs .....  | 10 |
| Figure 4. Typical nonlinear modulus characterization of unbound aggregate materials.....  | 14 |
| Figure 5. Stress dependency of fine-grained soils characterized by bilinear model .....   | 15 |
| Figure 6. ILLI-PAVE-based ANN backcalculation models for flexible pavements .....   | 16 |
| Figure 7. Pavement geometry and finite element mesh used for the ILLI-PAVE runs.....  | 19 |
| Figure 8. Iowa DOT FWD (JILS-20) sensor configuration.....  | 20 |
| Figure 9. $E_{AC}$ correlation with deflections (CFP) .....   | 21 |
| Figure 10. $K_B$ correlation with deflections (CFP).....  | 21 |
| Figure 11. $E_{Ri}$ correlation with deflections (CFP) .....  | 22 |
| Figure 12. Geometry and loading characteristics of pavement sections analyzed .....   | 27 |
| Figure 13. ANN, BAKFAA, and algorithms comparison for prediction of $E_{AC}$ .....  | 28 |
| Figure 14. ANN, BAKFAA, and algorithms comparison for prediction of $E_{Ri}$ .....  | 28 |
| Figure 15. Comparison of ANN-based models to statistical models for $E_{AC}$ .....  | 29 |
| Figure 16. Comparison of ANN-based models to statistical models for $E_{Ri}$ .....  | 29 |
| Figure 17. $E_{AC}$ predictions for IA – Clarke County (I-35) FWD deflection basin data (205085)..  | 31 |
| Figure 18. $E_{Ri}$ predictions for IA – Clarke County (I-35) FWD deflection basin data (205085)..  | 31 |
| Figure 19. $E_{AC}$ predictions for IA – Clarke County (I-35) FWD deflection basin data (205086)..  | 32 |
| Figure 20. $E_{Ri}$ predictions for IA – Clarke County (I-35) FWD deflection basin data (205086)..  | 32 |
| Figure 21. $E_{AC}$ predictions for IA – Clarke County (I-35) FWD deflection basin data (205087)..  | 33 |
| Figure 22. $E_{Ri}$ predictions for IA – Clarke County (I-35) FWD deflection basin data (205087)..  | 33 |
| Figure 23. $E_{AC}$ predictions for IA – Clarke County (I-35) FWD deflection basin data (205088)..  | 34 |
| Figure 24. $E_{Ri}$ predictions for IA – Clarke County (I-35) FWD deflection basin data (205088)..  | 34 |
| Figure 25. $E_{AC}$ predictions for IA – Clarke County (I-35) FWD deflection basin data (205089)..  | 35 |
| Figure 26. $E_{Ri}$ predictions for IA – Clarke County (I-35) FWD deflection basin data (205089)..  | 35 |
| Figure 27. $E_{AC}$ predictions for IA – Clarke County (I-35) FWD deflection basin data (205090)..  | 36 |
| Figure 28. $E_{Ri}$ predictions for IA – Clarke County (I-35) FWD deflection basin data (205090)..  | 36 |
| Figure 29. $E_{AC}$ predictions for IA – Clarke County (I-35) FWD deflection basin data (205091)..  | 37 |
| Figure 30. $E_{Ri}$ predictions for IA – Clarke County (I-35) FWD deflection basin data (205091)..  | 37 |
| Figure 31. $E_{AC}$ predictions for IA – Clarke County (I-35) FWD deflection basin data (501193)..  | 38 |
| Figure 32. $E_{Ri}$ predictions for IA – Clarke County (I-35) FWD deflection basin data (501193)..  | 38 |
| Figure 33. $E_{AC}$ predictions for IA – Jasper County (I-80) FWD deflection basin data (501194) ..   | 39 |
| Figure 34. $E_{Ri}$ predictions for IA – Jasper County (I-80) FWD deflection basin data (501194)..  | 39 |
| Figure 35. $E_{AC}$ predictions for IL – Henry County FWD deflection basin data .....   | 40 |
| Figure 36. $E_{Ri}$ predictions for IL – Henry County FWD deflection basin data .....   | 40 |
| Figure 37. Layout of full-depth flexible pavement systems .....   | 44 |
| Figure 38. $E_{AC}$ correlation with deflections (FD) .....   | 45 |
| Figure 39. $E_{Ri}$ correlation with deflections (FD) .....   | 45 |
| Figure 40. IL – Carlyle test road (K) FWD deflection basin data $E_{AC}$ predictions .....  | 52 |

|   |    |
|---|----|
| Figure 41. IL – Carlyle test road (K) FWD deflection basin data $E_{Ri}$ predictions .....  | 52 |
| Figure 42. IL – Carlyle test road (M2) FWD deflection basin data $E_{AC}$ predictions.....  | 53 |
| Figure 43. IL – Carlyle test road (M2) FWD deflection basin data $E_{Ri}$ predictions.....  | 53 |
| Figure 44. IL – Staley Road FWD deflection basin data $E_{AC}$ predictions.....   | 54 |
| Figure 45. IL – Staley Road FWD deflection basin data $E_{Ri}$ predictions .....  | 54 |
| Figure 46. IL – Windsor Road FWD deflection basin data $E_{AC}$ predictions .....   | 55 |
| Figure 47. IL – Windsor Road FWD deflection basin data $E_{Ri}$ predictions .....   | 55 |
| Figure 48. Full-depth $E_{AC}$ prediction comparisons with statistical algorithms .....   | 56 |
| Figure 49. Full-depth $E_{Ri}$ prediction comparisons with statistical algorithms .....   | 56 |
| Figure 50. $E_{AC}$ predictions for IA – Cedar County (I-80 EB) FWD deflection basin data<br>(166218).....  | 57 |
| Figure 51. $E_{Ri}$ predictions for IA – Cedar County (I-80 EB) FWD deflection basin data<br>(166218).....  | 57 |
| Figure 52. $E_{AC}$ predictions for IA – Cedar County (I-80 WB) FWD deflection basin data<br>(166219).....  | 58 |
| Figure 53. $E_{Ri}$ predictions for IA – Cedar County (I-80 WB) FWD deflection basin data<br>(166219).....  | 58 |
| Figure 54. Comparison of ISLAB2000, DIPLOMAT, KENSLAB program results and<br>Westergaard theoretical solutions.....                                   | 64 |
| Figure 55. Comparison of ISLAB2000, DIPLOMAT, and KENSLAB finite element model<br>solutions for different pavement and foundation configurations..... | 65 |
| Figure 56. ISLAB2000 finite element model mesh for the six-slab JPCP assembly .....   | 66 |
| Figure 57. A general view of the deflections under 9-kip loading in six-slab assembly.....  | 67 |
| Figure 58. Winkler foundation and coefficient of subgrade reaction ( $k_s$ ) .....  | 68 |
| Figure 59. Sensitivity study results for the number of hidden layers .....  | 71 |
| Figure 60. Sensitivity study results for the number of hidden neurons in each hidden layer.....   | 71 |
| Figure 61. Sensitivity study results for the learning rate .....  | 72 |
| Figure 62. Sensitivity study results for the momentum factor.....   | 72 |
| Figure 63. Sensitivity study results for the number of hidden layers .....  | 73 |
| Figure 64. Sensitivity study results for the number of hidden neurons in each hidden layer.....   | 73 |
| Figure 65. Sensitivity study results for the learning rate .....  | 74 |
| Figure 66. Sensitivity study results for the momentum factor.....   | 74 |
| Figure 67. $E_{PCC}$ correlation with deflections (RGD) .....   | 75 |
| Figure 68. $k_s$ correlation with deflections (RGD) .....   | 75 |
| Figure 69. Effect of layer thickness on $E_{PCC}$ backcalculation .....   | 82 |
| Figure 70. Effect of degree of layer bonding on $E_{PCC}$ backcalculation .....   | 83 |
| Figure 71. FWD deflection basins normalized to 9-kip load level for NAPTF-LRS section<br>(before trafficking).....                                    | 86 |
| Figure 72. FWD deflection basins normalized to 9-kip load level for NAPTF-LRS section (after<br>trafficking) .....                                    | 87 |
| Figure 73. Coefficient of subgrade reaction predictions using: (a) RGD- $k_s$ -(6) ANN model, and<br>(b) Closed-form equations .....                  | 88 |
| Figure 74. PCC layer elastic modulus predictions using: (a) RGD- $E_{PCC}$ -(4) ANN model, and (b)<br>Closed-form equations.....                      | 89 |
| Figure 75. Comparison of results from different backcalculation methods (NAPTF data) .....  | 90 |
| Figure 76. a) Iowa – Allamakee County (US 18) FWD data b) RGD- $E_{PCC}$ -(4) model predictions<br>c) RGD- $k_s$ -(6) model predictions .....         | 92 |
| Figure 77. a) Iowa – Fayette County (IA 150) FWD deflection basin data b) RGD- $E_{PCC}$ -(4)   |    |

|  |     |
|--|-----|
| model predictions c) RGD-ks-(6) model predictions .....  | 93  |
| Figure 78. a) Iowa – Franklin County (I 35) FWD deflection basin data b) RGD-E <sub>PCC</sub> -(4) model predictions c) RGD-ks-(6) model predictions ..... | 94  |
| Figure 79. a) Iowa – Wright County (I 35) FWD deflection basin data b) RGD-E <sub>PCC</sub> -(4) model predictions c) RGD-ks-(6) model predictions .....   | 95  |
| Figure 80. Schematic of AC overlaid PCC composite pavement structure.....  | 100 |
| Figure 81. DIPLOMAT layer configuration input options.....   | 100 |
| Figure 82. E <sub>AC</sub> modulus correlation with deflections (CP).....  | 101 |
| Figure 83. E <sub>PCC</sub> modulus correlation with deflections (CP) .....  | 102 |
| Figure 84. k <sub>s</sub> correlations with deflections (CP) .....   | 102 |
| Figure 85. Training and testing set histogram comparisons for (a) E <sub>AC</sub> , (b) E <sub>PCC</sub> , and (c) k .....                                 | 106 |
| Figure 86. Field data deflection basin before filtering.....   | 108 |
| Figure 87. Field data deflection basin after filtering .....   | 108 |
| Figure 88. AC layer moduli predictions using: (a) ANN-based models and (b) MODCOMP model.....  | 110 |
| Figure 89. PCC layer moduli predictions using: (a) ANN-based models and (b) MODCOMP model.....   | 111 |
| Figure 90. Iowa – Allamakee Co. (I-51): (a)E <sub>AC</sub> predictions, (b)E <sub>PCC</sub> predictions, (c)k <sub>s</sub> predictions.....                | 113 |
| Figure 91. Iowa – Black Hawk County (I-57): (a)E <sub>AC</sub> predictions, (b)E <sub>PCC</sub> predictions, (c)k <sub>s</sub> predictions.....            | 114 |
| Figure 92. Iowa – Butler County (I-14:) (a)E <sub>AC</sub> predictions, (b)E <sub>PCC</sub> predictions, (c)k <sub>s</sub> predictions.....                | 115 |
| Figure 93. Iowa – Chickasaw County (US-18): (a)E <sub>AC</sub> predictions, (b)E <sub>PCC</sub> predictions, (c) k <sub>s</sub> predictions.....           | 116 |
| Figure 94. FWD analysis program main menu .....  | 119 |
| Figure 95. General information window.....   | 120 |
| Figure 96. Sample pavement analysis: Excel sheet inputs .....  | 121 |
| Figure 97. Filter options menu.....  | 122 |
| Figure 98. Sample pavement analysis: Excel sheet outputs .....   | 123 |
| Figure 99. Sample pavement analysis: Excel sheet output statistics .....   | 123 |
| Figure 100. Plot option window .....   | 124 |
| Figure 101. Sample pavement analysis: Excel sheet charts.....  | 125 |
| Figure 102. Output statistics sheet.....   | 126 |



## LIST OF TABLES

|  |     |
|--|-----|
| Table 1. Pavement geometry and material property/model inputs of CFPs for ILLI-PAVE solutions .....                  | 18  |
| Table 2. Mesh constraints for AC layer .....   | 19  |
| Table 3. Summary of CFP-ANN backcalculation models .....   | 23  |
| Table 4. Prediction performance of CFP-ANN-based backcalculation models (with zero noise) .....                      | 25  |
| Table 5. Prediction performance of CFP-ANN-based backcalculation models (with noise) .....                           | 26  |
| Table 6. Prediction performance of CFP-ANN-based backcalculation models (forward) .....                              | 26  |
| Table 7. The Iowa CFP sections .....   | 30  |
| Table 8. Pavement geometry and material property/model inputs of FD flexible pavements for ILLI-PAVE solutions ..... | 44  |
| Table 9. FD-ANN models input/output configuration .....  | 46  |
| Table 10. Prediction performance of FD-ANN-based backcalculation models (virgin) .....                               | 49  |
| Table 11. Prediction performance of FD-ANN-based backcalculation models (noise) .....                                | 50  |
| Table 12. Prediction performance of FD-ANN-based backcalculation models (forward) .....                              | 51  |
| Table 13. The Illinois FD flexible pavement sections .....   | 52  |
| Table 14. Linear elastic layer analysis backcalculation programs .....   | 62  |
| Table 15. Nonlinear elastic layer analysis backcalculation programs .....  | 63  |
| Table 16. Ranges of input parameters used in the ISLAB2000 database generation .....                                 | 67  |
| Table 17. Ranges of the ISLAB2000 solution database (inputs of the ANN models) .....                                 | 68  |
| Table 18. RGD-ANN models (virgin) input/output configuration .....   | 70  |
| Table 19. RGD-ANN models (noise-introduced) input/output configuration .....   | 77  |
| Table 20. Architectures of the RGD-RRS and RGD- $\sigma_{PCC}$ ANN models .....                                      | 78  |
| Table 21. Prediction performance of RGD-ANN-based backcalculation models (with zero noise) .....                     | 80  |
| Table 22. Prediction performance of RGD-ANN-based backcalculation models (with noise) .....                          | 80  |
| Table 23. Prediction performance of RGD-ANN-based forward calculation models .....                                   | 80  |
| Table 24. Input ranges used in generating DIPLOMAT solutions .....   | 101 |
| Table 25. Abbreviations for ANN models .....   | 103 |
| Table 26. CP-ANN models input/output configuration .....   | 104 |
| Table 27. Prediction performance of CP-ANN-based backcalculation models (virgin) .....                               | 106 |
| Table 28. Prediction performance of CP-ANN-based backcalculation models (noise) .....                                | 107 |
| Table 29. Iowa composite pavement sections .....   | 112 |
| Table 30. Curvature check input parameters .....   | 122 |



## LIST OF SYMBOLS

|                    |   |
|--------------------|---|
| $E_{AC}$           | Modulus of Asphalt Concrete   |
| $E_{Ri}$           | Breakpoint Resilient Modulus  |
| $E_{PCC}$          | Modulus of portland cement concrete                                   |
| $E_i$              | Elastic modulus for layer i   |
| $K_B$              | Base Modulus Parameter  |
| $M_R$              | Resilient Modulus   |
| $k_s$              | Coefficient of subgrade reaction                                      |
| $\sigma_D$         | Subgrade deviator stress  |
| $\sigma_{PCC}$     | Tensile stress at the bottom of the PCC layer                         |
| $\theta$           | Bulk stress   |
| $\tau_{oct}$       | Octahedral shear stress   |
| $\varepsilon_{AC}$ | Tensile strain at the bottom of asphalt layer                         |
| $\varepsilon_{SG}$ | Compressive strain at the top of subgrade                             |
| $h_{AC}$           | Thickness of AC Layer   |
| $h_{PCC}$          | Thickness of PCC Layer  |
| $h_{SG}$           | Thickness of Subgrade   |
| $h_{base}$         | Thickness of Subbase  |
| $h_i$              | Thickness for layer i   |
| $D_r$              | Measured deflection at radial distance r                              |
| $\mu$              | Poisson's ratio   |
| $W$                | Slab width  |
| $L$                | Slab length   |
| $\gamma$           | PCC unit weight   |
| $LTE$              | Load transfer efficiency  |
| $h_{e-u}$          | Effective thickness of the unbonded PCC layer                         |
| $h_{e-p}$          | Effective thickness of the partially bonded PCC layers                |
| $x_{na}$           | Neutral axis distance from top of layer                               |
| $x$                | Degree of bonding which ranges between 0 and 1                        |
| $RRS$ or $l$       | Radius of relative stiffness  |
| $V_s$              | Shear wave velocity   |
| $X$                | Input vector (Neural network)   |
| $Y$                | Output vector (Neural Network)  |
| $Z$                | Intermediate output vector of hidden layer (Neural Network)           |
| $w_{ij}$           | Weights between the input and output layer (Neural Network)           |
| $b_{ij}$           | Bias between the input layer and the hidden layer (Neural Network)    |
| $w_{ik}$           | Weight between the hidden layer and the output layer (Neural Network) |
| $b_{ik}$           | Bias between the hidden layer and the output layer (Neural Network)   |
| $T$                | Expected output (Neural Network)                                      |
| $\eta$             | Learning rate (Neural Network)  |
| $\alpha$           | Momentum  |
| $CV$               | Coefficient of Variation  |
| $R^2$              | Coefficient of Determination  |

## LIST OF ACRONYMS

|                 |   |
|-----------------|---|
| <i>AAE</i>      | Average Absolute Error                        |
| <i>AC</i>       | Asphalt Concrete                              |
| <i>ANNs</i>     | Artificial Neural Networks                    |
| <i>ATB</i>      | Asphalt Treated Base                          |
| <i>BCI</i>      | Base Curvature Index                          |
| <i>BDI</i>      | Base Damage Index                             |
| <i>BP</i>       | Backpropagation                               |
| <i>BPNN</i>     | Backpropagation Neural Networks               |
| <i>CFP</i>      | Conventional Flexible Pavements               |
| <i>CP</i>       | Composite Pavement                            |
| <i>DL</i>       | Dense Liquid Subgrade Model                   |
| <i>DM</i>       | Dimensional Method                            |
| <i>DOT</i>      | Department of Transportation                  |
| <i>DR</i>       | Direct Method                                 |
| <i>ELPs</i>     | Elastic Layer Programs                        |
| <i>FAA</i>      | Federal Aviation Administration               |
| <i>FD</i>       | Full-Depth Flexible Pavement                  |
| <i>FE</i>       | Finite Element                                |
| <i>FWD</i>      | Falling Weight Deflectometer                  |
| <i>GPR</i>      | Ground Penetrating Radar                      |
| <i>GPS</i>      | General Pavement Sites                        |
| <i>GRNN</i>     | Generalized Regression Neural Networks        |
| <i>HMA</i>      | Hot-Mix Asphalt                               |
| <i>HWD</i>      | Heavy Weight Deflectometer                    |
| <i>Iowa DOT</i> | Iowa Department of Transportation             |
| <i>LTPP</i>     | Long-Term Pavement Performance                |
| <i>MEPDG</i>    | Mechanistic-Empirical Pavement Design Guide   |
| <i>NAPTF</i>    | National Airport Pavement Test Facility       |
| <i>NCHRP</i>    | National Cooperative Highway Research Program |
| <i>NDT</i>      | Nondestructive Testing                        |
| <i>PCA</i>      | Portland Cement Association                   |
| <i>PCC</i>      | Portland Cement Concrete                      |
| <i>PNN</i>      | Probabilistic Neural Networks                 |
| <i>RBFFN</i>    | Radial Basis Function Networks                |
| <i>RGD</i>      | Rigid Pavement                                |
| <i>RMSE</i>     | Root-Mean-Square Error                        |
| <i>SASW</i>     | Spectral-Analysis-of-Surface-Waves            |
| <i>SCI</i>      | Surface Curvature Index                       |
| <i>SHRP</i>     | Strategic Highway Research Program            |
| <i>SPS</i>      | Specific Pavement Sites                       |
| <i>UAB</i>      | Unbound Aggregate Base                        |

## **ACKNOWLEDGMENTS**

The authors gratefully acknowledge the Iowa Department of Transportation for sponsoring this study. The contents of this report reflect the views of the authors who are responsible for the facts and accuracy of the data presented within. The contents do not necessarily reflect the official views and policies of the Iowa DOT. This report does not constitute a standard, specification, or regulation.



## EXECUTIVE SUMMARY

Falling weight deflectometer (FWD) and heavy weight deflectometer (HWD) testing have become the main nondestructive testing (NDT) techniques to evaluate the structural condition of in-service pavements over the last 20 years. FWD testing is often preferred over destructive testing methods because it is faster than destructive tests and does not entail the removal of pavement materials. Pavement structural properties are “backcalculated” from the observed dynamic response of the pavement surface to an impulse load (the falling weight). The current pavement layer moduli backcalculation techniques used by the Iowa Department of Transportation (Iowa DOT) in the past have been cumbersome and more efficient and faster methods are now needed. This report documents the development of rapid models for backcalculation of pavement layer structural properties and prediction of critical pavement responses of pavement systems in Iowa in real time based on FWD deflection basins.

### Research Summary

The primary objective of this research is to develop an easy-to-use ANN-based pavement evaluation methodology that will utilize/interpret routinely collected nondestructive test data from Iowa pavements. The end product is a user-friendly Excel-based software toolkit incorporating the advanced structural models the pavement engineer can easily use for routine pavement structural evaluation purposes.

The backcalculation models proposed in this research were developed using the neural networks methodology. Artificial neural networks (ANNs) are very adaptable and easy to use for this purpose. ANNs also support the real-time applications of developed models. The user-friendly ANN-based Excel spreadsheet tool, which is the end product of this research, provides easy interfacing with solutions to all the developed models for Iowa pavements. Pavement type-specific models were developed for three broad categories: flexible (conventional and full-depth), rigid, and composite. For each pavement type, state-of-the-art pavement structural modeling concepts are combined with ANN methodology to produce a robust pavement evaluation tool. All developed, ANN-based pavement structural models were compared with the existing and commonly used commercial software packages in the market. The ANN models were then validated using actual field data from selected sites in Iowa.

In this study, the pavement layer stiffness properties and critical pavement responses were predicted from FWD test results. For the three pavement types, over 300 models total were developed for varying input parameters. The primary pavement types considered were flexible (conventional and full-depth), rigid, and composite. Predicted flexible pavement parameters were,  $E_{AC}$ -modulus of hot-mix asphalt (HMA),  $K_b$ -base modulus parameter,  $E_{Ri}$ -subgrade resilient modulus,  $\epsilon_{AC}$ -tensile strain at the bottom of asphalt layer,  $\epsilon_{SG}$ -compressive strain at the top of subgrade, and  $\sigma_D$ -subgrade deviator stress. For rigid pavements,  $E_{PCC}$ -modulus of portland cement concrete (PCC),  $k_s$ -coefficient of subgrade reaction,  $\sigma_{PCC}$ -tensile stress at the bottom of the PCC layer, and radius of relative stiffness (RRS) were predicted. In the case of composite pavements (CPs), where an asphalt concrete (AC) surface is overlaid on top of an existing PCC pavement,  $E_{AC}$ ,  $E_{PCC}$ ,  $k_s$ ,  $\sigma_{PCC}$  (tensile stress at the bottom of the PCC), and  $\epsilon_{AC}$  were predicted.

Field data from Iowa pavements were evaluated for each pavement type. The  $R^2$  (coefficient of determination) value and average absolute errors (AAE) were used to assess the quality of predictions.

## **Research Conclusions and Benefits**

- It was demonstrated that ANNs are capable of successfully predicting the pavement layer moduli values using the FWD field deflection measurements. Field moduli values were successfully predicted for the given deflection basins and comparison of the ANN-based predictions showed the strength of the ANN-based backcalculation approach.
- The ANN-based backcalculation models successfully predicted pavement layer moduli values (except for the base/subbase layer in flexible pavements) with an overall AAE value of less than 1.5 percent.
- The adoption of an ANN-based approach also resulted in both a drastic reduction in computation time and a simplification of the backcalculation approach from the viewpoint of a pavement designer/analyst. Rapid prediction ability of the ANN models, capable of analyzing 100,000 FWD deflection profiles in less than a second, provide a tremendous advantage to the pavement engineers by allowing them to nondestructively assess the condition of the transportation infrastructure system in real time, including when the FWD testing is conducted in the field.
- Elimination of the seed layer moduli selection step, combined with the integration of ANN-based direct backcalculation approach, can be invaluable for the state and federal agencies for rapidly analyzing a large number of pavement deflection basins needed for routine pavement evaluation for both project-specific and network-level FWD testing.
- Several ANN-based backcalculation models were developed that use different FWD sensor configurations. For example, there are 4-Deflection ( $D_0, D_{12}, D_{24}, D_{36}$ ), 6-Deflection ( $D_0, D_{12}, D_{24}, D_{36}, D_{48}, D_{60}$ ), 7-Deflection ( $D_0, D_8, D_{12}, D_{18}, D_{24}, D_{36}, D_{60}$ ), and 8-Deflection ( $D_0, D_8, D_{12}, D_{18}, D_{24}, D_{36}, D_{48}, D_{60}$ ) ANN-based backcalculation models to predict the pavement parameters.

## **Recommendations**

- Although advanced approaches to pavement layer backcalculation have been developed in this study, the accuracy of results will largely depend on the quality and integrity of FWD deflection data collected in the field. Future research efforts should focus on developing guidelines for the Iowa DOT that clearly define the FWD testing requirements, data analysis approach, and reporting requirements. The guidelines will provide Iowa DOT with an improved specification for acquiring FWD testing and backcalculation services, as well as provide guidance for Iowa DOT internal staff conducting FWD testing and analysis. Also, the guidelines will provide procedures

for standardized FWD calibration.

- Both the current research and past research studies have shown that to successfully backcalculate the pavement layer stiffness, or to predict the critical pavement responses (maximum stresses, strains and deflections), accurate layer thickness information is needed, especially at the FWD testing points. Future research efforts should focus on conducting sensitivity studies to determine the effect of pavement layer thickness on pavement performance data using the mechanistic-empirical based (the same concept used for developing NCHRP Project 1-37A) pavement design concepts. This will help to determine how much tolerance can be accommodated in assessing the pavement thickness by the means of NDT techniques and devices.



## INTRODUCTION

Evaluating the structural condition of existing, in-service pavements is a part of the routine maintenance and rehabilitation activities undertaken by most DOT agencies. In the field, the pavement deflection profiles, or basins, gathered from the nondestructive FWD test data are typically used to evaluate pavement structural conditions. The deflection-testing program is being conducted periodically to obtain the load-response characteristics of the pavement structure and subgrade. This kind of evaluation requires the use of backcalculation-type structural analysis to determine pavement layer stiffness and is used to estimate a pavement's remaining structural life.

FWD and HWD tests have become the main NDT techniques to structurally evaluate the in-service pavements over the last 20 years. The FWD equipment is mainly used for the structural evaluation of highway pavements, whereas the heavier version of the same test equipment, HWD, is used in airport pavements. This study deals with FWD testing. FWD testing is often preferred over destructive testing methods because FWD testing is faster than destructive tests and does not entail the removal of pavement materials. In addition, the testing apparatus is easily transportable. Pavement properties are backcalculated from the observed dynamic response of the pavement surface to an impulse load (the falling weight). Backcalculation of pavement layer properties is a very useful pavement design tool to evaluate the structural condition of in-service pavements and to characterize the layer properties as inputs into available numerical or analytical programs. Most backcalculation procedures estimate pavement properties by matching measured and calculated pavement surface deflection basins.

Several types of FWD equipment are shown in [Figure 1](#). The FWD can either be mounted in a vehicle or on a trailer and is equipped with a weight and several velocity transducer sensors. To perform a test, the vehicle is stopped and the loading plate (weight) is positioned over the desired location (see [Figure 2](#)). The sensors are then lowered to the pavement surface and the weight is dropped. The advantage of an impact load response measuring device over a steady state deflection measuring device is that it is quicker, the impact load can be easily varied, and it more accurately simulates the transient loading of moving traffic. Sensors located at specific radial distances monitor the deflection history. The deflections measured at radial distances away from the load form the deflection basin. In order to calculate the pavement structural capacity accurately, the deflection basins should be measured and analyzed accurately. Although there are numerous methods for evaluating the structural capacity of pavements from deflection basin data, there is no standard or universally accepted procedure that presently exists (PCS/Law Engineering 1993).

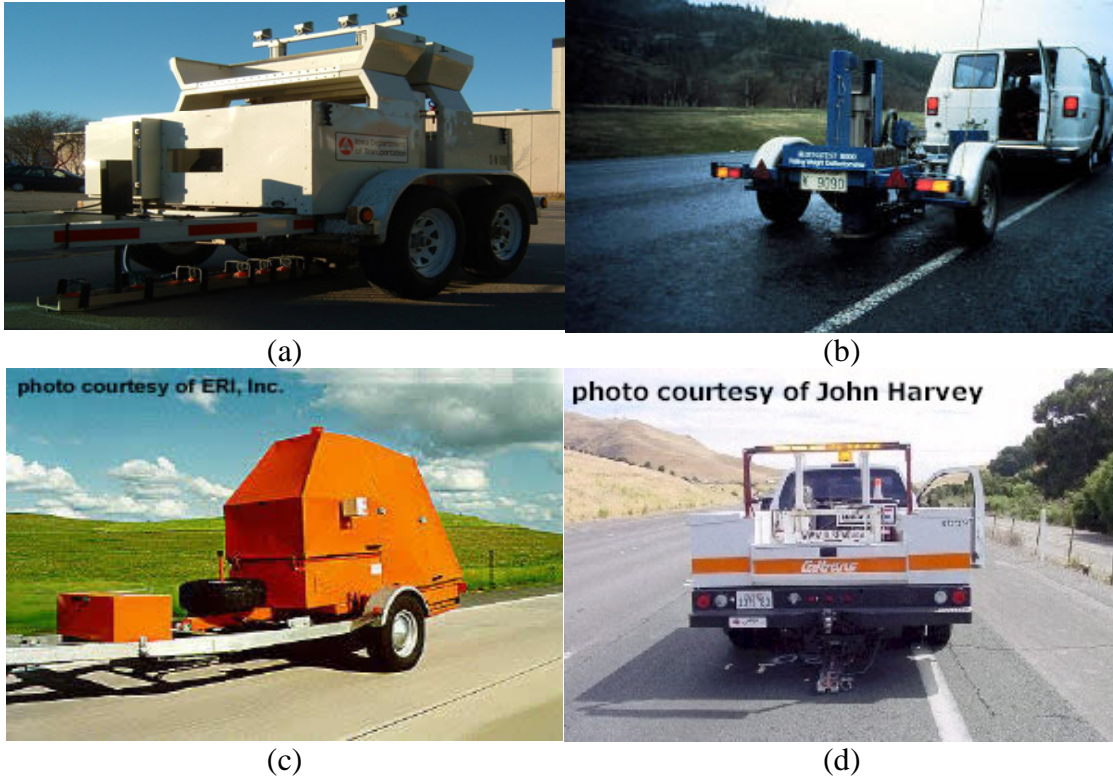


**Figure 1. FWD test equipments, (a) Iowa DOT FWD: JILS-20, (b) DYNATEST FWD, (c) KUAB FWD, and (d) JILS FWD (Source: [http://training.ce.washington.edu/WSDOT/Modules/09\\_pavement\\_evaluation/09-5\\_body.htm](http://training.ce.washington.edu/WSDOT/Modules/09_pavement_evaluation/09-5_body.htm))**



**Figure 2. FWD bottom view with sensor locations (Source: [http://training.ce.washington.edu/WSDOT/Modules/09\\_pavement\\_evaluation/09-5\\_body.htm](http://training.ce.washington.edu/WSDOT/Modules/09_pavement_evaluation/09-5_body.htm))**

The FWD equipment measures pavement surface deflections from an applied dynamic load that simulates a moving wheel (FAA 2004). There are many advantages to using FWD tests in lieu of, or to supplement, traditional destructive tests for pavement structural evaluation. Without

FWD testing, structural data must be obtained from numerous cores, borings, and excavation pits on existing highway/airport pavements. This process can be very disruptive to highway/airport operations. FWD tests are economical to perform and data can be collected at up to 250 locations per day. FWD devices have earned a major role in pavement management. The Strategic Highway Research Program (SHRP) adopted the FWD device as a key piece of equipment for assessing structural capacity of long-term pavement performance (LTPP) test sections. Under the LTPP program, FWD testing is used at all general pavement studies (GPS) and specific pavement studies (SPS) test sites.

In the past 10 years, there has been an increased interest in a few classes of computational intelligence systems, known as ANNs, for use in geomechanical and pavement system applications. ANNs have been found to be powerful and versatile computational tools for organizing and correlating information in ways that have proved useful for solving certain types of problems too complex, too poorly understood, or too resource-intensive to tackle using more-traditional computational methods. ANNs have been successfully used for tasks involving pattern recognition, function approximation, optimization, forecasting, data retrieval, and automatic control, to name a few. The adoption and use of ANN modeling techniques in the recently released Mechanistic-Empirical Pavement Design Guide (NCHRP project 1-37A: Development of the 2002 Guide for the Design of New and Rehabilitated Pavement Structures) has especially placed the emphasis on the successful use of neural networks in geomechanical and pavement systems. A Transportation Research Board (TRB) subcommittee, AFS50(1) (formerly A2K05(1)), has been focused on applications of nontraditional computing tools including neural networks with the primary mission to provide practitioners with a better understanding of use of the ANNs and other nontraditional computational intelligence techniques in pavement applications, as well as foster their use. In this research study, the ANN methodology was employed to develop robust structural tools for rapid structural evaluation of pavement systems based on routinely collected FWD data.

Previous research has demonstrated that the neural network method is a valuable tool to backcalculate pavement and foundation properties from FWD deflection basins. A recent study by Ceylan et al. (2004a) showed that the use of ANN models trained with ILLI-PAVE (a flexible pavement finite element structural model) solutions proved to give much better results than the statistical algorithms currently in use. Similarly, ANN-based backcalculation models trained with the results from the ISLAB2000 (a 2.5-D rigid pavement finite element structural modeling program) solutions were proposed for backcalculating rigid pavement layer properties. Also, ANN models trained with the DIPLOMAT structural analysis program were used to rapidly backcalculate the AC overlaid PCC-type composite pavement layer moduli properties. This report summarizes the research efforts related to the development of a suite of ANN backcalculation and critical response prediction models for all three pavement types found in Iowa: flexible, rigid, and composite.

## LITERATURE REVIEW

### Backcalculation of Pavement Layer Moduli

Several pavement layer moduli backcalculation programs have been proposed in the literature. The AREA method for flexible pavements (Hoffman et al. 1982), AREA method for rigid pavements (Ioannides et al. 1989; Ioannides 1990; and Barenberg et al. 1991), ILLI-SLAB (Foxworthy and Darter 1989), ILLI-BACK (Ioannides 1990), best fit algorithm (Hall et al. 1997; Smith et al. 1996), ELMOD (Ullidtz 1987), WESDEF (Van Cauwelaert 1989), DIPLOBACK (Khazanovich and Roesler 1997), and MODCOMP (Irwin and Szenbenyi 1991; Irwin 1994) are examples of FWD interpretation programs and algorithms for rigid, flexible, and composite pavements. Backcalculation programs based on multilayer elastic layer theory are generally used for AC pavements. For rigid pavements, plate theory for a slab resting on a Winkler foundation or elastic solid foundation is modeled. There is no widely accepted methodology for AC overlaid PCC-type of composite pavements on a Winkler foundation. The backcalculation programs WESDEF, BISDEF, and ELSDEF are based on multilayer elastic analysis programs WESLEA, BISAR and ELSYM, respectively. These programs require the thickness, Poisson's ratio, and a seed modulus as inputs. The forward elastic layer program iterates the given seed modulus until the given deflections match with calculated deflections. Thus, the modulus of pavement layer is highly affected by the seed modulus. Consequently, experienced engineers are required to use these backcalculation programs (Lytton, 1989).

Moreover, elastic layer programs (ELPs) used in asphalt pavement analysis assume linear elasticity. Pavement geomaterials do not, however, follow a linear type stress-strain behavior under repeated traffic loading (Brown and Pappin 1981; Raad and Figueroa 1980; Thompson and Elliot 1985; Garg et al. 1998). The ILLI-PAVE (Thompson and Elliot 1985; Garg et al. 1998; Gomez-Achecar and Thompson 1986; Thompson 1992) finite element program, which is commonly used in structural analysis of flexible pavements, takes into account nonlinear geomaterials characterization. Other finite element programs such as ABAQUS, ANSYS, and DYNA3D are very powerful programs because they can be used in three-dimensional nonlinear dynamic analysis. Several studies have focused on 3-D finite element modeling of pavements in the last decade (Mallela and George, 1994; Darter and Kuo, 1995; Kennedy, 1998). Drawbacks associated with these 3-D finite element programs include considerable computational resources and time required for developing a structural model for each problem.

There are also several finite-element-based programs, such as ISLAB2000, specifically designed for the analysis of rigid pavement systems (Tabatabaie and Barenberg 1978; Khazanovich 1994; Khazanovich et al. 2000). ISLAB2000 contains many advanced features that distinguish it from other pavement programs that are based on plate theory. KENSLABS (Huang 1985) and WESLIQID (Chou 1981) are pavement analysis programs for multi-wheel loading of one- or two-layered medium thick plates resting on a Winkler foundation or elastic solid. DIPLOMAT (Khazanovich 1994; Ioannides and Khazanovich 1994; Khazanovich and Ioannides 1995) provides the capability to model pavement layers as plates, springs and/or elastic layers. DIPLOMAT assumes infinite joints in the horizontal direction. An ANN-based backcalculation procedure was developed for composite pavements by Khazanovich and Roesler (1997) using

DIPLOMAT solutions and implemented into a program called DIPLOBACK. DIPLOBACK procedure solutions were compared with WESDEF solutions (Khazanovich and Roesler 1997).

### **Application of ANNs in Pavement Structural Evaluation**

The use of ANNs has increased tremendously in several areas of engineering over the last two decades. This chapter reviews a significant number of research publications that specifically deal with applications of ANNs to backcalculate the pavement parameters such as elastic moduli of the pavement layers, pavement layer thicknesses, coefficient of subgrade reaction, shear wave velocities of the layers, and pavement surface deflections.

In order to interpret the ground penetrating radar (GPR) thickness profile output from pavement thickness and structure surveys without any destructive coring, Attoh-Okine (1993) used a feed-forward neural network model with a four-layer backpropagation algorithm. GPR is a noncontact technique that has the potential to survey pavement thickness and structure while operating at highway speed. In this study, three output nodes were used to identify the three different types of surface-base interface for composite pavements, partial-designed pavements, and full-designed pavements. Based on the analysis, the author concluded that the combination of radar output and ANN had the potential to automate nondestructive evaluation of structural conditions of pavements.

Meier and Rix (1994) developed an approach to backcalculate pavement layer moduli from FWD deflection basins by using ANNs. Two backpropagation neural networks were trained to backcalculate pavement moduli for three-layer flexible pavement profiles by using synthetic deflection basins with a wide variety of layer moduli and thicknesses. The first model was trained with success using synthetic basins with no random noise added and the second model was trained using deflection basins with random noise added to simulate measurement errors. Even though the network trained and tested with noisy data exhibited much more scatter in the results, the network did a reasonably good job of predicting moduli. The authors developed a neural network model that operated 1,500–2,200 times faster than the conventional algorithmic programs used at that time. In this study, a static analysis of pavement response was investigated. The authors also trained a different model (Meier and Rix 1995) to backcalculate pavement layer moduli from synthetic deflection basins calculated by using a dynamic analysis of pavement response based on Green functions. This neural network, similar to the previous study, gave the successful results in real time.

Williams and Gucunski (1995) developed backpropagation and general regression neural network models to predict the elastic moduli and layer thicknesses of pavements from the spectral analysis of surface waves (SASW) test results. The SASW test is a seismic technique for the in situ evaluation of pavements and soil systems. Three-, four-, and five-layer backpropagation models with jump connections were trained in the study. All neural network models produced reasonably close results to the actual outputs. The authors concluded that backpropagation neural networks can provide a useful technique for the analysis of dispersion curves obtained from SASW tests.

In another study, Heiler et al. (1995) tackled the problem of automatic detection of asphalt thickness and depth to reinforcement in composite pavements using neural networks. The authors stated that in the past, GPR interpretation had been done manually by trained engineers and technicians with the aid of standard signal processing techniques. This method of collection produced vast quantities of data, and the interpretation required a great amount of time. Recently, parallel processing, in the form of ANNs, had been applied to the interpretation of GPR condition assessment data from highways. This paper introduced a general strategy for using ANNs for the interpretation of GPR data.

Neural networks were trained to perform an inversion procedure for SASW testing of asphalt concrete pavements (Gucunski and Krstic 1996). The training of the networks was completed by the dispersion curves for individual receiver spacing. Two different models were developed. The first model approach was based on the basis of the average dispersion curve and the second model was based on the individual receiver spacing dispersion curve approach. The results of the comparison of those two models showed that both models have the capability of predicting the shear wave velocities and thicknesses of all the layers with high accuracy except the thickness of the subbase,  $d_3$ . In order to reduce this problem, the authors suggested the use of the individual receiver spacing model,  $V_{s2}/V_{s1} < 1$  ( $V_{s1}$ : shear wave velocity of the AC surface layer;  $V_{s2}$ : shear wave velocity of the bituminous stabilized base course layer) and the average dispersion curve model for higher ratios.

Meier et al. (1997) augmented the WESDEF (Van Cauwelaert et al. 1989) backcalculation program, which minimizes the difference between a calculated basin and the measured basin by adjusting the modulus of the various layers through a series of iterations, by four ANN models trained to compute pavement surface deflections as a function of pavement layer moduli for a wide range of three-layered flexible pavements. The authors noted that WESDEF can backcalculate pavement layer moduli 42 times faster with success than it did before with the addition of the neural networks.

An ANN-based backcalculation procedure has been previously developed for AC over PCC (three-layer) composite pavement systems and has been implemented into a computer program called DIPLOBACK (Khazanovich and Roesler 1997). The pavement layer thicknesses and deflection profiles were given to the model as input variables to predict the  $E_{AC}$  and  $E_{PCC}$  as well as  $k_s$ . Theoretical deflection basins were generated by the DIPLOMAT (Khazanovich and Ioannides 1995) program, which solves AC overlays over PCC as elastic layers over a dense liquid (DL) subgrade, to create an ANN-based procedure to backcalculate  $E_{AC}$ ,  $E_{PCC}$ , and  $k_s$ . The results of backcalculation were compared with the actual elastic parameters of the theoretical deflection basins and good agreement was observed. In addition, the results of the backcalculation using field test data were compared with the results obtained by using WESDEF. Based on the comparison, similar trends were observed for elastic parameters of all three pavement layers.

Kim and Kim (1998) presented a study related to the prediction of layer moduli from FWD tests and surface wave measurements. Based on the observations and investigations in this study, a new modulus prediction algorithm was developed and presented. Hankel transforms were used in this study as a forward model. However, neural networks were used for the inverse process. This

method was applied to the evaluation of two pavement sites in North Carolina and it was concluded that the analysis procedure developed in this study was more sensitive to upper layer conditions and resulted in less variable sub-surface layer moduli.

The capability of ANN models to compute lateral and longitudinal tensile stresses, as well as deflections at the bottom of jointed concrete airfield pavements, as a function of type, level, and location of the applied gear load, slab thickness, slab modulus, subgrade support, pavement temperature gradient, and the load transfer efficiencies of the joints was illustrated by Ceylan et al. (1998, 1999a, 2000) and Ceylan (2002). The training sets were developed for prescribed gear and temperature loads using the ILLI-SLAB (Tabatabaie 1977) finite element program. The findings of these studies proved that ANN models could be successfully trained to capture the complex multidimensional mapping of a large-scale finite element pavement analysis problem in their connection weights and node biases.

Ceylan et al. (1999b) and Ceylan (2004b) trained ANNs to predict stresses and deflections in jointed concrete airfield pavements serving the Boeing B-777 aircraft. The results of the ILLI-SLAB finite element program were used to train the ANN models producing stress and deflections with average errors less than 0.5 percent of those obtained directly from the finite element analyses. The prediction capability of the ANN models appeared to be accurate when predicting the maximum stresses and deflections, slab thicknesses, subgrade supports, and the joint load transfer efficiencies matched exactly on the piecewise continuous functional relations obtained from the training of the models. The authors concluded that trained neural network models will eventually enable pavement engineers to easily incorporate current sophisticated state-of-the-art technology into routine practical analysis and design. In conclusion, the use of ANN as analysis and design tool was demonstrated in these studies by analyzing the concrete airfield pavements serving the Boeing 777 aircraft.

To estimate the elastic modulus of the asphalt concrete layer and the thickness in flexible pavements, Saltan et al. (2002) developed an ANN model. Seven different deflection values obtained from the FWD tests were used as input variables in the ANN model. The authors utilized the asphalt concrete elastic modulus and thickness of asphalt mixture as output variables in the backcalculation type ANN model. Based on the analysis results, Saltan et al. (2002) concluded that the ANNs can be used for backcalculation of the thickness of layers with great improvement and accuracy.

Ceylan and Guclu (2004c) demonstrated the use of ANNs as pavement analysis and design tools by analyzing concrete airfield pavements under the following three loading cases: (1) Airbus A380-800 new generation aircraft (NGA) gear loading only, (2) climatic loading only, and, most importantly, (3) simultaneous aircraft gear and climatic loading. For the three different loading cases, the ANN model predicted maximum bending stresses and deflections with an overall AAE of less than 2.1 percent. The authors concluded that ANNs are capable of successfully predicting the critical responses of a large-scale, nonlinear finite element model. Such ANN models provide invaluable help to pavement engineers for studying the effects of heavy-loading NGA.

In another study, Ceylan et al. (2004a) also investigated the use of the neural network-based structural models for rapid analysis of flexible pavements with unbound aggregate layers. Unlike

the linear elastic layer theory commonly used in pavement layer backcalculation, realistic nonlinear unbound aggregate base (UAB) and subgrade soil modulus models were used in the ILLI-PAVE program—originally developed by Duncan et al. (1968) and further modified by the Department of Civil Engineering at University of Illinois, and Construction Engineering Laboratory and Facilities Group in 1982—to account for the typical stiffening behavior of UABs and the fine-grained subgrade soil moduli decreasing with increasing stress states. The ANN models developed successfully predicted the layer moduli and critical pavement responses computed by the ILLI-PAVE finite element solutions and were much superior to the linear-elastic-layered forward and backcalculation analyses due to the nonlinear material characterization employed. ANN models were designed to predict the elastic modulus of the AC layer and the resilient modulus of the subgrade layer using only four pavement surface deflections,  $D_0$ ,  $D_{12}$ ,  $D_{24}$ , and  $D_{36}$ , and two layer thicknesses: asphalt concrete and granular base-layer thicknesses. The authors concluded that such ANN structural analysis tools can provide pavement engineers and designers with sophisticated finite element solutions, without the need for a high degree of expertise in the input and output of the problem, to rapidly analyze a large number of pavement deflection basins needed for routine pavement evaluation.

Ceylan et al. (2005a) also showed that ANN models could be developed to perform rapid and accurate predictions of flexible pavement layer moduli and critical pavement responses (stresses, strains, and deflections) from FWD deflection basins for a number of pavement input parameters considered in analysis and design. The virgin and the noise-introduced ANN models successfully predicted the pavement layer moduli and critical pavement responses obtained from the ILLI-PAVE finite element solutions, and they were much more superior to the linear elastic layer backcalculation analyses due to the nonlinear material characterization employed. Noise-introduced ANN models have been found to be more robust compared to the models trained with the virgin training data. Such ANN models provided more realistic predictions of pavement layer moduli and critical pavement responses because of their ability to tolerate the inaccuracies in the actual pavement deflection basins from field data and the layer thicknesses due to poor construction practices.

Seven ANN-based backcalculation and forward calculation models, using approximately 26,000 nonlinear ILLI-PAVE finite element solutions for the full-depth (FD) and conventional flexible pavements (CFPs), were developed by Ceylan et al. (2005b). In this study, six CFP sections were selected to further evaluate the performances of the ANN backcalculation models. ANN models predicted the layer moduli and critical pavement responses computed by the ILLI-PAVE finite element solutions and were much superior to the linear elastic layer forward and backcalculation analyses due to the nonlinear material characterization employed.

ANN-based backcalculation and forward calculation pavement structural models were developed in another study (Ceylan et al. 2005c) using the ILLI-PAVE 2000 full-depth asphalt finite element solutions with nonlinear, stress-dependent subgrade soil properties. The authors concluded that ANNs were capable of mapping complex relationships, such as those studied in complex finite element analyses, between the input parameters and the output variables for nonlinear, stress-dependent systems. ANN models could rapidly (50,000 analyses in less than a second) output the required solutions in analyzing a large number of pavement deflection basins needed for routine pavement evaluation. The rapid prediction ability of the ANN backcalculation models made them perfect evaluation tools for analyzing the FWD deflection data and assessing

the condition of the pavement sections in real time for both project-specific and network-level FWD testing.

In another work (Rakesh et al. 2006), ANN models have been developed for computing surface deflections using elastic moduli and thicknesses of pavement layers as inputs. The ANN models have been used in BACKGA (developed by the Indian Institute of Technology) for forward calculation of surface deflections to combine the computational efficiency of ANNs with the robustness of the genetic algorithms. The authors stated that the performance of the resulting model, BACKGA-ANN, has been evaluated and found to be satisfactory.

Goktepe et al. (2006) analyzed the role of learning algorithms and ANN architecture in ANN-based backcalculation of flexible pavements. In this study, 284 different ANN models were developed using synthetic training and testing databases obtained by layered elastic theory. Results indicated that both the learning algorithm and network architecture play important roles in the performance of the ANN-based backcalculation process to reach realistic results. Recently, Ceylan et al. (2007) successfully studied the TRB Nonlinear Pavement Analysis Project data sets using ANN-based, stress-dependent flexible pavement structural models.

## ARTIFICIAL NEURAL NETWORKS – A BRIEF REVIEW

A suite of ANN-based backcalculation and forward response prediction models based on FWD test data were developed in this study. The detailed information related to the developed ANN-based backcalculation models are given in the next sections. The Backpropagation (BP) training algorithm was employed in developing the neural network structural models. In the following sections, an in-depth review of the ANN and backpropagation algorithm is provided.

### ANNs

Imitating the biological nervous system, ANNs are information processing computational tools capable of solving nonlinear relations in a specific problem. Similar to the human brain, ANNs have the flexibility to learn from examples by means of massively interconnected processing units, namely neurons. Neural network architectures, arranged in layers, involve synaptic connections amid neurons that receive signals and transmit them to other neurons via activation functions. Each connection has its own connection weight and learning is the process of adjusting the connection weights between neurons to minimize the error between the predicted and given values. In the learning process, node biases are also adjusted in addition to the connection weights. Because interconnected neurons have the flexibility to adjust the weights, neural networks have powerful capacities in analyzing complex problems. ANNs, inspired by the neuronal architecture and operation of the human brain, contribute to our understanding of several complex, nonlinear pavement engineering problems with various pavement materials and pavement foundation variables. Figure 3 displays a typical structure of ANNs that consists of a number of neurons that are usually arranged in layers: an input layer, hidden layers, and an output layer.

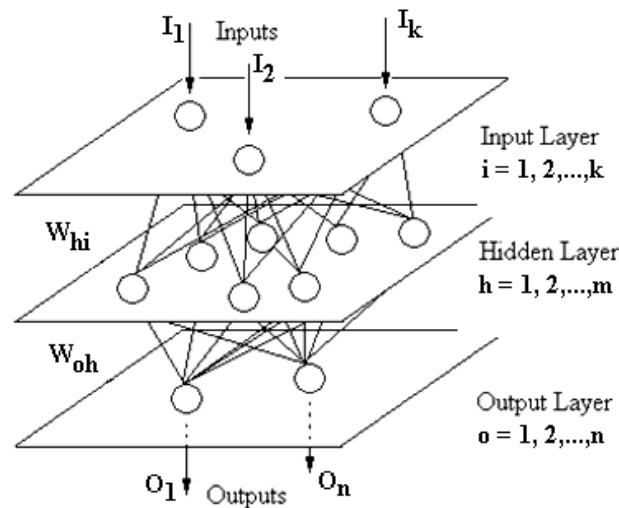


Figure 3. A general view of the ANNs

There are several different types of ANNs such as backpropagation neural networks (BPNN), radial basis function neural networks (RBFNN), probabilistic neural networks (PNN), and generalized regression neural networks (GRNN). Computing abilities of neural networks have been proven in the fields of prediction and estimation, pattern recognition, and optimization (Adeli and Hung 1995; Golden 1996; Mehrotra et al. 1997; Adeli and Park 1998; Haykin 1999). The best known example of a neural network training algorithm is backpropagation (Rumelhart et al. 1986; Haykin 1994; Fausett 1994; Patterson 1996), which is based on a gradient-descent optimization technique. The backpropagation neural networks have been described in many sources (Hegazy et al. 1994; Adeli and Hung 1995; Mehrotra et al. 1997; Topping and Bahreininejad 1997; Haykin 1999).

ANNs provide an analytical alternative to conventional techniques often limited by strict assumptions of normality, linearity, and variable independence. Because an ANN can capture many kinds of relationships, it allows the user to quickly and relatively easily model a phenomenon that may have otherwise been very difficult. Neural networks offer a number of advantages, including requiring less formal statistical training, the ability to implicitly detect complex nonlinear relationships between dependent and independent variables, the ability to detect all possible interactions between predictor variables, and the availability of multiple training algorithms. By simulating the human brain, neural networks are capable of learning from examples (learning ability), can perform nonlinear multidimensional mapping (nonlinearity), can memorize the patterns and restore the incomplete patterns (memorization), and can adapt themselves to the environment by virtue of learning (adaptivity). In order to construct a neural network to solve a particular problem, three components need to be determined first, including architecture, learning method, and neuron activation function.

### *Architecture*

One of the most important issues in the development of an ANN model is the architecture. Determination of the input and output variables, number of hidden layers, and number of hidden neurons in each hidden layer is crucial in the development part of the ANN models. The architecture of an ANN model has significant effects on the success of the developed models. Usually, a neural network with too few hidden neurons is unable to learn sufficiently from the training data set, whereas a neural network with too many hidden neurons will allow the network to memorize the training set instead of generalizing the acquired knowledge for unseen patterns (Lawrence and Fredricson 1993). Haykin (1994) recommends using two hidden layers—the first one for extracting local features and the second one for extracting global features. In addition, satisfactory results were obtained in the previous studies with these types of networks because of their ability to better facilitate the nonlinear functional mapping (Ceylan 2002; Ceylan et al. 2005b; Ceylan et al. 2005c). Thus, a network with two hidden layers was exclusively chosen for all ANN models trained in this study. However, trial and error is conventionally employed to select the appropriate number of hidden neurons in the hidden layer for the problem under investigation due to the still vague understanding of the impacts of the variation of ANN architecture.

## *Learning Method*

Many computational models can be described as functions mapping some numerical input vectors to numerical outputs. The outputs corresponding to some input vectors may be known from training data, but we may not know the mathematical function describing the actual process that generates the outputs from the input vectors. Function approximation is the task of learning or constructing a function based on available training data that generates approximately the same outputs from input vectors as the process being modeled.

At a high level, the tasks performed using neural networks can be classified as those requiring supervised or unsupervised learning. In supervised learning, a teacher is available to indicate whether a system is performing correctly, or to indicate a desired response, or to validate the acceptability of a system's responses, or to indicate the amount of error in system performance. This is in contrast with unsupervised learning, where no teacher is available and learning must rely on guidance obtained heuristically by the system examining different sample data or the environment. A concrete example of supervised learning is provided by classification problems, whereas clustering provides an example of unsupervised learning (Mehrotra et al. 1997). The backpropagation method, which was used in this research, falls into the category of supervised learning. It is one of the most popular learning methods for multiple-layer neural networks.

Backpropagation ANNs are very powerful and versatile networks that can be taught a mapping from one data space to another using a representative set of patterns/examples to be learned. The term "backpropagation network" actually refers to a multilayered, feed-forward neural network trained using an error backpropagation algorithm. The learning process performed by this algorithm is called "backpropagation learning," which is mainly an "error minimization technique" (see Haykin 1999; Hecht-Nielsen 1990; Parker 1985; Rumelhart et al. 1986; and Werbos 1974).

In the development of backpropagation ANN models, the connection weights and node biases are initially selected at random. Inputs from the mapping examples are propagated forward through each layer of the network to emerge as outputs. The errors between those outputs and the correct answers are then propagated backwards through the network and the connection weights and node biases are individually adjusted to reduce the error. After many examples (training patterns) are propagated through the network many times, the mapping function is learned with some specified error tolerance. This is called supervised learning because the network has adjusted functional mapping using the correct answers. Backpropagation ANNs excel at data modeling with their superior function approximation (Haykin 1999; Meier and Tutumluer 1998).

## ANN MODELS FOR CFP SYSTEMS

ELPs used in asphalt pavement analysis assume linear elasticity. Pavement geomaterials do not, however, follow a linear-type, stress-strain behavior under repeated traffic loading. In effect, the nonlinear stress-sensitive response of unbound aggregate materials and fine-grained subgrade soils has been well established (Brown and Pappin 1981; Thompson and Elliott 1985; Garg et al. 1998). Unbound aggregates exhibit stress hardening and fine-grained soils show stress-softening-type behavior. When these geomaterials are used as pavement layers, the layer stiffness, i.e., moduli, is no longer constant but functions as part of the applied stress state. Pavement structural analysis programs that take into account nonlinear geomaterial characterization, such as the ILLI-PAVE finite element program (Raad and Figueroa, 1980), need to be employed to more realistically predict pavement response needed for mechanistic-based pavement design.

In the field, the pavement deflection profiles are obtained from FWD measurements, which require the use of backcalculation-type structural analysis to determine pavement layer stiffness. Although ANN modeling was used in the past to aid in backcalculation (Meier and Rix 1995), the structural models used to train the ANN models did not account for realistic stress sensitive geomaterial properties. For this reason, the ILLI-PAVE finite element program, considering the nonlinear, stress-dependent geomaterial characterization, was utilized to generate a solution database for developing ANN-based structural models to accurately predict pavement deflection basins and pavement layer moduli from realistic FWD deflection profiles.

### Nonlinear Geomaterial Characterization

Considering increased serviceability and performance requirements of today's pavements, the field stress states, repeated application of moving traffic loads, field temperature, and moisture are among the most important factors to be correctly accounted for in pavement structural analysis. Under the repeated application of moving traffic loads, most of the deformations are recoverable and thus considered elastic. It has been customary to use resilient modulus ( $M_R$ ) for the elastic stiffness of the pavement materials, defined as the repeatedly applied wheel load stress divided by the recoverable strain determined after shakedown of the material. Repeated load triaxial tests are commonly employed to evaluate the resilient properties of unbound aggregate materials and cohesive subgrade soils. Therefore, emphasis should be given in structural pavement analysis to realistic nonlinear material modeling in the base/subbase and subgrade layers primarily based on repeated load triaxial test results (AASHTO T307-99, European CEN Std EN 13286-7).

Simple resilient modulus models, such as the K- $\theta$  (Hicks and Monismith 1971), Uzan (1985), and the Universal models (Uzan et al. 1992), consider the effects of stress dependency for modeling the nonlinear behavior of base/subbase aggregates. Given as follows, these models are generally suitable for finite element programming and practical design use:

$$\text{K-}\theta \text{ Model (Hicks and Monismith, 1971): } M_R = K \left( \theta / p_o \right)^n \quad (1)$$

$$\text{Uzan Model (Uzan, 1985): } M_R = K_1 \left(\frac{\theta}{p_o}\right)^{K_2} \left(\frac{\sigma_d}{p_o}\right)^{K_3} \quad (2)$$

$$\text{Universal Model (Uzan et al., 1992): } M_R = K_4 \left(\frac{\theta}{p_o}\right)^{K_5} \left(\frac{\tau_{oct}}{p_o}\right)^{K_6} \quad (3)$$

where  $\theta = \sigma_1 + \sigma_2 + \sigma_3 = \sigma_1 + 2\sigma_3 =$  bulk stress,  $\sigma_d = \sigma_1 - \sigma_3 =$  deviator stress,  $\tau_{oct} =$  octahedral shear stress  $= \sqrt{2/3} * \sigma_d$  in triaxial conditions,  $p_0$  is the unit reference pressure (1 kPa or 1 psi) used in the models to make the stresses non-dimensional, and  $K, n,$  and  $K_1$  to  $K_6$  are multiple regression constants obtained from repeated load triaxial test data on granular materials.

Figure 4 shows for two different-sized granular materials, crushed stone and sand, typical nonlinear resilient modulus characterizations obtained from AASHTO T307-99 test results using the  $K$ - $\theta$  and Uzan type models. The simpler  $K$ - $\theta$  model often adequately captures the overall stress dependency (bulk stress effects) of unbound aggregate behavior under compression-type field loading conditions. The Uzan (1985) model additionally considers the effects of deviator stresses and handles very well the modulus increase with increasing shear stresses even for extension-type field loading conditions. A more recent universal model (Uzan et al. 1992) also accounts for the stress dependency of the resilient behavior as power functions of the 3-D stress states.

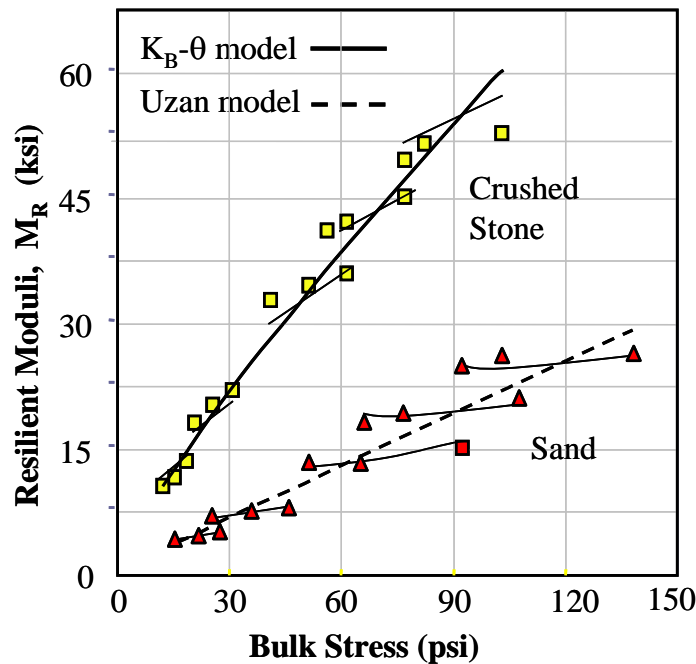


**Figure 4. Typical nonlinear modulus characterization of unbound aggregate materials**

The resilient modulus of fine-grained subgrade soils is also dependent upon the stress state. Typically, soil modulus decreases in proportion to the increasing stress levels, thus exhibiting stress-softening-type behavior. As a result, the most important parameter affecting the resilient modulus becomes the vertical deviator stress on top of the subgrade due to the applied wheel load. The bilinear or arithmetic model (Thompson and Elliot 1985) is the most commonly used

resilient modulus model for subgrade soils expressed by the modulus-deviator stress relationship given in Figure 5. As indicated by Thompson and Elliot (1985), the value of the resilient modulus at the breakpoint in the bilinear curve,  $E_{Ri}$ , (see Figure 5), can be used to classify fine-grained soils as being soft, medium, or stiff.

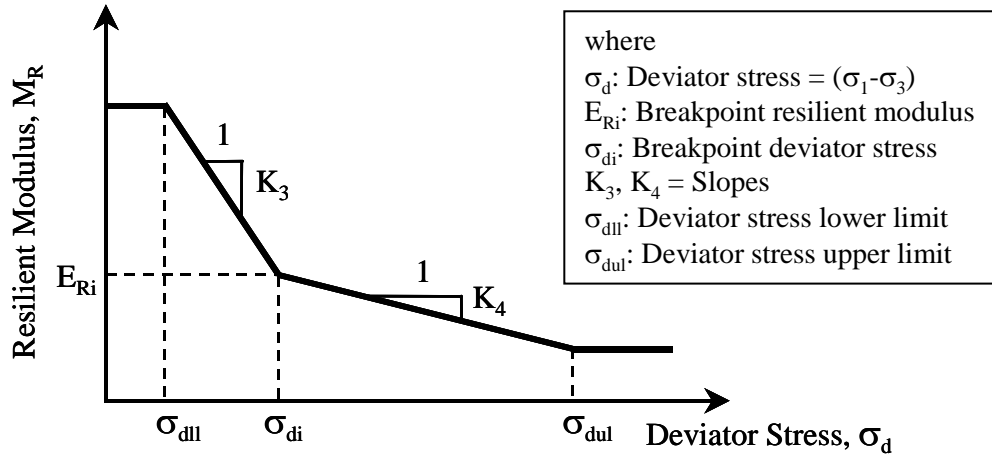


**Figure 5. Stress dependency of fine-grained soils characterized by bilinear model**

### ILLI-PAVE Finite Element Program

ILLI-PAVE is an axisymmetric finite element program commonly used in the structural analysis of flexible pavements. Most of the nonlinear, stress-dependent resilient modulus material models summarized in the previous section, and failure criteria for granular materials and fine-grained soils, are already incorporated into the finite element model. Granular materials are considered “stress hardening” (modulus increases as stress increases) and fine-grained soils are “stress-softening” (modulus decreases as stress increases). The principal stresses in the granular material and fine-grained soil layers are modified at the end of each iterative solution under the application of a single wheel loading such that they do not exceed their shear strength as defined by the Mohr-Coulomb theory of failure.

ILLI-PAVE was developed at the University of Illinois (Raad and Figueroa 1980) based on the finite element code used by Duncan et al. (1968) for highway pavement analysis. Since then, numerous research studies have demonstrated that the ILLI-PAVE model provides a realistic pavement structural response prediction for highway and airfield pavements (Thompson and Elliot 1985; Gomez-Achecar and Thompson 1986; Thompson 1992; Garg et al. 1998). Recent research studies at the Federal Aviation Administration’s (FAA) Center of Excellence established at the University of Illinois also supported the development of a new, updated version of the program, now known as the ILLI-PAVE 2000 (Gomez-Ramirez et al. 2002). Among the several modifications implemented in the new ILLI-PAVE 2000 finite element code were: (1) an increased number of elements (degrees of freedom); (2) new/updated material models for the granular materials and subgrade soils; (3) enhanced iterative solution methods;

(4) Fortran 90 Standard coding and compilation; and, (5) a new user-friendly Microsoft Visual Basic pre-/post-processing interface to assist in the analysis.

Analyses of flexible pavement systems were pursued under two subcategories: (1) analysis of CFPs, and (2) analysis of full-depth flexible pavements. For each category, a number of ILLI-PAVE-based ANN models were developed. The ANN-based methodology and model performances are described in the following subsections. A schematic tree representing the suite of ANN models developed for the analyses of flexible pavement systems is depicted in Figure 6.

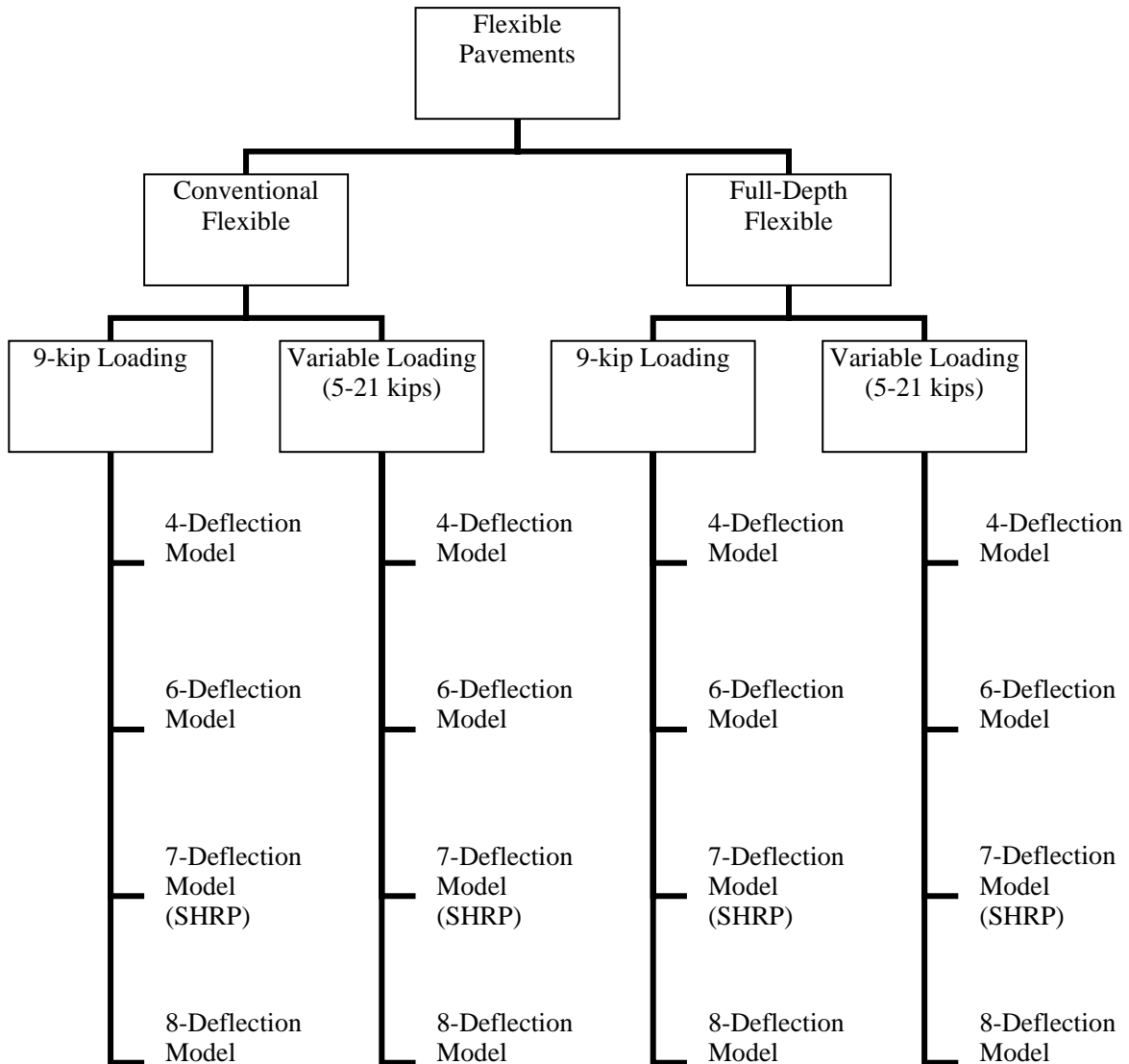


**Figure 6. ILLI-PAVE-based ANN backcalculation models for flexible pavements**

The ILLI-PAVE 2000 finite element program was used as the main validated nonlinear structural model for analyzing different geometries of flexible pavements with unbound aggregate bases (CFPs). The goal was to establish a database composed of pavement and loading input properties together with the corresponding ILLI-PAVE response solutions that would eventually constitute the training and testing data sets needed in the development of ANN-based structural models for the rapid forward and backcalculation analysis of flexible pavements with unbound aggregate bases. For this purpose, a convergence study was performed to determine the domain size extent for the finite element mesh discretization. The results indicated that a radial boundary placed at 30 times the contact area radius was sufficient to obtain convergence of deflections.

The top surface asphalt course was characterized as a linear elastic material with Young's Modulus,  $E_{AC}$ , and Poisson ratio,  $\mu$ . Due to its simplicity and ease in model parameter evaluation, the K- $\theta$  model (Hicks and Monismith 1971) was used as the nonlinear characterization model for the unbound aggregate layer. Based on the work of Rada and Witczak (1981) with a comprehensive granular material database, "K" and "n" model parameters can be correlated to characterize the nonlinear stress dependent behavior with only one model parameter using the following equation (Rada and Witczak 1981):

$$\text{Log}_{10}(K) = 4.657 - 1.807 \cdot n \quad R^2 = 0.68; \text{SEE} = 0.22 \quad (4)$$

According to Equation 4, good, quality granular materials show higher K and lower n values, whereas the opposite applies for low-quality granular materials. For the ILLI-PAVE runs and the ANN training/testing data generation, the K-value ranged from 3 ksi to 12 ksi and the corresponding n-value was obtained using the relationship in Equation 4. For Mohr-Coulomb strength characterization, all granular materials were assumed to have no cohesion (i.e.,  $c = 0$ ), and the friction angle  $\phi$ -values were entered in accordance with the quality level of the K-value.

Fine-grained soils were considered as "no-friction", but cohesion-only materials and modeled using the bilinear or arithmetic model (see Figure 5) for modulus characterization. The breakpoint deviator stress,  $E_{Ri}$ , was the main input for subgrade soils. The  $K_3$  and  $K_4$  slopes shown in Figure 5 were taken as constants, 1,100 and 200, respectively, corresponding to medium soils given by Thompson and Elliott (1985). According to a comprehensive Illinois subgrade soil study by Thompson and Robnett (1979), the breakpoint deviator stress,  $\sigma_{di}$ , was taken as 6 psi and 2 psi was used for the lower limit deviator stress,  $\sigma_{dli}$ . The soil's unconfined compressive strength,  $Q_u$ , or cohesion, was used to determine the upper limit deviator stress,  $\sigma_{duli}$ , (see Figure 5) as a function of the breakpoint deviator stress,  $E_{Ri}$ , using the following relationship (Thompson and Robnett, 1979):

$$\sigma_{duli}(\text{psi}) = 2 \times \text{cohesion}(\text{psi}) = Q_u(\text{psi}) = \frac{E_{Ri}(\text{ksi}) - 0.86}{0.307} \quad (5)$$

Therefore, asphalt concrete modulus,  $E_{AC}$ , granular base  $K$ - $\theta$  model parameter  $K$ , and the subgrade soil break point deviator stress,  $E_{Ri}$ , in the bilinear model were used as the layer stiffness inputs for all the different CFP geometries, i.e., layer thicknesses, analyzed using the ILLI-PAVE 2000 finite element program. The thickness and moduli ranges used are summarized in Table 1. Either a constant 9-kip wheel load was applied as a uniform pressure of 80 psi over a circular area of radius 6 inches or variable load was applied as uniform pressure ranged between 44 psi and 186 psi (5 and 21 kips loaded over a circular area of radius 6 inches).

**Table 1. Pavement geometry and material property/model inputs of CFPs for ILLI-PAVE solutions**

| Material Type          | Layer Thickness                        | Material Model                 | Layer Modulus Inputs  |
|------------------------|--|--------------------------------|---|
| Asphalt Concrete       | $h_{AC} = 3$ to 28 in.                 | Linear Elastic                 | $E_{AC} = 100$ to 6,000 ksi   |
| Unbound Aggregate Base | $h_{GB} = 4$ to 22 in.                 | Nonlinear $K$ - $\theta$ model | $M_R = K\theta^n$<br>“ $K$ ” = 3 to 12 ksi<br>“ $n$ ” from Equation 4 |
| Fine-grained Subgrade  | 300 in. minus total pavement thickness | Nonlinear Bilinear Model       | $M_R = f(E_{Ri})$ ; see Figure 5<br>$E_{Ri} = 1$ to 15 ksi            |

### Generating ILLI-PAVE Finite Element Solution Database

A total of 30,000 ILLI-PAVE finite element runs were conducted by randomly choosing the flexible pavement layer thicknesses and input variables within the given ranges in Table 1 to generate a knowledge database for ANN trainings. The finite element mesh used for generating the ILLI-PAVE analyses is shown in

Figure 7. An adaptive mesh was used; i.e., the total number of nodes and elements for each analysis were varied based on the thicknesses of the AC and the base layers. AC layer constraints for adaptive mesh generation are shown in Table 2. Granular base layer is divided into  $h_{GB}/2$  layers. The total analysis depth of the pavement system was taken as 300 inches. The subgrade thicknesses were calculated by subtracting the thicknesses of the AC and the base layers (for CFP) from the total analysis depth.

Figure 7 illustrates the finite element mesh for the example CFP system with a four-inch AC layer and 12-inch granular base with 9-kip loading. The location of the tire loading of 80 psi on the pavement surface is shown in

Figure 7. Choosing consistent meshes for generating accurate finite element solutions was previously highlighted as a necessity by Ceylan (2002) in order to successfully train ANN structural analysis models.

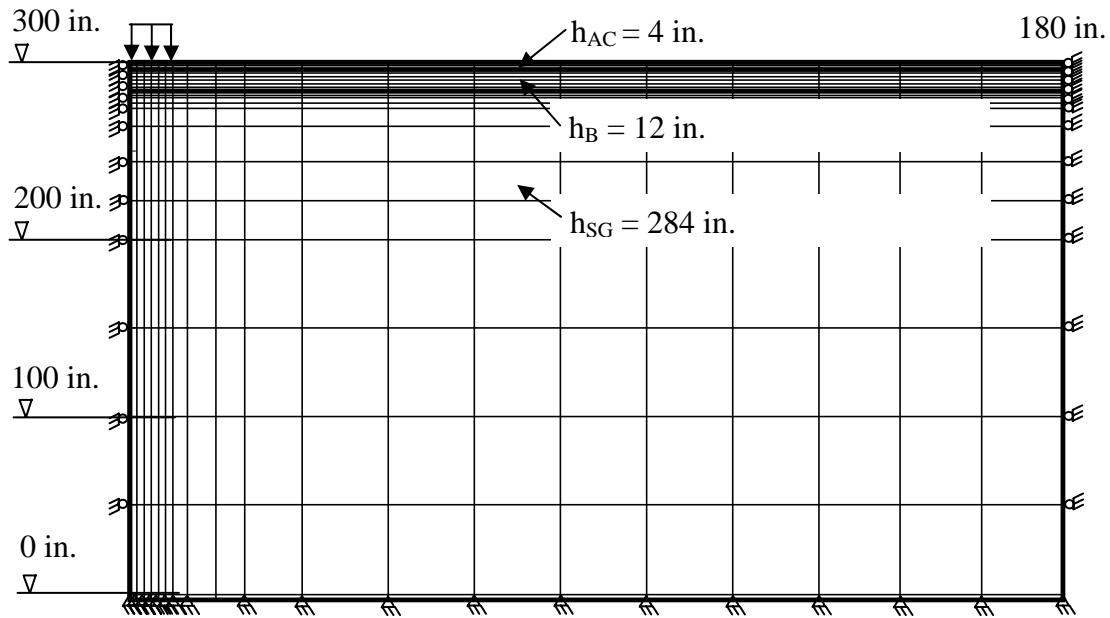


**Figure 7. Pavement geometry and finite element mesh used for the ILLI-PAVE runs**

**Table 2. Mesh constraints for AC layer**

| AC Layers     | Number of Layers<br>AC Layer Divided |
|---------------|--------------------------------------|
| $h_{AC} < 4$  | 3                                    |
| $h_{AC} < 7$  | 4                                    |
| $h_{AC} < 9$  | 5                                    |
| $h_{AC} < 11$ | 6                                    |
| $h_{AC} < 13$ | 7                                    |
| $h_{AC} < 16$ | 8                                    |
| $h_{AC} < 19$ | 9                                    |
| $h_{AC} < 22$ | 10                                   |
| $h_{AC} < 25$ | 11                                   |
| $h_{AC} < 28$ | 12                                   |
| $h_{AC} < 30$ | 13                                   |

The ILLI-PAVE finite element analyses were performed in the following manner. For each ILLI-PAVE run, the input variables for pavement thicknesses ( $h_{AC}$ ,  $h_B$ ),  $E_{AC}$ , base-layer K value of the  $K-\theta^n$  model, and the subgrade layer  $E_{Ri}$  value were recorded along with the pavement surface deflection basin and the critical pavement responses, radial strain at the bottom of the AC layer ( $\epsilon_{AC}$ ), vertical strain on top of the subgrade ( $\epsilon_{SG}$ ), and the  $\sigma_D$ . AC layer thicknesses were kept between 3 and 28 inches, and base layer thicknesses were varied between 4 and 22 inches to

consider typical flexible pavement design geometries. Similarly, the moduli ranges of the pavement layers given in Table 1 were selected in a way to represent the most commonly used flexible pavement material properties in practice.

In order to backcalculate the  $E_{AC}$ ,  $E_{Ri}$  and  $K_B$  values for the CFPs, different ANN models have been developed with different combinations of input parameters. The FWD surface deflections ( $D_0$ ,  $D_8$ ,  $D_{12}$ ,  $D_{18}$ ,  $D_{24}$ ,  $D_{36}$ ,  $D_{48}$ , and  $D_{60}$ ) were often collected at several different locations, at the drop location (0) and at radial offsets of 8 inches (203 mm), 12 inches (254 mm), 18 inches (457 mm), 24 inches (610 mm), 36 inches (914 mm), 48 inches (1219 mm), 60 inches (1524 mm), and 72 inches (1829 mm). The deflection parameters obtained from the FWD test are  $D_0$ ,  $D_8$ ,  $D_{12}$ ,  $D_{18}$ ,  $D_{24}$ ,  $D_{36}$ ,  $D_{48}$ , and  $D_{60}$  (

Figure 8). According to the results of sensitivity analyses illustrated in Figure 9 to Figure 11 below, correlation of deflections with pavement layer moduli values varied depending on the sensor offset distance. Therefore, ANN models were developed with different combinations of deflection inputs. This is because all the deflection parameters may not always be available and to also determine the optimum number of deflection inputs necessary to yield accurate predictions. ANN models with four deflections ( $D_0$ ,  $D_{12}$ ,  $D_{24}$ , and  $D_{36}$ ), six deflections ( $D_0$ ,  $D_{12}$ ,  $D_{24}$ ,  $D_{36}$ ,  $D_{48}$ ,  $D_{60}$ ), seven deflections ( $D_0$ ,  $D_8$ ,  $D_{12}$ ,  $D_{18}$ ,  $D_{24}$ ,  $D_{36}$ , and  $D_{60}$ ), and eight deflections ( $D_0$ ,  $D_8$ ,  $D_{12}$ ,  $D_{18}$ ,  $D_{24}$ ,  $D_{36}$ ,  $D_{48}$ , and  $D_{60}$ ) were successfully developed.

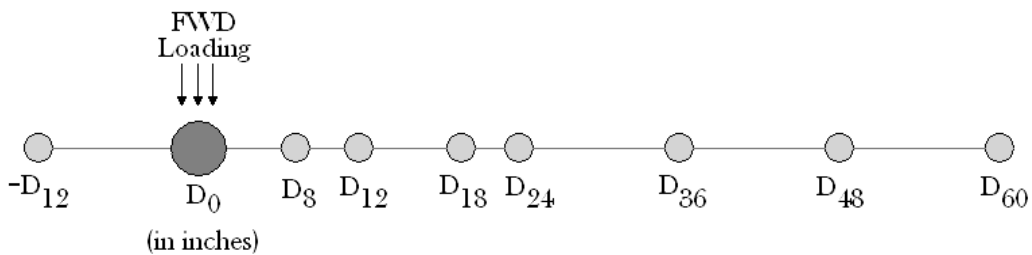


**Figure 8. Iowa DOT FWD (JILS-20) sensor configuration**

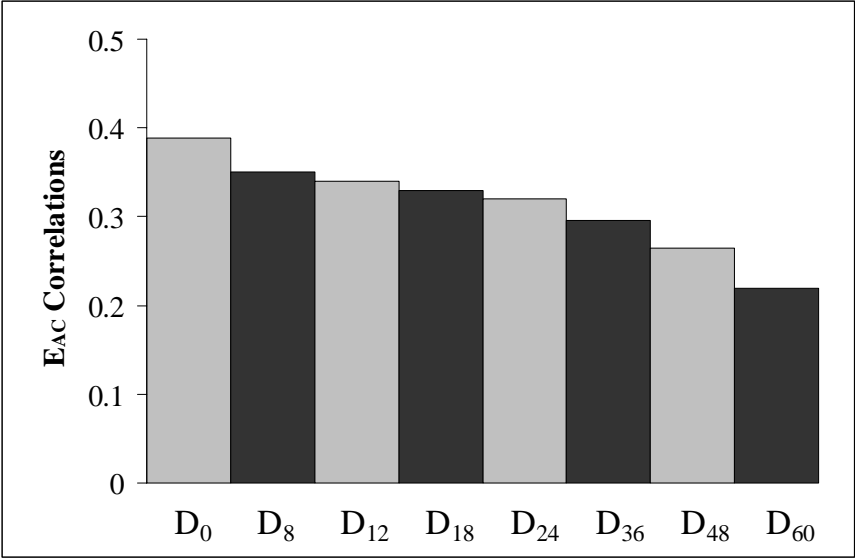


**Figure 9. E<sub>AC</sub> correlation with deflections (CFP)**

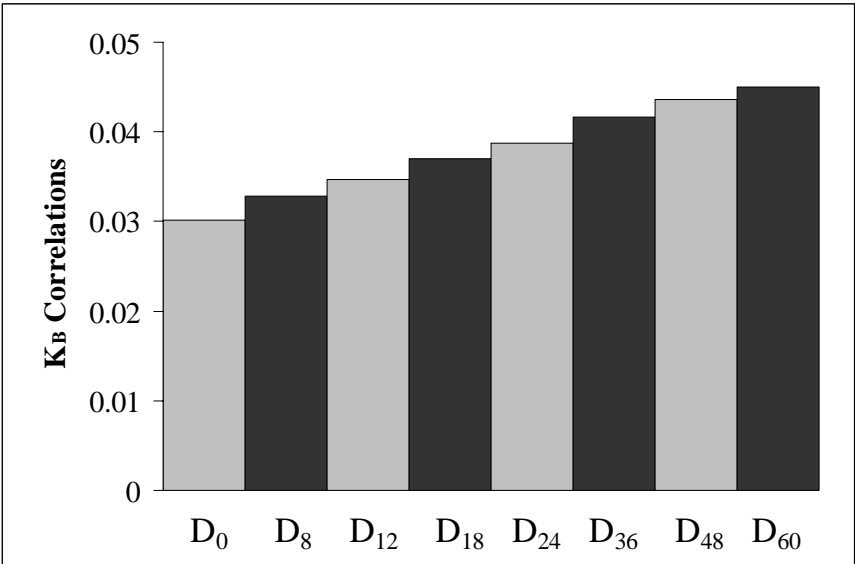


**Figure 10. K<sub>B</sub> correlation with deflections (CFP)**

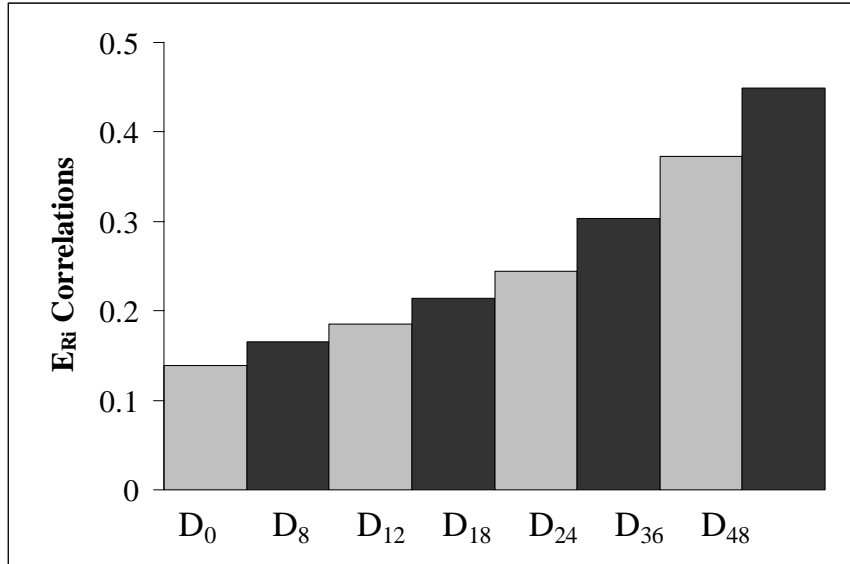


**Figure 11. E<sub>Ri</sub> correlation with deflections (CFP)**

### ANN-Based CFP Backcalculation Models

Backpropagation-type neural networks were used to develop ANN structural models with different network architectures for predicting the pavement layer moduli ( $E_{AC}$ ,  $K$ , and  $E_{Ri}$ ). For the modeling work, surface deflections at the FWD sensor radial offsets were obtained from the ILLI-PAVE results.

The backcalculation models were first developed based on the necessary number of deflection inputs determined by correlations shown in Figure 9 to Figure 11. As mentioned previously, four different deflection-based backcalculation models were developed: four-, six-, seven-, and eight-deflection ANN models. Second, each of these models was separately used to predict  $E_{AC}$  of the AC layer, the  $E_{Ri}$  value of the subgrade layer, and  $K$  of granular base. Finally, for each model, two sub-models were developed by FWD load level. The developed models were either for 9-kip FWD loading or for 5- to 21-kip FWD loading (varying FWD load level). A summary of all ANN models developed for CFP systems is shown in Table 3. A total of 1,500 data sets out of a 30,000 ILLI-PAVE solution database were set aside as an independent testing set to validate the performance of the trained ANN model. Neural network architecture with two hidden layers was exclusively chosen for the CFP models developed in this study. This was in accordance with the satisfactory results obtained previously with these types of networks because of their ability to better facilitate the nonlinear functional mapping (Ceylan 2002).

Several network architectures with two hidden layers were trained for predicting the properties of the pavement layer moduli with one output node. Overall, the training and testing mean-square errors (MSEs) decreased as the networks grew in size with an increasing number of neurons in the hidden layers. The error levels for both the training and testing sets matched closely when the number of hidden nodes approached 60, as in the case of the X-60-60-1 architecture (X inputs, 60 hidden nodes, and 1 output node).

**Table 3. Summary of CFP-ANN backcalculation models**

| <b>Model</b>                              | <b>Inputs</b>   | <b>Output</b>   |
|---|---|-----------------|
| <b>CFP-E<sub>AC</sub>-(4)-(9-kip)</b>     | D <sub>0</sub> , D <sub>12</sub> , D <sub>24</sub> , D <sub>36</sub> , h <sub>AC</sub> , h <sub>B</sub>   | E <sub>AC</sub> |
| <b>CFP-E<sub>AC</sub>-(6)-(9-kip)</b>     | D <sub>0</sub> , D <sub>12</sub> , D <sub>24</sub> , D <sub>36</sub> , D <sub>48</sub> , D <sub>60</sub> , h <sub>AC</sub> , h <sub>B</sub>   | E <sub>AC</sub> |
| <b>CFP-E<sub>AC</sub>-(7)-(9-kip)</b>     | D <sub>0</sub> , D <sub>8</sub> , D <sub>12</sub> , D <sub>18</sub> , D <sub>24</sub> , D <sub>36</sub> , D <sub>60</sub> , h <sub>AC</sub> , h <sub>B</sub>                                      | E <sub>AC</sub> |
| <b>CFP-E<sub>AC</sub>-(8)-(9-kip)</b>     | D <sub>0</sub> , D <sub>8</sub> , D <sub>12</sub> , D <sub>18</sub> , D <sub>24</sub> , D <sub>36</sub> , D <sub>48</sub> , D <sub>60</sub> , h <sub>AC</sub> , h <sub>B</sub>                    | E <sub>AC</sub> |
| <b>CFP-E<sub>Ri</sub>-(4)-(9-kip)</b>     | D <sub>0</sub> , D <sub>12</sub> , D <sub>24</sub> , D <sub>36</sub> , h <sub>AC</sub> , h <sub>B</sub>   | E <sub>Ri</sub> |
| <b>CFP-E<sub>Ri</sub>-(6)-(9-kip)</b>     | D <sub>0</sub> , D <sub>12</sub> , D <sub>24</sub> , D <sub>36</sub> , D <sub>48</sub> , D <sub>60</sub> , h <sub>AC</sub> , h <sub>B</sub>   | E <sub>Ri</sub> |
| <b>CFP-E<sub>Ri</sub>-(7)-(9-kip)</b>     | D <sub>0</sub> , D <sub>8</sub> , D <sub>12</sub> , D <sub>18</sub> , D <sub>24</sub> , D <sub>36</sub> , D <sub>60</sub> , h <sub>AC</sub> , h <sub>B</sub>                                      | E <sub>Ri</sub> |
| <b>CFP-E<sub>Ri</sub>-(8)-(9-kip)</b>     | D <sub>0</sub> , D <sub>8</sub> , D <sub>12</sub> , D <sub>18</sub> , D <sub>24</sub> , D <sub>36</sub> , D <sub>48</sub> , D <sub>60</sub> , h <sub>AC</sub> , h <sub>B</sub>                    | E <sub>Ri</sub> |
| <b>CFP-K<sub>B</sub>-(4)-(9-kip)</b>      | D <sub>0</sub> , D <sub>12</sub> , D <sub>24</sub> , D <sub>36</sub> , h <sub>AC</sub> , h <sub>B</sub>   | K <sub>B</sub>  |
| <b>CFP-K<sub>B</sub>-(6)-(9-kip)</b>      | D <sub>0</sub> , D <sub>12</sub> , D <sub>24</sub> , D <sub>36</sub> , D <sub>48</sub> , D <sub>60</sub> , h <sub>AC</sub> , h <sub>B</sub>   | K <sub>B</sub>  |
| <b>CFP-K<sub>B</sub>-(7)-(9-kip)</b>      | D <sub>0</sub> , D <sub>8</sub> , D <sub>12</sub> , D <sub>18</sub> , D <sub>24</sub> , D <sub>36</sub> , D <sub>60</sub> , h <sub>AC</sub> , h <sub>B</sub>                                      | K <sub>B</sub>  |
| <b>CFP-K<sub>B</sub>-(8)-(9-kip)</b>      | D <sub>0</sub> , D <sub>8</sub> , D <sub>12</sub> , D <sub>18</sub> , D <sub>24</sub> , D <sub>36</sub> , D <sub>48</sub> , D <sub>60</sub> , h <sub>AC</sub> , h <sub>B</sub>                    | K <sub>B</sub>  |
| <b>CFP-E<sub>AC</sub>-(4)-(5-21 kips)</b> | D <sub>0</sub> , D <sub>12</sub> , D <sub>24</sub> , D <sub>36</sub> , h <sub>AC</sub> , h <sub>B</sub> , P <sub>FWD</sub>  | E <sub>AC</sub> |
| <b>CFP-E<sub>AC</sub>-(6)-(5-21 kips)</b> | D <sub>0</sub> , D <sub>12</sub> , D <sub>24</sub> , D <sub>36</sub> , D <sub>48</sub> , D <sub>60</sub> , h <sub>AC</sub> , h <sub>B</sub> , P <sub>FWD</sub>                                    | E <sub>AC</sub> |
| <b>CFP-E<sub>AC</sub>-(7)-(5-21 kips)</b> | D <sub>0</sub> , D <sub>8</sub> , D <sub>12</sub> , D <sub>18</sub> , D <sub>24</sub> , D <sub>36</sub> , D <sub>60</sub> , h <sub>AC</sub> , h <sub>B</sub> , P <sub>FWD</sub>                   | E <sub>AC</sub> |
| <b>CFP-E<sub>AC</sub>-(8)-(5-21 kips)</b> | D <sub>0</sub> , D <sub>8</sub> , D <sub>12</sub> , D <sub>18</sub> , D <sub>24</sub> , D <sub>36</sub> , D <sub>48</sub> , D <sub>60</sub> , h <sub>AC</sub> , h <sub>B</sub> , P <sub>FWD</sub> | E <sub>AC</sub> |
| <b>CFP-E<sub>Ri</sub>-(4)-(5-21 kips)</b> | D <sub>0</sub> , D <sub>12</sub> , D <sub>24</sub> , D <sub>36</sub> , h <sub>AC</sub> , h <sub>B</sub> , P <sub>FWD</sub>  | E <sub>Ri</sub> |
| <b>CFP-E<sub>Ri</sub>-(6)-(5-21 kips)</b> | D <sub>0</sub> , D <sub>12</sub> , D <sub>24</sub> , D <sub>36</sub> , D <sub>48</sub> , D <sub>60</sub> , h <sub>AC</sub> , h <sub>B</sub> , P <sub>FWD</sub>                                    | E <sub>Ri</sub> |
| <b>CFP-E<sub>Ri</sub>-(7)-(5-21 kips)</b> | D <sub>0</sub> , D <sub>8</sub> , D <sub>12</sub> , D <sub>18</sub> , D <sub>24</sub> , D <sub>36</sub> , D <sub>60</sub> , h <sub>AC</sub> , h <sub>B</sub> , P <sub>FWD</sub>                   | E <sub>Ri</sub> |
| <b>CFP-E<sub>Ri</sub>-(8)-(5-21 kips)</b> | D <sub>0</sub> , D <sub>8</sub> , D <sub>12</sub> , D <sub>18</sub> , D <sub>24</sub> , D <sub>36</sub> , D <sub>48</sub> , D <sub>60</sub> , h <sub>AC</sub> , h <sub>B</sub> , P <sub>FWD</sub> | E <sub>Ri</sub> |
| <b>CFP-K<sub>B</sub>-(4)-(5-21 kips)</b>  | D <sub>0</sub> , D <sub>12</sub> , D <sub>24</sub> , D <sub>36</sub> , h <sub>AC</sub> , h <sub>B</sub> , P <sub>FWD</sub>  | K <sub>B</sub>  |
| <b>CFP-K<sub>B</sub>-(6)-(5-21 kips)</b>  | D <sub>0</sub> , D <sub>12</sub> , D <sub>24</sub> , D <sub>36</sub> , D <sub>48</sub> , D <sub>60</sub> , h <sub>AC</sub> , h <sub>B</sub> , P <sub>FWD</sub>                                    | K <sub>B</sub>  |
| <b>CFP-K<sub>B</sub>-(7)-(5-21 kips)</b>  | D <sub>0</sub> , D <sub>8</sub> , D <sub>12</sub> , D <sub>18</sub> , D <sub>24</sub> , D <sub>36</sub> , D <sub>60</sub> , h <sub>AC</sub> , h <sub>B</sub> , P <sub>FWD</sub>                   | K <sub>B</sub>  |
| <b>CFP-K<sub>B</sub>-(8)-(5-21 kips)</b>  | D <sub>0</sub> , D <sub>8</sub> , D <sub>12</sub> , D <sub>18</sub> , D <sub>24</sub> , D <sub>36</sub> , D <sub>48</sub> , D <sub>60</sub> , h <sub>AC</sub> , h <sub>B</sub> , P <sub>FWD</sub> | K <sub>B</sub>  |

### Noise-Introduced ANN Backcalculation Models

In addition to the training and testing sets prepared for backcalculation models, more ANN training sets were generated by introducing  $\pm 2\%$ ,  $\pm 5\%$  and  $\pm 10\%$  noise to the FWD deflection data used in backcalculation models. The purpose of introducing noisy patterns in the training sets was to develop more robust networks that can tolerate the noisy or inaccurate deflection patterns collected from the FWD deflection basins. Noise introduction to trained ANN models was as follows. The ILLI-PAVE solution database was first partitioned to create 28,500 training patterns and an independent testing set of 1,500 patterns to check the performance of the trained ANN models. Uniformly distributed random numbers ranging from -2 to 2% ( $\pm 2\%$ ),  $\pm 5\%$  and  $\pm 10\%$  noise patterns were generated each time to create noisy training patterns. After adding

randomly selected noise values only to the pavement surface deflections of  $D_0$ ,  $D_8$ ,  $D_{12}$ ,  $D_{18}$ ,  $D_{24}$ ,  $D_{48}$ , and  $D_{60}$ , new training data sets were developed for each noisy training set. By repeating the noise introduction procedure, three more training data sets were formed for each backcalculation model.

### **ANN-Based CFP Forward Calculation Models**

Backpropagation-type neural networks, which are very good in function approximation, were used in this study to develop ANN structural models for predicting critical pavement responses based on the known input variables of pavement layer thicknesses and deflection basin. Similar to ELP or ILLI-PAVE analyses, pavement responses were directly predicted from the known pavement design inputs in this forward computation process. Accordingly, this ANN model was named as the forward calculation (FC) model. The ANN FC model inputs consisted of the  $h_{AC}$ ,  $h_{GB}$ , and the pavement surface deflection basin to predict the critical pavement responses of strains  $\epsilon_{AC}$ ,  $\epsilon_{SG}$ , and  $\sigma_D$  under the standard 9-kip FWD loading or variable FWD loading within the range of 5–21 kips. The main advantage and use of the ANN FC model was in the rapid prediction ability of ILLI-PAVE results (critical pavement responses) from the pavement surface deflections at the sophistication level of the complicated finite element solutions that usually require a high degree of expertise to solve the problem.

### **Performance of CFP ANN Models**

To evaluate the performance of the developed ANN models, AAE and root-mean-square error (RMSE) values were calculated. In addition, goodness-of-fit is a commonly used approach to evaluate the performance of mathematical models. The AAE values for each of the developed ANN models are summarized in Table 4. One of the most important findings is that the AAE values decrease when the number of deflection inputs increase, which is as expected. For example, the AAE values of the CFP ANN models (with varying FWD load magnitude) are 1.03%, 1.10%, 1.03%, and 0.98% ( $E_{AC}$  predictions) for the four, five, seven, and eight deflection models, respectively. The rationale behind this is that as the number of deflection input parameters increase, the ANN can learn the mapping better. However, as will be seen later, this explanation is only valid for the synthetic data. When these ANN models were used to predict the  $E_{AC}$  value of the actual pavements obtained from the Iowa DOT, the predictions do not vary significantly with the number of deflection inputs. Figure B.1 to Figure B.48 in Appendix B summarize the performance of ANN models and accuracy of predictions.

The performance of noise-introduced ANN models is presented in Appendix C. The purpose of introducing noisy patterns in the training sets was to develop more robust networks that can tolerate the noisy or inaccurate deflection patterns collected from the FWD deflection basins. Therefore, in the case of the noise-introduced models, the 1,500 independent test data had more scatter around the line of equality and both the MSE and AAE values were relatively higher compared to zero-noise ANN models (see figures in Appendix C). However, the confidence interval of the input data increased.

Table 5 shows the AAE values of noise-introduced ANN models. The AAE increased from 1.11% to 2.74% in the CFP-4 deflection model at a 2% noise level, from 1.11% to 4.09% at a 5% noise level, and from 1.11% to 7.38 % at a 10% noise level for predicting the AC layer moduli. A similar trend is observed for other models (see Table 5).

Forward calculation models developed for predicting the critical pavement responses of  $\epsilon_{AC}$ ,  $\epsilon_{SG}$ , and  $\sigma_D$  directly from the FWD deflection data eliminated the need for predicting the pavement layer moduli and then computing the critical pavement responses needed for pavement analysis and design. This direct approach saved valuable time in analyzing the pavement sections using the FWD deflection basins. The AAE values for the forward calculation models (9-kip models) were 0.80% for predicting the critical tensile strains at the bottom of the AC layer and 5.51% for predicting the critical compressive strains on top of the subgrade layer. The AAE value for the critical deviator stresses on top of the subgrade layer was approximately 5.23% (see Table 6). Low error values indicate the proper training and prediction performance of the ANN backcalculation models developed in this study. Figure B.49 to Figure B.96 included in Appendix B show the prediction accuracy for forward calculation ANN models.

**Table 4. Prediction performance of CFP-ANN-based backcalculation models (with zero noise)**

| Load Level  | ANN Deflection Models | AAE (%)  |          |       |
|-------------|-----------------------|----------|----------|-------|
|             |                       | $E_{AC}$ | $E_{Ri}$ | $K_B$ |
| (9-kip)     | 4-Deflection          | 1.11     | 4.04     | 9.47  |
|             | 6-Deflection          | 1.25     | 3.46     | 14.17 |
|             | 7-Deflection          | 0.84     | 3.52     | 12.70 |
|             | 8 Deflection          | 1.08     | 3.49     | 12.59 |
| (5-21 kips) | 4 Deflection          | 1.03     | 4.71     | 17.37 |
|             | 6 Deflection          | 1.10     | 4.04     | 19.80 |
|             | 7 Deflection          | 1.03     | 3.91     | 23.01 |
|             | 8 Deflection          | 0.98     | 3.93     | 24.83 |

**Table 5. Prediction performance of CFP-ANN-based backcalculation models (with noise)**

| Noise Level  | ANN Deflection Models | AAE (%)  |          |       |
|--|-----------------------|----------|----------|-------|
|  |                       | $E_{AC}$ | $E_{Ri}$ | $K_B$ |
| 9-kip<br>( $\pm 2\%$ )<br><br>( $\pm 5\%$ )<br><br>( $\pm 10\%$ )        | 4-Deflection          | 2.74     | 7.11     | 13.64 |
|  | 6-Deflection          | 1.74     | 6.75     | 16.50 |
|  | 7-Deflection          | 1.63     | 6.30     | 13.41 |
|  | 8-Deflection          | 2.79     | 4.50     | 18.14 |
|  | 4-Deflection          | 4.09     | 10.18    | 18.78 |
|  | 6-Deflection          | 2.78     | 5.85     | 17.21 |
|  | 7-Deflection          | 2.52     | 6.01     | 21.56 |
|  | 8-Deflection          | 2.76     | 7.65     | 18.37 |
|  | 4-Deflection          | 7.38     | 22.43    | 25.66 |
|  | 6-Deflection          | 7.95     | 8.54     | 26.57 |
|  | 7-Deflection          | 6.17     | 12.52    | 25.41 |
|  | 8-Deflection          | 4.30     | 10.38    | 26.98 |
| 5-21<br>kips<br>( $\pm 2\%$ )<br><br>( $\pm 5\%$ )<br><br>( $\pm 10\%$ ) | 4-Deflection          | 3.09     | 7.70     | 21.24 |
|  | 6-Deflection          | 2.38     | 7.65     | 19.18 |
|  | 7-Deflection          | 1.73     | 8.91     | 25.25 |
|  | 8-Deflection          | 1.89     | 6.28     | 20.59 |
|  | 4-Deflection          | 6.36     | 10.33    | 27.75 |
|  | 6-Deflection          | 3.15     | 7.50     | 23.34 |
|  | 7-Deflection          | 3.40     | 10.39    | 27.42 |
|  | 8-Deflection          | 3.07     | 7.81     | 24.20 |
|  | 4-Deflection          | 8.78     | 16.86    | 32.51 |
|  | 6-Deflection          | 11.67    | 9.69     | 33.56 |
|  | 7-Deflection          | 6.20     | 13.69    | 32.22 |
|  | 8-Deflection          | 7.10     | 7.30     | 30.47 |

**Table 6. Prediction performance of CFP-ANN-based backcalculation models (forward)**

| Load Level     | ANN Deflection Models | AAE (%)         |                 |            |
|----------------|-----------------------|-----------------|-----------------|------------|
|                |                       | $\epsilon_{AC}$ | $\epsilon_{SG}$ | $\sigma_D$ |
| (9-kip)        | 4-Deflection          | 0.80            | 5.51            | 5.23       |
|                | 6-Deflection          | 0.77            | 4.95            | 5.25       |
|                | 7-Deflection          | 0.83            | 6.17            | 5.28       |
|                | 8-Deflection          | 0.85            | 5.15            | 5.25       |
| (5-21<br>kips) | 4-Deflection          | 1.33            | 6.74            | 5.68       |
|                | 6-Deflection          | 0.95            | 6.72            | 5.51       |
|                | 7-Deflection          | 1.16            | 6.19            | 5.54       |
|                | 8-Deflection          | 1.29            | 6.63            | 5.59       |

## Validation of CFP-ANN Models

Six deflection basins were selected from CFP sections in Clarke County, Iowa. The thickness of the AC layer and granular base were 16 inches and 17 inches, respectively. The pavement sections were part of I-35 on Clarke County. Pavement sections had the geometry and loading characteristics, as shown in Figure 12. The pavements were first analyzed using the CFP-4 (four deflections) varying load ANN backcalculation model. These deflections were also used in an ELP-based backcalculation program, BAKFAA, developed by the FAA, to backcalculate the pavement layer moduli (<http://www.airtech.tc.faa.gov/naptf/download/>). Also, the following statistically based moduli-prediction algorithms (Thompson 1989) were used to further evaluate the performance of the models using FWD data from Henry County, Illinois:

$$\text{Log}E_{AC} = 1.48 + 1.76 \log(AREA / D_o) + 0.26(AREA / h_{AC}) \quad (\text{ksi}) \quad (6)$$

$$\text{Log}E_{Ri} = 1.51 - 0.19D_{36} + 0.27 \log D_{36} \quad (\text{ksi}) \quad (7)$$

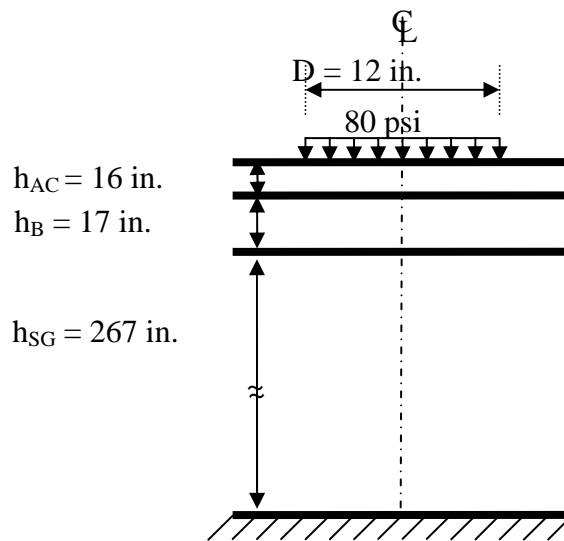


**Figure 12. Geometry and loading characteristics of pavement sections analyzed**

Figure 13 and Figure 14 compare the results of the BAKFAA moduli prediction algorithm results with those of ANN predictions for  $E_{AC}$  and  $E_{Ri}$ , respectively. In general, for six sets of predictions, the AAE values of BAKFAA were rather high compared to both the ANN- and moduli-algorithm-based predictions for both  $E_{AC}$ , and  $E_{Ri}$ . The ANN models gave the lowest moduli for both  $E_{AC}$  and  $E_{Ri}$ . The moduli algorithm predictions and ANN results are further compared using the Henry County, Illinois data (see Figure 15 and Figure 16).

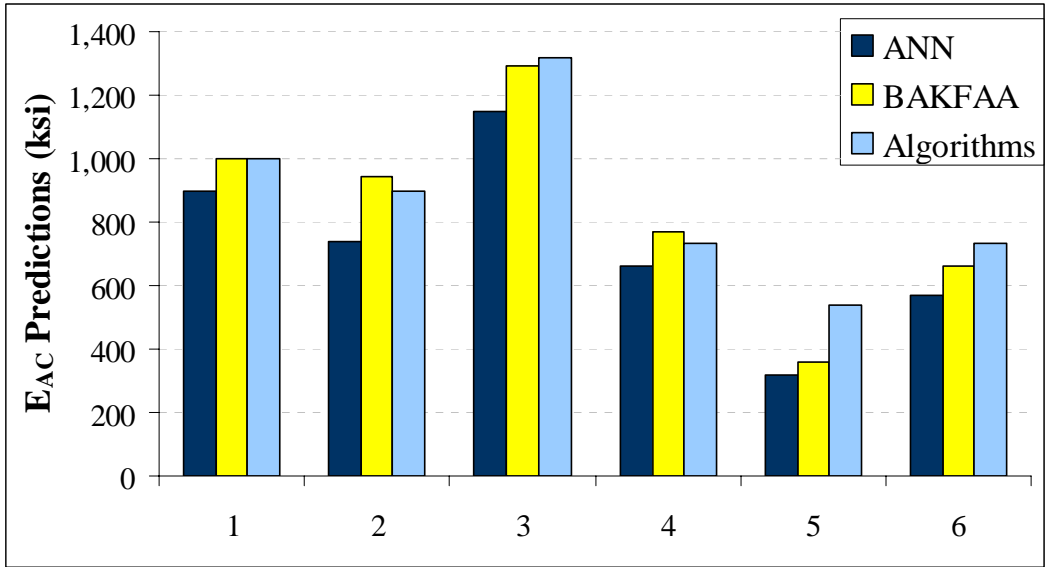


Figure 13. ANN, BAKFAA, and algorithms comparison for prediction of  $E_{AC}$

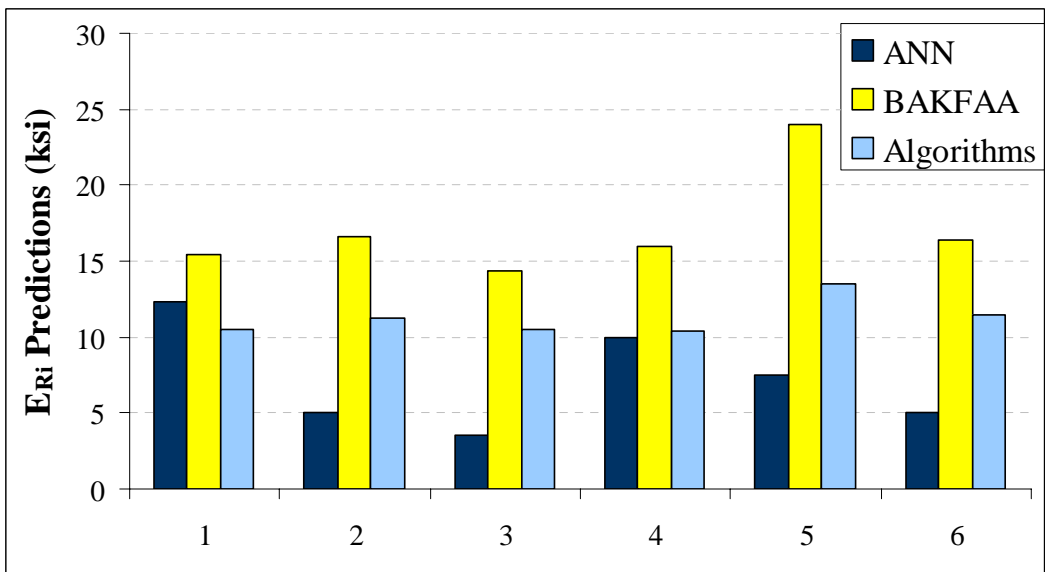


Figure 14. ANN, BAKFAA, and algorithms comparison for prediction of  $E_{Ri}$

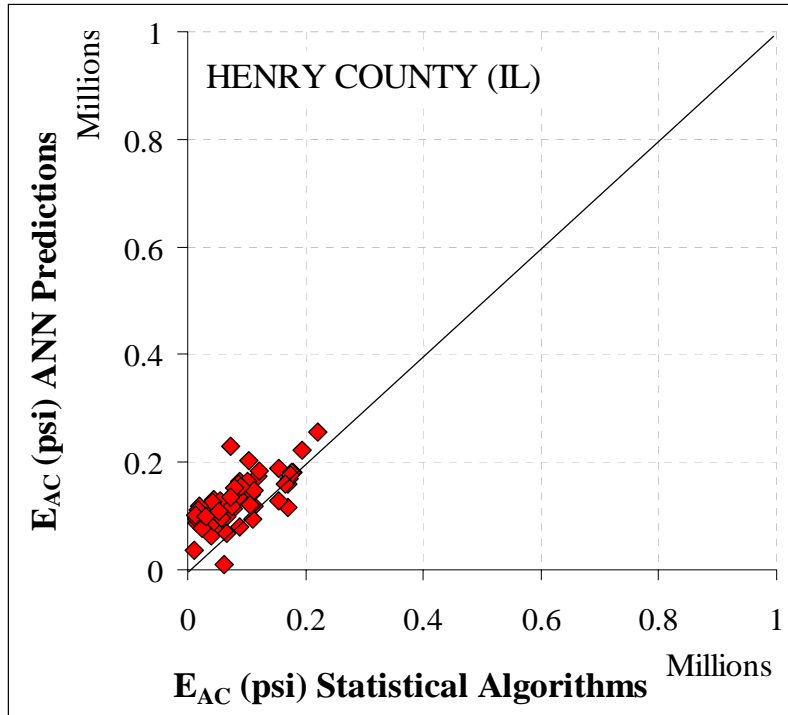


Figure 15. Comparison of ANN-based models to statistical models for  $E_{AC}$

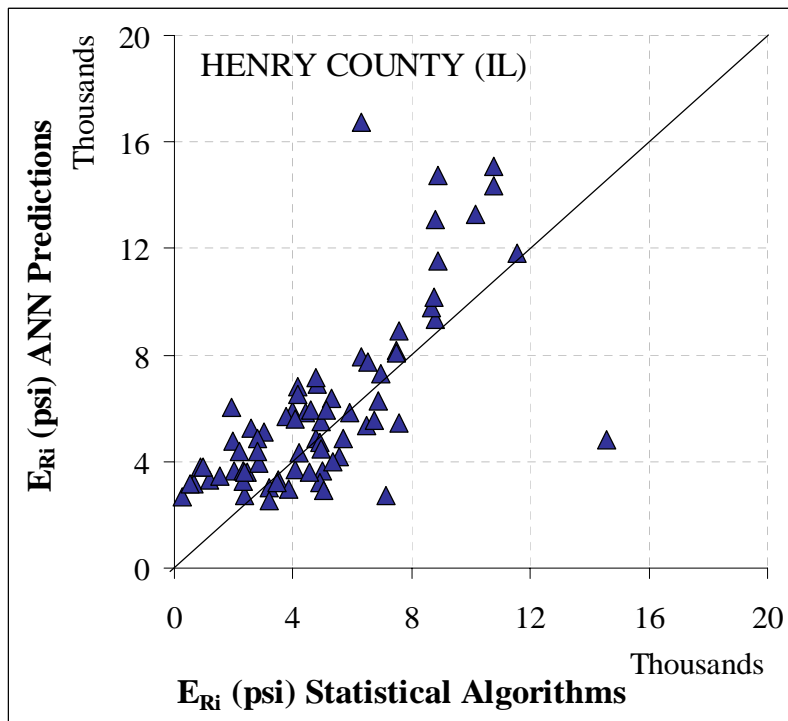


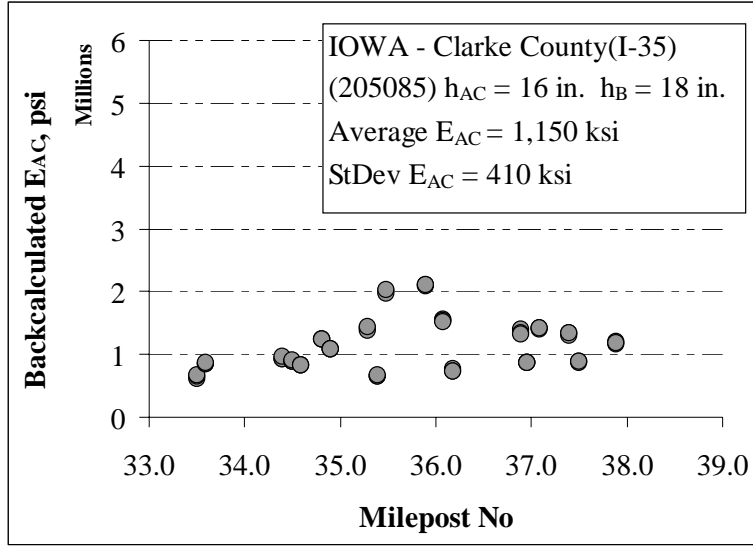
Figure 16. Comparison of ANN-based models to statistical models for  $E_{Ri}$

## Case Studies of Individual Pavement Sections

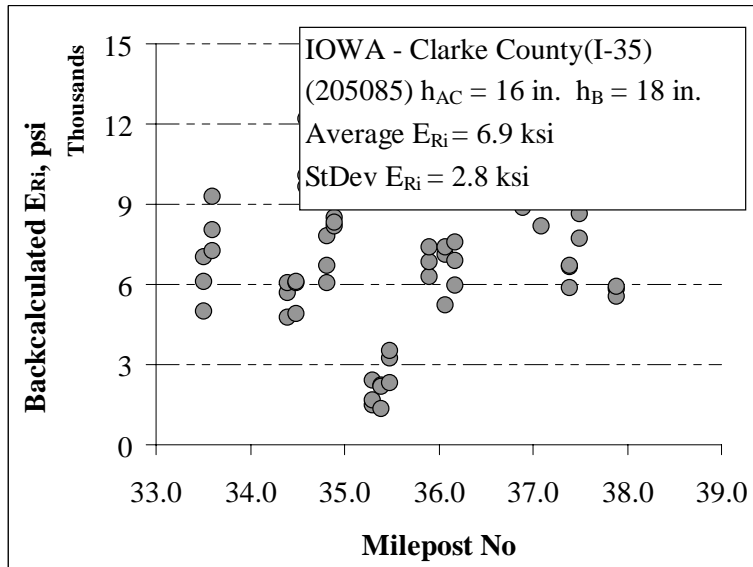
The CFP-ANN models were evaluated using actual FWD data from the Iowa DOT. First, CFP systems were identified using the DOT milepost book. The layer thicknesses from the milepost book were entered as inputs for ANN models along with the FWD measurements at these sites. For this study, 10 different CFP sites were selected. The list of selected sites is given in Table 7. In Figure 17 to Figure 36, the ANN prediction performance for the selected sites is shown.

**Table 7. The Iowa CFP sections**

| <b>Pavement Type</b> | <b>Location &amp; Milepost</b>                   | <b><math>h_{AC}</math> (in.)</b> | <b><math>h_B</math> (in.)</b> |
|----------------------|--|----------------------------------|-------------------------------|
| CFP                  | IA-Clarke County (I-35)<br>(Milepost No:33-38)   | 16                               | 18                            |
| CFP                  | IA-Clarke County (I-35)<br>(Milepost No:33-38)   | 16                               | 18                            |
| CFP                  | IA-Clarke County (I-35)<br>(Milepost No:38-39)   | 17                               | 18                            |
| CFP                  | IA-Clarke County (I-35)<br>(Milepost No:38-42)   | 17                               | 18                            |
| CFP                  | IA-Clarke County (I-35)<br>(Milepost No:39-40)   | 17                               | 18                            |
| CFP                  | IA-Clarke County (I-35)<br>(Milepost No:40-41)   | 17                               | 18                            |
| CFP                  | IA-Clarke County (I-35)<br>(Milepost No:41-43)   | 17                               | 18                            |
| CFP                  | IA-Jasper County (I-80)<br>(Milepost No:174-180) | 8                                | 9.5                           |
| CFP                  | IA-Jasper County (I-80)<br>(Milepost No:174-182) | 8                                | 9.5                           |
| CFP                  | IL – Henry County                                | 3.5                              | 16                            |



**Figure 17.  $E_{AC}$  predictions for IA – Clarke County (I-35) FWD deflection basin data (205085)**



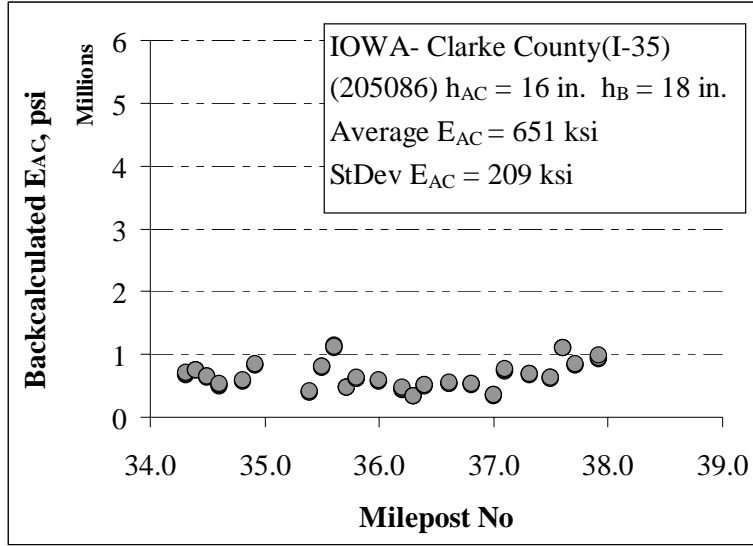


Figure 19.  $E_{AC}$  predictions for IA – Clarke County (I-35) FWD deflection basin data (205086)

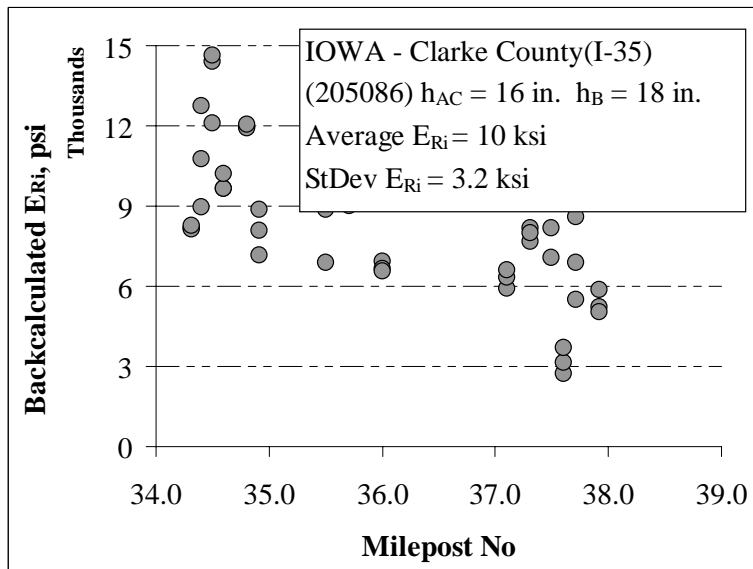


Figure 20.  $E_{Ri}$  predictions for IA – Clarke County (I-35) FWD deflection basin data (205086)

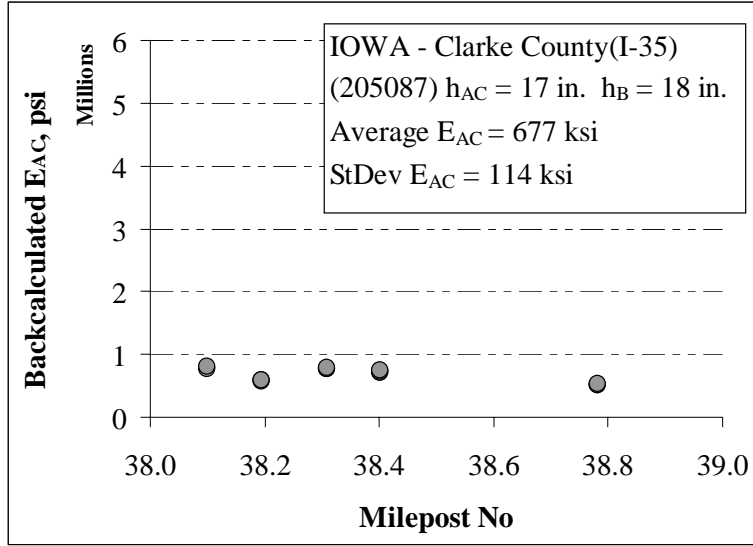


Figure 21.  $E_{AC}$  predictions for IA – Clarke County (I-35) FWD deflection basin data (205087)

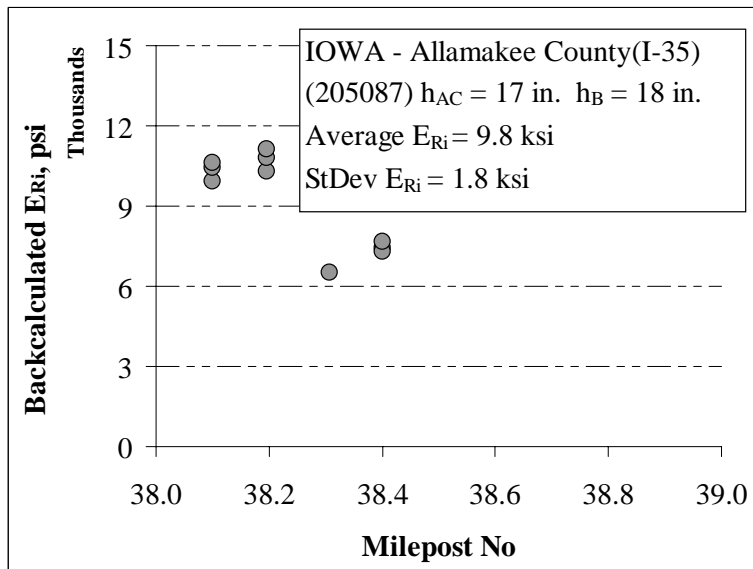


Figure 22.  $E_{Ri}$  predictions for IA – Clarke County (I-35) FWD deflection basin data (205087)

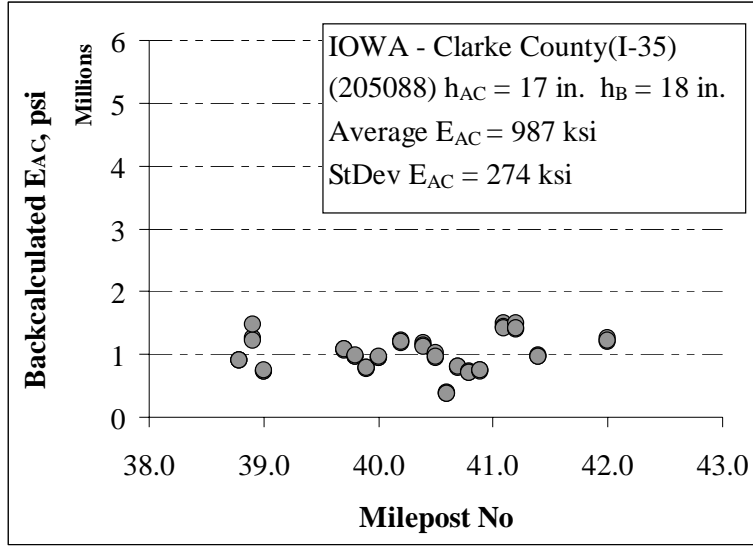


Figure 23.  $E_{AC}$  predictions for IA – Clarke County (I-35) FWD deflection basin data (205088)

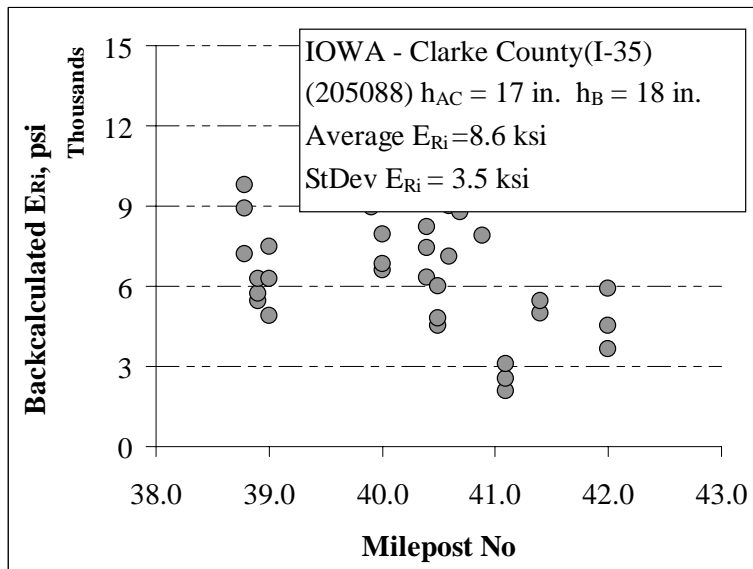


Figure 24.  $E_{Ri}$  predictions for IA – Clarke County (I-35) FWD deflection basin data (205088)

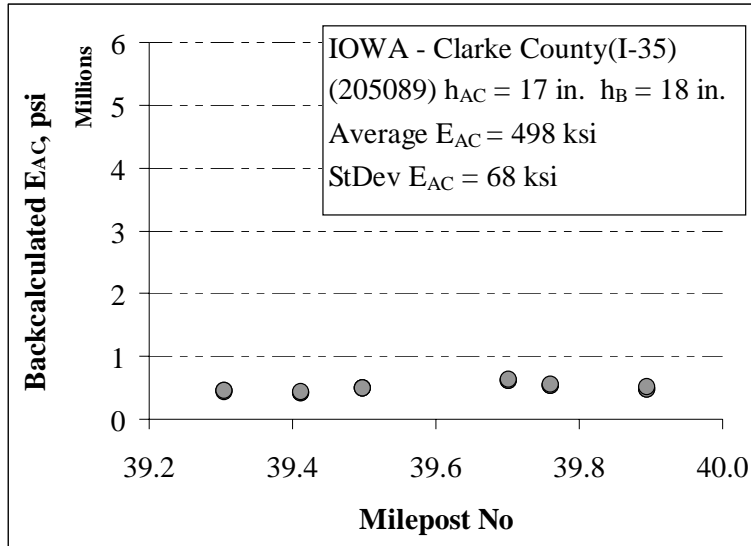


Figure 25.  $E_{AC}$  predictions for IA – Clarke County (I-35) FWD deflection basin data (205089)

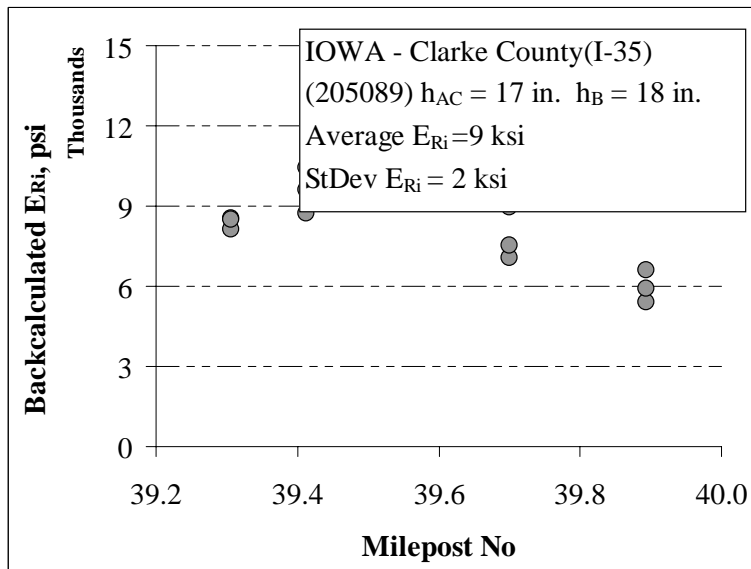


Figure 26.  $E_{Ri}$  predictions for IA – Clarke County (I-35) FWD deflection basin data (205089)

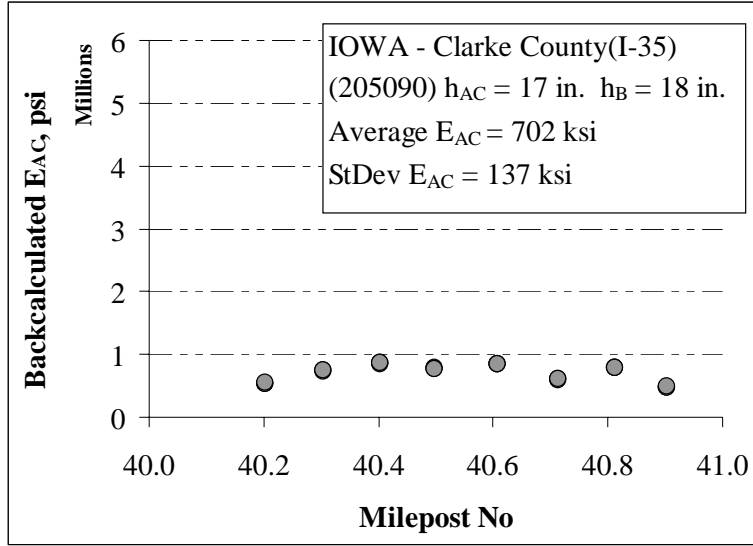


Figure 27.  $E_{AC}$  predictions for IA – Clarke County (I-35) FWD deflection basin data (205090)

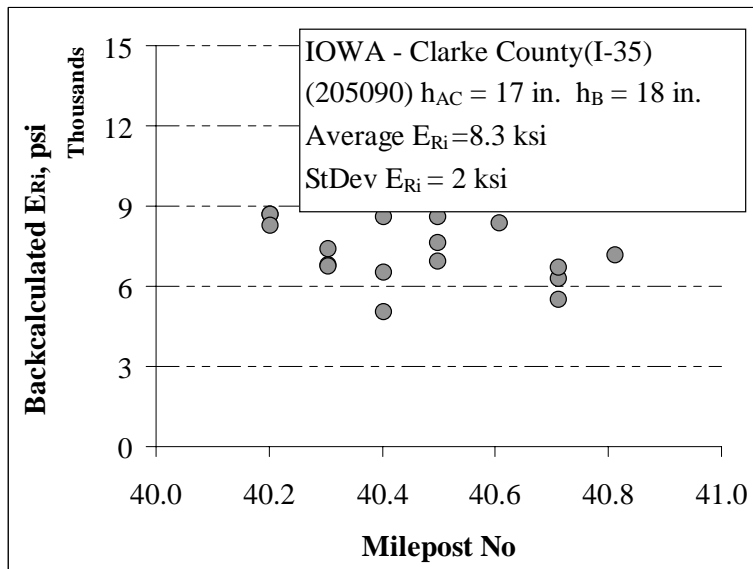


Figure 28.  $E_{Ri}$  predictions for IA – Clarke County (I-35) FWD deflection basin data (205090)

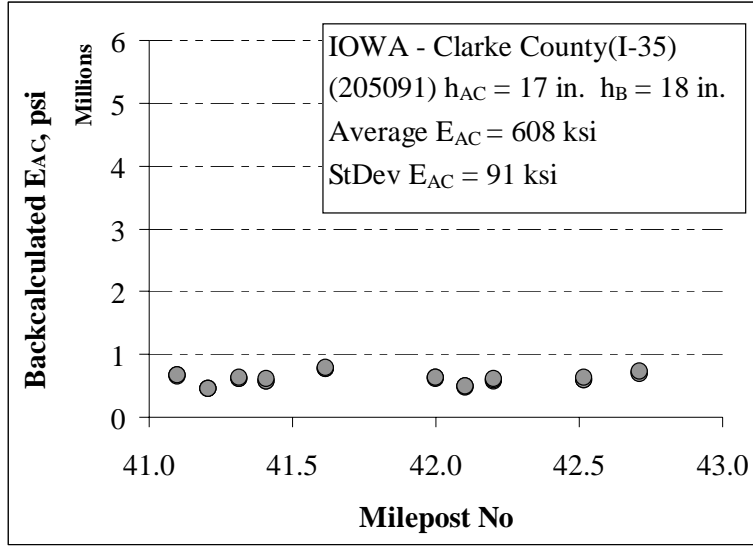


Figure 29.  $E_{AC}$  predictions for IA – Clarke County (I-35) FWD deflection basin data (205091)

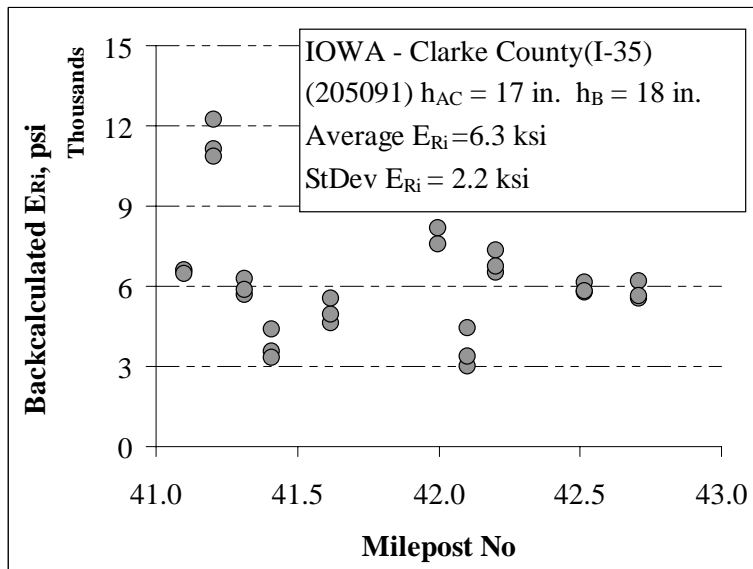


Figure 30.  $E_{Ri}$  predictions for IA – Clarke County (I-35) FWD deflection basin data (205091)

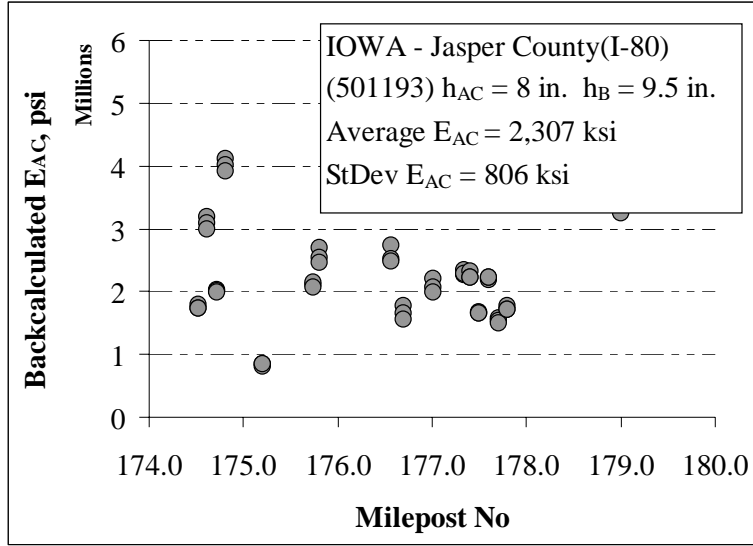


Figure 31.  $E_{AC}$  predictions for IA – Clarke County (I-35) FWD deflection basin data (501193)

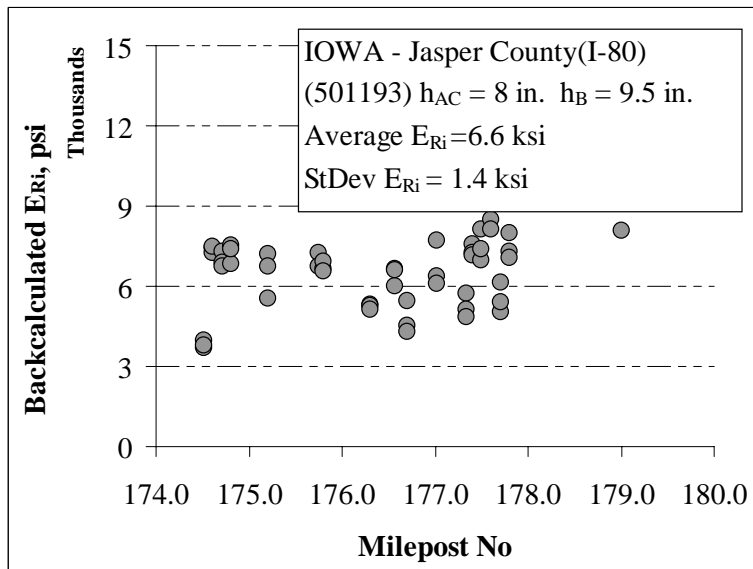
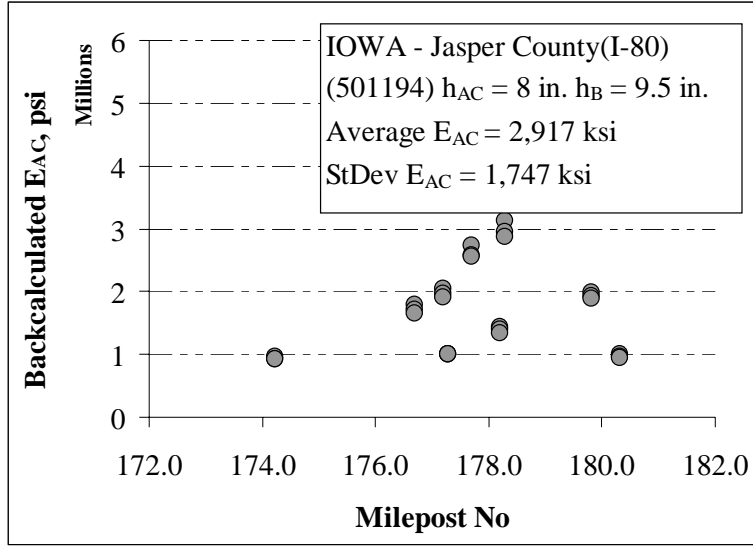
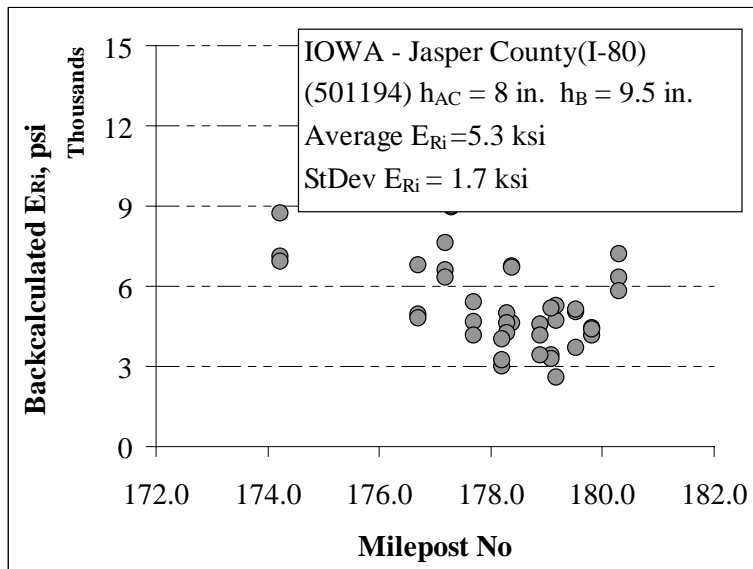


Figure 32.  $E_{Ri}$  predictions for IA – Clarke County (I-35) FWD deflection basin data (501193)



**Figure 33.  $E_{AC}$  predictions for IA – Jasper County (I-80) FWD deflection basin data (501194)**



**Figure 34.  $E_{Ri}$  predictions for IA – Jasper County (I-80) FWD deflection basin data (501194)**

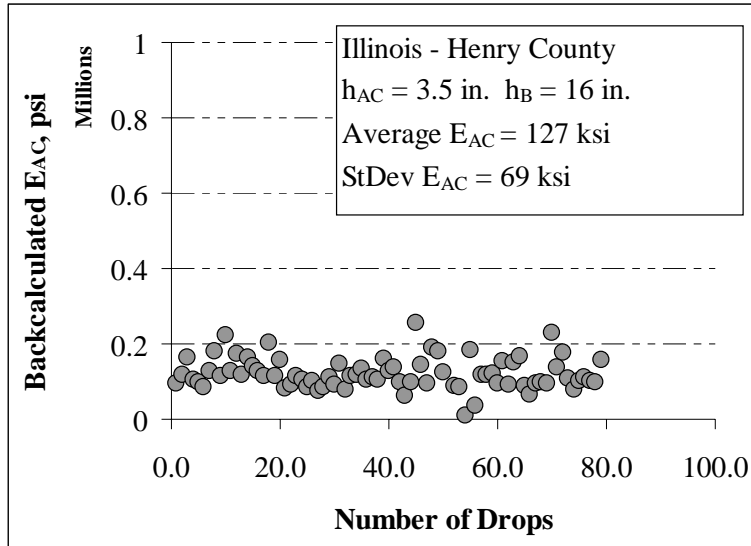


**Figure 35.  $E_{AC}$  predictions for IL – Henry County FWD deflection basin data**

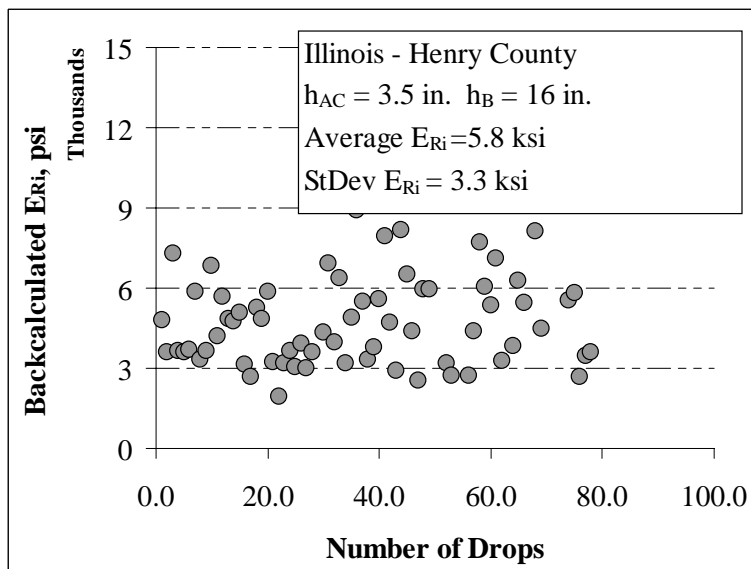


**Figure 36.  $E_{Ri}$  predictions for IL – Henry County FWD deflection basin data**

## ANN Models for CFP Systems – Summary and Conclusions

### *Summary*

The primary objective in this section was to show that ANN models could be developed to perform rapid predictions of CFP layer moduli and critical pavement responses from the FWD deflection basins for a number of pavement input parameters considered in analysis and design. Unlike the linear elastic layer theory commonly used in pavement layer backcalculation, realistic soil modulus models were used in the ILLI-PAVE program to account for the typical softening

behavior of the fine-grained subgrade soils. The developed forward- and back-calculation ANN models successfully predicted the pavement layer moduli, and critical pavement responses obtained from the ILLI-PAVE finite element solutions. ANN predictions had very low AAE even for noisy deflection basins when compared to the ILLI-PAVE solutions.

It was shown that ANNs are capable of mapping complex relationships, such as those studied in complex finite element analyses, between the input parameters and the output variables for nonlinear, stress-dependent systems. Such ANN-based structural analysis models can provide pavement engineers and designers with sophisticated finite element solutions without the need for a high degree of expertise in the input and output of the problem. ANN models can rapidly output the required solutions in analyzing a large number of pavement deflection basins needed for routine pavement evaluation. The rapid prediction ability of the ANN backcalculation models makes them perfect evaluation tools for analyzing the FWD deflection data, and thus assessing the condition of the pavement sections, in real time for both project-specific and network-level FWD testing.

### *Conclusions*

Major findings related to ANN-based prediction of elastic modulus of asphalt concrete ( $E_{AC}$ ) layer can be summarized as follows:

- In total, eight different ANN-based backcalculation models were developed for  $E_{AC}$ : CFP- $E_{AC}$ -(4-deflection)-(9 kip), CFP- $E_{AC}$ -(6-deflection)-(9 kip), CFP- $E_{AC}$ -(7-deflection)-(9 kip), CFP- $E_{AC}$ -(8-deflection)-(9 kip), CFP- $E_{AC}$ -(4-deflection)-(5-21 kips), CFP- $E_{AC}$ -(6-deflection)-(5-21 kips), CFP- $E_{AC}$ -(7-deflection)-(5-21 kips), and CFP- $E_{AC}$ -(8-deflection)-(5-21 kips).
- The AAE values of ANN trainings are around 1% for almost all the developed  $E_{AC}$  prediction models.
- Almost all the developed models showed similar prediction accuracy for the same FWD data collected in the field.
- The 4-deflection CFP-ANN model gave slightly better results in terms of standard deviation.
- The standard deviations were low for all the models.
- The ANN predictions are consistent with statistically based moduli prediction algorithms and the ELP-based BAKFAA backcalculation program.
- In addition to the developed models, noise-introduced models were additionally developed ( $\pm 2\%$ ,  $\pm 5\%$ , and  $\pm 10\%$ ) for predicting  $E_{AC}$ .
- When the introduced noise in the deflection data increased, the AAE (%) value also increased as expected.

Major findings for prediction of subgrade soil break point deviator stress ( $E_{Ri}$ ) can be summarized as follows:

- In total, eight different ANN-based backcalculation models were developed for  $E_{Ri}$ : CFP- $E_{Ri}$ -(4-deflection)-(9 kip), CFP- $E_{Ri}$ -(6-deflection)-(9 kip), CFP- $E_{Ri}$ -(7-

- deflection)-(9 kip), CFP- $E_{Ri}$ -(8-deflection)-(9 kip), CFP- $E_{Ri}$ -(4-deflection)-(5-21 kips), CFP- $E_{Ri}$ -(6-deflection)-(5-21 kips), CFP- $E_{Ri}$ -(7-deflection)-(5-21 kips), and CFP- $E_{Ri}$ -(8-deflection)-(5-21 kips).
- The AAE values of ANN predictions were around 4% for almost all the  $E_{Ri}$  prediction models.
  - Scatter was higher compared to  $E_{AC}$  predictions, which is as expected because the subgrade variability is higher.
  - In general, the standard deviations of  $E_{Ri}$  predictions were higher compared to  $E_{AC}$ .
  - The 6-deflection models gave better results than the 4-deflection models in terms of standard deviations.
  - Using the variable load level  $E_{Ri}$  prediction models, the nonlinear, stress-dependent behavior of subgrade soils could be verified.
  - In addition to the developed models, noise-introduced models were additionally developed ( $\pm 2\%$ ,  $\pm 5\%$ , and  $\pm 10\%$ ) for predicting  $E_{AC}$ .
  - When the introduced noise in the deflection data increased, the AAE (%) value also increased as expected.

The major findings related to the development of CFP-ANN FC models can be summarized as follows:

- ANN-based forward calculation models developed for predicting the critical pavement responses of  $\epsilon_{AC}$ ,  $\epsilon_{SG}$ , and  $\sigma_D$  directly from the FWD deflection data eliminated the need for first predicting the pavement layer moduli and then computing the critical pavement responses needed for pavement analysis and design.
- Different ANN forward calculation models were developed for prediction of critical pavement responses of strains ( $\epsilon_{AC}$  and  $\epsilon_{SG}$ ) and the subgrade deviator stress ( $\sigma_D$ ).
- The ANN FC model inputs consisted of the thicknesses of AC and granular base layers, and the pavement surface deflection basin to predict the critical pavement responses of strains  $\epsilon_{AC}$  and  $\epsilon_{SG}$  and subgrade deviator stress  $\sigma_D$  under the standard 9-kip FWD loading or varying FWD loading within the range of 5-21 kips.
- The average AAE values of ANN predictions were around 1%, 6%, and 5% for  $\epsilon_{AC}$ ,  $\epsilon_{SG}$ , and  $\sigma_D$ , respectively.

## ANN MODELS FOR FULL-DEPTH FLEXIBLE PAVEMENT SYSTEMS

The full-depth flexible pavement systems were constructed by placing one or more layer of hot mix asphalt (HMA) directly on the subgrade. Therefore, the basic difference from CFPs was the base layer on top of the subgrade. For this analysis, HMA with a thickness varying between 3 and 28 inches over a subgrade, with a total thickness of about 300 inches, was selected as the FD pavement system. The asphalt surface layer was characterized as a linear elastic material modeling with  $E_{AC}$ , and Poisson's ratio,  $\nu$ . The AC layer moduli were kept between the realistic range of 100 ksi and 6,000 ksi, and the Poisson's ratio was constant as 0.35. The  $E_{Ri}$  was the main input for subgrade soils. The  $K_3$  and  $K_4$  slopes were taken as constants, 1,100 and 200, respectively, corresponding to medium-strength soils, as reported by Thompson and Elliott (1985). Based on the results from a comprehensive Illinois subgrade soil study conducted by Thompson and Robnett (1979), the breakpoint deviator stress,  $\sigma_{di}$ , was taken as 6 psi and a value of 2 psi was used for the lower limit deviator stress,  $\sigma_{dli}$ . The soil's unconfined compressive strength,  $Q_u$ , or cohesion, was used to determine the upper limit deviator stress,  $\sigma_{duli}$ , (see Figure 5) as a function of the breakpoint deviator stress,  $E_{Ri}$ , using Equation 5.

### Generating ILLI-PAVE Finite Element Solution Database

To generate the ILLI-PAVE 2000 solution database, a uniform random number generator was utilized to obtain values for each independent variable:  $h_{AC}$ ,  $E_{AC}$ , and  $E_{Ri}$ . A total of 30,000 input files were generated and the corresponding pavement layer model parameters for the subgrade layer were calculated using the randomly selected  $E_{Ri}$  values. The ILLI-PAVE 2000 pavement geometry and material model inputs are given in Table 8, which were selected to cover, within range, the most typical AC thickness and AC and subgrade layer stiffness of field constructed full-depth asphalt pavements.

The finite element mesh used for generating the ILLI-PAVE runs was determined according to the stress concentration effect and FWD sensor locations. A fine mesh was used under the FWD loading where the highest stress concentration occurred. The horizontal mesh size was arranged to match the FWD sensor distances. An aspect ratio of one, or close to one, was selected for high stress concentration areas. The total analysis depth of the pavement was 300 inches. The radial boundary of the mesh was placed at 30 times the contact area radius.

A total of 30,000 ILLI-PAVE analyses were performed to adequately cover the typical geometries and layer properties of most full-depth asphalt pavements practically constructed in the field (see Table 8). For each ILLI-PAVE run, the input values for  $h_{AC}$ ,  $E_{AC}$ , and the  $E_{Ri}$  were recorded along with the surface deflections ( $D_0$  for centerline or 0-inch radially away,  $D_8$ ,  $D_{12}$ ,  $D_{18}$ ,  $D_{24}$ ,  $D_{36}$ ,  $D_{48}$ , and  $D_{60}$ ), critical pavement responses, i.e.,  $\epsilon_{AC}$  at the bottom of the AC layer,  $\epsilon_{SG}$  on top of the subgrade, and the  $\sigma_D$  on top of the subgrade layer, at the center line of the applied FWD loading (see Figure 37). Either a constant 9-kip wheel load was applied as a uniform pressure of 80 psi over a circular area of radius six inches (152 mm) or a variable load was applied as uniform pressure ranging between 44 psi and 186 psi (5 and 21 kips load over a circular area of 6-inch radius).

**Table 8. Pavement geometry and material property/model inputs of FD flexible pavements for ILLI-PAVE solutions**

| Material Type         | Layer Thickness           | Material Model           | Layer Modulus Inputs                                       |
|-----------------------|---------------------------|--------------------------|--|
| Asphalt Concrete      | $h_{AC} = 3-28$ in.       | Linear Elastic           | $E_{AC} = 100$ to 6,000 ksi                                |
| Fine-grained Subgrade | $h_{SG} = (300 - h_{AC})$ | Nonlinear Bilinear Model | $M_R = f(E_{Ri})$ ; see Figure 5<br>$E_{Ri} = 1$ to 15 ksi |

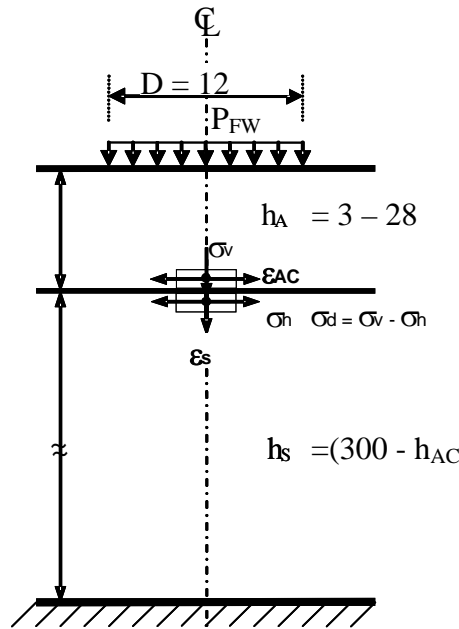


**Figure 37. Layout of full-depth flexible pavement systems**

A total of 30,000 of ILLI-PAVE analysis results were used for generating ANN training and testing sets. Deflection parameters obtained from an ILLI-PAVE solution database at radial distances contained diverse information about pavement layer moduli. In order to reveal which deflection parameter had more effect on individual layers, a multivariate correlation statistic was used. The results of this statistical analysis are summarized in Figure 38 and Figure 39. This analysis resulted in multiple ANN models based on different combinations of deflection parameters. These models are described in the following sections. Each model had its own training and testing sets prepared from the ILLI-PAVE 2000 solution database. Noisy ANN training sets were generated by introducing 10% ( $\pm 5\%$ ) and 20% ( $\pm 10\%$ ) noise to the FWD deflection values used in backcalculation models. The purpose of introducing noisy patterns in the training sets was to develop more robust ANN models that can tolerate the noisy or inaccurate deflection patterns collected from the field FWD deflection basins.

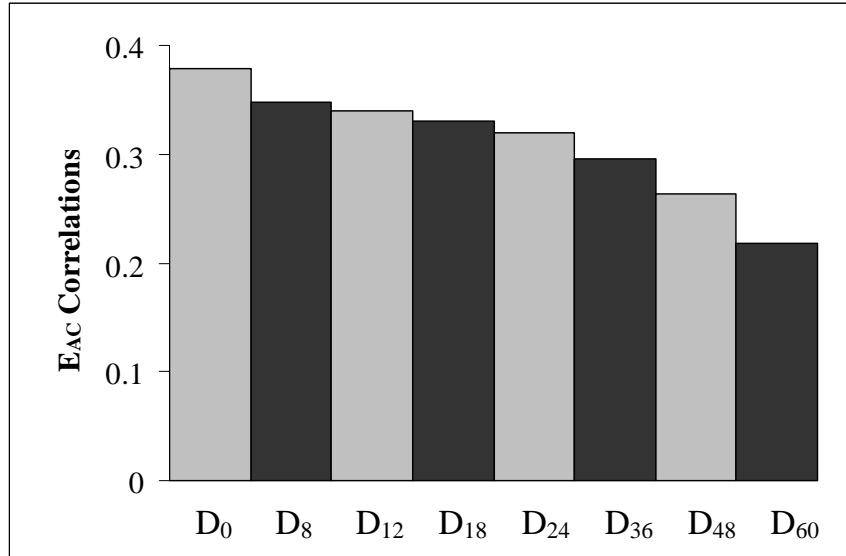


**Figure 38. E<sub>AC</sub> correlation with deflections (FD)**

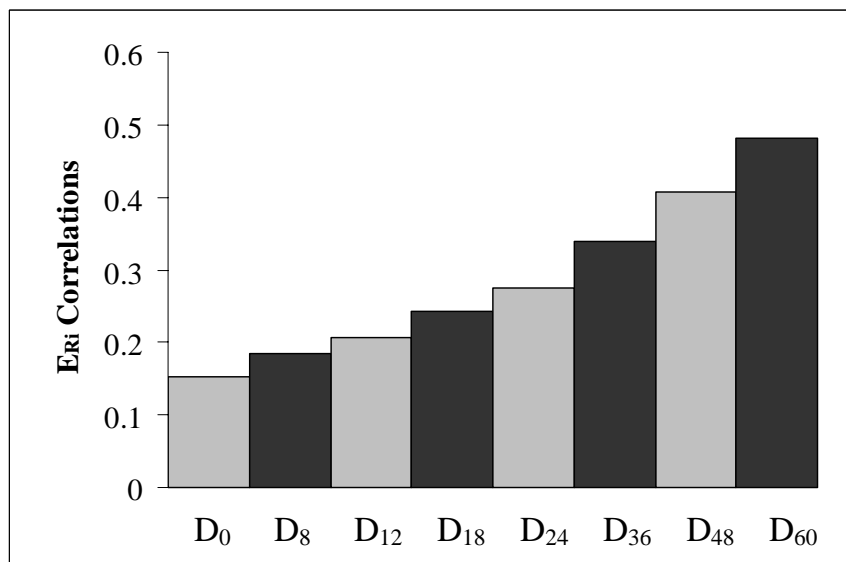


**Figure 39. E<sub>RI</sub> correlation with deflections (FD)**

### ANN-Based FD Backcalculation Models

Backpropagation-type neural networks were used to develop ANN structural models with different network architectures for predicting the pavement layer moduli ( $E_{AC}$ , and  $E_{RI}$ ) of FD flexible pavement systems. The backcalculation models were first developed based on the necessary number of deflection inputs determined by correlations. Four different deflection-based backcalculation models were developed based on correlation statistics: four-, six-, seven-, and eight-deflection ANN models. Second, each of these models was separately used to predict  $E_{AC}$  of the AC layer and the  $E_{RI}$  value of the subgrade layer. Finally, for each model, two sub-

models were developed by FWD load level. The developed models were either for 9-kip FWD loading or for 5–21 kip FWD loading (variable FWD load level). The summary of all ANN models can be seen in Table 9 below. To train the ANN models, a training data file was formed using the 30,000 ILLI-PAVE runs. Of these, 1,500 data sets were set aside for use as an independent testing set to validate the performance of the trained ANN model. Neural network architecture with two hidden layers was exclusively chosen for the FD models developed in this study. This was in accordance with the satisfactory results previously obtained with these types of networks because of their ability to better facilitate the nonlinear functional mapping (Ceylan 2002).

Several network architectures with two hidden layers were trained for predicting the properties of the pavement layer moduli with one output node (either  $E_{AC}$  or  $E_{Ri}$ ). Overall, the training and testing MSEs decreased as the networks grew in size with an increasing number of neurons in the hidden layers. The error levels for both the training and testing sets matched closely when the number of hidden nodes approached 60, as in the case of 60-60-1 architecture (60 hidden nodes, and 1 output node, respectively).

**Table 9. FD-ANN models input/output configuration**

| <b>Model</b>                                  | <b>Inputs</b>   | <b>Output</b> |
|---|---|---------------|
| <b>FD-<math>E_{AC}</math>-(4)-(9-kip)</b>     | $D_0, D_{12}, D_{24}, D_{36}, h_{AC}$                                       | $E_{AC}$      |
| <b>FD-<math>E_{AC}</math>-(6)-(9-kip)</b>     | $D_0, D_{12}, D_{24}, D_{36}, D_{48}, D_{60}, h_{AC}$                       | $E_{AC}$      |
| <b>FD-<math>E_{AC}</math>-(7)-(9-kip)</b>     | $D_0, D_8, D_{12}, D_{18}, D_{24}, D_{36}, D_{60}, h_{AC}$                  | $E_{AC}$      |
| <b>FD-<math>E_{AC}</math>-(8)-(9-kip)</b>     | $D_0, D_8, D_{12}, D_{18}, D_{24}, D_{36}, D_{48}, D_{60}, h_{AC}$          | $E_{AC}$      |
| <b>FD-<math>E_{Ri}</math>-(4)-(9-kip)</b>     | $D_0, D_{12}, D_{24}, D_{36}, h_{AC}$                                       | $E_{Ri}$      |
| <b>FD-<math>E_{Ri}</math>-(6)-(9-kip)</b>     | $D_0, D_{12}, D_{24}, D_{36}, D_{48}, D_{60}, h_{AC}$                       | $E_{Ri}$      |
| <b>FD-<math>E_{Ri}</math>-(7)-(9-kip)</b>     | $D_0, D_8, D_{12}, D_{18}, D_{24}, D_{36}, D_{60}, h_{AC}$                  | $E_{Ri}$      |
| <b>FD-<math>E_{Ri}</math>-(8)-(9-kip)</b>     | $D_0, D_8, D_{12}, D_{18}, D_{24}, D_{36}, D_{48}, D_{60}, h_{AC}$          | $E_{Ri}$      |
| <b>FD-<math>E_{AC}</math>-(4)-(5-21 kips)</b> | $D_0, D_{12}, D_{24}, D_{36}, h_{AC}, P_{FWD}$                              | $E_{AC}$      |
| <b>FD-<math>E_{AC}</math>-(6)-(5-21 kips)</b> | $D_0, D_{12}, D_{24}, D_{36}, D_{48}, D_{60}, h_{AC}, P_{FWD}$              | $E_{AC}$      |
| <b>FD-<math>E_{AC}</math>-(7)-(5-21 kips)</b> | $D_0, D_8, D_{12}, D_{18}, D_{24}, D_{36}, D_{60}, h_{AC}, P_{FWD}$         | $E_{AC}$      |
| <b>FD-<math>E_{AC}</math>-(8)-(5-21 kips)</b> | $D_0, D_8, D_{12}, D_{18}, D_{24}, D_{36}, D_{48}, D_{60}, h_{AC}, P_{FWD}$ | $E_{AC}$      |
| <b>FD-<math>E_{Ri}</math>-(4)-(5-21 kips)</b> | $D_0, D_{12}, D_{24}, D_{36}, h_{AC}, P_{FWD}$                              | $E_{Ri}$      |
| <b>FD-<math>E_{Ri}</math>-(4)-(5-21 kips)</b> | $D_0, D_{12}, D_{24}, D_{36}, D_{48}, D_{60}, h_{AC}, P_{FWD}$              | $E_{Ri}$      |
| <b>FD-<math>E_{Ri}</math>-(4)-(5-21 kips)</b> | $D_0, D_8, D_{12}, D_{18}, D_{24}, D_{36}, D_{60}, h_{AC}, P_{FWD}$         | $E_{Ri}$      |
| <b>FD-<math>E_{Ri}</math>-(4)-(5-21 kips)</b> | $D_0, D_8, D_{12}, D_{18}, D_{24}, D_{36}, D_{48}, D_{60}, h_{AC}, P_{FWD}$ | $E_{Ri}$      |

### Noise-Introduced ANN-Based FD Backcalculation Models

In addition to the training and testing sets prepared for backcalculation models, more ANN training sets were generated by introducing  $\pm 2\%$ ,  $\pm 5\%$  and  $\pm 10\%$  noise to the FWD deflection data used in backcalculation models (see Table 9). The purpose of introducing noisy patterns in the training sets was to develop more robust networks that can tolerate the noisy or inaccurate deflection patterns collected from the FWD deflection basins. The following procedure was followed when introducing noise in the trained ANN models. The ILLI-PAVE solution database was first partitioned to create training sets of 28,500 training patterns and an independent testing

set of 1,500 patterns. Uniformly distributed random numbers in the range of  $\pm 2\%$ ,  $\pm 5\%$ , and  $\pm 10\%$  noise patterns were individually generated. After adding randomly selected noise values to only the pavement surface deflections, new training data sets were developed for each noisy training set. By repeating the noise introduction procedure, three more training data sets were formed for each backcalculation model. Including the original training set with no noise in it, a total of 115,500 patterns were used to train the noise-introduced ANN backcalculation models.

### **ANN-Based FD Forward Calculation Models**

Backpropagation-type neural network models were designed to develop ANN-based tools for predicting the critical pavement responses and pavement surface deflections based on the known deflection basins and AC layer thickness. In forward calculation models, the network-input layer consisted of  $h_{AC}$  and the deflection parameters. The output variables of this model were the critical pavement responses of strains and the subgrade deviator stress under the standard 9-kip FWD or variable FWD loading (within the range of 5–21 kips). The pavement surface deflections ( $D_0$ ,  $D_8$ ,  $D_{12}$ ,  $D_{18}$ ,  $D_{24}$ ,  $D_{36}$ ,  $D_{48}$ , and  $D_{60}$ ) were typically obtained from FWD tests at several different offset locations at the drop location (0) and at radial offsets of 8 inches, 12 inches, 18 inches, 24 inches, 36 inches, 48 inches, and 60 inches. These ANN-based FC models could rapidly predict the ILLI-PAVE responses directly from pavement surface deflections, thus bypassing the complicated finite element analysis sequence that usually require a high degree of expertise in the input and output of the problem.

## Performance of FD-ANN Models

To evaluate the performance of the developed FD-ANN models, AAE and RMSE values were calculated. In addition, goodness-of-fit is a commonly used approach to evaluate the performance of these models. ANN predictions for the 1,500 independent testing set fell on the line of equality for the two pavement layer moduli, thus indicating a proper training and exceptional performance of the ANN model. AAEs were calculated as sum of the individual absolute errors divided by the 1,500 independent testing patterns. The AAE for the AC layer moduli was around 0.60% (9-kip, 4-deflection model) and the AAE for the  $E_{Ri}$  was around 0.49% (9-kip, 4-deflection model). The AAE values for each of the developed backcalculation FD-ANN models are summarized in Table 10. Figure D.1 to Figure D.32 in Appendix D summarize the performance and accuracy of ANN-based  $E_{AC}$  and  $E_{Ri}$  predictions. Robust (noisy) networks could tolerate the differences between the actual field values and the fixed material property values assigned for AC and subgrade layers in the ILLI-PAVE 2000 model. Backcalculation models without noise were sensitive to even very small changes in the deflection values used to train them. Therefore, different noise levels were introduced to the FWD deflection values to develop robust backcalculation models. Because of the noise introduction, the 1,500 independent testing data had more scatter around the line of equality and both the MSE and AAE values increased for the robust ANN models (see Appendix D). However, the confidence interval of the input data increased. Figures in Appendix D show the performance of noise-introduced robust networks for predicting the layer moduli of FD flexible pavement systems.

Table 11 shows the AAE values of noise-introduced ANN models. The AAE value increased from 0.60% to 1.71% in the FD 4-deflection model (9-kip) for a 2% noise level, from 0.60% to 4.40% for a 5% noise level, and from 0.60% to 8.11% for a 10% noise level for predicting the AC layer moduli. A similar trend is observed in the results for other models (see Table 11). Considering the 5% and 10% level of noise introduced in the FWD deflection data, the performance of the robust backcalculation models can still be considered superior, which is an indicator of the powerful function approximation/fitting by the ANN models. For analyzing FWD field data using the backcalculation models, such as those developed in this study, it is suggested to consider at least 2%–3% of noise in the deflection basins instead of using backcalculation models that have no noise in them. Selecting the appropriate level of noise depends on the quality of the FWD data. Factors such as surface conditions of the pavement, the “overall condition” of the FWD machine used to collect the deflection data, and the reasonableness of the backcalculated modulus values are important factors to consider.

The AAE values for forward models were 0.91% for predicting  $\epsilon_{AC}$  and 1.01% for  $\epsilon_{SG}$ . The AAE value for the critical deviator stresses on top of the subgrade layer was approximately 2.77% (see Table 12). Low error values indicate the proper training and prediction performance of the ANN backcalculation models developed in this study. Figure D.33 to Figure D.80 show the prediction accuracy for ANN models. It should be restated that the forward calculation models developed to predict the critical pavement responses of  $\epsilon_{AC}$ ,  $\epsilon_{SG}$ , and  $\sigma_D$  directly from the FWD deflection data eliminates the need for predicting the pavement layer moduli and then computing the critical pavement responses needed for pavement analysis and design. The directness of this approach saves invaluable time in analyzing the pavement sections using the FWD deflection basins.

A major benefit of applying the developed ANN-based backcalculation techniques in routine FWD evaluations will come from the high-speed data processing and analyses that can be performed in the field. The ANN models developed in this study are approximately two million times faster than the ILLI-PAVE 2000 finite element model solutions and they do not require lengthy and detailed finite element pre- and post-processing tasks. This aspect alone makes accurate nonlinear stress-dependent geomaterial characterizations possible and practically applicable in FWD backcalculation. With the current move toward adopting a Rolling Wheel Deflectometer (RWD)-type FWD-testing-on-the-run concept, the time saved using the ANN models can be invaluable to the pavement engineer for evaluating hundreds or thousands of FWD/RWD test scenarios and data for a network-level testing. The rapid prediction ability of the ANN backcalculation models makes them perfect tools for analyzing the FWD deflection data, and thus assessing the condition of the pavement sections, in real time during the field tests.

**Table 10. Prediction performance of FD-ANN-based backcalculation models (virgin)**

| Load Level  | ANN<br>Deflection<br>Models | AAE (%)  |          |
|-------------|-----------------------------|----------|----------|
|             |                             | $E_{AC}$ | $E_{Ri}$ |
| (9-kip)     | 4-Deflection                | 0.60     | 0.49     |
|             | 6-Deflection                | 0.61     | 0.43     |
|             | 7-Deflection                | 0.62     | 0.31     |
|             | 8-Deflection                | 0.45     | 0.36     |
| (5-21 kips) | 4-Deflection                | 0.63     | 0.87     |
|             | 6-Deflection                | 0.57     | 0.78     |
|             | 7-Deflection                | 0.63     | 0.76     |
|             | 8-Deflection                | 0.59     | 0.86     |

**Table 11. Prediction performance of FD-ANN-based backcalculation models (noise)**

| Noise Level   | ANN<br>Deflection<br>Models | AAE (%)  |          |
|---|-----------------------------|----------|----------|
|   |                             | $E_{AC}$ | $E_{Ri}$ |
| 9-kip<br><br>( $\pm 2\%$ )<br><br><br><br>( $\pm 5\%$ )<br><br><br><br>( $\pm 10\%$ )     | 4-Deflection                | 1.71     | 1.79     |
|   | 6-Deflection                | 0.68     | 5.15     |
|   | 7-Deflection                | 0.72     | 1.27     |
|   | 8-Deflection                | 0.90     | 3.80     |
|   | 4-Deflection                | 4.40     | 6.45     |
|   | 6-Deflection                | 1.52     | 1.78     |
|   | 7-Deflection                | 1.43     | 5.07     |
|   | 8-Deflection                | 1.91     | 2.26     |
|   | 4-Deflection                | 8.11     | 12.68    |
|   | 6-Deflection                | 3.65     | 4.04     |
|   | 7-Deflection                | 3.35     | 8.10     |
|   | 8-Deflection                | 5.47     | 3.81     |
| 5-21 kips<br><br>( $\pm 2\%$ )<br><br><br><br>( $\pm 5\%$ )<br><br><br><br>( $\pm 10\%$ ) | 4-Deflection                | 1.88     | 2.49     |
|   | 6-Deflection                | 2.53     | 2.21     |
|   | 7-Deflection                | 1.05     | 2.40     |
|   | 8-Deflection                | 1.31     | 3.18     |
|   | 4-Deflection                | 3.94     | 7.05     |
|   | 6-Deflection                | 2.67     | 2.72     |
|   | 7-Deflection                | 3.60     | 3.17     |
|   | 8-Deflection                | 3.42     | 2.14     |
|   | 4-Deflection                | 7.89     | 18.46    |
|   | 6-Deflection                | 4.20     | 7.59     |
|   | 7-Deflection                | 4.53     | 7.21     |
|   | 8-Deflection                | 4.39     | 4.72     |

**Table 12. Prediction performance of FD-ANN-based backcalculation models (forward)**

| Load Level  | ANN Deflection Models | AAE (%)         |                 |            |
|-------------|-----------------------|-----------------|-----------------|------------|
|             |                       | $\epsilon_{AC}$ | $\epsilon_{SG}$ | $\sigma_D$ |
| (9-kip)     | 4-Deflection          | 0.91            | 1.01            | 2.77       |
|             | 6-Deflection          | 0.58            | 0.61            | 2.86       |
|             | 7-Deflection          | 0.61            | 0.67            | 2.93       |
|             | 8-Deflection          | 0.49            | 0.86            | 2.90       |
| (5-21 kips) | 4-Deflection          | 1.30            | 1.94            | 3.35       |
|             | 6-Deflection          | 1.30            | 1.85            | 3.52       |
|             | 7-Deflection          | 1.05            | 1.74            | 3.43       |
|             | 8-Deflection          | 1.11            | 1.48            | 3.52       |

### Validation of FD-ANN Models

To demonstrate the applicability of the ANN-based methodology for analyzing existing full-depth flexible pavement sections and to further validate the ANN models, field deflection data were collected from various FWD tests conducted in Illinois. To backcalculate the pavement layer moduli for typical full-depth asphalt pavements having AC thickness and layer properties within the ranges given in Table 13, the following statistical algorithms, currently used by the Iowa DOT for nondestructive pavement evaluation, were also used:

$$AREA = 6(D_0 + 2D_{12} + 2D_{24} + D_{36}) / D_0 \quad (8)$$

$$E_{AC} = 10^{1.85 - (4.90 \text{Log}(D_0 - D_{12}))} + 5.19 \text{Log}(D_0 - D_{24}) - 1.28 \text{Log}(D_{12} - D_{36}) \quad (\text{ksi}) \quad (9)$$

$$E_{Ri} = 24.7 - 5.41D_{36} + 0.31D_{36}^2 \quad (\text{ksi}) \quad (10)$$

In these equations,  $D_x$  refers to surface deflections measured at  $x$  inches offset from the center of load plate. Three full-depth flexible pavement sections selected for field validation were Staley Road, Windsor Road and Carlyle Road sections (K and M2) located in Champaign County, Illinois. All of these sections were tested with a standard 9-kip plate load. Deflections were obtained from FWD tests conducted in March 29, 2000, when the pavement temperature was 51°F. The Windsor Road nondestructive FWD test data were collected in May 18, 1994, at a pavement temperature of 70°F. For Carlyle Road, the AC layer was 9.5 inches thick in section K and M2. The Carlyle pavement temperature measurements ranged from 61°F to 96°F for the different testing times. Four pavement surface deflections of  $D_0$ ,  $D_{12}$ ,  $D_{24}$ , and  $D_{36}$  and  $h_{AC}$  of these four field sites were used in the FD 4-deflection model to predict the  $E_{AC}$  and  $E_{Ri}$  values (see Figure 40 to Figure 47). Note that no temperature corrections were made in the predicted AC moduli. Predicted  $E_{AC}$  values correspond to the asphalt concrete moduli for the measured pavement temperature during the FWD testing. The same FWD deflection data were also used in the ILLI-PAVE-based algorithms to compare the calculated moduli with the ANN predictions. The algorithm comparison results are presented in Figure 48 and Figure 49.

**Table 13. The Illinois FD flexible pavement sections**

| Pavement Type | Location                            | $h_{AC}$ (in.) |
|---------------|-------------------------------------|----------------|
| FD            | IL – Carlyle test road (Section K)  | 9.5            |
| FD            | IL – Carlyle test road (Section M2) | 9.5            |
| FD            | IL – Staley Road 2000               | 12             |
| FD            | IL – Windsor Road                   | 9.5            |

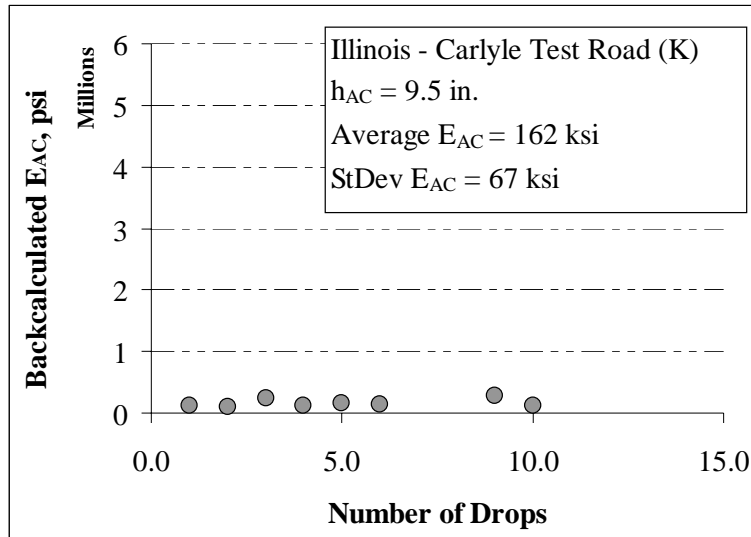


**Figure 40. IL – Carlyle test road (K) FWD deflection basin data  $E_{AC}$  predictions**

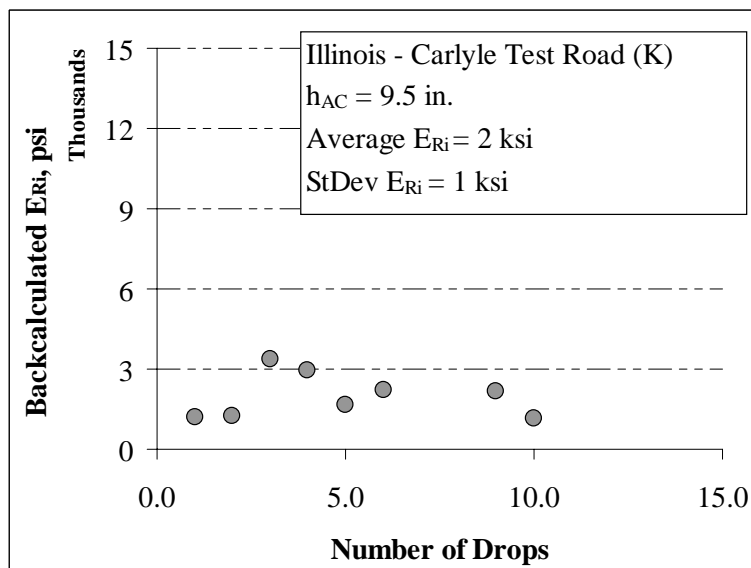


**Figure 41. IL – Carlyle test road (K) FWD deflection basin data  $E_{Ri}$  predictions**

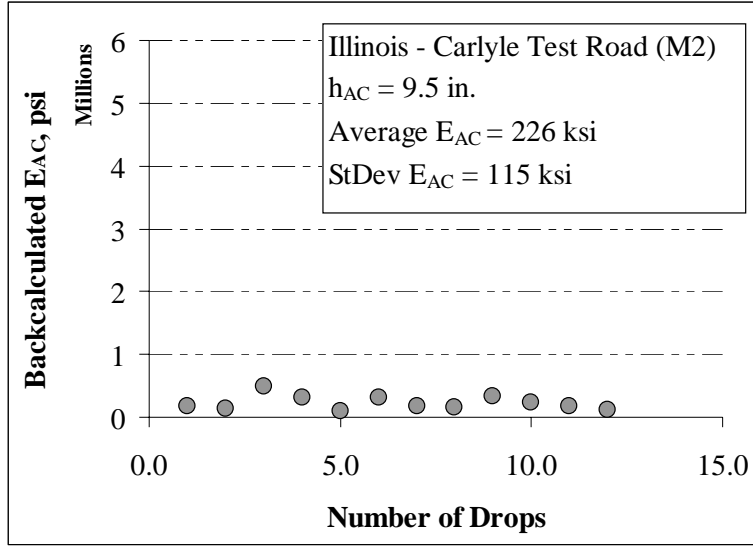


Figure 42. IL – Carlyle test road (M2) FWD deflection basin data  $E_{AC}$  predictions

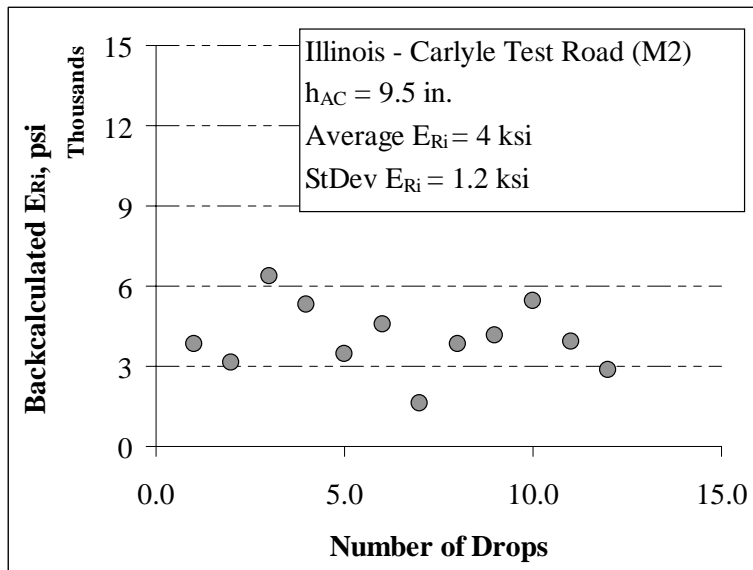


Figure 43. IL – Carlyle test road (M2) FWD deflection basin data  $E_{Ri}$  predictions

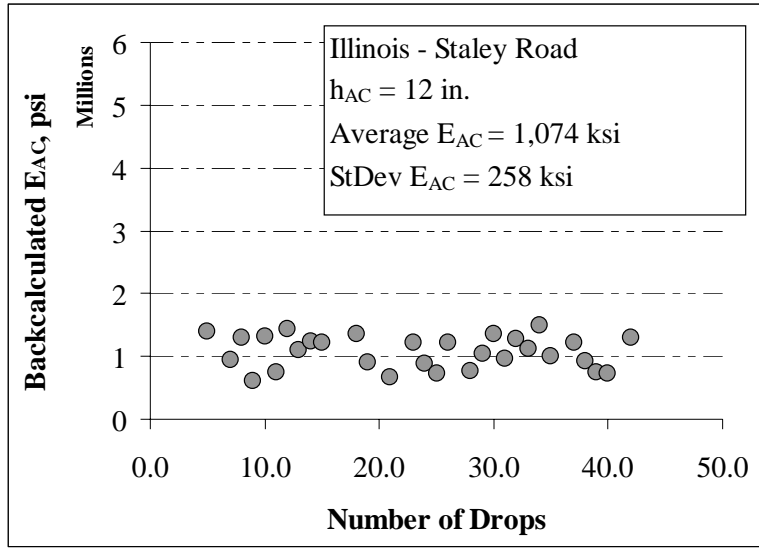


Figure 44. IL – Staley Road FWD deflection basin data  $E_{AC}$  predictions

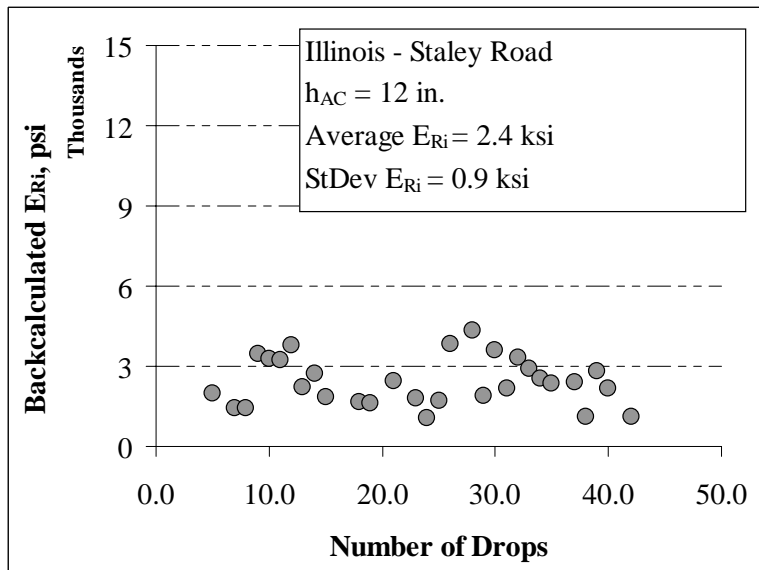


Figure 45. IL – Staley Road FWD deflection basin data  $E_{Ri}$  predictions

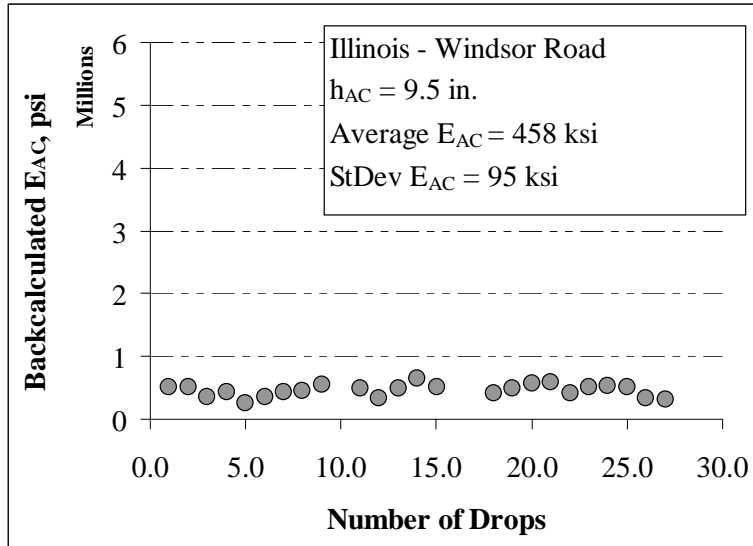


Figure 46. IL – Windsor Road FWD deflection basin data  $E_{AC}$  predictions

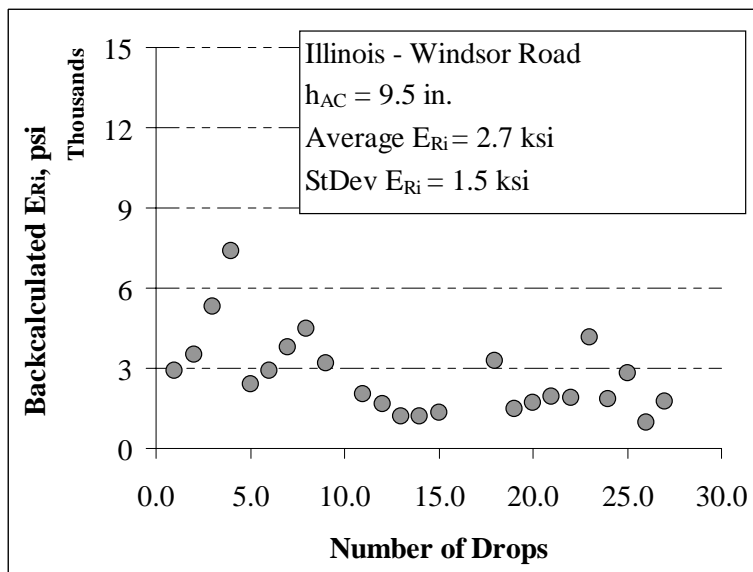
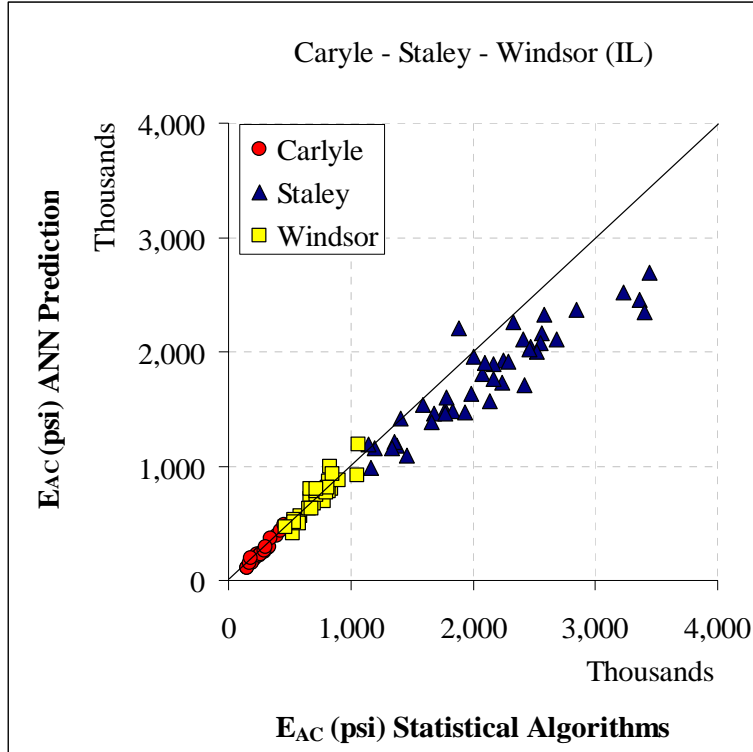
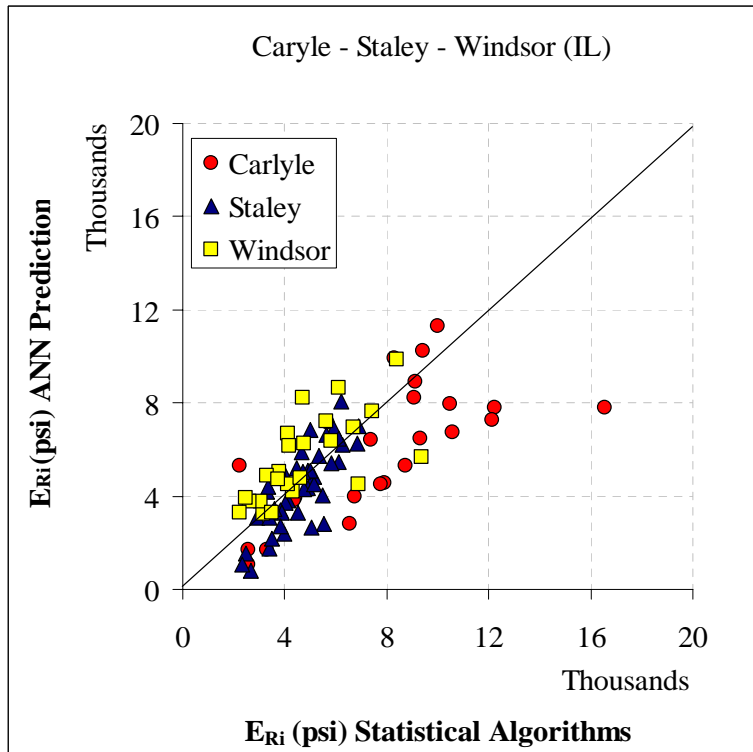


Figure 47. IL – Windsor Road FWD deflection basin data  $E_{Ri}$  predictions



**Figure 48. Full-depth E<sub>AC</sub> prediction comparisons with statistical algorithms**



**Figure 49. Full-depth E<sub>Ri</sub> prediction comparisons with statistical algorithms**

## Case Studies of Individual Pavement Sections – Iowa DOT Data

ANN models were evaluated using actual FWD data from the Iowa DOT. FD systems were identified using the DOT milepost book. The layer thicknesses from the milepost book were entered as inputs for ANN models along with the FWD measurements at these sites. For this study, two sections from Cedar County were selected. Figure 50 to Figure 53 show the prediction of the pavement properties of these sites.

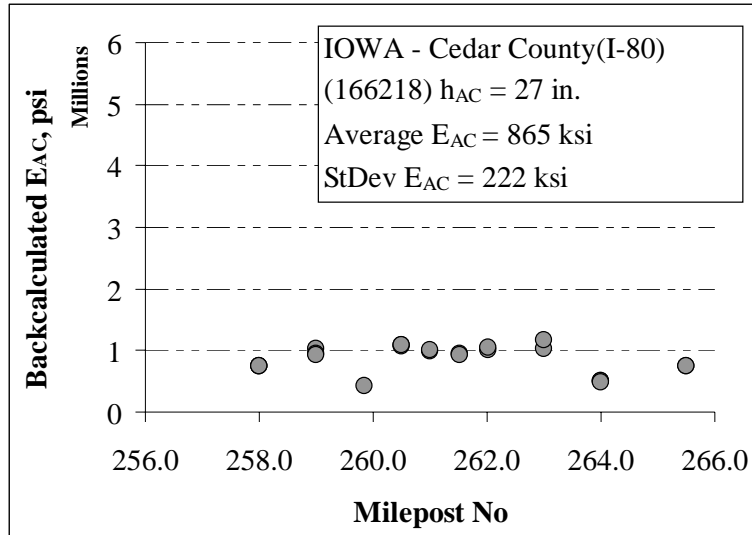


Figure 50.  $E_{AC}$  predictions for IA – Cedar County (I-80 EB) FWD deflection basin data (166218)

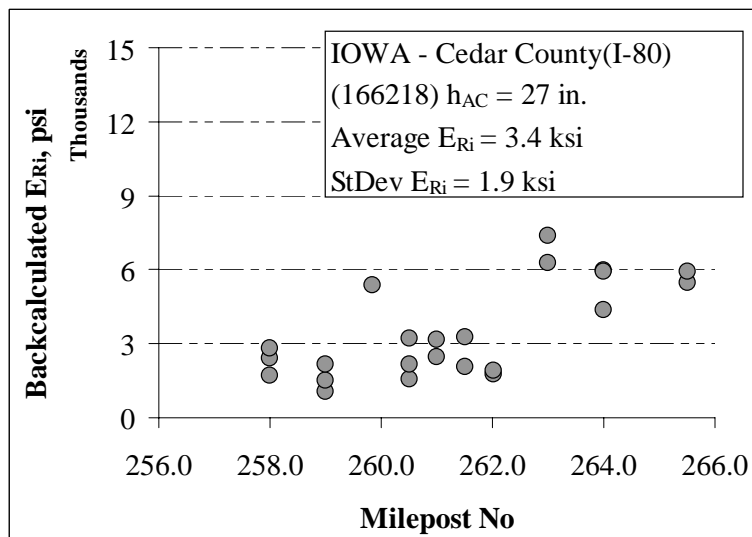
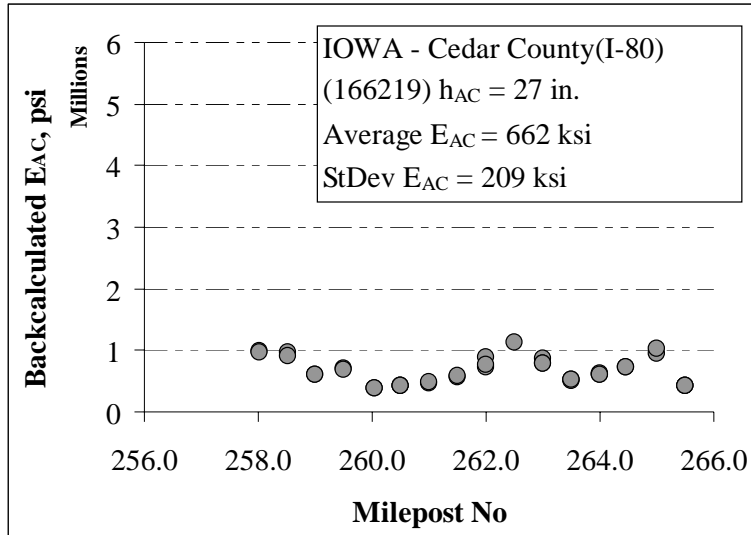
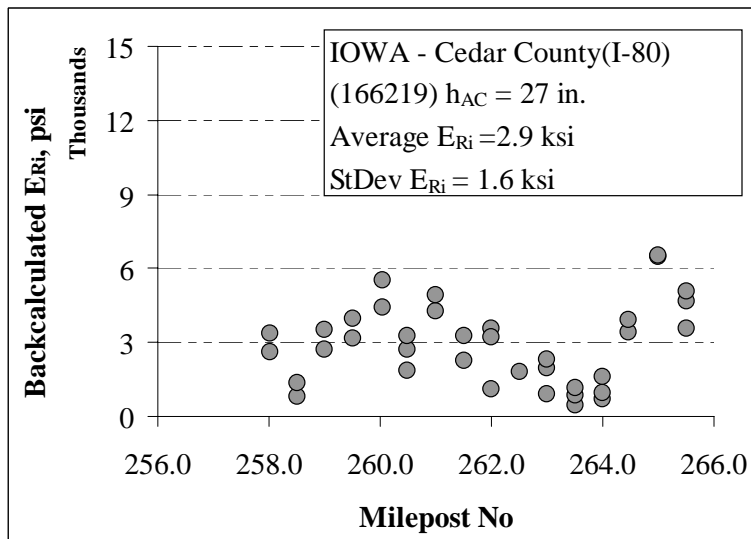


Figure 51.  $E_{Ri}$  predictions for IA – Cedar County (I-80 EB) FWD deflection basin data (166218)



**Figure 52.  $E_{AC}$  predictions for IA – Cedar County (I-80 WB) FWD deflection basin data (166219)**



**Figure 53.  $E_{Ri}$  predictions for IA – Cedar County (I-80 WB) FWD deflection basin data (166219)**

### ANN Models for Full-Depth Flexible Pavement Systems – Summary and Conclusions

#### Summary

ANN-based backcalculation and forward calculation pavement structural models were developed using the ILLI-PAVE full-depth asphalt finite element solutions with nonlinear, stress-dependent subgrade soil properties. The ANN models described in this section successfully predicted the

pavement layer moduli and critical responses computed by the ILLI-PAVE finite element model and thus satisfied the main objective of this study.

### *Conclusions*

Major findings for prediction of elastic modulus of asphalt concrete layer ( $E_{AC}$ ) for FD pavement systems can be summarized as follows:

- In total, eight different ANN-based backcalculation models were developed for  $E_{AC}$ : FD- $E_{AC}$ -(4-deflection)-(9 kip), FD - $E_{AC}$ -(6-deflection)-(9 kip), FD- $E_{AC}$ -(7-deflection)-(9 kip), FD - $E_{AC}$ -(8-deflection)-(9 kip), FD - $E_{AC}$ -(4-deflection)-(5-21 kips), FD- $E_{AC}$ -(6-deflection)-(5-21 kips), FD- $E_{AC}$ -(7-deflection)-(5-21 kips), and FD- $E_{AC}$ -(8-deflection)-(5-21 kips).
- The AAE values of ANN trainings for all the FD-ANN  $E_{AC}$  prediction models were less than one percent.
- The 4-deflection model gave slightly better results in terms of standard deviation.
- In general, the standard deviations were low for all the models.
- The ANN-based  $E_{AC}$  predictions were consistent with the closed-form algorithms.
- Noise-introduced FD-ANN models were successfully developed ( $\pm 2\%$ ,  $\pm 5\%$ , and  $\pm 10\%$ ) for predicting  $E_{AC}$ .
- When the noise introduced in the FWD deflection data increased, the AAE (%) value also increased as expected.

Major findings for prediction of subgrade soil break point resilient modulus ( $E_{Ri}$ ) can be summarized as follows:

- In total, eight different ANN-based backcalculation models were developed for  $E_{Ri}$ : FD- $E_{Ri}$ -(4-deflection)-(9 kip), FD- $E_{Ri}$ -(6-deflection)-(9 kip), FD- $E_{Ri}$ -(7-deflection)-(9 kip), FD- $E_{Ri}$ -(8-deflection)-(9 kip), FD- $E_{Ri}$ -(4-deflection)-(5-21 kips), FD- $E_{Ri}$ -(6-deflection)-(5-21 kips), FD- $E_{Ri}$ -(7-deflection)-(5-21 kips), and FD- $E_{Ri}$ -(8-deflection)-(5-21 kips).
- The AAE values of ANN predictions were less than 1 percent.
- The scattering was higher compared to  $E_{AC}$  predictions as expected because the subgrade variability was expected to be higher.
- The 6-deflection models gave better results than the 4-deflection models in terms of standard deviations.
- In general, the standard deviations were higher compared to  $E_{AC}$ .
- The nonlinear stress dependent behavior of subgrade soils was confirmed with variable FWD load levels.
- Also, noise-introduced models were developed ( $\pm 2\%$ ,  $\pm 5\%$ , and  $\pm 10\%$ ) for  $E_{Ri}$ .
- When the noise introduced in the deflection data increased, the AAE (%) value also increased as expected.

Major findings related to ANN FC models can be summarized as follows:

- Different ANN-based forward calculation models were developed for prediction of critical pavement responses of strains and the subgrade deviator stress.
- Mean AAE values of ANN predictions are around 1%, 1%, and 3% for  $\epsilon_{AC}$ ,  $\epsilon_{SG}$ , and  $\sigma_D$ , respectively.

## ANN MODELS FOR RIGID PAVEMENT (RGD) SYSTEMS

Backcalculated pavement layer parameters play a crucial role in pavement management systems in project-specific and network-level pavement testing and evaluation for the Iowa DOT to make decisions on overall maintenance and budget plans. The overall objective of this project is to rapidly analyze a large number of pavement deflection basins needed for routine pavement evaluation for both project-specific and network-level FWD testing. The efforts related to the flexible pavement analysis were addressed in the previous sections. This section of the report documents the research efforts related to the development of ANN models for rapid and accurate predictions of  $E_{PCC}$ ,  $k_s$ , radius of relative stiffness of the pavement system (RRS), and  $\sigma_{PCC}$  at the bottom of the PCC layer values from FWD deflection data for RGD systems. When compared with the other approaches, the trained ANN models successfully predicted the pavement layer moduli and critical responses with several additional advantages.

### Review of Existing RGD Layer Moduli Backcalculation Models

Several methods are available for backcalculating the PCC slab, base, and subgrade moduli or  $k_s$  from the FWD deflection data. Each method has its own strengths and limitations. The following procedures are typically considered for rigid pavements:

- Backcalculation software and procedures based on elastic layered analysis
- Backcalculation procedures specifically developed for rigid pavements that are based on slab on elastic solid or slab on dense-liquid models that can further be classified as:
  - AREA method-based procedures
  - Best-fit-based procedures

Table 14 and Table 15 summarize the significant features of several commonly used linear and nonlinear elastic layer-based backcalculation software, respectively.

**Table 14. Linear elastic layer analysis backcalculation programs**

| <b>Program name</b> | <b>Developed by</b>                               | <b>Calculation subroutine</b> | <b>Rigid layer analysis</b> | <b>Layer interface analysis</b> | <b>Maximum number of layers</b>                                 | <b>Convergence routine</b>   |
|---------------------|---|-------------------------------|-----------------------------|---------------------------------|---|------------------------------|
| BAKFAA              | FAA   | LEAF                          | Yes                         | Variable                        | 10  | RMS                          |
| BISDEF              | U.S. Army Corps of Engineers-WES                  | BISAR (Proprietary)           | Yes                         | Variable                        | Cannot exceed no. of deflections. Works best for three unknowns | Sum of sq. of absolute error |
| CHEVDEF             | U.S. Army Corps of Engineers-WES                  | CHEVRON                       | Yes                         | Fixed (rough)                   | Cannot exceed no. of deflections. Works best for three unknowns | Sum of sq. of absolute error |
| ELSDEF              | Texas A&M Univ.; U.S. Army Corps of Engineers WES | ELSYM5                        | Yes                         | Fixed (rough)                   | Cannot exceed no. of deflections. Works best for three unknowns | Sum of sq. of absolute error |
| MODULUS             | Texas Trans Institute                             | WESLEA                        | Yes Variable                | Fixed                           | Up to four unknowns, plus stiff layer                           | Sum of relative sq. error    |
| WESDEF              | U.S. Army Corps of Engineers-WES                  | WESLEA                        | Yes                         | Variable                        | Up to five layers   | Sum of sq. of absolute error |
| MICHBACK            | Michigan State                                    | CHEVRON                       | Yes                         | Fixed                           | Up to four unknowns, plus stiff layer                           | Sum of relative sq. error    |

All programs use multilayer elastic theory during the backcalculation. All programs, except MODULUS, use an iterative backcalculation method; MODULUS uses a database search procedure. "Seed" moduli are required for all programs. A range of acceptable modulus values is required for all programs except MICHBACK. All programs allow the user to fix the modulus value for a layer. All programs contain an error convergence function.

**Table 15. Nonlinear elastic layer analysis backcalculation programs**

| <b>Program name</b> | <b>Developed by</b>                | <b>Calculation subroutine</b> | <b>Rigid layer analysis</b> | <b>Layer interface analysis</b> | <b>Maximum number of layers</b>            | <b>Convergence routine</b>       |
|---------------------|------------------------------------|-------------------------------|-----------------------------|---------------------------------|--|----------------------------------|
| BOUSDEF             | Zhou, et al.<br>Oregon State Univ. | Odemark-Boussinesq            | Yes                         | Fixed (rough)                   | Five, works best for three unknowns        | Sum of percent errors            |
| ELMOD/<br>ELCON     | P. Ullidtz,<br>Dynatest            | Odemark-Boussinesq            | Yes<br>(Variable)           | Fixed (rough)                   | Up to four, excluding rigid layer          | Relative error on five sensors   |
| EMOD                | PCS/LAW                            | CHEVRON                       | No                          | Fixed (rough)                   | Three                                      | Sum of relative sq. error        |
| EVERCALC            | J. Mahoney et al.                  | CHEVRON                       | Yes                         | Fixed (rough)                   | Three, excluding layer                     | Sum of absolute error            |
| FREDDI              | W. Uddin                           | BASINPT                       | Yes<br>(Variable)           | Fixed (rough)                   | Unknown                                    | Unknown                          |
| ISSEM4              | R. Stubstad                        | ELSYM5                        | No                          | Fixed (rough)                   | Four                                       | Relative defl. errors            |
| MODCOMP             | L. Irwin<br>Szebenyi               | CHEVRON                       | Yes                         | Fixed (rough)                   | Two to 15 layers, max. five unknown layers | Relative defl. errors at sensors |
| PADAL               | S. F. Brown et al.                 | Unknown                       | Unknown                     | Fixed                           | Unknown                                    | Sum of relative sq. error        |
| RoSy<br>DESIGN      | Carl Bro<br>Group                  | Odemark-Boussinesq            | No                          | Fixed (rough)                   | Up to four layers                          | Relative error on six sensors    |

All programs, except BOUSDEF and ELMOD/ELCON, use multilayer elastic theory during the backcalculation. BOUSDEF and ELMOD/ELCON use the Odemark-Boussinesq method. All programs use an iterative backcalculation method. Nonlinear analysis for ELMOD/ELCON, EMOD, and PADA is limited to the subgrade. “Seed” moduli are required for all programs except ELMOD/ELCON and FREDDI. With the exception of ELMOD/ELCON, a range of acceptable modulus values is required. All programs, except FREDDI and PADAL, allow users to fix the modulus value for a layer. Only BOUSDEF contains an error convergence function.

### **ISLAB2000 Finite Element Program**

Today a variety of finite element programs are available for the analysis and design of pavement systems. The ISLAB2000 finite element program, extensively tested and validated for over 20 years, has been used as an advanced structural model for solving the responses of the rigid pavement systems and generating a large knowledge database. ANN-based models trained with

the results from the ISLAB2000 solutions were later developed for both backcalculation and forward calculation (i.e., prediction of critical pavement responses directly from FWD deflection data).

This chapter contains a detailed review of the database structure and data preprocessing in the development of ANN models. Data preprocessing is the prelude to the ANN modeling process, and it involves transferring the original database into formats appropriate for the modeling purposes.

### *Selection of the Forward Calculation Methodology*

A sensitivity study was first performed to analyze the differences in the slab-center deflections ( $D_0$ , the maximum FWD deflection) obtained from ISLAB2000, DIPLOMAT, and KENSLABS programs and Westergaard’s closed-form solutions. For this purpose, different combinations of  $E_{PCC}$ ,  $h_{PCC}$ , and  $k_s$ , to represent a variety of pavement structural configurations, were defined and the  $D_0$  deflections obtained from ISLAB2000, DIPLOMAT, and KENSLABS programs and Westergaard’s solutions were compared with each other (see Figure 54). The pavement surface deflection profiles obtained from ISLAB2000, DIPLOMAT, and KENSLABS models for three pavement configurations are presented in Figure 54 and Figure 55. The results obtained from different models are consistent.

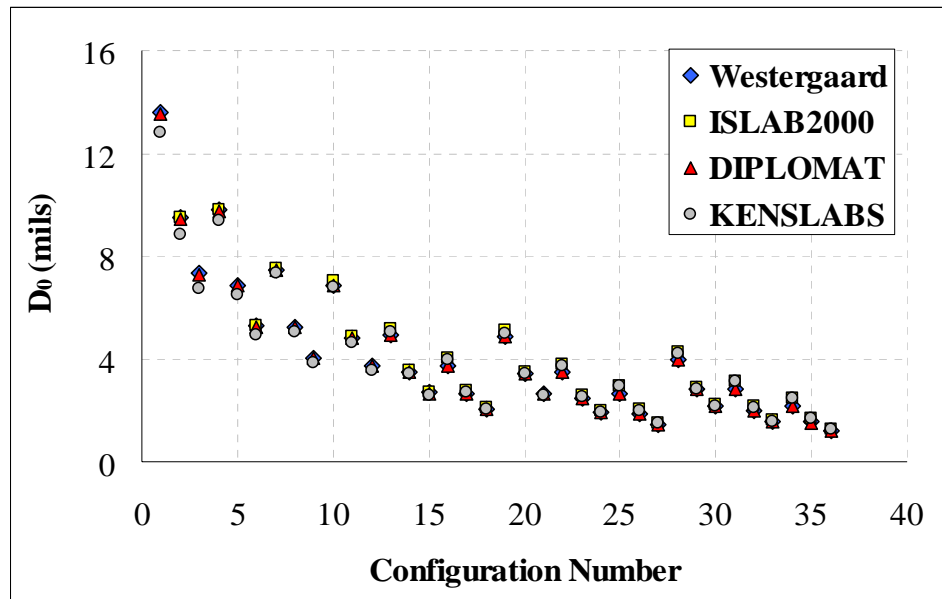


**Figure 54. Comparison of ISLAB2000, DIPLOMAT, KENSLAB program results and Westergaard theoretical solutions**

The ISLAB2000 finite element program was chosen for solving the responses of the rigid pavement systems and generating the database because of the ease of modeling and flexibility in the analysis compared to other methods. ISLAB2000 also allows the user to define an “unlimited” number of nodes, pavement layers, and wheel loads. In addition, ISLAB2000 can

analyze partially bonded layers, the effects of nonlinear temperature distribution throughout the constructed layers, the mismatched joints and cracks, and the effect of voids under the slab.

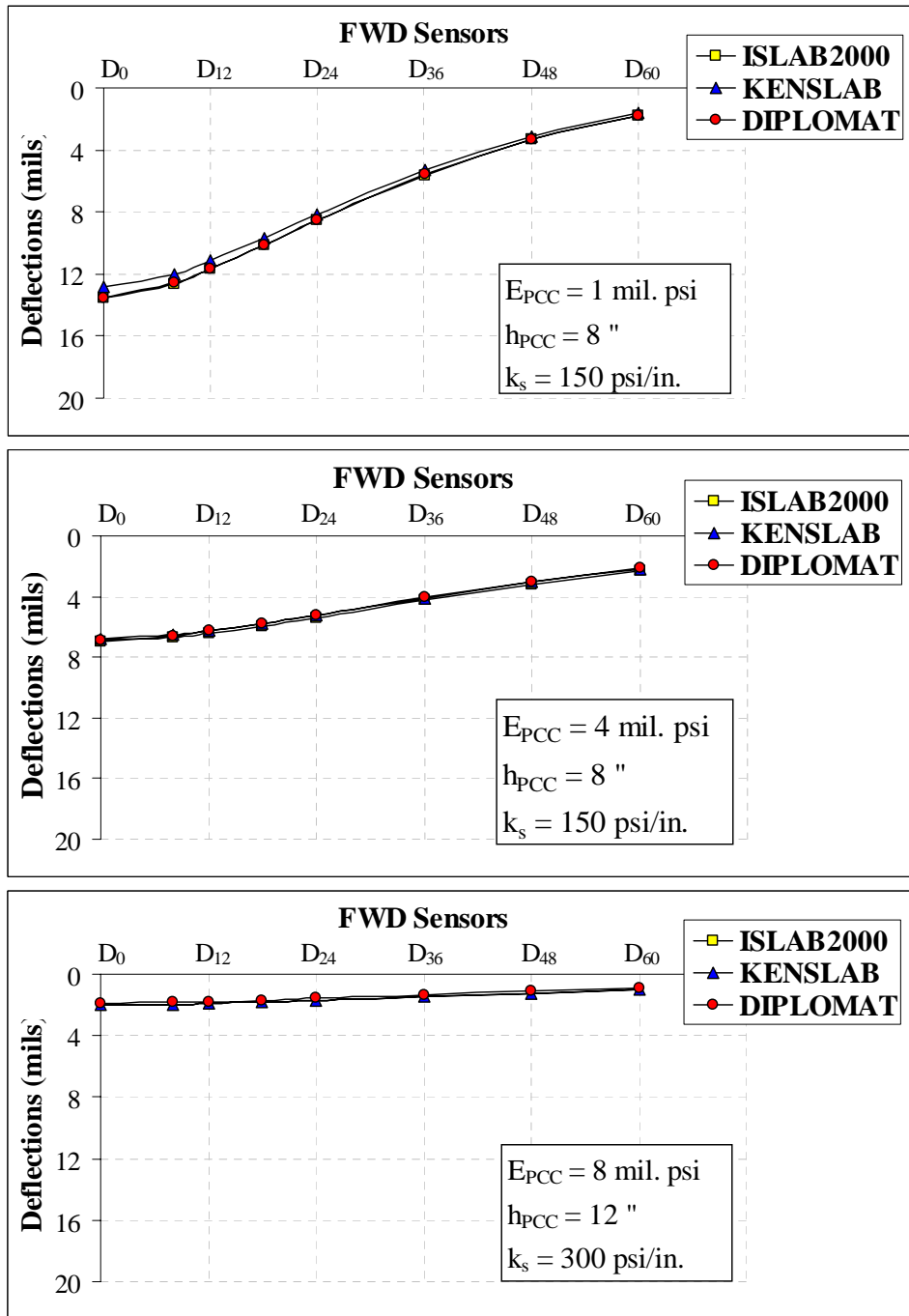


**Figure 55. Comparison of ISLAB2000, DIPLOMAT, and KENSLAB finite element model solutions for different pavement and foundation configurations**

## Generating ISLAB2000 Finite Element Solution Database

A total of 51,714 ISLAB2000 runs were generated by modeling slab-on-grade concrete pavement systems. A single slab layer resting on a Winkler foundation was analyzed in all cases. Concrete pavements analyzed in this study were represented by a six-slab assembly with each slab having dimensions of 20 feet by 20 feet (6.1 m by 6.1 m) (see Figure 56).

To maintain the same level of accuracy in the results for all analyses, a standard ISLAB2000 finite element mesh was constructed for the slab. This mesh consisted of 10,004 elements with 10,209 nodes. The ISLAB2000 solutions database was generated by varying the  $E_{PCC}$ ,  $k_s$ , and  $h_{PCC}$  over a range of values representative of realistic variations in the field. The ranges used in the analyses are shown in Table 16. The Poisson's ratio ( $\mu$ ), the slab width ( $W$ ), the slab length ( $L$ ), PCC unit weight ( $\gamma$ ), and load transfer efficiency (LTE) were set at constant values of 0.15, 20 feet (6.1 m), 20 feet (6.1 m), 0.087 lb/in<sup>3</sup> (2408.15 kg/m<sup>3</sup>), and 50%, respectively. A general view of the ISLAB2000 finite element solution database is shown in Figure 57.

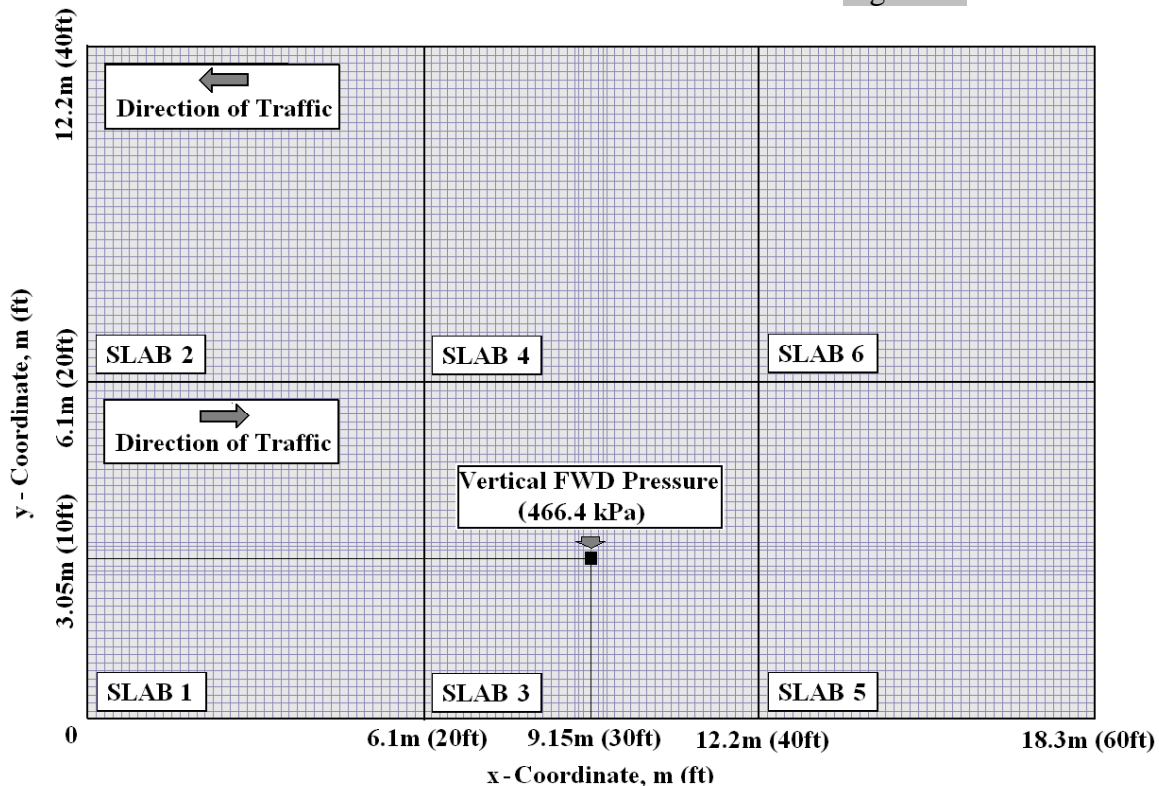
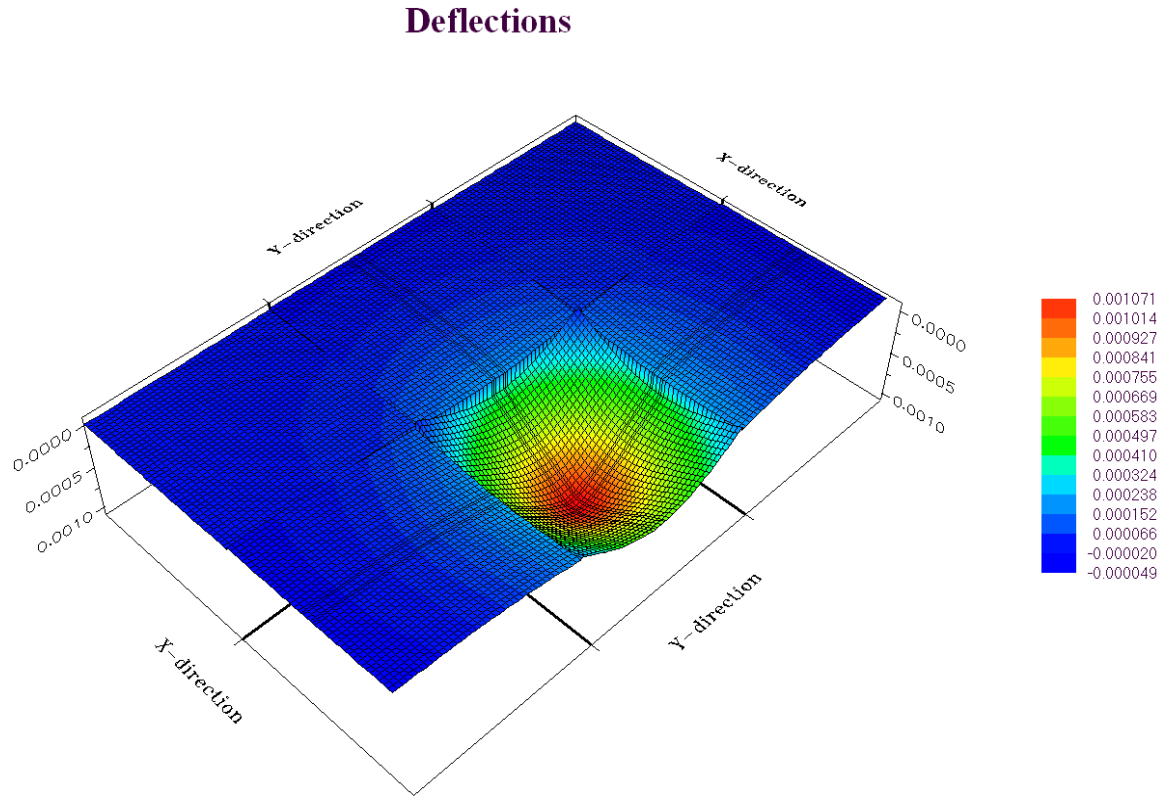


Figure 56. ISLAB2000 finite element model mesh for the six-slab JPCP assembly

**Table 16. Ranges of input parameters used in the ISLAB2000 database generation**

| Pavement System Inputs | Min. Value | Max. Value |
|------------------------|------------|------------|
| $E_{PCC}$ , psi        | 1,000,000  | 15,000,000 |
| $h_{PCC}$ , in.        | 6          | 25         |
| $k_s$ , psi/in.        | 50         | 1,000      |



**Figure 57. A general view of the deflections under 9-kip loading in six-slab assembly**

The DL model, proposed by Winkler (1864), was used to characterize the subgrade behavior in this study. Accurate modeling of subgrade support for pavement systems is not a simple task because many soil types exhibit nonlinear, stress-dependent elasto-plastic behavior especially under the moving heavy wheel loads. Nevertheless, experience in rigid pavements analysis and design has shown that subgrade layer may be modeled as linear elastic because of the lower levels of vertical stresses acting on rigid pavement foundations.

A plate on a DL foundation is the most widely adopted mechanistic idealization for analysis of concrete pavements (NCHRP 2003). Consideration of the critical load transfer phenomena, occurring at the PCC slab joints, and the concomitant development of major distress types, such as faulting, pumping, and corner breaking, are the significant advantages of this approach. The DL foundation is the simplest foundation model and requires only one parameter: the coefficient of subgrade reaction,  $k_s$ , which is the proportionality constant between the applied pressure and

the load plate deflection (Figure 58). Subgrade deformations are local in character; that is, they develop only beneath the load plate. Furthermore, their behavior is considered linear-elastic and deformations are recoverable upon removal of load (NCHRP 2003).

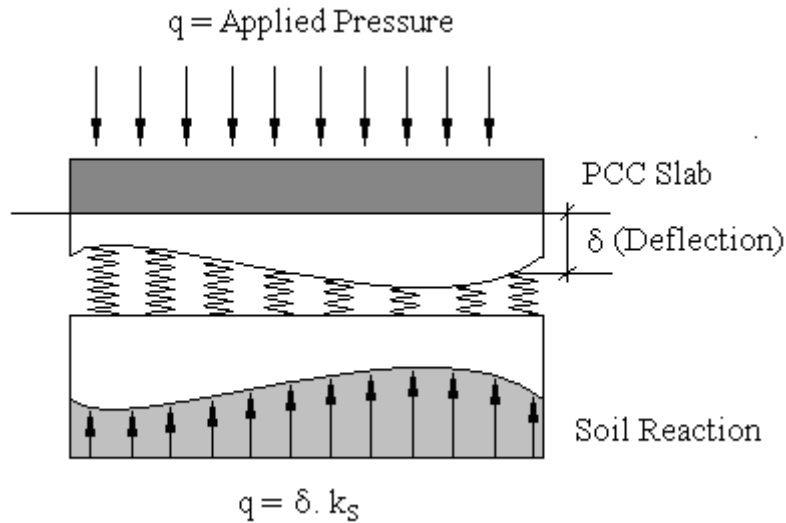


**Figure 58. Winkler foundation and coefficient of subgrade reaction ( $k_s$ )**

### Data Preprocessing for ANN Modeling

The ranges of the pavement surface deflections calculated by ISLAB2000 are given in Table 17. All pavement surface deflection values were normalized between the maximum value of the  $D_0$  (36.26 mils) and the minimum value of  $D_{60}$  (0 mils). According to LeCun (1993), each input variable should be preprocessed so that its mean value, averaged over the entire training set, is close to zero. Thus, inputs were normalized between +2 and -2. In a similar way, outputs were normalized between 0.1 and 0.9 because of the effective ranges of the sigmoid activation function considered in the backpropagation-type ANN trainings.

**Table 17. Ranges of the ISLAB2000 solution database (inputs of the ANN models)**

|                   | $D_0$<br>(mils) | $D_8$<br>(mils) | $D_{12}$<br>(mils) | $D_{18}$<br>(mils) | $D_{24}$<br>(mils) | $D_{36}$<br>(mils) | $D_{48}$<br>(mils) | $D_{60}$<br>(mils) |
|-------------------|-----------------|-----------------|--------------------|--------------------|--------------------|--------------------|--------------------|--------------------|
| <b>Min. Value</b> | 0.29            | 0.29            | 0.28               | 0.27               | 0.27               | 0.25               | 0.22               | 0.00               |
| <b>Max. Value</b> | 36.26           | 33.95           | 31.69              | 27.82              | 23.78              | 16.26              | 10.25              | 6.84               |

### Formation of Data Sets for Training and Testing Sets

The database was separated into training and testing data sets. The testing set was reserved for testing the ANN models only and not used in the training process. ANNs are considered successful only if the system can perform well on the testing set on which the system has not

been trained. All the presented AAE values belong to the testing data sets and show the prediction capability of the developed ANN models described in the following sections.

The total number of the ISLAB2000 runs conducted in this study was 51,714. However, some of the deflections obtained from ISLAB2000, especially  $D_{48}$ ,  $D_{60}$  and the deflections at further offsets, had negative values (upward) due to very low magnitudes of  $E_{PCC}$ ,  $h_{PCC}$ , and  $k_s$  in combination. Therefore, the finite element runs with negative deflections were excluded from the database used for the ANN trainings. In view of irregularity of the data in the database, this part is the crucial step for the model development. To guarantee the reliable performance of neural networks for backcalculation, it is important that quality data be utilized for network training.

The number of patterns included in the ANN trainings was 51,539 for  $k_s$  prediction and 41,026 for  $E_{PCC}$  predictions. For each training the ISLAB2000 solution database was first portioned to create training sets of 49,539 (97.5 %, for  $k_s$ ) and 39,026 (95 % for  $E_{PCC}$ ) and then to an independent, randomly chosen testing set of 2,000 patterns to check the prediction performance of the trained ANN models.

### **ANN-Based RGD Backcalculation Models**

This section presents the modeling framework design and procedures used for the development of ANN models developed in this study. The main objective of ANN modeling in this research was to attain a set of weight matrices, which is the abstracted underlying knowledge from the example data after many loops of training. In ANN modeling, a framework first needs to be designed according to the characteristics of the problem under study. For this purpose, the architecture of each ANN model must be designed, which is the design-making process. This process includes determining the number of layers, the number of neurons in each layer, and the variables to be included in the input layer and output layer. After finishing the ANN architecture design, the ANN architecture needs to be trained and tested.

In this study, mainly two groups of ANN-based backcalculation models were developed, which were RGD- $k_s$  models (for backcalculating  $k_s$ ) and RGD- $E_{PCC}$  models (for backcalculating  $E_{PCC}$ ). FWD deflection readings [ $D_0$  (0 mm),  $D_8$ (203 mm),  $D_{12}$ (304 mm),  $D_{18}$ (457 mm),  $D_{24}$ (610 mm),  $D_{36}$ (914 mm),  $D_{48}$ (1,219 mm), and  $D_{60}$ (1,524 mm)] and  $h_{PCC}$  were used as input parameters in the developed ANN backcalculation models. Separate ANN architectures were used for the backcalculation of the elastic modulus of the slab and the coefficient of subgrade reaction. Four-, six-, seven-, and eight-deflection ANN models were developed for backcalculating the  $k_s$  and  $E_{PCC}$  values (see [Table 18](#)).

**Table 18. RGD-ANN models (virgin) input/output configuration**

| ANN<br>Models       | Input<br>Parameters  | Output<br>Parameter<br>r | AAE<br>(%) | ANN<br>Architecture<br>e |
|---------------------|--|--------------------------|------------|--------------------------|
| RGD- $k_s$ -(4)     | $D_0, D_{12}, D_{24}, D_{36}$  | $k_s$                    | 0.28       | 4-60-60-1                |
| RGD- $k_s$ -(6)     | $D_0, D_{12}, D_{24}, D_{36}, D_{48}, D_{60}$                        | $k_s$                    | 0.20       | 6-60-60-1                |
| RGD- $k_s$ -(7)     | $D_0, D_8, D_{12}, D_{18}, D_{24}, D_{36}, D_{60}$                   | $k_s$                    | 0.19       | 7-60-60-1                |
| RGD- $k_s$ -(8)     | $D_0, D_8, D_{12}, D_{18}, D_{24}, D_{36}, D_{48}, D_{60}$           | $k_s$                    | 0.22       | 8-60-60-1                |
| RGD- $E_{PCC}$ -(4) | $D_0, D_{12}, D_{24}, D_{36} + h_{PCC}$                              | $E_{PCC}$                | 0.34       | 5-60-60-1                |
| RGD- $E_{PCC}$ -(6) | $D_0, D_{12}, D_{24}, D_{36}, D_{48}, D_{60} + h_{PCC}$              | $E_{PCC}$                | 0.32       | 7-60-60-1                |
| RGD- $E_{PCC}$ -(7) | $D_0, D_8, D_{12}, D_{18}, D_{24}, D_{36}, D_{60} + h_{PCC}$         | $E_{PCC}$                | 0.29       | 8-60-60-1                |
| RGD- $E_{PCC}$ -(8) | $D_0, D_8, D_{12}, D_{18}, D_{24}, D_{36}, D_{48}, D_{60} + h_{PCC}$ | $E_{PCC}$                | 0.30       | 9-60-60-1                |

### *Model Architecture*

The selection of ANN architecture is not a straightforward decision-making process. Most of the time, trial, and error combined with engineering judgment are jointly employed to determine the appropriate architecture for a particular problem. Therefore, a sensitivity study was conducted to determine the most appropriate architecture for the backcalculation of the rigid pavement parameters ( $E_{PCC}$  and  $k_s$ ). For this purpose, different architectures were tried to obtain the minimum AAE value which is considered as an indicator of the success of the developed ANN-based backcalculation models. The number of hidden layers, the number of neurons in each hidden layer, the learning rate, and the momentum factor were varied, and the AAE values were compared. The results of the ANN architecture sensitivity study are presented in Figure 59 to Figure 62 and in Figure 63 to Figure 66 for the elastic modulus of concrete layer ( $E_{PCC}$ ) and coefficient of subgrade reaction ( $k_s$ ), respectively. Based on the results of these sensitivity studies, networks with two hidden layers with 60 neurons in each hidden layer were exclusively chosen for all models trained in this study.

Similar to the traditional regression methods, the output variables, variables that appear in the output layer, are the dependent variables, which are defined according to the problem under study. Variables that appear in the input layer are independent variables. To show the individual effect of each deflection (input parameters of developed ANN models) on the rigid pavement parameters (outputs of the developed ANN models), multivariate correlation analyses were conducted.  $R^2$  values obtained from these statistical analyses are presented in Figure 67 and Figure 68. As seen from the results, the correlation between the deflections and elastic modulus of the slab is much higher for the deflections close to the loading point ( $D_0, D_{12}$ ) than the outer deflections ( $D_{48}, D_{60}$ ). However, the opposite is true for the coefficient of subgrade reaction, which is highly correlated with the outer deflections ( $D_{48}, D_{60}$ ). To be able to compare the backcalculated rigid pavement parameters, as mentioned above, four-, six-, seven-, and eight-deflection ANN models were developed in this study. The results are presented in the following sections.

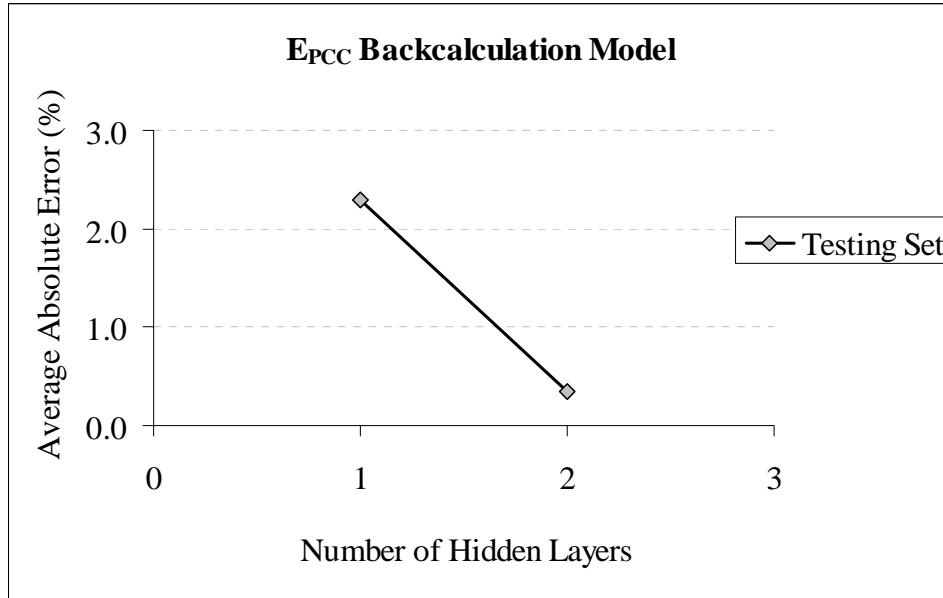


**Figure 59. Sensitivity study results for the number of hidden layers**

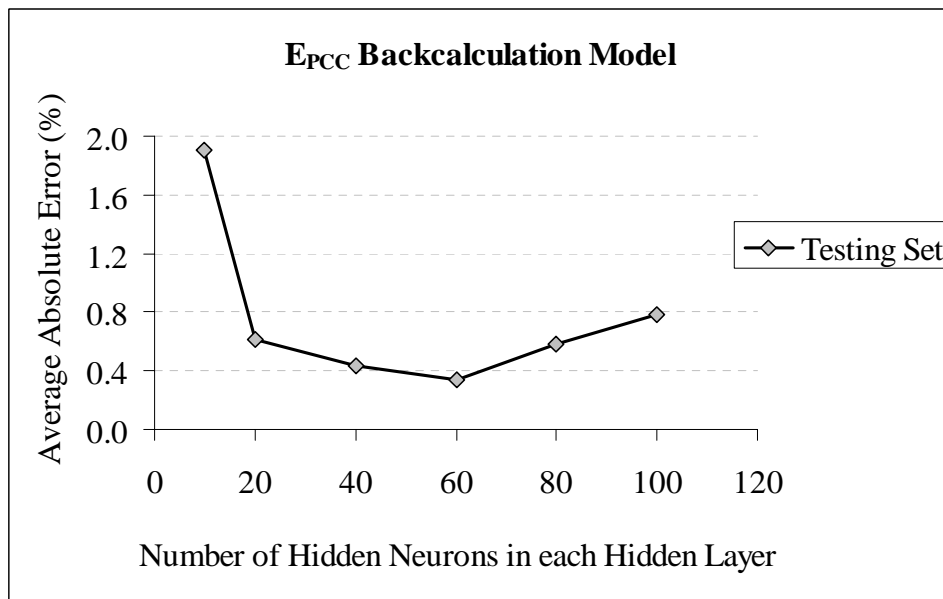


**Figure 60. Sensitivity study results for the number of hidden neurons in each hidden layer**

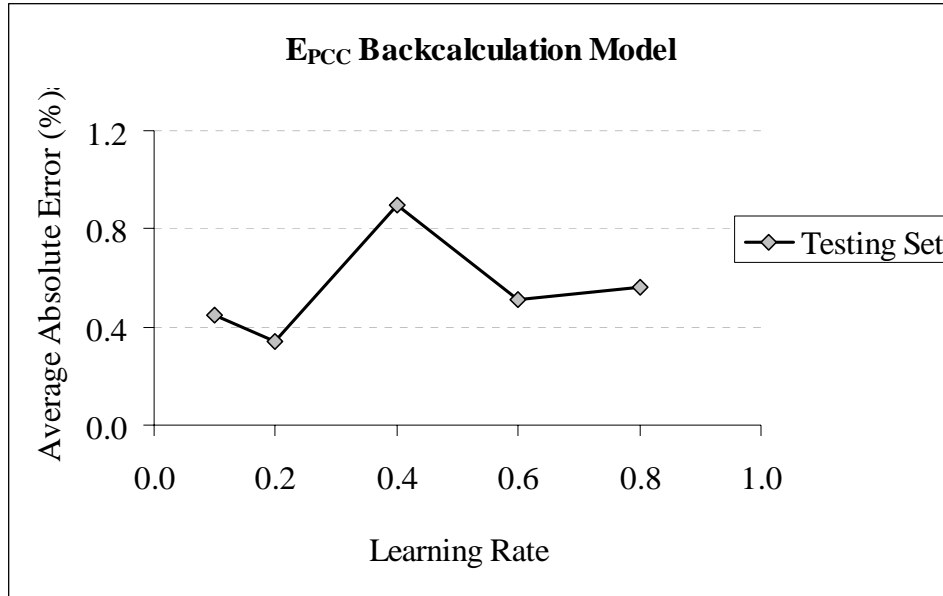


**Figure 61. Sensitivity study results for the learning rate**

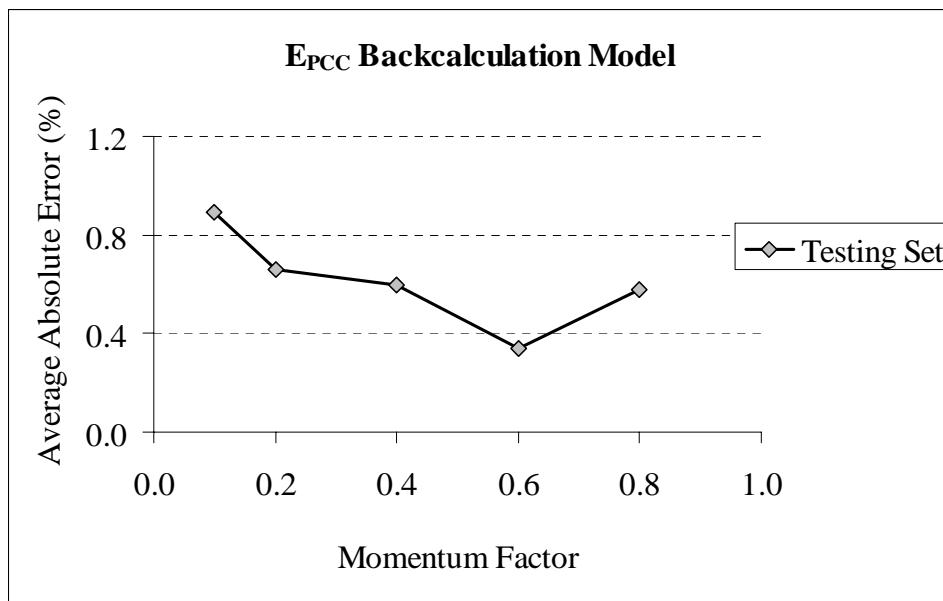


**Figure 62. Sensitivity study results for the momentum factor**

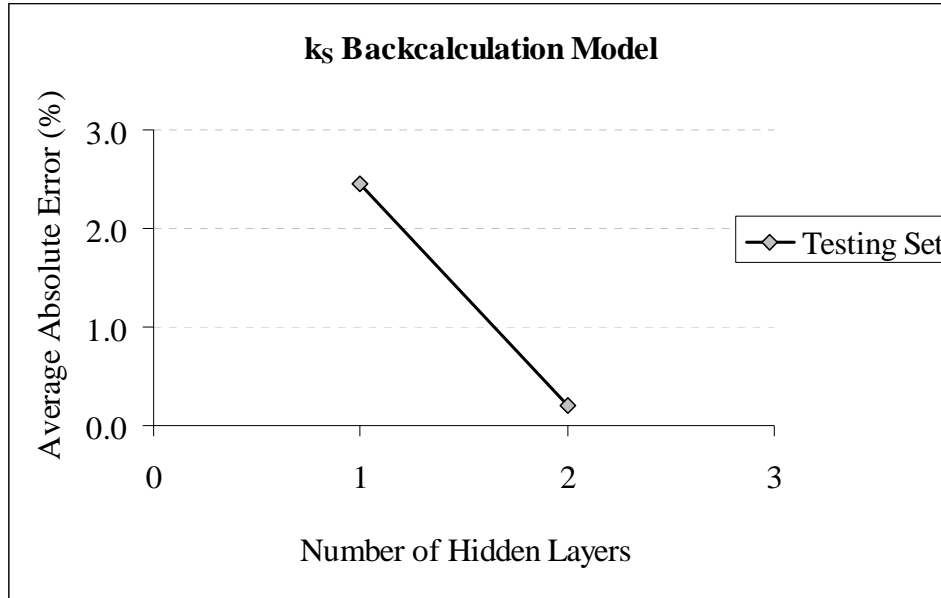


**Figure 63. Sensitivity study results for the number of hidden layers**

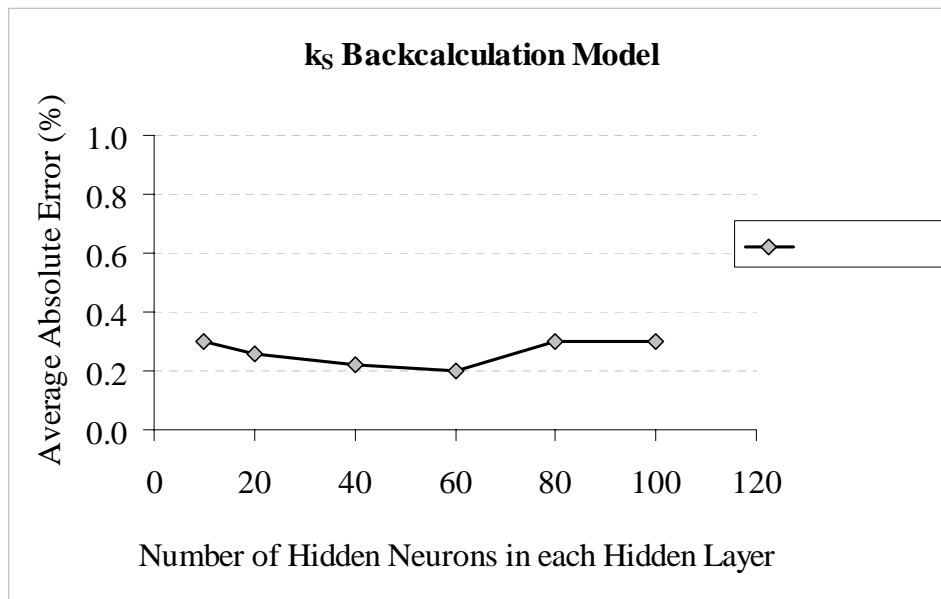


**Figure 64. Sensitivity study results for the number of hidden neurons in each hidden layer**

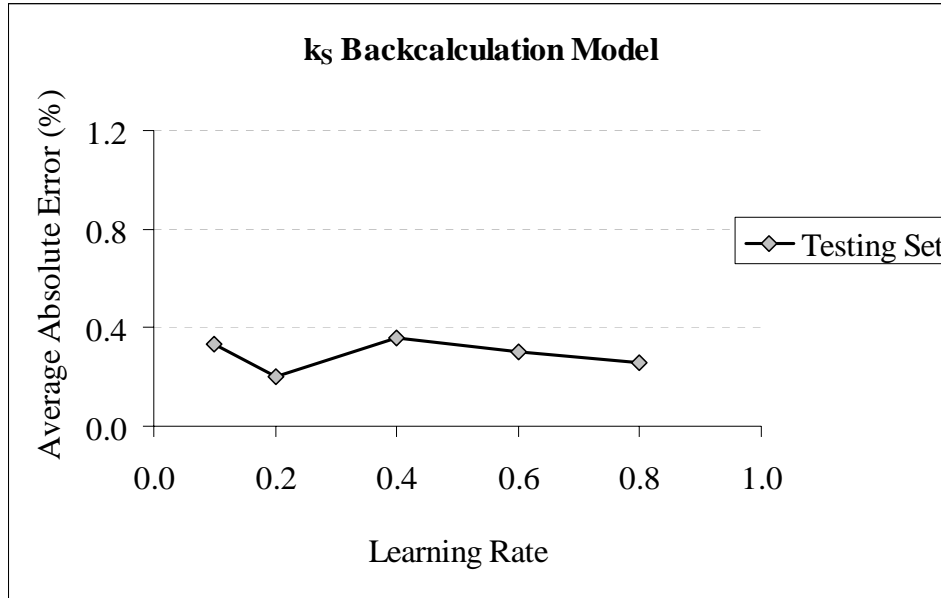


**Figure 65. Sensitivity study results for the learning rate**

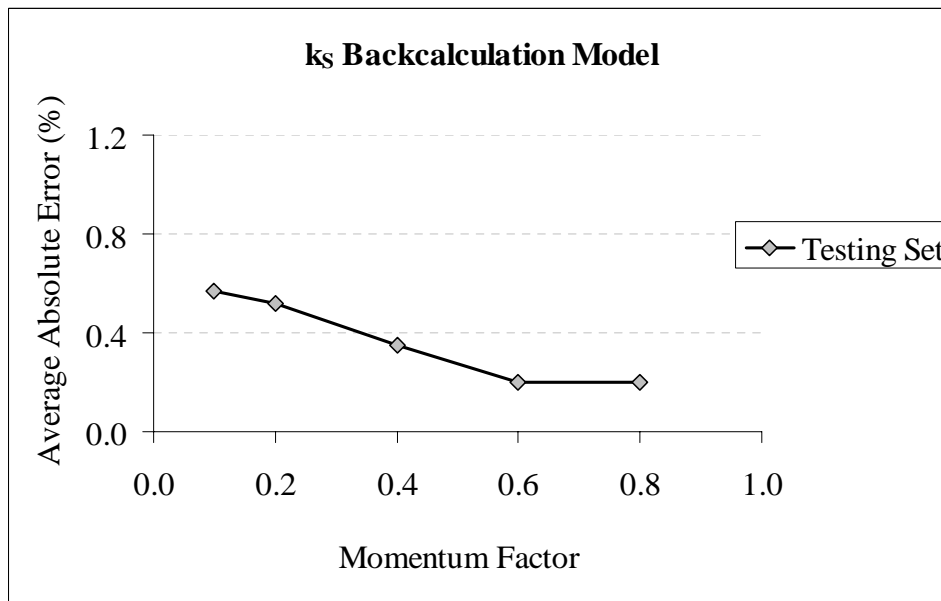


**Figure 66. Sensitivity study results for the momentum factor**

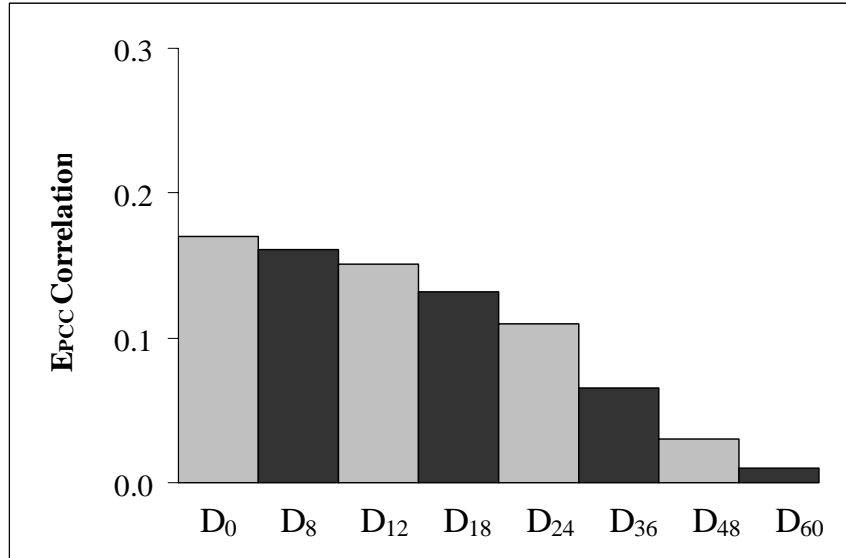


**Figure 67.  $E_{PCC}$  correlation with deflections (RGD)**

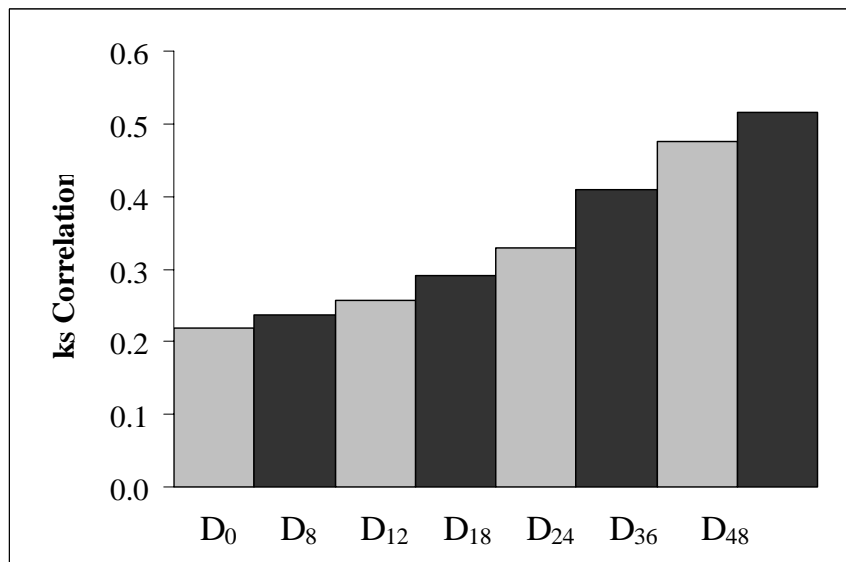


**Figure 68.  $k_s$  correlation with deflections (RGD)**

### Noise-Introduced RGD-ANN Backcalculation Models

In addition to the training and testing sets prepared for the virgin (zero-noise) RGD- $E_{PCC}$  and RGD- $k_s$  models, more ANN training sets were generated by introducing 4% ( $\pm 2\%$ ), 10% ( $\pm 5\%$ ) and 20% ( $\pm 10\%$ ) noise to the FWD deflection data used in both backcalculation models. As was done with the CFP-ANN models, the purpose of introducing noisy patterns in the training sets in the RGD-ANN models was to develop more robust networks that can tolerate the noisy or inaccurate deflection patterns collected from the FWD deflection basins. Noise introduction to trained ANN- $E_{PCC}$  (and  $k_s$ ) models was as follows. ISLAB2000 solution databases were first partitioned to create training sets of the values 39,026 for  $E_{PCC}$  and 49,539 for  $k_s$  patterns, as well

as an independent testing set of 2,000 patterns to check the performance of the trained ANN models. Uniformly distributed random numbers ranging from 0% to 4% ( $\pm 2\%$ ) and 10% ( $\pm 5\%$ ) for low-noise levels, and another set of values of 39,026 for  $E_{PCC}$  and 49,539 for  $k_s$  with a range from 0% to 20% ( $\pm 10\%$ ) for high-noise patterns were generated each time to create noisy training patterns. By repeating the noise introduction procedure, four more training data sets were formed for each backcalculation model. Including the original training set with no noise in it, a total of 195,130 patterns for  $E_{PCC}$  and 247,695 patterns for  $k_s$  were used to train the noise-introduced ANN backcalculation models. The architectures of the noise-introduced ANN-based backcalculation models are given in Table 19. As can be seen in Figures F.1 to F.48 in Appendix F, the AAE values increased when high levels of noise were introduced to the deflection data.

**Table 19. RGD-ANN models (noise-introduced) input/output configuration**

| ANN Models                               | Input Parameters   | Output Parameter | ANN Architecture |
|--|--|------------------|------------------|
| RGD-E <sub>PCC</sub> -(4)-( $\pm 2\%$ )  | D <sub>0</sub> , D <sub>12</sub> , D <sub>24</sub> , D <sub>36</sub> + h <sub>PCC</sub>  | E <sub>PCC</sub> | 5-60-60-1        |
| RGD-E <sub>PCC</sub> -(4)-( $\pm 5\%$ )  | D <sub>0</sub> , D <sub>12</sub> , D <sub>24</sub> , D <sub>36</sub> + h <sub>PCC</sub>  | E <sub>PCC</sub> | 5-60-60-1        |
| RGD-E <sub>PCC</sub> -(4)-( $\pm 10\%$ ) | D <sub>0</sub> , D <sub>12</sub> , D <sub>24</sub> , D <sub>36</sub> + h <sub>PCC</sub>  | E <sub>PCC</sub> | 5-60-60-1        |
| RGD-E <sub>PCC</sub> -(6)-( $\pm 2\%$ )  | D <sub>0</sub> , D <sub>12</sub> , D <sub>24</sub> , D <sub>36</sub> , D <sub>48</sub> , D <sub>60</sub> + h <sub>PCC</sub>                                    | E <sub>PCC</sub> | 7-60-60-1        |
| RGD-E <sub>PCC</sub> -(6)-( $\pm 5\%$ )  | D <sub>0</sub> , D <sub>12</sub> , D <sub>24</sub> , D <sub>36</sub> , D <sub>48</sub> , D <sub>60</sub> + h <sub>PCC</sub>                                    | E <sub>PCC</sub> | 7-60-60-1        |
| RGD-E <sub>PCC</sub> -(6)-( $\pm 10\%$ ) | D <sub>0</sub> , D <sub>12</sub> , D <sub>24</sub> , D <sub>36</sub> , D <sub>48</sub> , D <sub>60</sub> + h <sub>PCC</sub>                                    | E <sub>PCC</sub> | 7-60-60-1        |
| RGD-E <sub>PCC</sub> -(7)-( $\pm 2\%$ )  | D <sub>0</sub> , D <sub>8</sub> , D <sub>12</sub> , D <sub>18</sub> , D <sub>24</sub> , D <sub>36</sub> , D <sub>60</sub> + h <sub>PCC</sub>                   | E <sub>PCC</sub> | 8-60-60-1        |
| RGD-E <sub>PCC</sub> -(7)-( $\pm 5\%$ )  | D <sub>0</sub> , D <sub>8</sub> , D <sub>12</sub> , D <sub>18</sub> , D <sub>24</sub> , D <sub>36</sub> , D <sub>60</sub> + h <sub>PCC</sub>                   | E <sub>PCC</sub> | 8-60-60-1        |
| RGD-E <sub>PCC</sub> -(7)-( $\pm 10\%$ ) | D <sub>0</sub> , D <sub>8</sub> , D <sub>12</sub> , D <sub>18</sub> , D <sub>24</sub> , D <sub>36</sub> , D <sub>60</sub> + h <sub>PCC</sub>                   | E <sub>PCC</sub> | 8-60-60-1        |
| RGD-E <sub>PCC</sub> -(8)-( $\pm 2\%$ )  | D <sub>0</sub> , D <sub>8</sub> , D <sub>12</sub> , D <sub>18</sub> , D <sub>24</sub> , D <sub>36</sub> , D <sub>48</sub> , D <sub>60</sub> + h <sub>PCC</sub> | E <sub>PCC</sub> | 9-60-60-1        |
| RGD-E <sub>PCC</sub> -(8)-( $\pm 5\%$ )  | D <sub>0</sub> , D <sub>8</sub> , D <sub>12</sub> , D <sub>18</sub> , D <sub>24</sub> , D <sub>36</sub> , D <sub>48</sub> , D <sub>60</sub> + h <sub>PCC</sub> | E <sub>PCC</sub> | 9-60-60-1        |
| RGD-E <sub>PCC</sub> -(8)-( $\pm 10\%$ ) | D <sub>0</sub> , D <sub>8</sub> , D <sub>12</sub> , D <sub>18</sub> , D <sub>24</sub> , D <sub>36</sub> , D <sub>48</sub> , D <sub>60</sub> + h <sub>PCC</sub> | E <sub>PCC</sub> | 9-60-60-1        |
| RGD- k <sub>s</sub> -(4)-( $\pm 2\%$ )   | D <sub>0</sub> , D <sub>12</sub> , D <sub>24</sub> , D <sub>36</sub>   | k <sub>s</sub>   | 4-60-60-1        |
| RGD- k <sub>s</sub> -(4)-( $\pm 5\%$ )   | D <sub>0</sub> , D <sub>12</sub> , D <sub>24</sub> , D <sub>36</sub>   | k <sub>s</sub>   | 4-60-60-1        |
| RGD- k <sub>s</sub> -(4)-( $\pm 10\%$ )  | D <sub>0</sub> , D <sub>12</sub> , D <sub>24</sub> , D <sub>36</sub>   | k <sub>s</sub>   | 4-60-60-1        |
| RGD- k <sub>s</sub> -(6)-( $\pm 2\%$ )   | D <sub>0</sub> , D <sub>12</sub> , D <sub>24</sub> , D <sub>36</sub> , D <sub>48</sub> , D <sub>60</sub>   | k <sub>s</sub>   | 6-60-60-1        |
| RGD- k <sub>s</sub> -(6)-( $\pm 5\%$ )   | D <sub>0</sub> , D <sub>12</sub> , D <sub>24</sub> , D <sub>36</sub> , D <sub>48</sub> , D <sub>60</sub>   | k <sub>s</sub>   | 6-60-60-1        |
| RGD- k <sub>s</sub> -(6)-( $\pm 10\%$ )  | D <sub>0</sub> , D <sub>12</sub> , D <sub>24</sub> , D <sub>36</sub> , D <sub>48</sub> , D <sub>60</sub>   | k <sub>s</sub>   | 6-60-60-1        |
| RGD- k <sub>s</sub> -(7)-( $\pm 2\%$ )   | D <sub>0</sub> , D <sub>8</sub> , D <sub>12</sub> , D <sub>18</sub> , D <sub>24</sub> , D <sub>36</sub> , D <sub>60</sub>                                      | k <sub>s</sub>   | 7-60-60-1        |
| RGD- k <sub>s</sub> -(7)-( $\pm 5\%$ )   | D <sub>0</sub> , D <sub>8</sub> , D <sub>12</sub> , D <sub>18</sub> , D <sub>24</sub> , D <sub>36</sub> , D <sub>60</sub>                                      | k <sub>s</sub>   | 7-60-60-1        |
| RGD- k <sub>s</sub> -(7)-( $\pm 10\%$ )  | D <sub>0</sub> , D <sub>8</sub> , D <sub>12</sub> , D <sub>18</sub> , D <sub>24</sub> , D <sub>36</sub> , D <sub>60</sub>                                      | k <sub>s</sub>   | 7-60-60-1        |
| RGD- k <sub>s</sub> -(8)-( $\pm 2\%$ )   | D <sub>0</sub> , D <sub>8</sub> , D <sub>12</sub> , D <sub>18</sub> , D <sub>24</sub> , D <sub>36</sub> , D <sub>48</sub> , D <sub>60</sub>                    | k <sub>s</sub>   | 8-60-60-1        |
| RGD- k <sub>s</sub> -(8)-( $\pm 5\%$ )   | D <sub>0</sub> , D <sub>8</sub> , D <sub>12</sub> , D <sub>18</sub> , D <sub>24</sub> , D <sub>36</sub> , D <sub>48</sub> , D <sub>60</sub>                    | k <sub>s</sub>   | 8-60-60-1        |
| RGD- k <sub>s</sub> -(8)-( $\pm 10\%$ )  | D <sub>0</sub> , D <sub>8</sub> , D <sub>12</sub> , D <sub>18</sub> , D <sub>24</sub> , D <sub>36</sub> , D <sub>48</sub> , D <sub>60</sub>                    | k <sub>s</sub>   | 8-60-60-1        |

## RGD-ANN Forward Calculation Models

In addition to RGD- $E_{PCC}$  and RGD- $k_s$  models, two different groups of ANN models were also developed in order to calculate the radius of relative stiffness of the pavement system (RGD-RRS models) and the tensile stress at the bottom of the PCC layer (RGD- $\sigma_{PCC}$  models). The architectures of the developed RGD-RRS and RGD- $\sigma_{PCC}$  ANN models are given in Table 20, and the prediction success of the developed ANN-based models are presented in the following section.

**Table 20. Architectures of the RGD-RRS and RGD- $\sigma_{PCC}$  ANN models**

| ANN Models               | Input Parameters   | Output Parameter | ANN Architecture |
|--------------------------|--|------------------|------------------|
| RGD-RRS-(4)              | $D_0, D_{12}, D_{24}, D_{36} + h_{PCC}$                              | RRS              | 4-60-60-1        |
| RGD-RRS-(6)              | $D_0, D_{12}, D_{24}, D_{36}, D_{48}, D_{60} + h_{PCC}$              | RRS              | 6-60-60-1        |
| RGD-RRS-(7)              | $D_0, D_8, D_{12}, D_{18}, D_{24}, D_{36}, D_{60} + h_{PCC}$         | RRS              | 7-60-60-1        |
| RGD-RRS-(8)              | $D_0, D_8, D_{12}, D_{18}, D_{24}, D_{36}, D_{48}, D_{60} + h_{PCC}$ | RRS              | 8-60-60-1        |
| RGD- $\sigma_{PCC}$ -(4) | $D_0, D_{12}, D_{24}, D_{36} + h_{PCC}$                              | $\sigma_{PCC}$   | 5-60-60-1        |
| RGD- $\sigma_{PCC}$ -(6) | $D_0, D_{12}, D_{24}, D_{36}, D_{48}, D_{60} + h_{PCC}$              | $\sigma_{PCC}$   | 7-60-60-1        |
| RGD- $\sigma_{PCC}$ -(7) | $D_0, D_8, D_{12}, D_{18}, D_{24}, D_{36}, D_{60} + h_{PCC}$         | $\sigma_{PCC}$   | 8-60-60-1        |
| RGD- $\sigma_{PCC}$ -(8) | $D_0, D_8, D_{12}, D_{18}, D_{24}, D_{36}, D_{48}, D_{60} + h_{PCC}$ | $\sigma_{PCC}$   | 9-60-60-1        |

## Performance of ANN Models

After completing the training process, the subsequent step was to evaluate the performance of the developed ANN models. For this purpose, the ISLAB2000 inputs ( $E_{PCC}$  and  $k_s$ ) were compared with the ANN model predictions. To evaluate the performance of the developed ANN models, AAE and RMSE values were calculated. In addition, goodness-of-fit was a commonly used approach to evaluate performance of models. In this research, the performance of the ANN-based backcalculation models were further evaluated by comparing the  $R^2$  of the ANN models and ISLAB2000 inputs ( $E_{PCC}$  and  $k_s$ ).

The equations used in this performance evaluation study are given below.

AAE is calculated using Equation 11.

$$AAE (\%) = \frac{\sum_{i=1}^n |o_i - p_i|}{n} \left( \frac{1}{o_i} \times 100 \right) \quad (11)$$

Where,

- $n$  = number of observations,
- $o_i$  = observed value of observation i, and
- $p_i$  = predicted value of observation i.

RMSE is calculated using Equation 12.

$$\text{RMSE} = \sqrt{\frac{\sum_{i=1}^n (o_i - p_i)^2}{n}} \quad (12)$$

Where,

- RMSE = root-mean-square-error,
- $o_i$  = observed value of observation i, and
- $p_i$  = predicted value of observation i.

$R^2$  value is calculated using Equation 13.

$$R^2 = 1 - \frac{\sum (x_{act} - x_{pred})^2}{\sum (x_{act} - x_{avg})^2} \quad (13)$$

Where,

- $x_{act}$  = actual value,
- $x_{pred}$  = predicted value by ANN model, and
- $x_{avg}$  = average value.

The performance evaluation plots and associated progress curves of each developed ANN model are presented in Figure E.1 to Figure E.32 in Appendix E. In addition, the summary of the AAE values of the developed RGD-ANN models is provided in Table 21 to Table 23.

**Table 21. Prediction performance of RGD-ANN-based backcalculation models (with zero noise)**

| ANN Deflection Models | AAE (%)   |       |   |
|-----------------------|-----------|-------|---|
|                       | $E_{PCC}$ | $k_s$ |   |
| 4-Deflection          | 0.34      | 0.28  | — |
| 6-Deflection          | 0.32      | 0.20  | — |
| 7-Deflection          | 0.29      | 0.19  | — |
| 8-Deflection          | 0.30      | 0.22  | — |

**Table 22. Prediction performance of RGD-ANN-based backcalculation models (with noise)**

| Noise Level    | ANN Deflection Models | AAE (%)   |       |   |
|----------------|-----------------------|-----------|-------|---|
|                |                       | $E_{PCC}$ | $k_s$ |   |
| ( $\pm 2\%$ )  | 4-Deflection          | 2.57      | 1.65  | — |
|                | 6-Deflection          | 1.11      | 1.46  | — |
|                | 7-Deflection          | 1.04      | 1.21  | — |
|                | 8-Deflection          | 1.42      | 1.17  | — |
| ( $\pm 5\%$ )  | 4-Deflection          | 5.96      | 4.23  | — |
|                | 6-Deflection          | 2.59      | 2.69  | — |
|                | 7-Deflection          | 2.37      | 1.74  | — |
|                | 8-Deflection          | 1.75      | 1.58  | — |
| ( $\pm 10\%$ ) | 4-Deflection          | 11.61     | 7.51  | — |
|                | 6-Deflection          | 5.22      | 3.60  | — |
|                | 7-Deflection          | 4.54      | 2.71  | — |
|                | 8-Deflection          | 3.33      | 2.23  | — |

**Table 23. Prediction performance of RGD-ANN-based forward calculation models**

| ANN Deflection Models | AAE (%)        |      |   |
|-----------------------|----------------|------|---|
|                       | $\sigma_{PCC}$ | RRS  |   |
| 4-Deflection          | 0.45           | 0.14 | — |
| 6-Deflection          | 0.44           | 0.14 | — |
| 7-Deflection          | 0.43           | 0.23 | — |
| 8-Deflection          | 0.43           | 0.14 | — |

### **The Significance of Layer Bonding and Thickness in Backcalculation of Rigid Pavement Layer Moduli**

Two of the important issues in the backcalculation of the rigid pavement parameters are the degree of bonding between layers and the thickness of the PCC and base layers. To simplify the ANN-based backcalculation methodology developed in this study, only one thickness value,

effective PCC thickness, was considered in the analysis. The effective thickness of the pavement structure was directly related to the bonding conditions between the PCC layer and the base layer. Because it was difficult to construct a long pavement section with a uniform thickness value during the backcalculation of the pavement parameters, it was assumed that pavement thickness is uniform for a given section and that it is the value taken from the project files. To determine the effective thickness of a two-layer pavement section for bonded, unbonded, and partially bonded cases, the equations below are considered (Ioannides et al. 1992).

Effective thickness for fully bonded PCC layers was computed using the following equation:

$$h_{e-b} = \left\{ h_1^3 + \frac{E_2}{E_1} h_2^3 + 12 \left[ \left( x_{na} - \frac{h_1}{2} \right)^2 h_1 + \frac{E_2}{E_1} \left( h_1 - x_{na} + \frac{h_2}{2} \right)^2 h_2 \right] \right\}^{1/3} \quad (14)$$

$$x_{na} = \frac{E_1 h_1 \frac{h_1}{2} + E_2 h_2 \left( h_1 + \frac{h_2}{2} \right)}{E_1 h_1 + E_2 h_2} \quad (15)$$

Effective thickness for unbonded PCC layers is computed using the following equation:

$$h_{e-u} = \left( h_1^3 + \frac{E_2}{E_1} h_2^3 \right)^{1/3} \quad (16)$$

Effective thickness for partially bonded PCC layers is computed using the following equation:

$$h_{e-p} = (1-x)h_{e-u} + (x)h_{e-b} \quad (17)$$

$$x = \frac{h_{e-p} - h_{e-u}}{h_{e-b} - h_{e-u}} \quad (18)$$

Where:

$h_{e-b}$  = Effective thickness of the fully bonded PCC layers

$h_{e-u}$  = Effective thickness of the unbonded PCC layers

$h_{e-p}$  = Effective thickness of the partially bonded PCC layers

$E_1$  or  $E_2$  = Elastic modulus for layer 1 or 2

- $h_1$  or  $h_2$  = Thickness for layer 1 or 2
- $x_{na}$  = Neutral axis distance from top of layer
- $x$  = Degree of bonding which ranges between 0 and 1

*The Effect of the Layer Thickness in the  $E_{PCC}$  Predictions*

The predicted layer moduli were very sensitive to the pavement layer thickness. Even a small change in the assumed PCC layer thickness caused considerable differences in the backcalculated elastic moduli of the PCC layer. To demonstrate the effect of the PCC thickness on the backcalculated  $E_{PCC}$  values, one FWD deflection basin data collected from the FAA’s National Airport Pavement Test Facility (NAPTF) was used. Thickness value was varied from 10 inches (25.4 cm) to 14 inches (35.6 cm) and all other values were kept constant. Predicted  $E_{PCC}$  values obtained from the developed RGD- $E_{PCC}$ -(4) model are presented in Figure 69. As expected, the predicted  $E_{PCC}$  values decreased dramatically as the assumed PCC thickness increased.

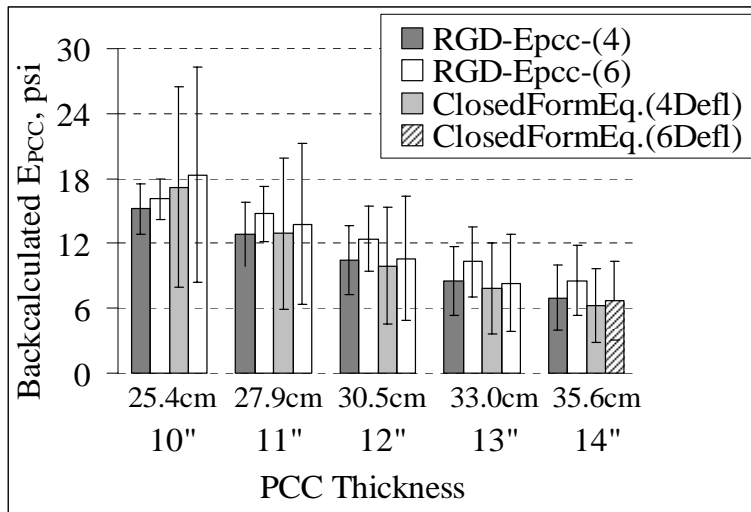


**Figure 69. Effect of layer thickness on  $E_{PCC}$  backcalculation**

*The Effect of the Pavement Layer Bonding in the  $E_{PCC}$  Predictions*

The LRS (rigid [R] pavement with stabilized [S] base over low-strength [L] subgrade) data was used to investigate the sensitivity of the bonding degree between the layers. The thickness and elastic modulus values for the LRS test section were assumed as follows:  $E_{PCC} = 34.5$  GPa (5,000,000 psi),  $E_{base} = 6.9$  GPa (1,000,000 psi),  $h_{PCC} = 11$  inches (28 cm.), and  $h_{base} = 6 \frac{1}{8}$  inches (15.6 cm). Unbonded, 25% bonded, 50% bonded, 75% bonded, and fully bonded cases, as well as the equations presented above, were investigated using developed ANN-based backcalculation models. The variation of the backcalculated  $E_{PCC}$  values is presented in Figure 70. As expected, the predicted  $E_{PCC}$  values decreased as the assumed bonding degree increased.

As seen in Figure 70, the degree of layer bonding resulting in a 1-inch (2.5-cm) change in the effective thickness of the pavement system may change the backcalculated  $E_{PCC}$  value of 17 GPa ( $2.5 \times 10^6$  psi) with the assumed PCC and base layer moduli values. Therefore, results from this sensitivity analysis show the significance of the degree of bonding in the  $E_{PCC}$  backcalculation procedure.

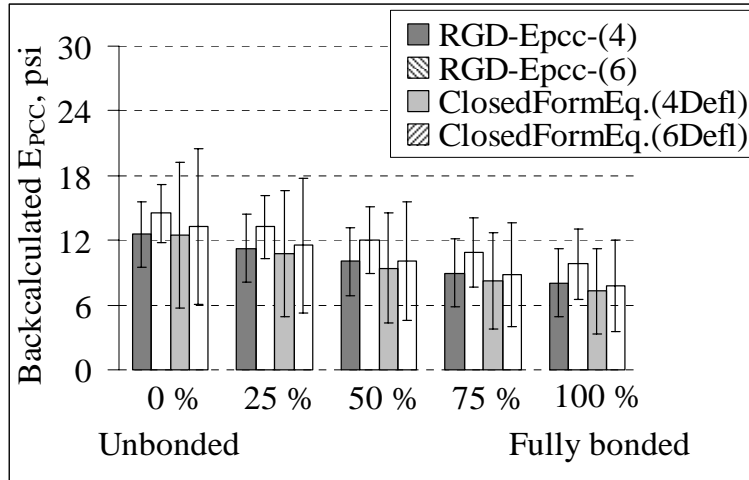


**Figure 70. Effect of degree of layer bonding on  $E_{PCC}$  backcalculation**

### Case Study of Individual Pavement Sections

To validate the developed models, ANN-based backcalculation models were compared with the closed-form solutions, EverCalc 5.0 and BAKFAA backcalculation computer programs, for the NAPTF FWD data. The FWD tests were conducted on the NAPTF's LRS, MRS, and HRS sections. Each NAPTF test section is identified using a three-character code where the first character indicates the subgrade strength (L for low, M for medium, and H for high), the second character indicates the test pavement type (F for flexible and R for rigid), and the third character signifies whether the base material is conventional (C) or stabilized (S). The three rigid pavement sections are designated as follows: (a) LRS – rigid pavement with a stabilized base over low-strength subgrade, (b) MRS – rigid pavement with a stabilized base over medium-strength subgrade, and (c) HRS – rigid pavement with a stabilized base over high-strength subgrade.

In the first comparison, ANN model backcalculation results were compared with the closed-form equation results using the LRS-FWD test data obtained from the NAPTF. The FWD deflection profiles obtained from the NAPTF's LRS test sections are depicted in Figure 71 and Figure 72. All FWD test results were normalized to nine kip (40 kN) to compare the results. Results from FWD tests conducted on the center of the PCC slab alone are considered. The ANN RGD- $k_s$ -(6) model predictions and closed-form equation solutions (Equations 20, 22, and 23) are presented in Figure 73 for backcalculating the  $k_s$  using the NAPTF-LRS FWD data. In addition, ANN RGD- $E_{PCC}$ -(4) model predictions and closed-form equation solutions (Equations 19, 21, 23, and 24) were compared and results are presented in Figure 74 for backcalculating the  $E_{PCC}$  using the same FWD data. As seen from the comparison of ANN models and closed-form equation

predictions, the standard deviations for the ANN-based predictions are lower than the ones for closed-form equations. In addition, the scatter of the predictions is strongly dependent on the FWD test dates because of the repeated trafficking at NAPTF and the subsequent deterioration of test pavements (see Figure 71 and Figure 72). Higher scatter in  $E_{PCC}$  predictions can be explained with  $E_{PCC}$  being dependent on the PCC layer thickness and the degree of bonding between the PCC and the stabilized base (econocrete) layers.

Because the exact thickness of the PCC layer and the degree of bonding between the PCC and the Econocrete layers are not exactly known, more scatter is expected in  $E_{PCC}$  predictions. In addition, the time of the FWD testing is also crucial in the  $E_{PCC}$  backcalculation due to curling problems in rigid pavements. The results of previous studies indicate that the variations in temperature between two separate FWD tests affect primarily the elastic modulus of the slab (Ioannides et al. 1989). Due to the slab curling, temperature difference across the depth of the concrete pavement in the NAPTF-LRS section is another major reason for the scatter in  $E_{PCC}$  predictions (Bayrak et al. 2006). In summary, the major reasons for the scatter in  $E_{PCC}$  predictions are the curling and warping issues, the bonding degree between the PCC and econocrete layers, and the thickness of the PCC layer. To improve the  $E_{PCC}$  backcalculation, it is suggested that GPR measurements or cores can be taken along the test sections to determine the exact thickness of the pavement layers at the FWD test points. Also, the time of the FWD tests due to curling and warping issues and the shape of the PCC slab should be taken into account in the interpretation of the deflection data for backcalculation purposes.

$$AREA_4 = 6 * \left[ 1 + 2 \left( \frac{D_{12}}{D_0} \right) + 2 \left( \frac{D_{24}}{D_0} \right) + \left( \frac{D_{36}}{D_0} \right) \right] \quad (19)$$

$$AREA_6 = 6 * \left[ 1 + 2 \left( \frac{D_{12}}{D_0} \right) + 2 \left( \frac{D_{24}}{D_0} \right) + 2 \left( \frac{D_{36}}{D_0} \right) + 2 \left( \frac{D_{48}}{D_0} \right) + \left( \frac{D_{60}}{D_0} \right) \right] \quad (20)$$

$$RRS_4 = (-128.9885) + (5.4081 * AREA_4) + (1.0224 * (AREA_4 - 30.8637)^2) + (0.1919 * (AREA_4 - 30.8637)^3) + (0.0145 * (AREA_4 - 30.8637)^4) \quad (21)$$

$$RRS_6 = (-49.1500) + (1.9800 * AREA_6) + (0.1146 * (AREA_6 - 44.3008)^2) + (0.0075 * (AREA_6 - 44.3008)^3) + (0.0002 * (AREA_6 - 44.3008)^4) \quad (22)$$

$$k_s = \left( \frac{P}{8D_0 RRS_i^2} \right) \left\{ 1 + \left( \frac{1}{2\pi} \right) \left[ \ln \left( \frac{a}{2RRS_i} \right) - 0.673 \right] \left( \frac{a}{RRS_i} \right)^2 \right\} \quad (23)$$

$$E_{PCC} = \left( \frac{12RRS_i^4 k_s (1 - \nu^2)}{h_{PCC}^3} \right) \quad (24)$$

Next, a representative FWD deflection profile from each test section was selected (see Figure 75) to compare the backcalculated rigid pavement layer parameters from different methodologies. All FWD test results were normalized to nine kip (40 kN) to compare the results. Also, for each pavement structure (LRS, MRS, and HRS), the effective thickness value was calculated for the PCC slab as Ioannides et al. (1992) proposed.

The comparison of the  $E_{PCC}$  and  $k_s$  predictions obtained from four different methodologies is presented in Figure 75. Closed-form solution equations used to backcalculate the concrete pavement layer parameters are provided in Equations 19–24. As seen from the results, there are some differences in the predictions of four methodologies although not significant. The ANN predictions seem to be more conservative compared to other methodologies.

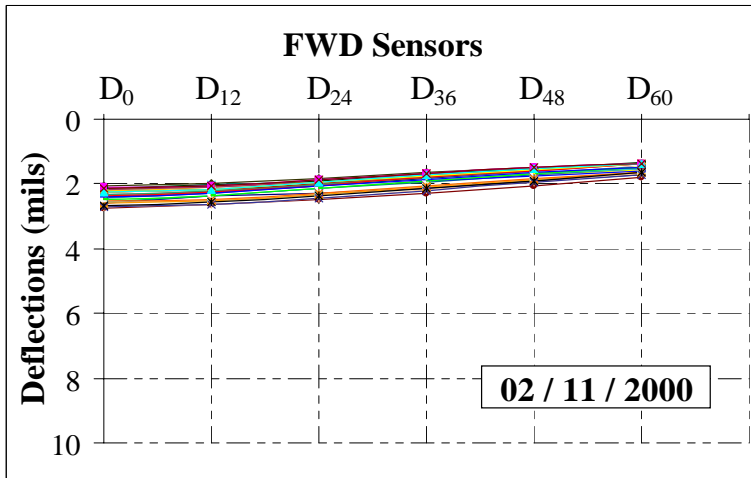
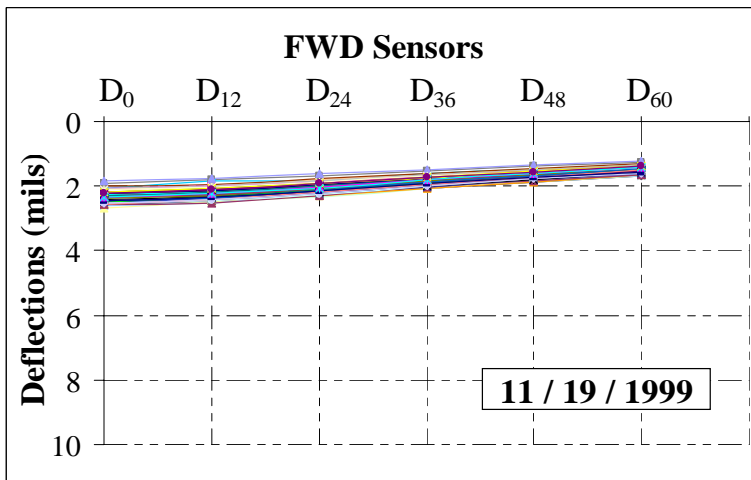
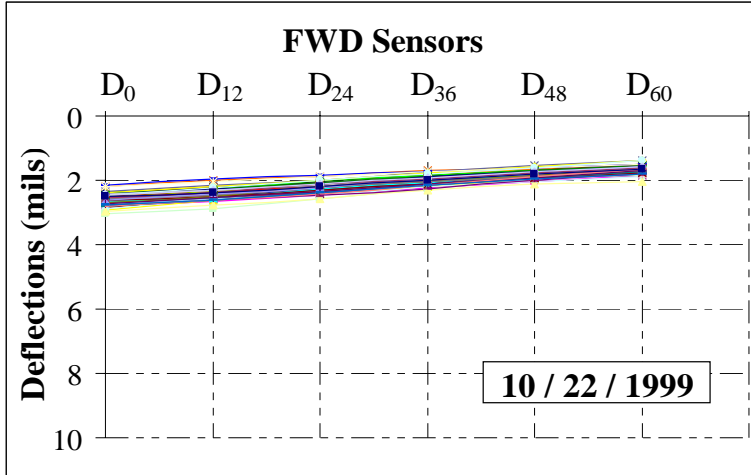


Figure 71. FWD deflection basins normalized to 9-kip load level for NAPTF-LRS section (before trafficking)

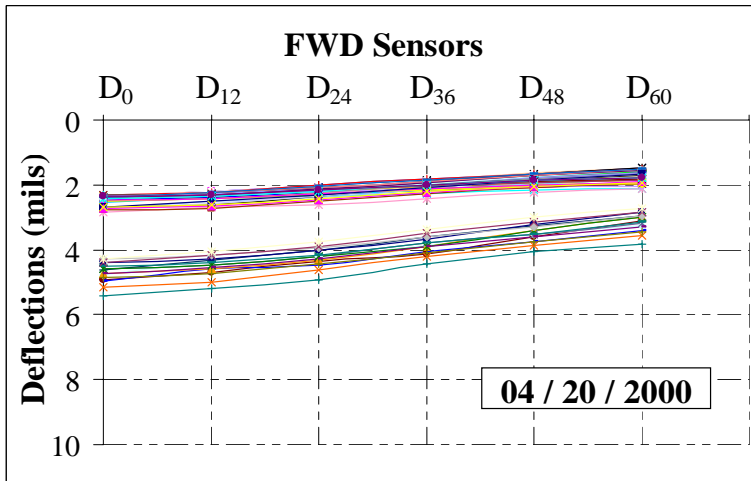
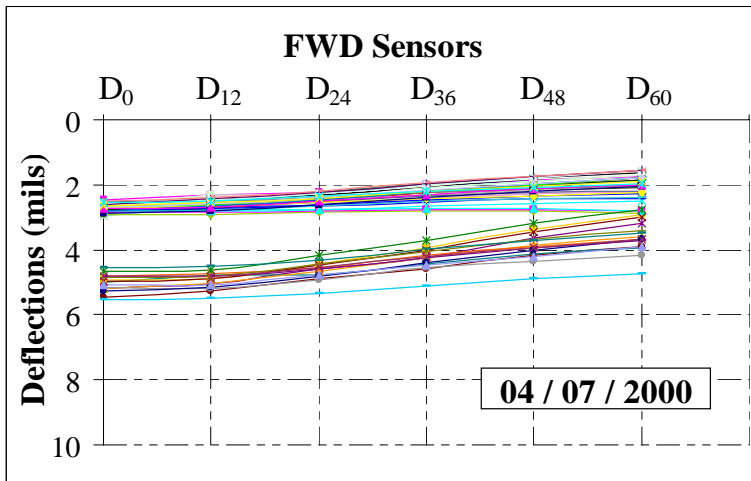
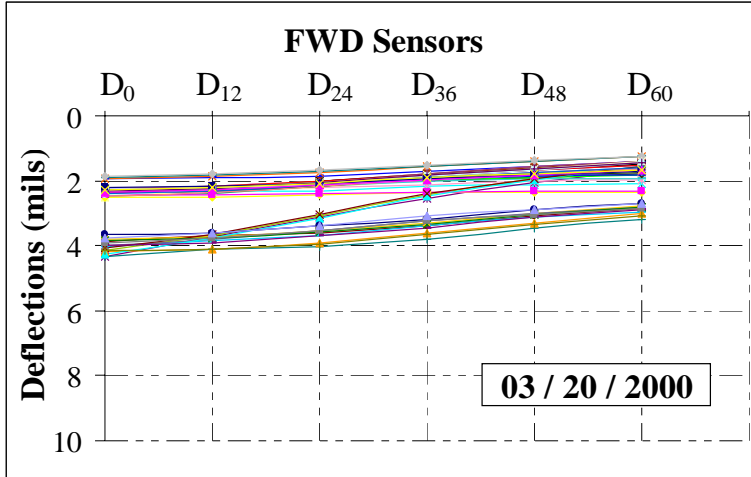
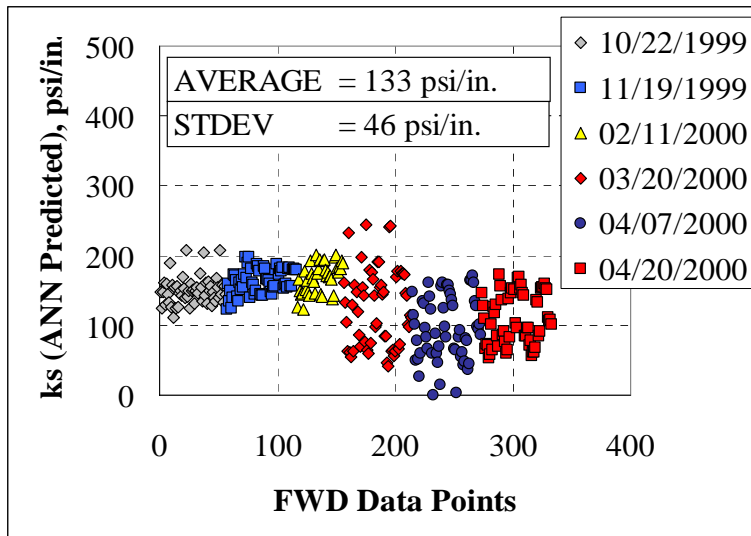
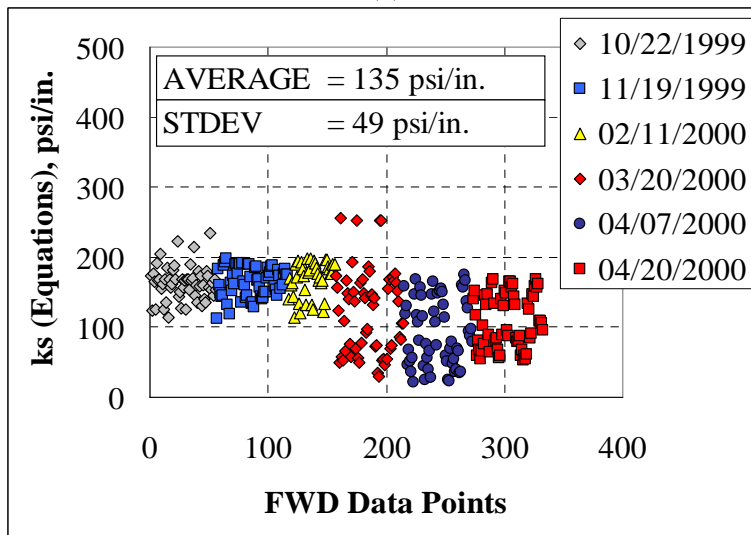


Figure 72. FWD deflection basins normalized to 9-kip load level for NAPTF-LRS section (after trafficking)

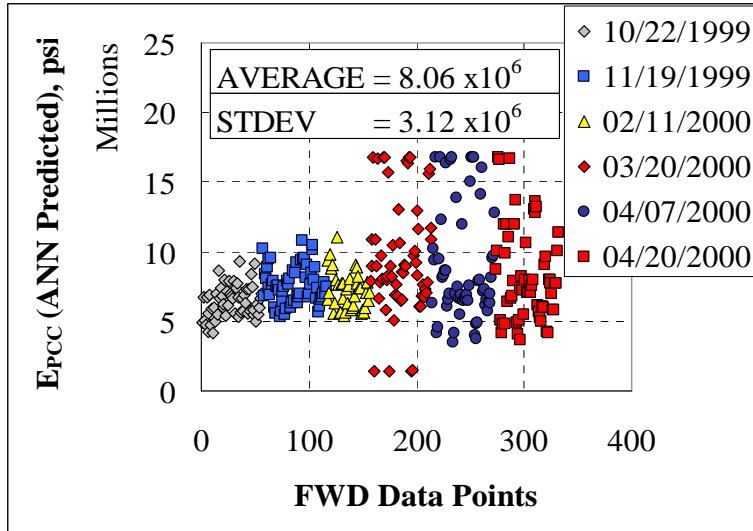


(a)

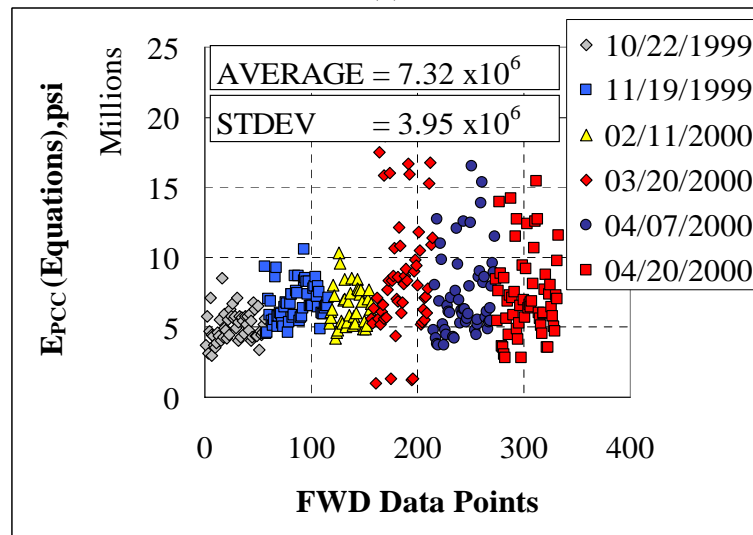


(b)

**Figure 73. Coefficient of subgrade reaction predictions using: (a) RGD-ks-(6) ANN model, and (b) Closed-form equations**

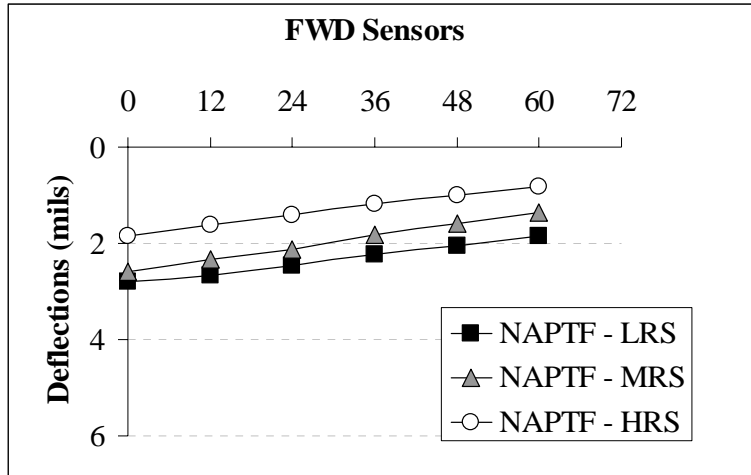


(a)

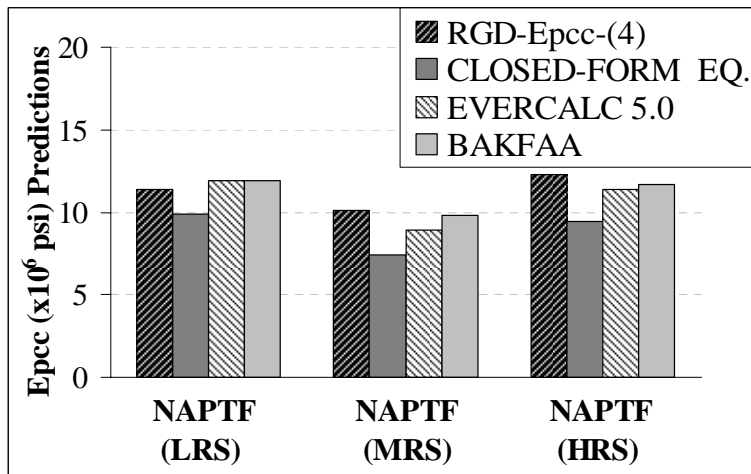


(b)

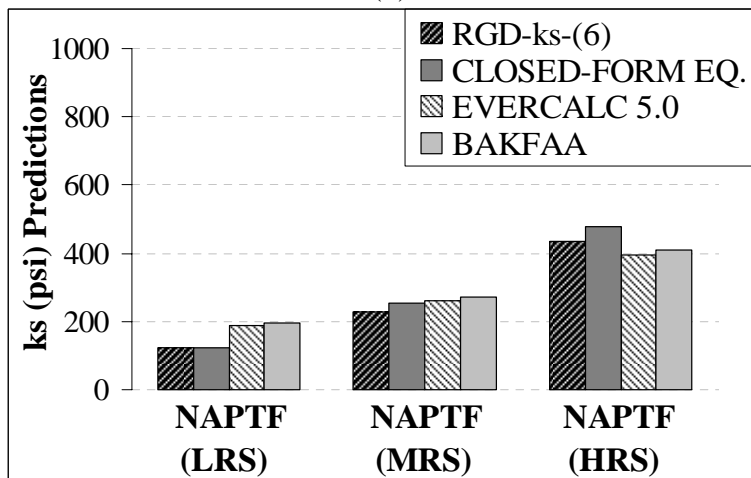
**Figure 74. PCC layer elastic modulus predictions using: (a) RGD- $E_{PCC}$ -(4) ANN model, and (b) Closed-form equations**



(a)



(b)



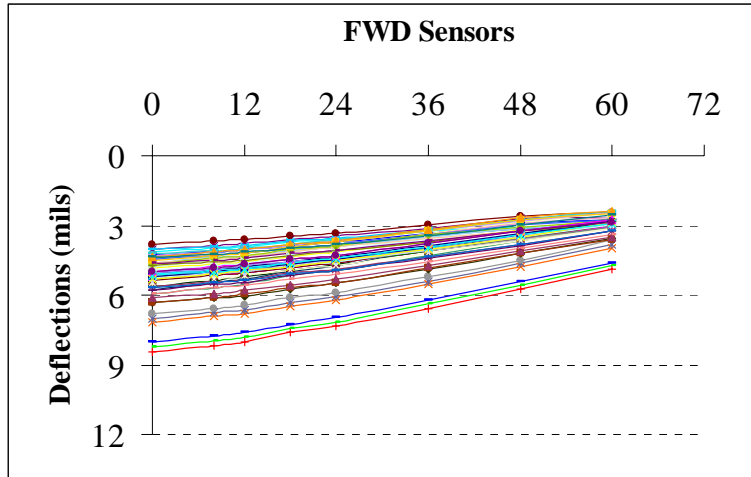
(c)

Figure 75. Comparison of results from different backcalculation methods (NAPTF data)

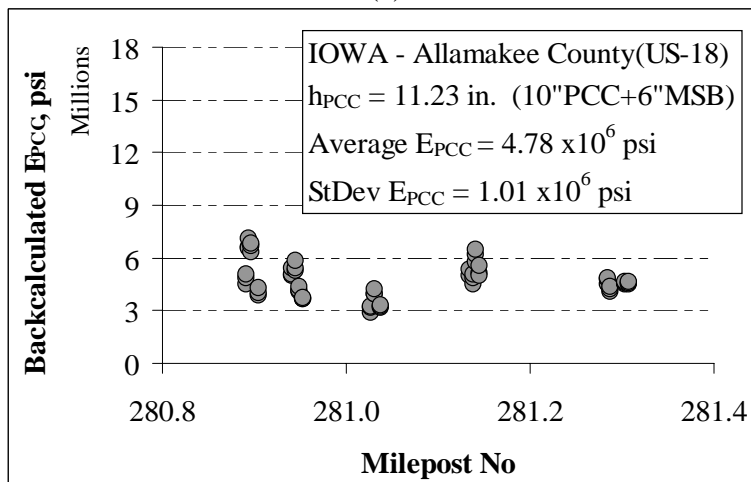
## *Iowa FWD Data Analysis*

The proposed ANN models were also utilized to backcalculate the concrete pavement layer parameters for different FWD data sets obtained from four different counties in Iowa (Allamakee, Fayette, Franklin, and Wright County). The elastic modulus of the PCC slab and the coefficient of subgrade reaction predictions obtained from proposed ANN models are shown in **Figure 76 to Figure 79**. The standard deviation values obtained from these analyses are very low and the predictions seem to be very consistent. All FWD test data was normalized to nine kip to compare the results. There was no base layer in Allamakee and Fayette pavement test sections; therefore, PCC slab thickness was taken directly from the given information. However, in Franklin and Wright County, there was a four-inch asphalt treated base (ATB) layer and effective thickness value was calculated for these analyses by assuming 50% bonding degree, as proposed by **Ioannides et al. (1992)**.

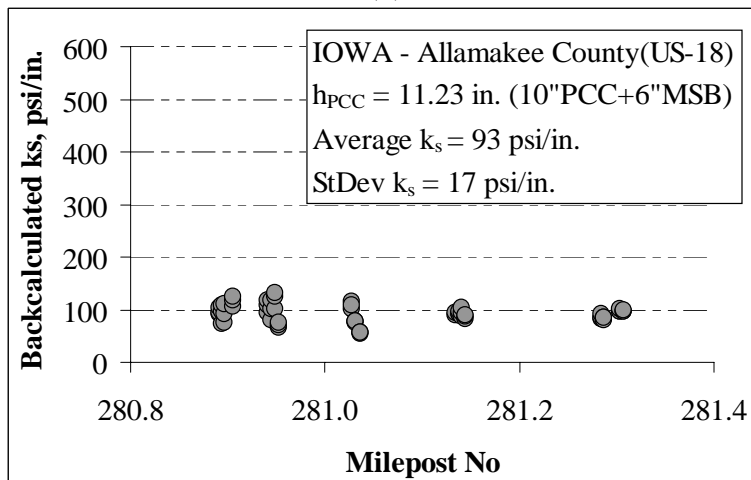
Also, the assumed elastic modulus values for the PCC and base layers for the effective thickness calculations are as follows:  $E_{PCC} = 34.5 \text{ GPa}$  (5,000,000 psi), and  $E_{\text{base-ATB}} = 6.9 \text{ GPa}$  (1,000,000 psi). The backcalculated coefficient of subgrade reaction is independent of the assumed PCC slab thickness but even a small change in the assumed PCC slab thickness causes critical differences in the backcalculated elastic moduli of the PCC slab (**Ioannides et al. 1989**). That's why the PCC slab thickness is crucial in  $E_{PCC}$  backcalculation. In addition, the FWD deflection profiles, which seemed to be very erroneous, were filtered from the analyzed database.



(a)

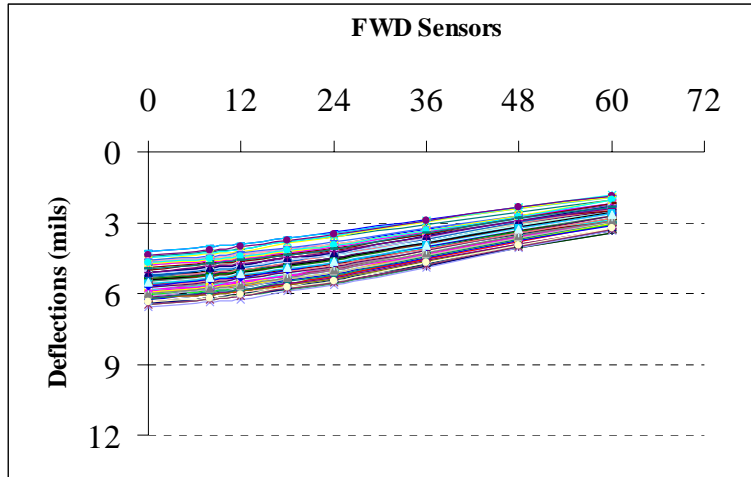


(b)

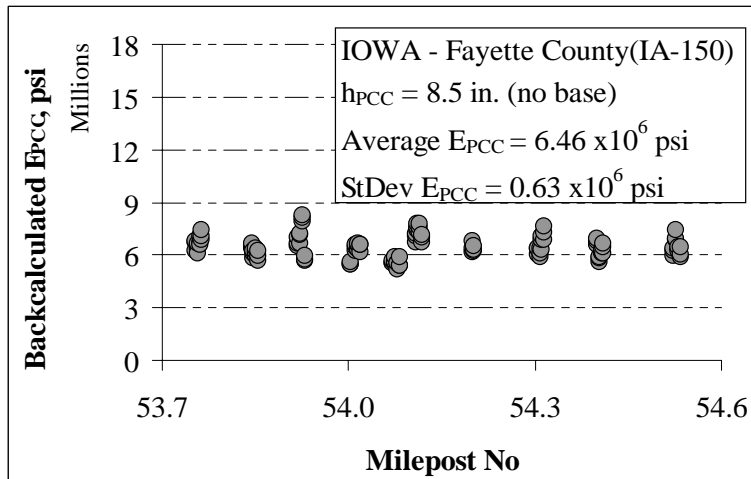


(c)

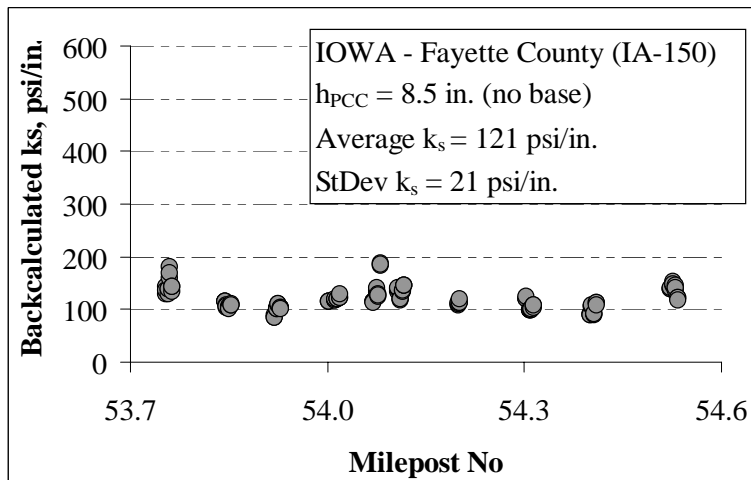
**Figure 76. a) Iowa – Allamakee County (US 18) FWD data b) RGD- $E_{PCC}$ -(4) model predictions c) RGD- $k_s$ -(6) model predictions**



(a)

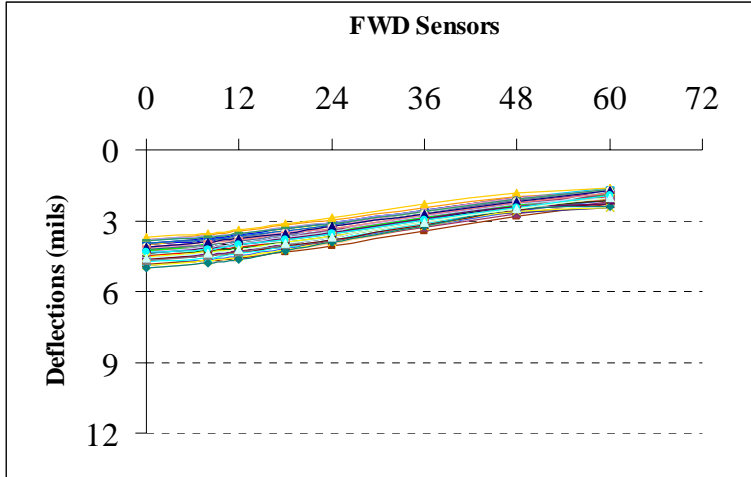


(b)

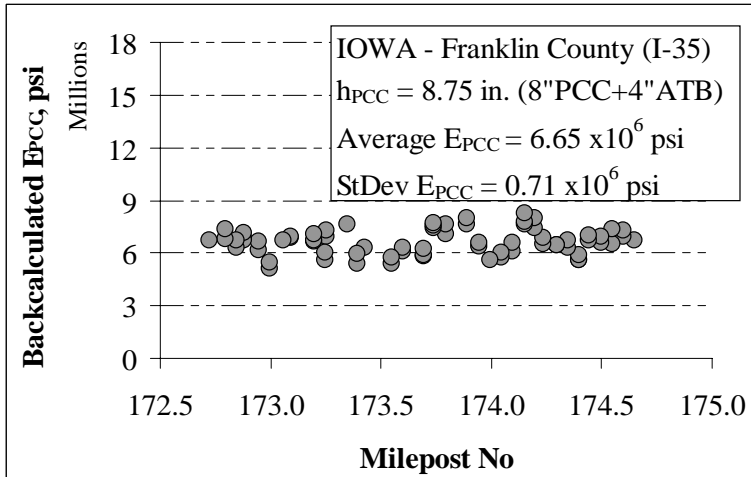


(c)

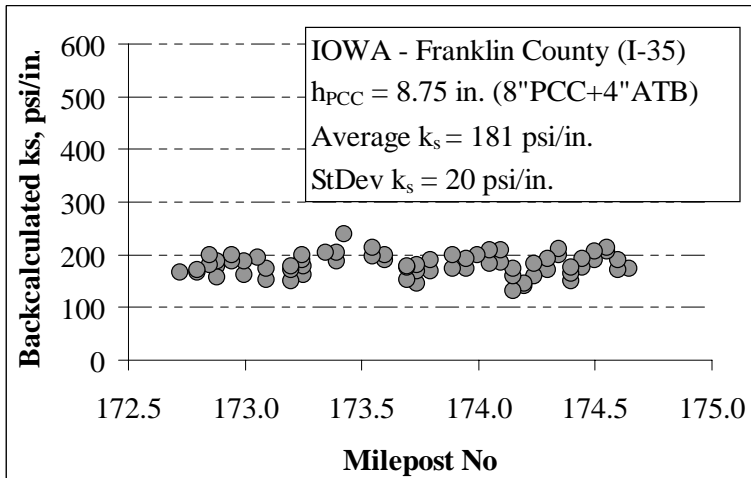
**Figure 77. a) Iowa – Fayette County (IA 150) FWD deflection basin data  
b) RGD- $E_{PCC}$ -(4) model predictions c) RGD- $k_s$ -(6) model predictions**



(a)

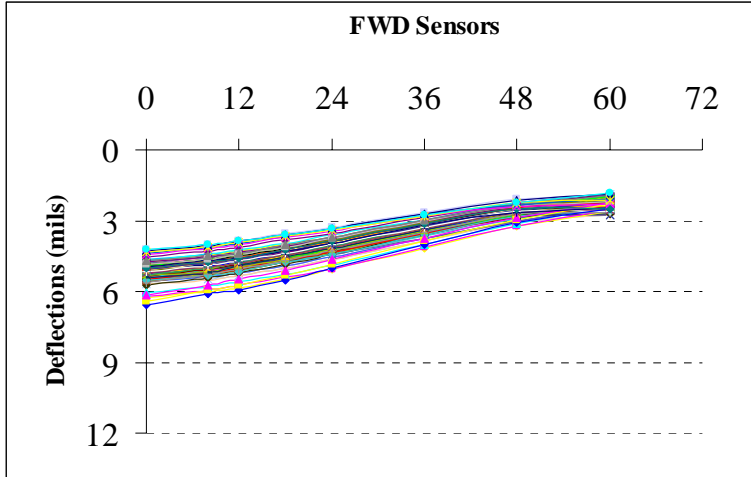


(b)

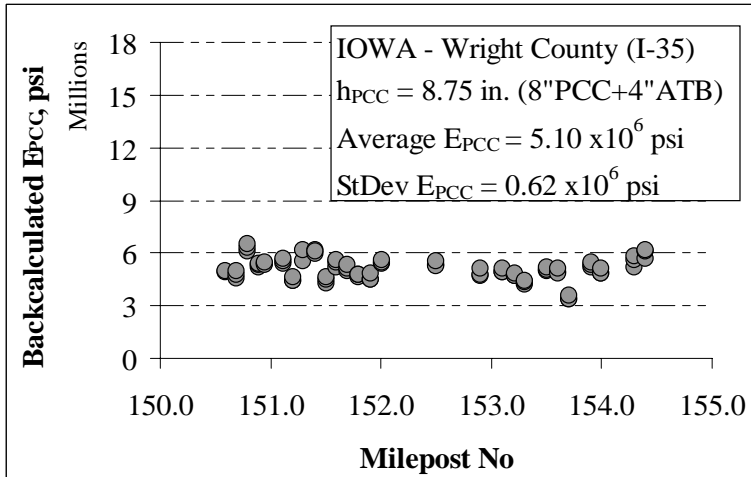


(c)

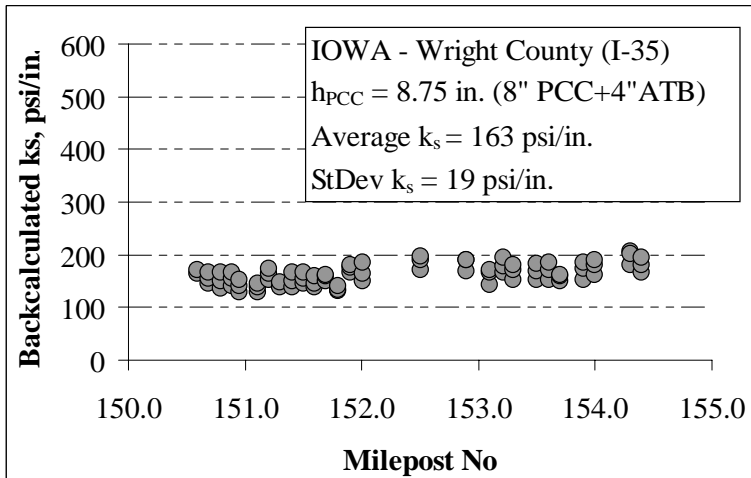
**Figure 78. a) Iowa – Franklin County (I 35) FWD deflection basin data b) RGD- $E_{PCC}$ -(4) model predictions c) RGD- $k_s$ -(6) model predictions**



(a)



(b)



(c)

**Figure 79. a) Iowa – Wright County (I 35) FWD deflection basin data  
 b) RGD- $E_{PCC}$ -(4) model predictions c) RGD- $k_s$ -(6) model predictions**

## ANN Models for Rigid Pavement Systems - Summary and Conclusions

### *Summary*

This section documents the research efforts related to the development of ANN-based rigid pavement backcalculation techniques. Based on the results of this study, the developed ANN models can be utilized to predict the PCC layer modulus and the coefficient of subgrade reaction with very low AAE values (<0.4% for the theoretical deflection basins). Also, different ANN-based forward calculation structural models were developed that can successfully predict the radius of relative stiffness of the pavement system and the tensile stress at the bottom of the PCC layer from FWD deflection basins. Rapid prediction ability of the ANN models, capable of analyzing 100,000 FWD deflection profiles in one second, provides a tremendous advantage to the pavement engineers by allowing them to nondestructively assess the condition of the transportation infrastructure in real time while the FWD testing takes place in the field. Finally, it can be concluded that ANN-based analysis models can provide pavement engineers and designers with state-of-the-art solutions, without the need for a high degree of expertise in the input and output of the problem, to rapidly analyze a large number of rigid pavement deflection basins needed for project-specific and network-level pavement testing and evaluation.

### *Conclusions*

- A total of 32 virgin (zero-noise) ANN-based backcalculation models were developed in this study that can backcalculate the elastic modulus of the PCC slab and coefficient of subgrade reaction from the FWD deflection basin data and the thickness of the slab ( $h_{PCC}$ ).
- During the backcalculation of the concrete pavement parameters, the bonding degree between layers should be carefully taken into account because a completely different deflection profile is obtained if bonding degree is varied, even if every single parameter is kept constant. Therefore, if erroneous values are used for bonding degree in the backcalculation process, unrealistic and meaningless results might emerge.
- The developed ANN models (not noise-introduced) give very low AAE values for all models (<0.4%) for synthetic databases. However, this not the case when the actual field data is utilized in the developed backcalculation models. There might always be some errors in the values of the slab thickness and bonding degree used in the backcalculation analysis that will directly affect the backcalculated pavement parameters. In addition, there also might be some noise in the collected data, errors in the data collection process due to FWD machine sensor calibration, and some operator mistakes. Therefore, actual FWD deflections, which are the basic inputs of the backcalculation models, are not always as perfect as synthetic data. Thus, more ANN training sets were generated by introducing 4% ( $\pm 2\%$ ), 10% ( $\pm 5\%$ ) and 20% ( $\pm 10\%$ ) noise to the FWD deflection data used in both backcalculation models. The purpose of introducing noisy patterns in the training sets was to develop more robust networks that can tolerate the noisy or inaccurate deflection patterns collected from

the FWD deflection basins. Also, as a matter of fact, some meaningless FWD deflection data should be filtered and extracted from the data analysis.

- For validation purposes, the results of the developed ANN-based models were compared with the closed-form solutions and two widely used backcalculation programs, EverCalc 5.0, and BAKFAA. Representative deflection basins were selected from three different test sites from NAPTF data for the comparison study. The predictions of four different methods for this specific data were presented in [Figure 75](#). There are some differences in the predictions obtained from different methodologies. The results seem not very different from each other, but the real time prediction capability (< 1 sec.) of the ANN-based models makes them very powerful tools over the other methods.
- Four different sets of actual FWD deflection basin data were utilized to backcalculate the elastic modulus of the PCC slab and coefficient of subgrade reaction in four different pavement test sections.  $E_{PCC}$  and  $k_s$  predictions for the Iowa counties of Allamakee, Fayette, Franklin, and Wright were presented in [Figure 76 to Figure 79](#). Consistent results were obtained from the developed ANN-based backcalculation models by using actual FWD deflection basins. It should be noted that  $k_s$  values show considerable seasonal changes throughout the year and the time of the FWD testing used for backcalculation should be taken into account in the design level. All FWD testings used in this case study were conducted in May 2006. The average of the four backcalculated  $k_s$  value for four Iowa counties is approximately 140 psi/in., which is a reasonable value for Iowa.
- Also, FWD tests were recently conducted on sections of old US Highway 218 near Donnelson. Each FWD drop was done with the 9-12-15-kip load sequence. According to visual observations, these pavements had numerous fatigue cracks and the pavement surface was not very old. ANN-based backcalculation models developed at this research were used to determine the pavement layer moduli and assess the structural integrity of these sections. The primary goal was to determine what kind of and how much subgrade support is being provided in these sections. Based on the subgrade moduli prediction results, it appears that the subgrade support may not be adequate in two highway sections analyzed in this report.
- The thickness of the PCC slab was not used as an input parameter in the developed  $k_s$  backcalculation models. However, the thickness of the PCC slab playing a crucial role in the  $E_{PCC}$  backcalculation is one of the most important parameters in the  $E_{PCC}$  prediction models. Generally, slab thickness exhibits considerable variability in the field, which has a large impact on the backcalculated PCC slab properties. Consequently, a given error in the estimate of the thickness of the PCC slab will have significant effects on the backcalculated slab modulus.
- In addition, the time of day for the FWD testing is also crucial in the  $E_{PCC}$  backcalculation due to curling problems in concrete pavements. The results of previous studies indicate that the variations in temperature between two separate FWD tests affect primarily the elastic modulus of the slab (Ioannides 1989). Due to

the curling and warping issues, the bonding degree between the PCC and base layers, and the thickness of the PCC slab, more scatter is expected in  $E_{PCC}$  predictions.

- Also, eight additional ANN models were developed than can predict the radius of relative stiffness of pavement systems and tensile stresses at the bottom of the PCC layer. Average AAE values of ANN predictions are less than 0.5% and 0.2% for radius of relative stiffness of pavement systems and tensile stresses at the bottom of the PCC layer, respectively.
- The backcalculated properties are significantly affected by the number of the FWD sensors. As the number of sensors increase, the mean value of elastic modulus of PCC slab increases and the mean values of coefficient of subgrade reaction decreases.  $D_0$  and  $D_{12}$  deflections are relatively more insensitive to changes in the elastic modulus of PCC slab compared to  $D_{48}$  and  $D_{60}$  deflections. However,  $D_{48}$  and  $D_{60}$  deflections are much more sensitive to the changes in the subgrade support ( $k_s$ ).
- In conclusion, the RGD- $E_{PCC}$ -(4) model (inputs:  $D_0$ ,  $D_{12}$ ,  $D_{24}$ ,  $D_{36}$ , and  $h_{PCC}$ ) is proposed for the PCC slab elastic modulus predictions, and the RGD- $k_s$ -(6) model (inputs:  $D_0$ ,  $D_{12}$ ,  $D_{24}$ ,  $D_{36}$ ,  $D_{48}$ , and  $D_{60}$ ) is proposed for the coefficient of subgrade reaction predictions. However, the backcalculated rigid pavement parameters obtained from the RGD- $E_{PCC}$ -(4) and RGD- $k_s$ -(6) models should be compared with the values obtained from other developed ANN-based backcalculation models.

## **ANN MODELS FOR COMPOSITE PAVEMENT (CP) SYSTEMS**

This section describes the research efforts related to the development of ANN-based structural models for rapid backcalculation of AC overlaid PCC-type composite pavement layer moduli parameters. The pavement structural properties that are of interest in this study are: (1)  $E_{AC}$ , (2)  $E_{PCC}$ , and (3)  $k_s$ . To generate a synthetic database for training the ANN, the DIPLOMAT (Khazanovich, 1994) structural analysis program was chosen. DIPLOMAT is chosen specifically for its capability to analyze pavement layers as plates, elastic, and springs. The results from DIPLOMAT were compared with those produced by ISLAB2000, ILLI-PAVE, and BISAR. DIPLOMAT deflection basins were then used to train ANN models for backcalculation of the pavement structural properties. When compared with the actual DIPLOMAT analysis, the trained ANN models successfully predicted the pavement layer moduli values but with several added advantages.

The primary objective of this section is to describe the development of ANN based backcalculation models for AC over PCC-type composite pavements using FWD deflection basins. The layout of this section is as follows:

- Generating solution database using DIPLOMAT
- Development of ANN structural analysis models for composite pavements
- Field testing and validation of ANN models

### **DIPLOMAT Model**

DIPLOMAT is a multilayered linear-elastic structural analysis program for computing pavement responses (stresses, strains, and displacements) under single- or multi-wheel traffic loads where each load is applied over a circular area with a uniform pressure (Khazanovich 1994). Each component of the multilayered pavement system can be an isotropic, an elastic layer, a plate, or a spring layer. The solution algorithm is based on a generalization of Burmister's layered elastic theory (Burmister 1943; 1945). Tensile stresses and downward displacements are assumed to be positive (Khazanovich 1994). DIPLOMAT can accommodate solutions for a plate on an elastic layer, an elastic layer on a plate, or spring models. Because DIPLOMAT analyzes using numerical integration methods it is faster than finite element programs.

### **Generating DIPLOMAT Solution Database**

It is intended to generate a set of data to represent measured deflection basins for ANN training using the DIPLOMAT software by varying input parameters such as layer thickness and E-moduli. A schematic of composite pavement structure is shown in [Figure 80](#). [Figure 81](#) shows the DIPLOMAT user interface for inputting layer configuration details.

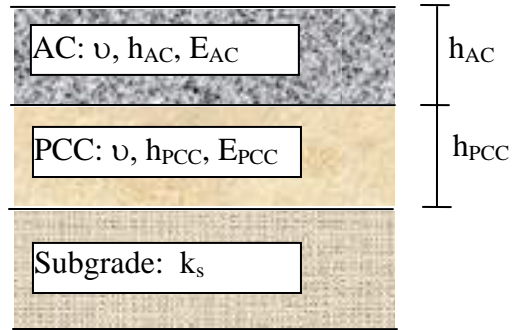


**Figure 80. Schematic of AC overlaid PCC composite pavement structure**

The screenshot shows the DIPLOMAT layer configuration input options dialog box. It features a blue title bar with a close button. The main area is light gray and contains the following controls:

- Total number of layers:** A text box containing the value '3'.
- Rigid Layer:** Radio buttons for 'Yes' (selected) and 'No'.
- Type:** Radio buttons for 'Normal' (selected), '2 unbonded plates', and '2 bonded plates'.
- Radius, r:** A text box containing the value '5.900'.
- Buttons:** 'Create files' and 'Run DIPLOMAT' buttons.
- Layer Configuration Table:** A table with three rows (Layer 1, Layer 2, Layer 3) and columns for 'Elastic', 'Plate', 'Spring', 'Bonded', 'Unbonded', and 'Poisson ratio'.
 

| Layer   | Elastic                          | Plate                            | Spring                           | Bonded | Unbonded | Poisson ratio |
|---------|----------------------------------|----------------------------------|----------------------------------|--------|----------|---------------|
| Layer 1 | <input checked="" type="radio"/> | <input type="radio"/>            | <input type="radio"/>            |        |          | 0.4           |
| Layer 2 | <input type="radio"/>            | <input checked="" type="radio"/> | <input type="radio"/>            |        |          | 0.2           |
| Layer 3 | <input type="radio"/>            | <input type="radio"/>            | <input checked="" type="radio"/> |        |          |               |

**Figure 81. DIPLOMAT layer configuration input options**

The ranges of composite pavement layer property inputs used in generating the synthetic database is summarized in Table 24. A total of 20,000 synthetic deflection basins were created, of which 18,500 were used as the training set and 1,500 as the test set.

**Table 24. Input ranges used in generating DIPLOMAT solutions**

|      | AC Modulus | PCC Modulus | $k_s$         | $h_{PCC}$ | $h_{AC}$ | $E_{PCC}/k_s$ | $E_{AC}/E_{PCC}$ |
|------|------------|-------------|---------------|-----------|----------|---------------|------------------|
| Min. | 100 ksi    | 1,000 ksi   | 50psi/in.     | *6 in.    | 2 in.    | 1,023.9       | 0.008            |
| Max. | 3,000 ksi  | 12,000 ksi  | 1,000 psi/in. | 20 in.    | 16 in.   | 230,674       | 2.92             |

\* The  $h_{PCC}$  minimum value was increased from 4 in. to 6 in. to improve the prediction performance of ANN models (see Appendix J)

### ANN-Based CP Backcalculation Models

Backpropagation-type ANN models were trained in this study with the results from the DIPLOMAT model and were used as rapid analysis design tools for predicting layer moduli of AC overlaid PCC composite pavements.

#### *Data Preprocessing*

DIPLOMAT-generated data included deflection values at 0-, 8-, 12-, 24-, 36-, 48-, and 60-inch radial distances away from the load center. The correlation of each input parameter to the pavement modulus value can be studied using a multivariate type of statistics. The correlation of each variable with the composite pavement layer moduli values is shown in [Figure 82](#) to [Figure 84](#).

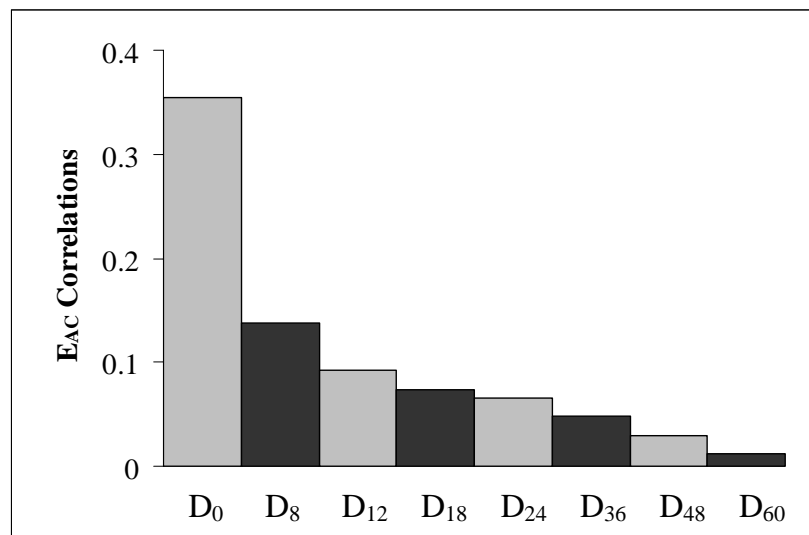


**Figure 82. E<sub>AC</sub> modulus correlation with deflections (CP)**

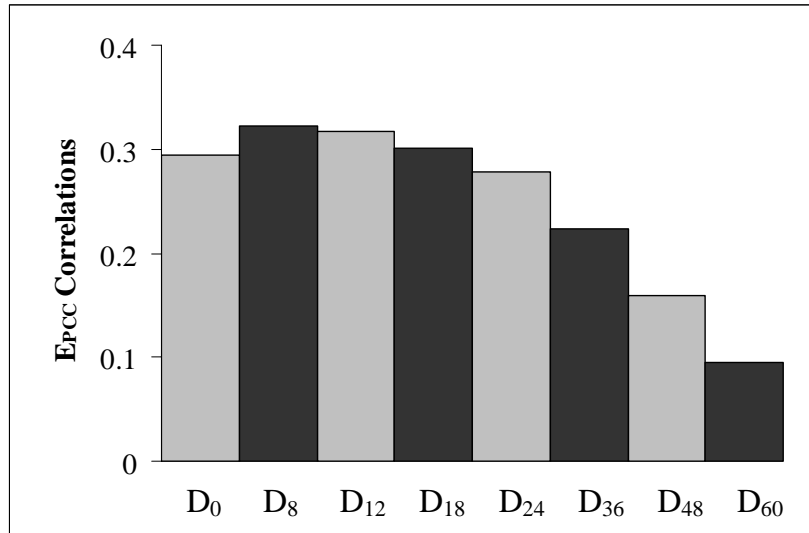


**Figure 83.  $E_{PCC}$  modulus correlation with deflections (CP)**

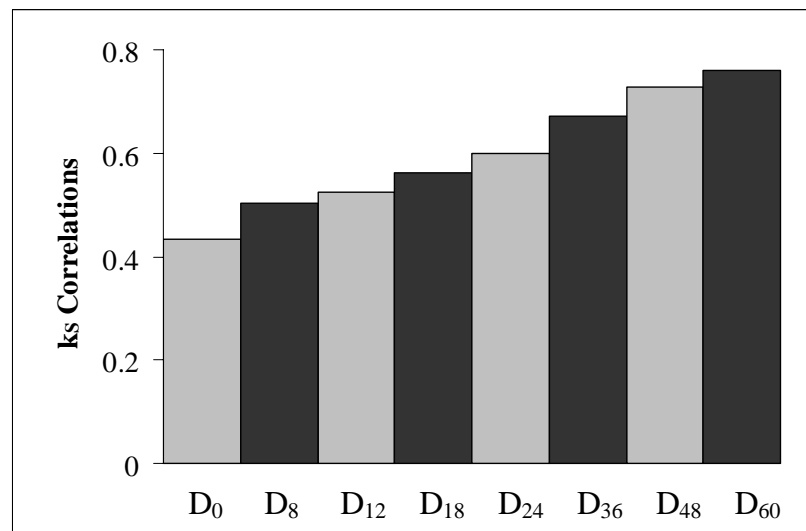


**Figure 84.  $k_s$  correlations with deflections (CP)**

### *ANN Network Architecture*

ANN models were developed by considering the following:

- Output neuron: (1) EAC model, (2) EPCC model, and (3)  $k_s$  model.
- Correlation study between inputs and outputs (4-Deflection model, 6-Deflection model, 7-Deflection model (SHRP model), 8-Deflection model)
- Use of Principle of Dimensional Analysis (Direct model and Dimensional model)

**Table 25** lists some of the abbreviations used in this section.

**Table 25. Abbreviations for ANN models**

| <b>Model</b>               | <b>Abbreviation</b>          |
|----------------------------|------------------------------|
| <b>Composite Pavements</b> | CP                           |
| <b>Dimensional Method</b>  | DM                           |
| <b>Direct Method</b>       | DR                           |
| <b>Deflection models</b>   | 4, 6, 7, 8                   |
| <b>Output models</b>       | $E_{AC}$ , $E_{PCC}$ , $k_s$ |

Both direct method and dimensional method runs had inputs of deflections at radial distances of 0, 8, 12, 18, 24, 36, 48, and 60 inches (0, 20, 30, 45, 61, 91, 122, 152 cm) away from the load, which were represented by  $D_0$ ,  $D_8$ ,  $D_{12}$ ,  $D_{18}$ ,  $D_{24}$ ,  $D_{36}$ ,  $D_{48}$ , and  $D_{60}$ , respectively, and pavement layer thickness information to predict the layer moduli of composite pavement systems. The thickness of AC and PCC were represented as  $h_{AC}$ , and  $h_{PCC}$ , respectively. The outputs were: (1) AC modulus, (2) PCC modulus, and (3)  $k_s$  – coefficient of subgrade reaction.

A total of 20 different ANN models were developed (see [Table 26](#)). Dimensional analysis inputs contained the dimensionless ratio parameters of  $E_{AC}/E_{PCC}$  and  $E_{PCC}/k_s$ . In CPDM- $E_{AC}$  models,  $E_{PCC}/k_s$  ratio was added as one of the inputs to improve ANN learning. CPDM models were developed to predict  $E_{AC}$  and  $E_{PCC}$  in stepwise fashion. First the  $k_s$  value was predicted using CPDR- $k_s$  model. Then, using the predicted  $k_s$  value and CPDM- $E_{PCC}$  run, the  $E_{PCC}$  value was predicted. Finally, having known the  $E_{PCC}$  value, the  $E_{AC}$  was predicted using the CPDM- $E_{AC}$  models.

**Table 26. CP-ANN models input/output configuration**

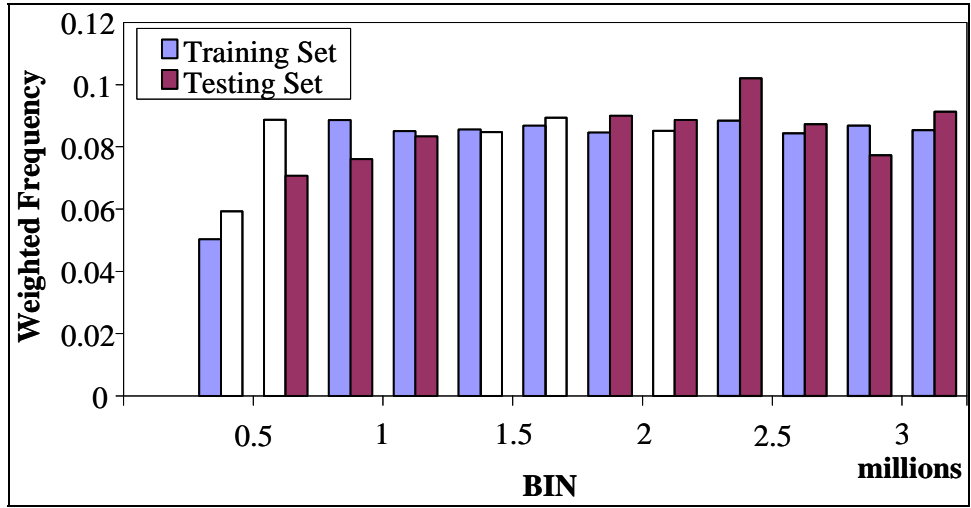
| <b>Model</b>                 | <b>Inputs</b>   | <b>Outputs</b>                     |
|------------------------------|---|------------------------------------|
| <b>CPDR4-E<sub>AC</sub></b>  | D <sub>0</sub> , D <sub>12</sub> , D <sub>24</sub> , D <sub>36</sub> , h <sub>AC</sub> , h <sub>PCC</sub>   | E <sub>AC</sub>                    |
| <b>CPDR6-E<sub>AC</sub></b>  | D <sub>0</sub> , D <sub>12</sub> , D <sub>24</sub> , D <sub>36</sub> , D <sub>48</sub> , D <sub>60</sub> , h <sub>AC</sub> , h <sub>PCC</sub>   | E <sub>AC</sub>                    |
| <b>CPDR7-E<sub>AC</sub></b>  | D <sub>0</sub> , D <sub>8</sub> , D <sub>12</sub> , D <sub>18</sub> , D <sub>24</sub> , D <sub>36</sub> , D <sub>60</sub> , h <sub>AC</sub> , h <sub>PCC</sub>  | E <sub>AC</sub>                    |
| <b>CPDR8-E<sub>AC</sub></b>  | D <sub>0</sub> , D <sub>8</sub> , D <sub>12</sub> , D <sub>18</sub> , D <sub>24</sub> , D <sub>36</sub> , D <sub>48</sub> , D <sub>60</sub> , h <sub>AC</sub> , h <sub>PCC</sub>                                    | E <sub>AC</sub>                    |
| <b>CPDR4-E<sub>PCC</sub></b> | D <sub>0</sub> , D <sub>12</sub> , D <sub>24</sub> , D <sub>36</sub> , h <sub>AC</sub> , h <sub>PCC</sub>   | E <sub>PCC</sub>                   |
| <b>CPDR6-E<sub>PCC</sub></b> | D <sub>0</sub> , D <sub>12</sub> , D <sub>24</sub> , D <sub>36</sub> , D <sub>48</sub> , D <sub>60</sub> , h <sub>AC</sub> , h <sub>PCC</sub>   | E <sub>PCC</sub>                   |
| <b>CPDR7-E<sub>PCC</sub></b> | D <sub>0</sub> , D <sub>8</sub> , D <sub>12</sub> , D <sub>18</sub> , D <sub>24</sub> , D <sub>36</sub> , D <sub>60</sub> , h <sub>AC</sub> , h <sub>PCC</sub>  | E <sub>PCC</sub>                   |
| <b>CPDR8-E<sub>PCC</sub></b> | D <sub>0</sub> , D <sub>8</sub> , D <sub>12</sub> , D <sub>18</sub> , D <sub>24</sub> , D <sub>36</sub> , D <sub>48</sub> , D <sub>60</sub> , h <sub>AC</sub> , h <sub>PCC</sub>                                    | E <sub>PCC</sub>                   |
| <b>CPDR4-k<sub>s</sub></b>   | D <sub>0</sub> , D <sub>12</sub> , D <sub>24</sub> , D <sub>36</sub> , h <sub>AC</sub> , h <sub>PCC</sub>   | k <sub>s</sub>                     |
| <b>CPDR6-k<sub>s</sub></b>   | D <sub>0</sub> , D <sub>12</sub> , D <sub>24</sub> , D <sub>36</sub> , D <sub>48</sub> , D <sub>60</sub> , h <sub>AC</sub> , h <sub>PCC</sub>   | k <sub>s</sub>                     |
| <b>CPDR7-k<sub>s</sub></b>   | D <sub>0</sub> , D <sub>8</sub> , D <sub>12</sub> , D <sub>18</sub> , D <sub>24</sub> , D <sub>36</sub> , D <sub>60</sub> , h <sub>AC</sub> , h <sub>PCC</sub>  | k <sub>s</sub>                     |
| <b>CPDR8-k<sub>s</sub></b>   | D <sub>0</sub> , D <sub>8</sub> , D <sub>12</sub> , D <sub>18</sub> , D <sub>24</sub> , D <sub>36</sub> , D <sub>48</sub> , D <sub>60</sub> , h <sub>AC</sub> , h <sub>PCC</sub>                                    | k <sub>s</sub>                     |
| <b>CPDM4-E<sub>AC</sub></b>  | D <sub>0</sub> , D <sub>12</sub> , D <sub>24</sub> , D <sub>36</sub> , h <sub>AC</sub> , h <sub>PCC</sub> , E <sub>PCC</sub> /k <sub>s</sub>  | E <sub>AC</sub> / E <sub>PCC</sub> |
| <b>CPDM6-E<sub>AC</sub></b>  | D <sub>0</sub> , D <sub>12</sub> , D <sub>24</sub> , D <sub>36</sub> , D <sub>48</sub> , D <sub>60</sub> , h <sub>AC</sub> , h <sub>PCC</sub> , E <sub>PCC</sub> /k <sub>s</sub>                                    | E <sub>AC</sub> / E <sub>PCC</sub> |
| <b>CPDM7-E<sub>AC</sub></b>  | D <sub>0</sub> , D <sub>8</sub> , D <sub>12</sub> , D <sub>18</sub> , D <sub>24</sub> , D <sub>36</sub> , D <sub>60</sub> , h <sub>AC</sub> , h <sub>PCC</sub> , E <sub>PCC</sub> /k <sub>s</sub>                   | E <sub>AC</sub> / E <sub>PCC</sub> |
| <b>CPDM8-E<sub>AC</sub></b>  | D <sub>0</sub> , D <sub>8</sub> , D <sub>12</sub> , D <sub>18</sub> , D <sub>24</sub> , D <sub>36</sub> , D <sub>48</sub> , D <sub>60</sub> , h <sub>AC</sub> , h <sub>PCC</sub> , E <sub>PCC</sub> /k <sub>s</sub> | E <sub>AC</sub> / E <sub>PCC</sub> |
| <b>CPDM4-E<sub>PCC</sub></b> | D <sub>0</sub> , D <sub>12</sub> , D <sub>24</sub> , D <sub>36</sub> , h <sub>AC</sub> , h <sub>PCC</sub>   | E <sub>PCC</sub> / k <sub>s</sub>  |
| <b>CPDM6-E<sub>PCC</sub></b> | D <sub>0</sub> , D <sub>12</sub> , D <sub>24</sub> , D <sub>36</sub> , D <sub>48</sub> , D <sub>60</sub> , h <sub>AC</sub> , h <sub>PCC</sub>   | E <sub>PCC</sub> / k <sub>s</sub>  |
| <b>CPDM7-E<sub>PCC</sub></b> | D <sub>0</sub> , D <sub>8</sub> , D <sub>12</sub> , D <sub>18</sub> , D <sub>24</sub> , D <sub>36</sub> , D <sub>60</sub> , h <sub>AC</sub> , h <sub>PCC</sub>  | E <sub>PCC</sub> / k <sub>s</sub>  |
| <b>CPDM8-E<sub>PCC</sub></b> | D <sub>0</sub> , D <sub>8</sub> , D <sub>12</sub> , D <sub>18</sub> , D <sub>24</sub> , D <sub>36</sub> , D <sub>48</sub> , D <sub>60</sub> , h <sub>AC</sub> , h <sub>PCC</sub>                                    | E <sub>PCC</sub> / k <sub>s</sub>  |

The ANN data set consisted of 20,000 DIPLOMAT solutions. This data set was separated into 18,500 training and 1,500 independent testing sets. ANNs learned the relationship between input parameters and output variables using the information provided in the training data set. Then the independent 1,500 test data set was used to test how well the ANN models learned the relationship between the input parameters and output variables. The test data set should be a good representative of total data; i.e., the distribution of the test set should match the distribution of the total data set.

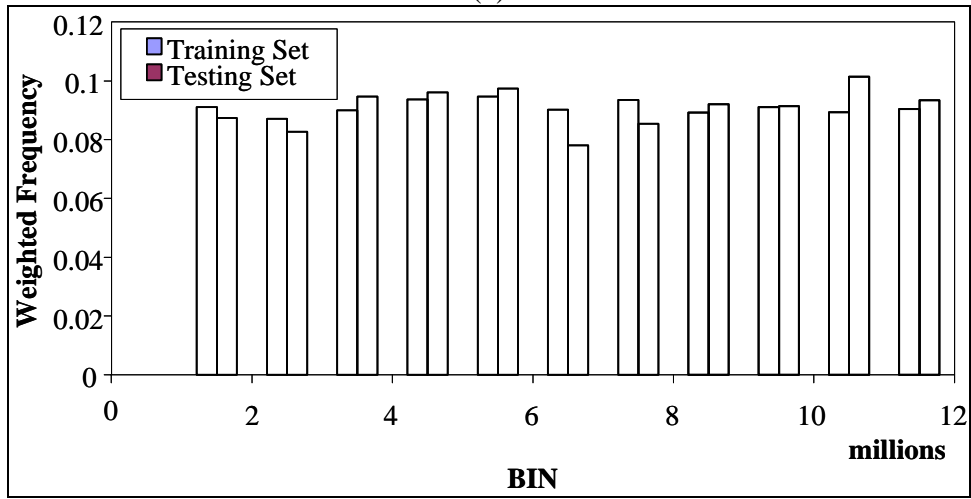
Figure 85 shows histograms of the training and testing set for each output value. For comparison, a weighted frequency of data was used. The weighted frequency was calculated by dividing the frequency for each bin by the total number of data sets. A network with two hidden layers and 60 neurons in each layer was exclusively chosen for the ANN models trained in this study. Satisfactory results were obtained in the previous studies with these types of networks because of their ability to better facilitate functional mapping (Ceylan 2002; Ceylan and Guclu 2005c).

Table 27 summarizes the AAE values for each ANN-based model. Figure H.1 to Figure H.24 in Appendix H summarize the results for the CPDR models and Figure H.25 to Figure H.40 summarize results predicted by the CPDM models. Progress curves depict the calculated MSE at

each epoch for training and testing of the output of the models. The MSEs decreased as the networks grew in size with an increasing number of epochs. The testing MSEs were, in general, for all models, slightly lower than the training ones. The lowest training MSEs were in the order of  $2.0 \times 10^{-5}$  for  $E_{AC}$ ,  $5.2 \times 10^{-5}$  for  $E_{PCC}$ ,  $3.6 \times 10^{-6}$  for  $k_s$ ,  $6.0 \times 10^{-5}$  for  $E_{AC}/E_{PCC}$  ratio, and for  $1.3 \times 10^{-4}$   $E_{PCC}/k_s$  ratio.



(a)



(b)

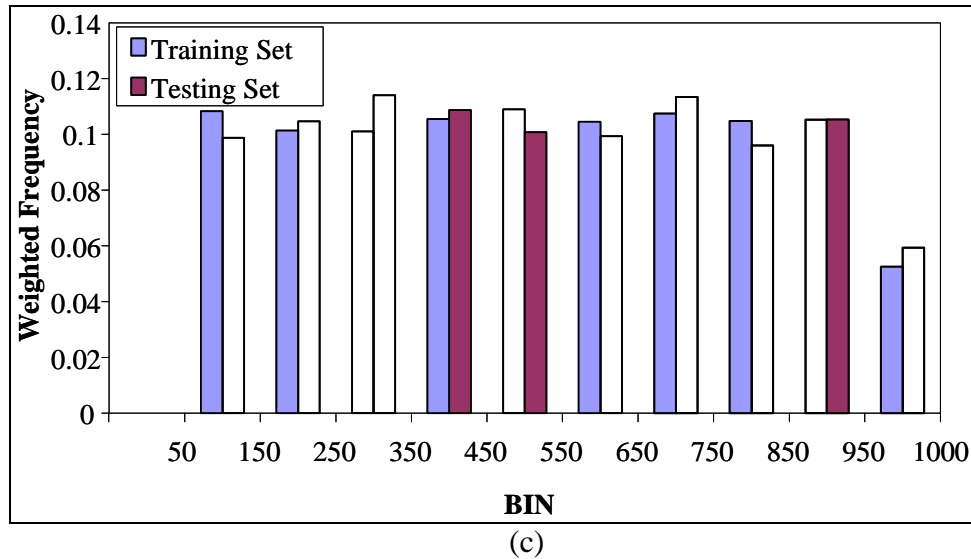


Figure 85. Training and testing set histogram comparisons for (a)  $E_{AC}$ , (b)  $E_{PCC}$ , and (c)  $k$

Table 27. Prediction performance of CP-ANN-based backcalculation models (virgin)

| ANN Deflection Models | AAE (%)              |           |       |                           |               |
|-----------------------|----------------------|-----------|-------|---------------------------|---------------|
|                       | Direct Method (CPDR) |           |       | Dimensional Method (CPDM) |               |
|                       | $E_{AC}$             | $E_{PCC}$ | $k_s$ | $E_{AC}/E_{PCC}$          | $E_{PCC}/k_s$ |
| 4-Deflection          | 0.37                 | 0.89      | 0.36  | 4.1                       | 2.83          |
| 6-Deflection          | 0.53                 | 0.70      | 0.23  | 4.05                      | 2.76          |
| 7-Deflection          | 0.63                 | 0.79      | 0.20  | 2.59                      | 2.57          |
| 8-Deflection          | 0.45                 | 0.77      | 0.23  | 2.37                      | 3.02          |

### Noise-Introduced CP-ANN Backcalculation Models

In addition to the training and testing data sets prepared for the backcalculation models, more ANN training data sets were generated by introducing  $\pm 2\%$ ,  $\pm 5\%$  and  $\pm 10\%$  noise to the FWD deflection data used in the backcalculation models (Table 28). The purpose of introducing noisy patterns in the training data sets was to develop more robust networks that can tolerate the noisy or inaccurate deflection patterns collected from the FWD deflection basins. Noise introduction to trained ANN models was as follows. The DIPLOMAT solution database was first partitioned to create training sets of 18,500 training patterns and an independent testing set of 1,500 patterns to check the performance of the trained ANN models. Uniformly distributed random numbers in the ranges of  $\pm 2\%$ ,  $\pm 5\%$ , and  $\pm 10\%$  were generated to create noisy training patterns. After adding the randomly selected noise values to only the pavement surface deflections, new training data sets were developed for each noisy training set. By repeating the noise introduction procedure, four more training data sets were formed for each backcalculation model. Including the original training set with no noise in it, a total of 94,000 patterns were used to train the noise-introduced ANN backcalculation model. Appendix I includes the prediction performance results of all noise-introduced ANN models.

**Table 28. Prediction performance of CP-ANN-based backcalculation models (noise)**

| Noise Amount | ANN Deflection Models | AAE (%)  |           |       |
|--------------|-----------------------|----------|-----------|-------|
|              |                       | $E_{AC}$ | $E_{PCC}$ | $k_s$ |
| ±2%          | 4-Deflection          | 6.46     | 5.46      | 3.51  |
|              | 6-Deflection          | 6.99     | 4.57      | 0.63  |
|              | 7-Deflection          | 4.52     | 3.45      | 0.72  |
|              | 8-Deflection          | 5.21     | 4.13      | 0.64  |
| ±5%          | 4-Deflection          | 12.46    | 11.81     | 5.32  |
|              | 6-Deflection          | 12.15    | 8.34      | 1.36  |
|              | 7-Deflection          | 11.45    | 7.80      | 1.32  |
|              | 8-Deflection          | 11.14    | 6.75      | 2.09  |
| ±10%         | 4-Deflection          | 18.21    | 18.17     | 9.53  |
|              | 6-Deflection          | 15.37    | 10.45     | 3.74  |
|              | 7-Deflection          | 17.13    | 10.43     | 3.16  |
|              | 8-Deflection          | 16.33    | 10.78     | 2.54  |

### CP-ANN Forward Calculation Models

Backpropagation-type neural networks were employed to develop ANN structural models for predicting pavement responses based on the known input variables of pavement layer thickness and deflection basin. This ANN model called forward calculation model consisted of the AC and PCC thicknesses and the pavement surface deflection basin to predict the pavement responses of  $\epsilon_{AC}$  at the bottom of AC,  $\sigma_{PCCx}$  at the bottom of PCC, and vertical stress in the subgrade. The main advantage and use of the ANN FC model is in the rapid prediction of the DIPLOMAT results from the pavement surface deflections. Prediction performance graphs presented in Figure H.41 to Figure H.46 in Appendix H show that the AAEs for  $\epsilon_{AC}$ ,  $\sigma_{PCCx}$ , and  $\sigma_{SGz}$  predictions are 0.62%, 0.86%, and 0.64%, respectively.

### Validation of ANN Models

To analyze the actual field data, the noise in the data should be minimized. To minimize the error, data errors and anomalies in the FWD deflection data should be identified. The majority of the errors and anomalies associated with the deflection data can be classified as:

- Operator errors (incorrect lane designation, station number, drop height, etc.)
- FWD equipment errors (calibration errors, incorrect sensor positioning, etc.)
- Irregularities of pavement surface

These errors result in inconsistent deflection basins. To identify the inconsistent deflection basins, the following filtering technique was developed:

- The deflection values should decrease with increasing radial offsets from the load center (i.e.,  $D_0$  should be maximum and  $D_{60}$  should be minimum).
- Maximum deflection should be obtained from maximum weight drop.
- The maximum and minimum of deflection data should be within the ANN training database range.

Figure 86 and Figure 87 shows unfiltered and filtered FWD data, respectively for the sake of illustration.

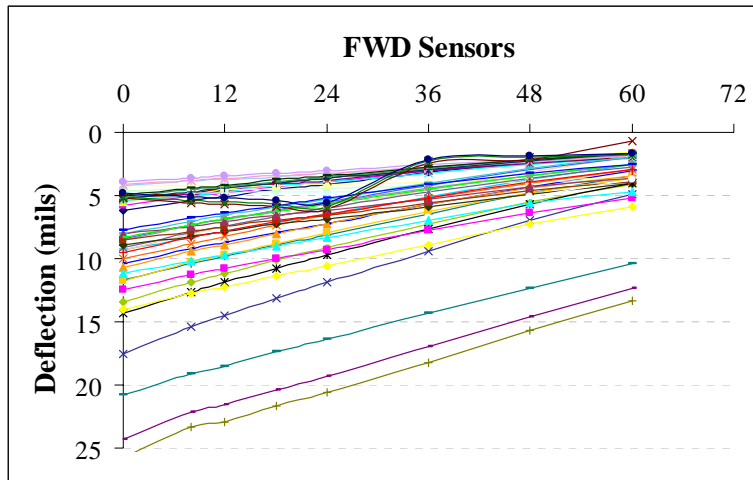


**Figure 86. Field data deflection basin before filtering**

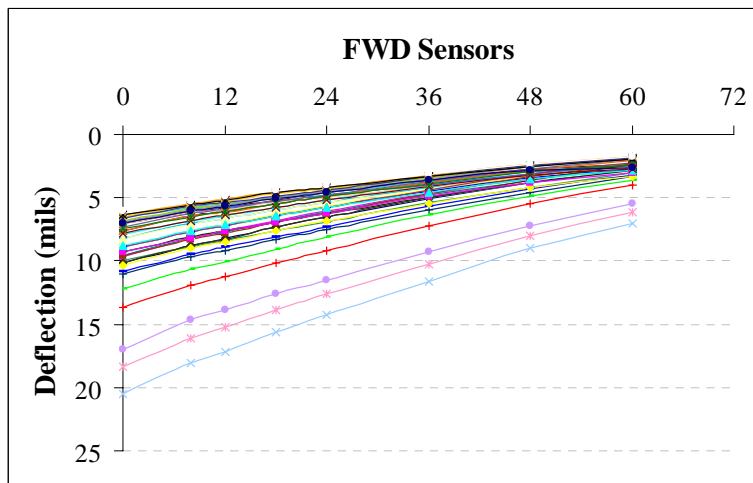
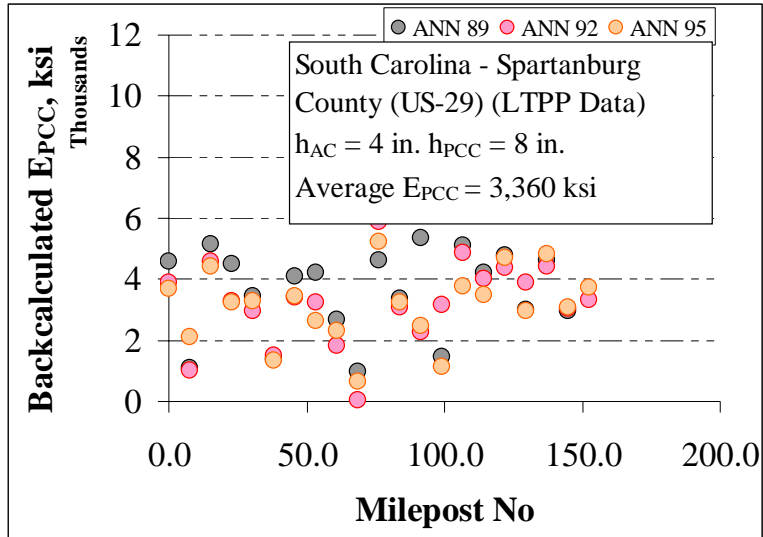


**Figure 87. Field data deflection basin after filtering**

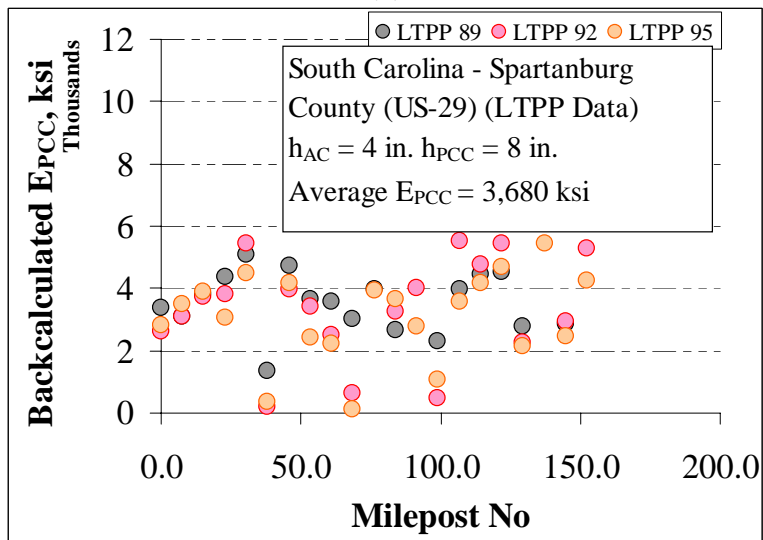
The performance of ANN models were tested with FWD data. LTPP field data for AC overlaid PCC pavements were used with ANN-CPDR-SHRP models (7-deflection). In addition, ANN model performances were compared with MODCOMP backcalculation software performance results provided in the LTPP database. The LTPP data site 45-7019 was selected. The FWD data was obtained from the pavement test sections on US 29, Spartanburg County, South Carolina.

The original construction date for this site was 1946. It is an AC overlaid PCC-type composite pavement system. FWD deflections were taken from the “MON\_DEFL\_DROP\_DATA\_MT\_TN” Microsoft Access file of LTPP standard data release 20 (FHWA, 2005). The LTPP database contains data for the same section for years 1989, 1992, and 1995. The centerline pavement deflections were chosen for this analysis. LTPP MODCOMP v4.2 backcalculated values are presented for comparison in Figure 88 and Figure 89. MODCOMP uses elastic layer theory, embodied in the CHEVRON computer code, as the method of forward calculation within an iterative approach.

Figure 88 shows the ANN-predicted CPDR-7-AC moduli and LTPP MODCOMP AC moduli predictions, respectively. Similarly, Figure 89 shows the PCC moduli predictions for both the CPDR-7-PCC ANN model and LTPP MODCOMP, respectively. As seen in figures, the  $E_{AC}$  predictions are more consistent than the  $E_{PCC}$  predictions. Both MODCOMP and ANN-based  $E_{AC}$  values lie within the  $\pm 200$  ksi range. This range goes up to  $\pm 1,000$  ksi in the case of  $E_{PCC}$ . As seen from both the AC and PCC prediction plots, the ANN and MODCOMP predictions, in general, are in good agreement. The ANN-based average  $E_{AC}$  prediction is 3.2 GPa, and the  $E_{PCC}$  average is 23.2 GPa. The average MODCOMP prediction for  $E_{AC}$  is 4.1 GPa, and  $E_{PCC}$  average is 25.4 GPa. Few spikes observed in the plots are due to faulty deflection basins. The scatter in ANN predictions is lesser compared to MODCOMP predictions (see the standard deviation values presented in Figure 88 and Figure 89), which demonstrates the power of the ANN-based approach. In addition, ANN moduli predictions for years 1989, 1992, and 1995 are more consistent compared to the MODCOMP predictions listed in the LTPP database.

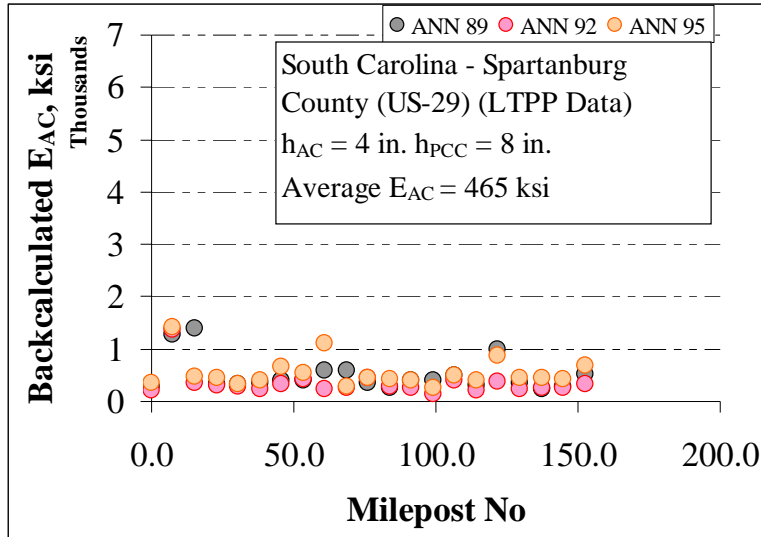


(a)

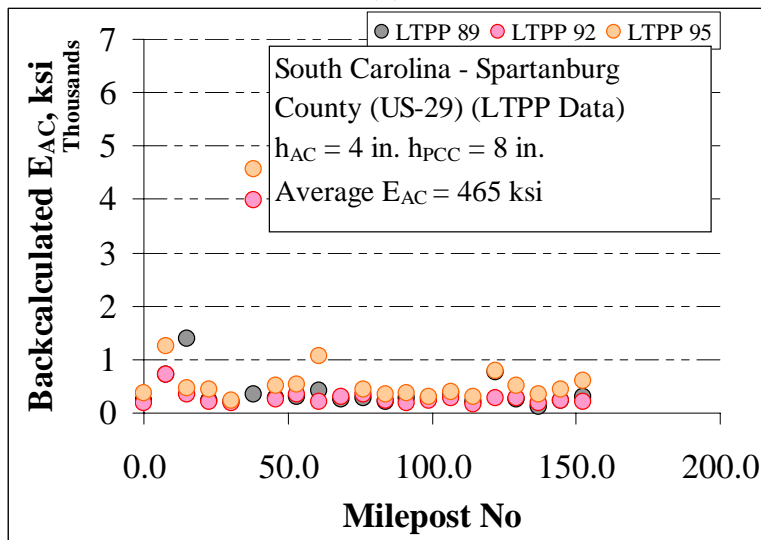


(b)

Figure 88. AC layer moduli predictions using: (a) ANN-based models and (b) MODCOMP model.



(a)



(b)

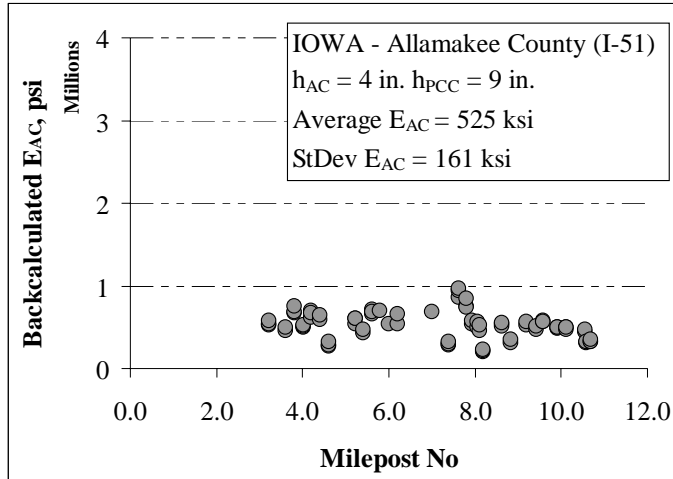
**Figure 89. PCC layer moduli predictions using: (a) ANN-based models and (b) MODCOMP model.**

### Case Studies of Individual Pavement Sections

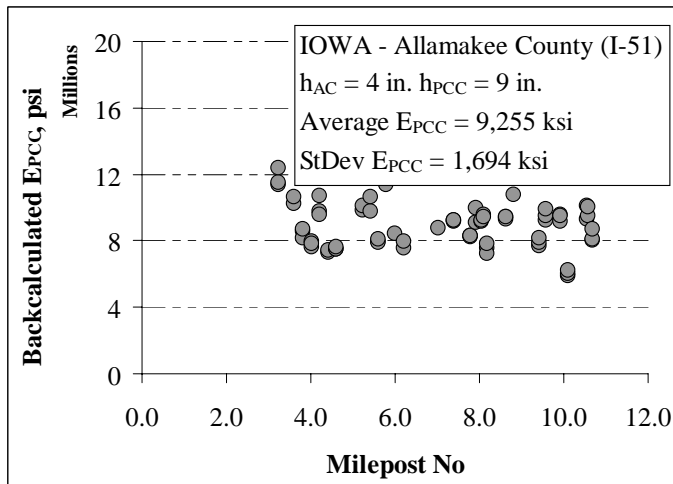
ANN models were evaluated using actual FWD data from the Iowa DOT. First, composite pavement systems were identified using the DOT milepost book. Then the layer thicknesses from the milepost book were entered as inputs for ANN models along with the FWD measurements at these sites. For this study, nine different sites were selected. A list of selected sites is given in [Table 29](#).

**Table 29. Iowa composite pavement sections**

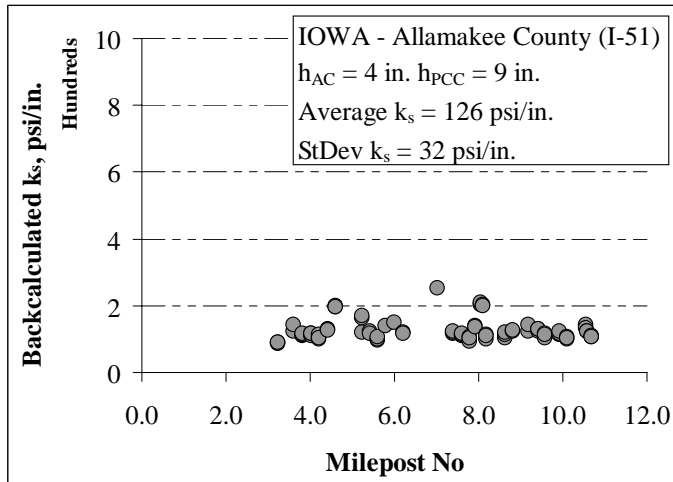
| <b>Pavement Type</b> | <b>Location &amp; Milepost</b>                         | <b>h<sub>AC</sub> (in.)</b> | <b>h<sub>PCC</sub> (in.)</b> |
|----------------------|--|-----------------------------|------------------------------|
| CP                   | IA-Allamakee County (I-51)<br>(Milepost No: 3-11)      | 4                           | 9                            |
| CP                   | IA-Black Hawk County (I-57)<br>(Milepost No: 37-40)    | 5.5                         | 8                            |
| CP                   | IA-Butler County (US-14)<br>(Milepost No: 152-158)     | 3                           | 8                            |
| CP                   | IA- Chickasaw County (US-18)<br>(Milepost No: 221-227) | 8.5                         | 7                            |



(a)

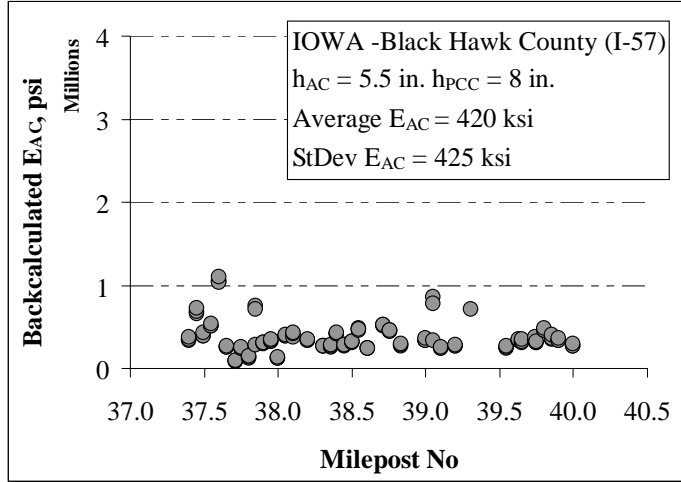


(b)

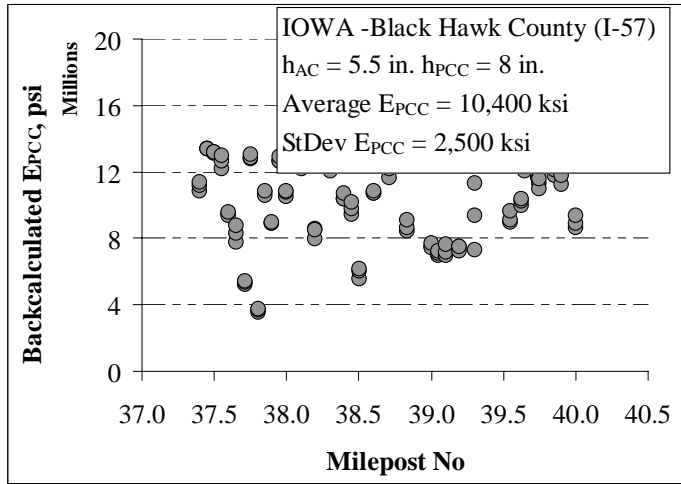


(c)

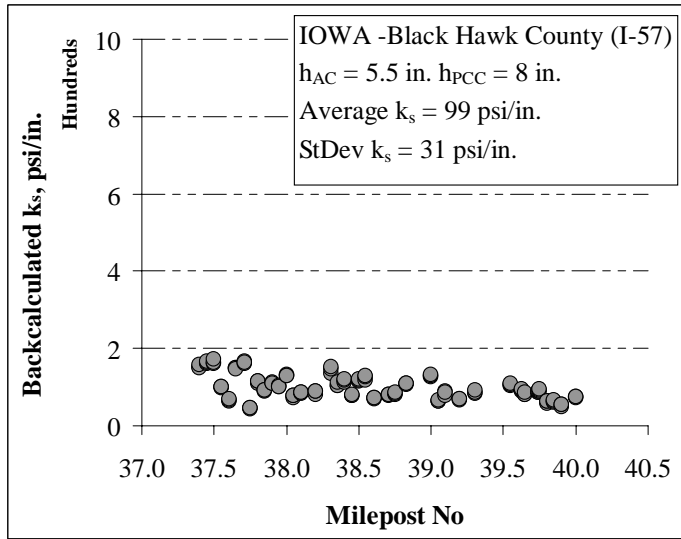
**Figure 90. Iowa – Allamakee Co. (I-51): (a) $E_{AC}$  predictions, (b) $E_{PCC}$  predictions, (c) $k_s$  predictions**



(a)

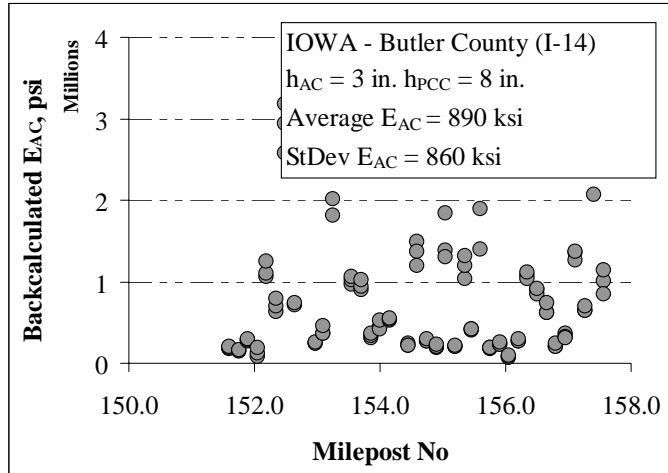


(b)

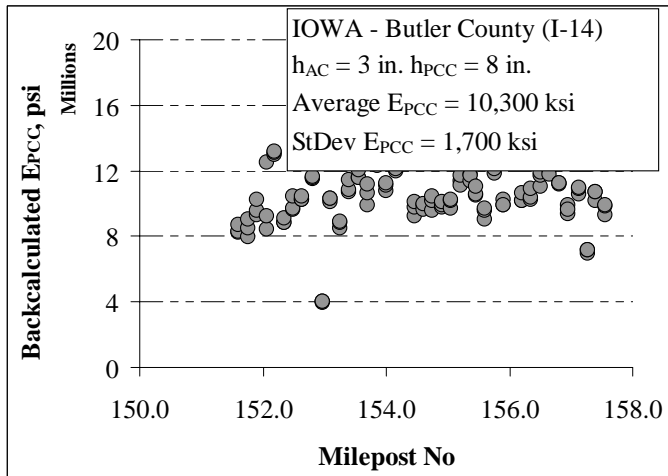


(c)

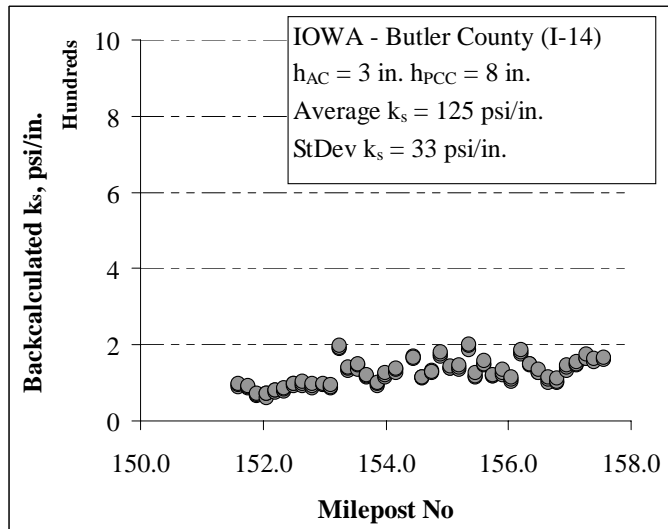
**Figure 91. Iowa – Black Hawk County (I-57): (a) $E_{AC}$  predictions, (b) $E_{PCC}$  predictions, (c) $k_s$  predictions**



(a)

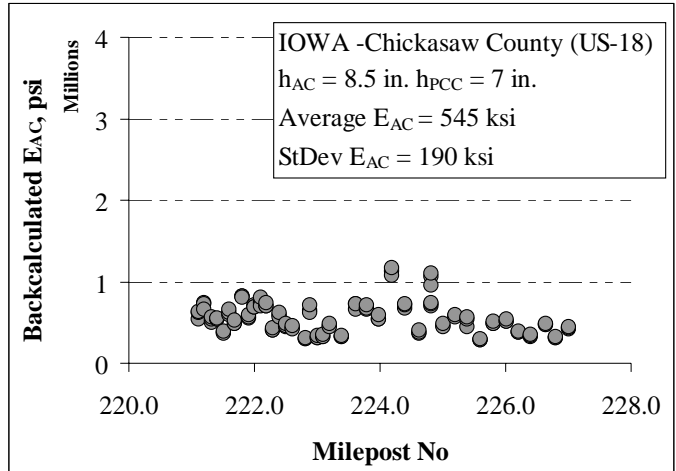


(b)

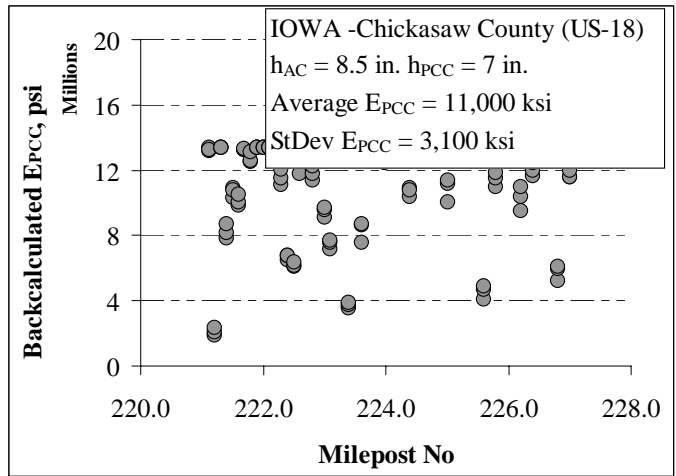


(c)

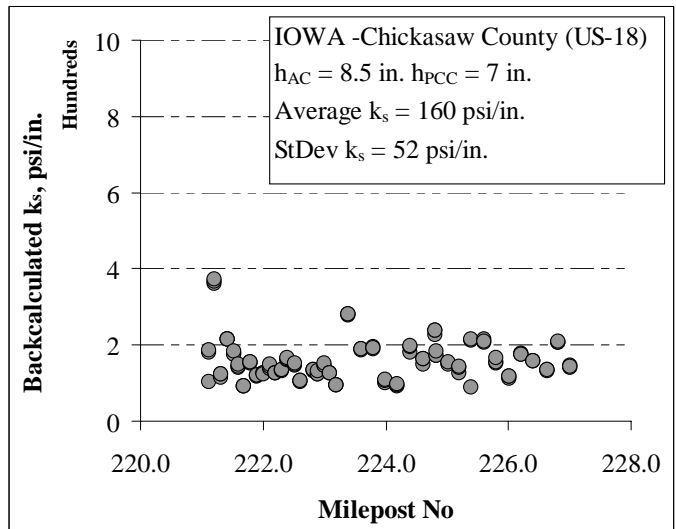
Figure 92. Iowa – Butler County (I-14): (a) $E_{AC}$  predictions, (b) $E_{PCC}$  predictions, (c) $k_s$  predictions



(a)



(b)



(c)

**Figure 93. Iowa – Chickasaw County (US-18): (a) $E_{AC}$  predictions, (b) $E_{PCC}$  predictions, (c)  $k_s$  predictions**

## ANN Models for Composite Pavements — Summary and Conclusions

### *Summary*

ANN-based structural models were successfully developed for analyzing AC overlaid PCC-type composite pavement systems. A total of 20 different ANN-based backcalculation models were developed for predicting composite pavement layer moduli using approximately 20,000 DIPLOMAT model solutions.

### *Conclusions*

- The ANN-based models successfully predicted pavement layer moduli values of EAC, EPCC, and ks with an overall AAE value of less than 1.5 percent. Similarly, ANN-based backcalculation models predicted the EAC/EPCC ratio and EPCC/ks ratio with an AAE of 3.0% for models in which dimensional analysis was used.
- It was demonstrated that ANNs are capable of successfully predicting the pavement layer moduli values using the LTPP-FWD field deflection measurements. Field moduli values were successfully predicted for the given deflection basins, and the comparison of the ANN-based predictions with the ones listed in the LTPP database showed the strength of the ANN-based backcalculation approach.
- The adoption of the ANN-based approach also resulted in both a drastic reduction in computation time and a simplification of the complicated traditional layer backcalculation approaches. Rapid prediction ability of the ANN models — capable of analyzing 100,000 FWD deflection profiles in one second — provide a tremendous advantage to the pavement engineers by allowing them to nondestructively assess the condition of the transportation infrastructure systems in real time while the FWD testing takes place in the field.
- Elimination of selecting seed layer moduli with the integration of an ANN-based direct backcalculation approach can be invaluable for the state and federal agencies for rapidly analyzing a large number of composite pavement deflection basins needed for routine pavement evaluation for both project-specific and network-level FWD testing.

# DEVELOPMENT OF A USER-FRIENDLY SPREADSHEET ANALYSIS TOOL FOR DEVELOPED ANN MODELS

## Introduction

One of the primary objectives of this study is to develop a nondestructive pavement evaluation software toolbox to assess pavement condition, estimate pavement remaining life, and eventually help assess pavement rehabilitation strategies by the pavement management team at the Iowa DOT. The Microsoft Excel-based pavement evaluation toolbox, which incorporates all the developed ANN models, provides the city, county, and Iowa DOT engineers with the ability to analyze FWD deflection data in real time, if necessary, and display the results in a graphical environment. The Excel toolbox allows an engineer to analyze FWD data quickly and efficiently using the neural network-based algorithms incorporated in it.

Pavement layer moduli values and critical pavement responses for various pavement types (flexible, rigid, and composite) are the outputs provided by the toolbox. Using the toolbox, the variations of pavement layer properties over the length of the analyzed section can also be observed numerically and graphically. The software was developed using the model parameters and results described in previous chapters. The toolbox program includes flexible (full-depth and conventional), rigid, and composite types of pavement analysis. Pavement data collection and analysis is a vital step in the evaluation of pavement structures. Proper collection of FWD data and pavement information is required for accurate FWD data analysis with the developed software.

## Program Overview

The password-protected, Excel-based software toolbox was developed using Microsoft's Visual Basic programming language and Excel macros. In case of troubleshooting, the user is requested to change the macro security (Tools → Macro → Security) to the "medium" or "low" level to allow macros to run. The Excel spreadsheets provide the user interaction for data editing and pasting, displaying results, charts, and tables, and for displaying statistical information. The Excel sheets include a main menu, analysis menu (for each pavement type), plotting menu, and summary menu.

### *Program Menus and Pavement Analysis Menu*

The program starts by displaying the main menu (Figure 94). As a first step, users are expected to select the pavement type (full-depth, conventional flexible, composite or rigid pavements) by clicking on it to activate the selected pavement analysis Excel sheet/interface. The software toolbox is programmed to give warning messages if the user clicks anywhere else.

While working with the toolbox, all other Excel features are accessible, including open, close, copy, paste, save, save as, print, and print settings. When the user quits the toolbox, all the charts and results for the analysis, except the last data entered, will be deleted. To retain the results, they should be copied into another spreadsheet.

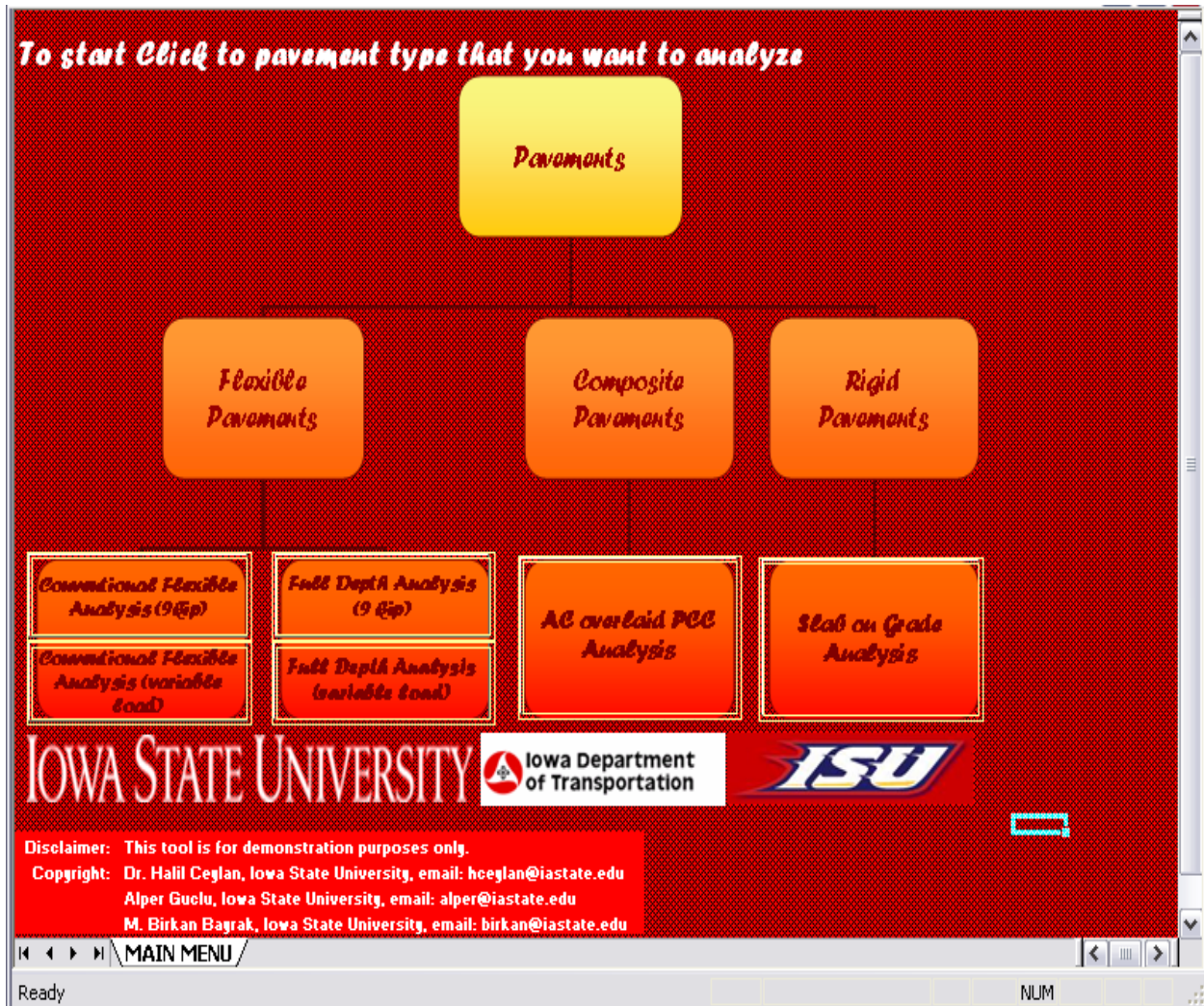


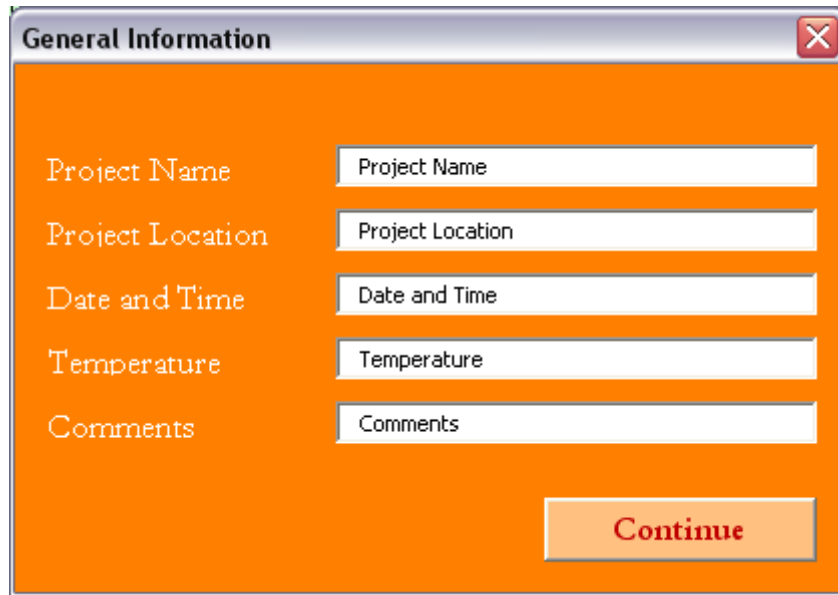
**Figure 94. FWD analysis program main menu**

### *Pavement Analysis Using the Excel Sheets*

There are six Excel pavement analysis sheets, including the CFP analysis module with 9-kip and variable FWD load, the full-depth flexible pavements analysis module with 9-kip and variable FWD load, and the composite and rigid pavement analysis module with 9-kip FWD loadings. After selecting one of the pavement types from the main menu, a general information window

appears. Its purpose is to get information that represents a project site at the beginning of each analysis (see Figure 95). The user is required to fill in the information to continue with pavement analysis.

General information inputs will be displayed with each graph to identify the project information.



The image shows a software dialog box titled "General Information". The dialog has a light blue title bar with a close button (X) in the top right corner. The main area has an orange background. There are five input fields, each with a label to its left: "Project Name", "Project Location", "Date and Time", "Temperature", and "Comments". Each input field contains the same text as its label. At the bottom right of the dialog is a "Continue" button with a red border and text.

**Figure 95. General information window**

At the next step, users are expected to enter the FWD deflection database and inputs for the program. Required analysis parameters are deflection data, pavement layer information (layer thicknesses), and FWD load (for variable FWD load analysis). Depending on pavement type, the number of layers can be changed. As shown in the Figure 96, the input requirements for conducting 9-kip CFP analyses are FWD deflection data, asphalt concrete thicknesses, granular base thickness, and FWD load (9-kip-constant). If any of the required parameter is missing, the program will display an error message of “No Data” in the results section.

The default units used in the program are based on US customary units. FWD deflection data ( $D_0$  till  $D_{60}$ ) should be entered in mils ( $10^{-3}$  inches), layer thickness in inches, and FWD load should be in kips. The program will not run correctly if these input parameters are not in the desired ranges. The user is requested to refer to the report for the appropriate ranges of these parameters. Reported results are modulus values, strains, and stresses. Modulus and stress values are reported in psi and strains are reported in micro-strains ( $\times 10^6$ ).

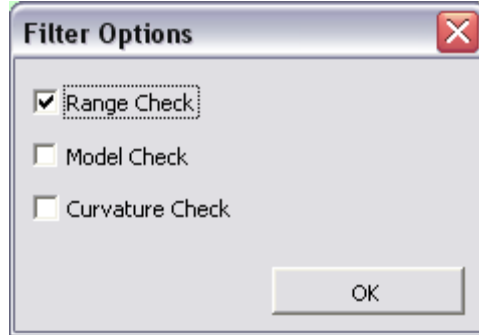
| Location | FWD Deflections (mils) |     |       |      |      |      |      | Asphalt Concrete Thickness (inch) | Granular Base Thickness (inch) | FWD Load (kip) | 4 Deflections-Eac (psf) (D0-D12-D24-D36) |    |    |    |
|----------|------------------------|-----|-------|------|------|------|------|-----------------------------------|--------------------------------|----------------|--|----|----|----|
|          | D-0                    | D-8 | D-12  | D-18 | D-24 | D-36 | D-48 | D-60                              | $h_{AC}$                       | $h_{GB}$       | Load                                     | 0% | 2% | 5% |
| 1        | 5.94                   |     | 10.00 |      | 3.66 | 2.86 | 2.16 | 2.08                              | 16.00                          | 18.00          | 9.00                                     |    |    |    |
| 2        | 5.94                   |     | 4.73  |      | 3.66 | 2.86 | 2.16 | 2.08                              | 16.00                          | 18.00          | 9.00                                     |    |    |    |
| 3        | 7.27                   |     | 5.78  |      | 4.46 | 3.49 | 2.64 | 2.24                              | 16.00                          | 18.00          | 9.00                                     |    |    |    |
| 4        | 5.56                   |     | 4.31  |      | 3.48 | 2.85 | 2.42 | 2.14                              | 16.00                          | 18.00          | 9.00                                     |    |    |    |
| 5        | 7.00                   |     | 5.45  |      | 4.38 | 3.60 | 2.93 | 2.73                              | 16.00                          | 18.00          | 9.00                                     |    |    |    |
| 6        | 8.50                   |     | 6.60  |      | 5.32 | 4.36 | 3.52 | 2.85                              | 16.00                          | 18.00          | 9.00                                     |    |    |    |
| 7        | 8.81                   |     | 7.30  |      | 5.84 | 4.70 | 3.62 | 3.10                              | 16.00                          | 18.00          | 9.00                                     |    |    |    |
| 8        | 6.16                   |     | 5.04  |      | 4.00 | 3.13 | 2.40 | 2.02                              | 16.00                          | 18.00          | 9.00                                     |    |    |    |
| 9        | 7.73                   |     | 6.30  |      | 4.99 | 3.90 | 2.97 | 2.57                              | 16.00                          | 18.00          | 9.00                                     |    |    |    |
| 10       | 9.44                   |     | 7.63  |      | 6.05 | 4.76 | 3.60 | 3.12                              | 16.00                          | 18.00          | 9.00                                     |    |    |    |
| 11       | 6.68                   |     | 5.06  |      | 3.99 | 3.12 | 2.40 | 2.15                              | 16.00                          | 18.00          | 9.00                                     |    |    |    |
| 12       | 8.37                   |     | 6.35  |      | 5.05 | 3.95 | 2.97 | 2.41                              | 16.00                          | 18.00          | 9.00                                     |    |    |    |
| 13       | 10.21                  |     | 7.75  |      | 6.14 | 4.82 | 3.61 | 2.92                              | 16.00                          | 18.00          | 9.00                                     |    |    |    |
| 14       | 5.53                   |     | 4.06  |      | 3.21 | 2.53 | 1.90 | 1.54                              | 16.00                          | 18.00          | 9.00                                     |    |    |    |
| 15       | 7.10                   |     | 5.21  |      | 4.13 | 3.23 | 2.42 | 2.02                              | 16.00                          | 18.00          | 9.00                                     |    |    |    |
| 16       | 8.58                   |     | 6.28  |      | 4.99 | 3.89 | 2.92 | 2.37                              | 16.00                          | 18.00          | 9.00                                     |    |    |    |
| 17       | 6.83                   |     | 5.61  |      | 4.61 | 3.77 | 2.96 | 2.57                              | 16.00                          | 18.00          | 9.00                                     |    |    |    |
| 18       | 8.19                   |     | 6.71  |      | 5.52 | 4.51 | 3.52 | 2.75                              | 16.00                          | 18.00          | 9.00                                     |    |    |    |
| 19       | 4.26                   |     | 3.61  |      | 3.18 | 2.85 | 2.62 | 2.48                              | 16.00                          | 18.00          | 9.00                                     |    |    |    |
| 20       | 4.71                   |     | 3.52  |      | 3.06 | 2.66 | 2.33 | 2.19                              | 16.00                          | 18.00          | 9.00                                     |    |    |    |
| 21       | 6.61                   |     | 5.32  |      | 4.34 | 3.49 | 2.69 | 2.30                              | 16.00                          | 18.00          | 9.00                                     |    |    |    |
| 22       | 8.07                   |     | 6.46  |      | 5.27 | 4.23 | 3.26 | 2.82                              | 16.00                          | 18.00          | 9.00                                     |    |    |    |
| 23       | 8.44                   |     | 6.68  |      | 5.22 | 4.03 | 3.00 | 2.55                              | 16.00                          | 18.00          | 9.00                                     |    |    |    |
| 24       | 10.69                  |     | 8.44  |      | 6.57 | 5.07 | 3.74 | 2.95                              | 16.00                          | 18.00          | 9.00                                     |    |    |    |
| 25       | 12.69                  |     | 10.02 |      | 7.82 | 5.99 | 4.42 | 3.46                              | 16.00                          | 18.00          | 9.00                                     |    |    |    |
| 26       | 5.68                   |     | 4.76  |      | 3.94 | 3.17 | 2.47 | 2.19                              | 16.00                          | 18.00          | 9.00                                     |    |    |    |
| 27       | 7.24                   |     | 6.05  |      | 4.97 | 4.00 | 3.06 | 2.57                              | 16.00                          | 18.00          | 9.00                                     |    |    |    |

Figure 96. Sample pavement analysis: Excel sheet inputs

After entering the FWD data, there is a data preprocessing unit for filtering the data. It is optional to use the filtering window. Figure 97 shows the available options for filtering. The three options are:

- Range Check: Deflection basin should form a bowl shape and, therefore, deflections should be in decreasing order. Data that falls outside this range are red colored.
- Model Check: ANN models are normalized according to the model ranges and, therefore, any input outside the range used in ANN training will form a poor quality input. As a result, the model check will determine the outliers and color them in red.
- Curve check: Curvature Index is checked in order to make sure that the FWD deflection basins form a bowl curvature. The curvature index check is applied as follows:  $SCI > BDI > BCI$ . The curvature check parameters are described in Table 30. Curve check should be applied only to flexible pavements.

The filtering is applied by changing the color of the input parameter to red. Filtered data is also shown with red color in charts. Therefore, results for these parameters are also calculated. With this approach, engineers will have a better understanding of the sources of errors.



**Figure 97. Filter options menu**

**Table 30. Curvature check input parameters**

---

Surface Curvature Index (SCI);  $SCI = D_0 - D_{12}$

Base Damage Index (BDI);  $BDI = D_{12} - D_{24}$

Base Curvature Index (BCI);  $BCI = D_{24} - D_{36}$

---

After preprocessing the data, clicking the “Run” button will activate a neural network-based analysis of pavements. The program will analyze model by model for the pavement properties. For each model (see previous chapters for the developed models), the analysis results will be displayed on the right side of the screen. The user should scroll right to see all results. Also, disabled menu commands of plots and the summary will be activated. Figure 98 illustrates the analysis result of a CFP with 9-kip FWD loading. As described in the previous chapters, each model has a different number of input parameters depending on the number of deflections. Failure to supply all the input parameters will be reflected in the results column of that model. The program will automatically write “No Data.” For example, if  $D_{48}$  is missing in the input data, then all six- and eight-deflection model columns will display the error message of “No Data.”

At the end of each column, statistical information regarding that model is presented (see Figure 99). The collection of these statistics is summarized in summary sheets.

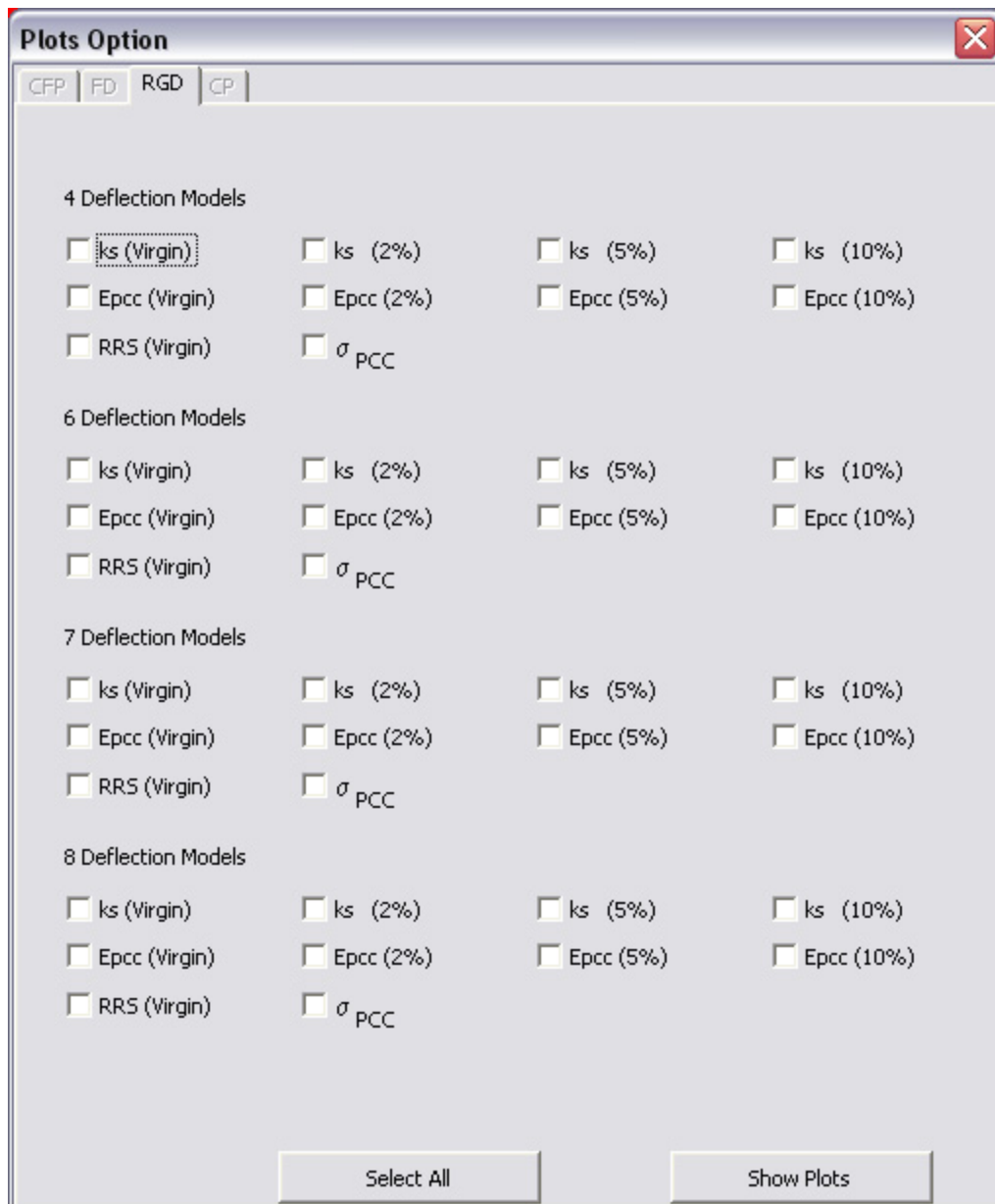
| Location | Granular Base Thickness (inch) |      | FWD Load (kip) | IOWA STATE UNIVERSITY<br>   | 4 Deflections-Eac (psi) (D0-D12-D24-D36) |           |           |           | 4 Deflections-Eri (psi) (D0-D12-D24-D36) |        |        |        |        |
|----------|--------------------------------|------|----------------|--|--|-----------|-----------|-----------|--|--------|--------|--------|--------|
|          | h <sub>gb</sub>                |      |                |  | 0%                                       | 2%        | 5%        | 10%       | 0%                                       | 2%     | 5%     | 10%    | 0%     |
|          | Load                           |      |                |  |  |           |           |           |  |        |        |        |        |
| 1        | 18.00                          | 9.00 | 9.00           | Total Data Set: 77<br><br><b>Run</b><br><br>Iowa Department of Transportation<br><br><b>Main Menu</b><br><br>Conventional Flexible Pavement (9 kip)<br><br><b>Plots</b><br><br><b>Summary</b><br><br><b>Filter</b> | 4,883,150                                | 377,266   | 533,962   | 86,003    | 16,750                                   | 16,705 | 15,340 | 6,025  | 1,875  |
| 2        | 18.00                          | 9.00 | 9.00           |  | 601,997                                  | 567,491   | 532,754   | 559,775   | 16,632                                   | 11,086 | 11,037 | 10,411 | 2,114  |
| 3        | 18.00                          | 9.00 | 9.00           |  | 497,094                                  | 450,880   | 427,986   | 391,252   | 16,254                                   | 7,592  | 7,398  | 7,843  | 1,911  |
| 4        | 18.00                          | 9.00 | 9.00           |  | 648,861                                  | 698,045   | 647,493   | 672,229   | 5,821                                    | 9,277  | 9,602  | 9,859  | 13,120 |
| 5        | 18.00                          | 9.00 | 9.00           |  | 508,610                                  | 532,879   | 492,385   | 475,471   | 3,941                                    | 5,979  | 5,941  | 6,402  | 13,104 |
| 6        | 18.00                          | 9.00 | 9.00           |  | 413,897                                  | 430,013   | 408,351   | 405,153   | 2,644                                    | 3,875  | 3,604  | 4,430  | 12,843 |
| 7        | 18.00                          | 9.00 | 9.00           |  | 510,725                                  | 435,958   | 413,986   | 423,838   | 8,348                                    | 2,759  | 2,326  | 3,321  | 1,875  |
| 8        | 18.00                          | 9.00 | 9.00           |  | 654,732                                  | 593,850   | 556,678   | 569,417   | 16,634                                   | 8,091  | 7,754  | 7,773  | 1,904  |
| 9        | 18.00                          | 9.00 | 9.00           |  | 529,828                                  | 457,734   | 442,670   | 406,206   | 16,032                                   | 5,495  | 4,697  | 5,524  | 1,876  |
| 10       | 18.00                          | 9.00 | 9.00           |  | 430,392                                  | 368,668   | 351,139   | 336,615   | 9,222                                    | 3,190  | 2,721  | 3,742  | 1,875  |
| 11       | 18.00                          | 9.00 | 9.00           |  | 479,479                                  | 484,027   | 446,534   | 442,493   | 10,228                                   | 9,413  | 9,821  | 9,640  | 5,192  |
| 12       | 18.00                          | 9.00 | 9.00           |  | 386,669                                  | 386,702   | 367,515   | 333,269   | 6,499                                    | 5,853  | 5,817  | 6,839  | 3,895  |
| 13       | 18.00                          | 9.00 | 9.00           |  | 314,841                                  | 305,681   | 287,929   | 275,993   | 4,455                                    | 3,610  | 3,529  | 4,752  | 3,207  |
| 14       | 18.00                          | 9.00 | 9.00           |  | 541,535                                  | 589,197   | 560,166   | 583,538   | 8,997                                    | 12,847 | 13,093 | 12,670 | 13,118 |
| 15       | 18.00                          | 9.00 | 9.00           |  | 415,323                                  | 440,612   | 403,418   | 386,657   | 6,377                                    | 8,751  | 9,414  | 9,584  | 13,072 |
| 16       | 18.00                          | 9.00 | 9.00           |  | 337,896                                  | 357,565   | 337,931   | 301,739   | 4,971                                    | 6,209  | 6,506  | 7,386  | 12,414 |
| 17       | 18.00                          | 9.00 | 9.00           |  | 645,900                                  | 623,059   | 584,420   | 557,763   | 6,195                                    | 4,361  | 3,953  | 4,559  | 2,042  |
| 18       | 18.00                          | 9.00 | 9.00           |  | 542,632                                  | 510,400   | 479,290   | 502,456   | 3,996                                    | 2,734  | 2,394  | 3,334  | 1,997  |
| 19       | 18.00                          | 9.00 | 9.00           |  | 1,490,041                                | 1,657,542 | 1,569,909 | 1,472,183 | 1,568                                    | 2,975  | 3,085  | 3,954  | 13,125 |
| 20       | 18.00                          | 9.00 | 9.00           |  | 838,815                                  | 1,050,242 | 999,305   | 921,920   | 724                                      | 8,022  | 8,337  | 8,123  | 13,125 |
| 21       | 18.00                          | 9.00 | 9.00           |  | 611,602                                  | 595,235   | 554,384   | 542,587   | 8,252                                    | 5,861  | 5,437  | 6,044  | 2,087  |
| 22       | 18.00                          | 9.00 | 9.00           |  | 496,354                                  | 473,590   | 451,291   | 443,354   | 5,303                                    | 3,938  | 3,310  | 3,996  | 2,077  |
| 23       | 18.00                          | 9.00 | 9.00           |  | 434,959                                  | 385,657   | 372,876   | 332,949   | 15,125                                   | 5,741  | 5,300  | 6,506  | 1,877  |
| 24       | 18.00                          | 9.00 | 9.00           |  | 344,550                                  | 291,379   | 270,685   | 250,223   | 9,268                                    | 3,588  | 2,879  | 3,816  | 1,876  |
| 25       | 18.00                          | 9.00 | 9.00           |  | 296,199                                  | 240,995   | 209,281   | 162,633   | 6,191                                    | 1,777  | 1,712  | 2,359  | 1,875  |
| 26       | 18.00                          | 9.00 | 9.00           |  | 827,216                                  | 784,341   | 731,916   | 743,658   | 13,375                                   | 5,833  | 5,407  | 5,926  | 1,894  |
| 27       | 18.00                          | 9.00 | 9.00           |  | 651,385                                  | 582,523   | 553,902   | 530,333   | 9,916                                    | 3,776  | 3,119  | 3,895  | 1,876  |

Figure 98. Sample pavement analysis: Excel sheet outputs

| Location | Asphalt Concrete Thickness (inch) |      | Granular Base Thickness (inch) | FWD Load (kip) | IOWA STATE UNIVERSITY<br> | 4 Deflections-Eac (psi) (D0-D12-D24-D36) |                 |                |                | 4 Deflections-Eri (psi) (D0-D12-D24-D36) |              |              |              |       |        |        |
|----------|-----------------------------------|------|--------------------------------|----------------|--|--|-----------------|----------------|----------------|--|--------------|--------------|--------------|-------|--------|--------|
|          | D-48                              | D-60 |                                |                |  | h <sub>ac</sub>                          | h <sub>gb</sub> | Load           | 0%             | 2%                                       | 5%           | 10%          | 0%           | 2%    | 5%     | 10%    |
|          | 61                                | 2.03 |                                |                |  | 1.70                                     | 16.00           | 18.00          | 9.00           | 309,099                                  | 350,107      | 307,529      | 322,063      | 7,777 | 13,182 | 14,000 |
| 62       | 2.47                              | 1.94 | 16.00                          | 18.00          | 9.00   | 247,490                                  | 271,488         | 257,689        | 198,840        | 6,974                                    | 10,230       | 11,200       | 11,200       |       |        |        |
| 63       | 3.04                              | 2.37 | 16.00                          | 18.00          | 9.00   | 204,142                                  | 211,741         | 204,486        | 174,665        | 5,265                                    | 6,369        | 7,400        | 7,400        |       |        |        |
| 64       | 2.52                              | 2.17 | 16.00                          | 18.00          | 9.00   | 734,449                                  | 769,000         | 711,405        | 730,620        | 5,305                                    | 6,351        | 6,300        | 6,300        |       |        |        |
| 65       | 3.11                              | 2.66 | 16.00                          | 18.00          | 9.00   | 568,752                                  | 578,218         | 540,694        | 519,633        | 3,444                                    | 4,153        | 3,700        | 3,700        |       |        |        |
| 66       | 3.74                              | 3.09 | 16.00                          | 18.00          | 9.00   | 474,901                                  | 476,622         | 443,819        | 472,608        | 2,138                                    | 2,583        | 2,300        | 2,300        |       |        |        |
| 67       | 2.44                              | 1.92 | 16.00                          | 18.00          | 9.00   | 690,927                                  | 697,294         | 645,851        | 672,777        | 10,065                                   | 7,879        | 8,000        | 8,000        |       |        |        |
| 68       | 2.94                              | 2.33 | 16.00                          | 18.00          | 9.00   | 522,772                                  | 523,087         | 491,088        | 466,017        | 4,814                                    | 4,984        | 4,500        | 4,500        |       |        |        |
| 69       | 2.95                              | 2.62 | 16.00                          | 18.00          | 9.00   | 529,619                                  | 544,064         | 507,347        | 484,496        | 3,827                                    | 5,000        | 4,600        | 4,600        |       |        |        |
| 70       | 3.46                              | 2.92 | 16.00                          | 18.00          | 9.00   | 440,644                                  | 445,383         | 421,760        | 428,065        | 2,909                                    | 3,423        | 2,900        | 2,900        |       |        |        |
| 71       | 2.55                              | 2.22 | 16.00                          | 18.00          | 9.00   | 652,922                                  | 626,060         | 582,347        | 583,186        | 10,896                                   | 6,167        | 5,700        | 5,700        |       |        |        |
| 72       | 3.15                              | 2.50 | 16.00                          | 18.00          | 9.00   | 498,295                                  | 465,398         | 444,486        | 434,086        | 6,321                                    | 3,981        | 3,200        | 3,200        |       |        |        |
| 73       | 3.77                              | 3.07 | 16.00                          | 18.00          | 9.00   | 413,935                                  | 376,856         | 344,455        | 338,313        | 4,032                                    | 2,139        | 2,000        | 2,000        |       |        |        |
| 74       | 2.61                              | 2.15 | 16.00                          | 18.00          | 9.00   | 539,218                                  | 491,994         | 464,991        | 436,900        | 16,027                                   | 7,453        | 7,200        | 7,200        |       |        |        |
| 75       | 3.12                              | 2.64 | 16.00                          | 18.00          | 9.00   | 453,219                                  | 403,271         | 390,781        | 360,403        | 12,525                                   | 4,952        | 4,400        | 4,400        |       |        |        |
| 76       | 2.35                              | 2.13 | 16.00                          | 18.00          | 9.00   | 499,036                                  | 526,727         | 482,939        | 501,806        | 6,708                                    | 9,679        | 10,100       | 10,100       |       |        |        |
| 77       | 2.80                              | 2.35 | 16.00                          | 18.00          | 9.00   | 407,482                                  | 428,600         | 398,615        | 369,515        | 4,997                                    | 6,740        | 6,900        | 6,900        |       |        |        |
| 78       |                                   |      |                                |                |  |  |                 |                |                |  |              |              |              |       |        |        |
| 79       |                                   |      |                                |                |  |  |                 |                |                |  |              |              |              |       |        |        |
| 80       |                                   |      |                                |                |  | <b>AVERAGE</b>                           | <b>529,392</b>  | <b>463,621</b> | <b>437,295</b> | <b>415,020</b>                           | <b>8,596</b> | <b>6,502</b> | <b>6,300</b> |       |        |        |
| 81       |                                   |      |                                |                |  | <b>STDEV</b>                             | <b>205,011</b>  | <b>199,282</b> | <b>188,124</b> | <b>193,291</b>                           | <b>4,553</b> | <b>3,064</b> | <b>3,200</b> |       |        |        |
| 82       |                                   |      |                                |                |  | <b>CV</b>                                | <b>49%</b>      | <b>43%</b>     | <b>43%</b>     | <b>47%</b>                               | <b>53%</b>   | <b>47%</b>   | <b>50%</b>   |       |        |        |
| 83       |                                   |      |                                |                |  |  |                 |                |                |  |              |              |              |       |        |        |
| 84       |                                   |      |                                |                |  |  |                 |                |                |  |              |              |              |       |        |        |
| 85       |                                   |      |                                |                |  |  |                 |                |                |  |              |              |              |       |        |        |
| 86       |                                   |      |                                |                |  |  |                 |                |                |  |              |              |              |       |        |        |
| 87       |                                   |      |                                |                |  |  |                 |                |                |  |              |              |              |       |        |        |

Figure 99. Sample pavement analysis: Excel sheet output statistics

The plot button will be enabled after the backcalculation analysis is complete. The plot option window appears after clicking on the plot button (see Figure 100). With this window, the user can select the models to display on charts. Selected models will be plotted as parameter versus location. Provided that the data is from a specified section, the first data will be represented as start, and each data afterward is assumed to be the data along the path of the pavement system. Filtered data from the preprocessor will be displayed in red, whereas all others will be in blue. The upper right corner will display a textbox containing general information about the project. Figure 101 illustrates the color-coded CFP analysis with 9-kip loading.



**Figure 100. Plot option window**

#### 4 Deflection - AC Modulus Prediction

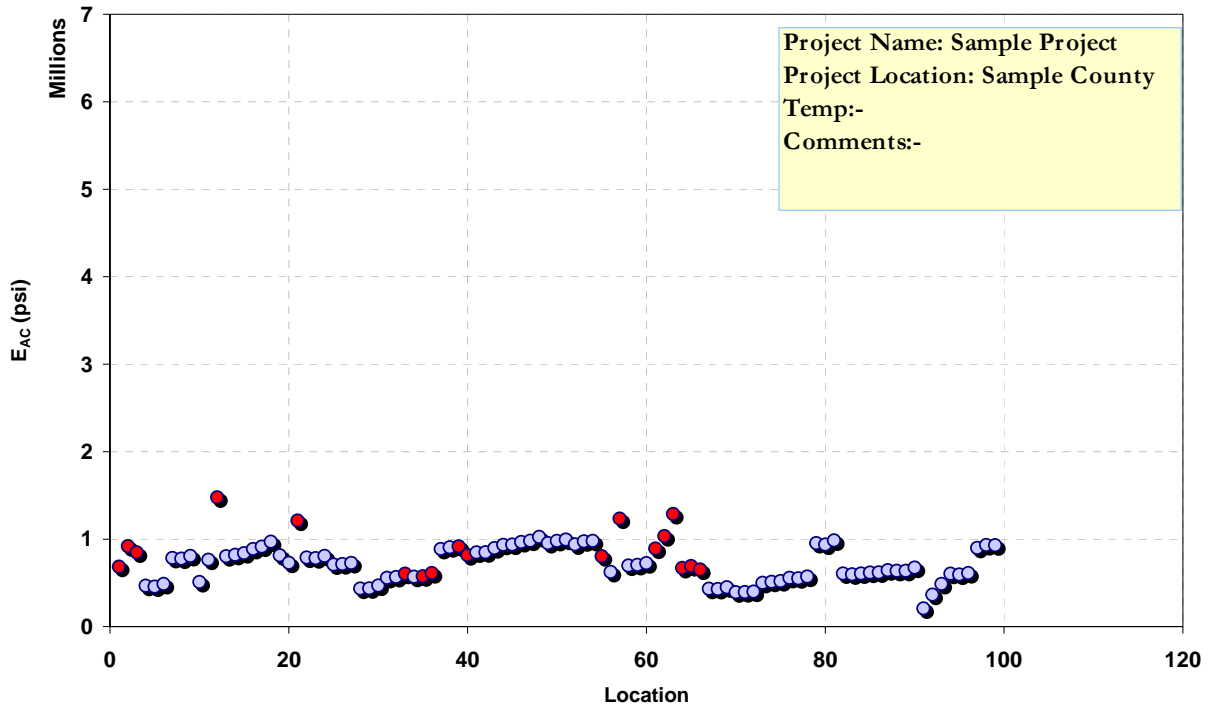


**Figure 101. Sample pavement analysis: Excel sheet charts**

Another button within the pavement analysis Excel sheet is the summary button. It is disabled until the “Run” button is clicked. It summarizes the statistical information for each model. It opens up a new Excel sheet with tables of each output and their statistics for every model (see [Figure 102](#)). The statistics variables used for the program are:

- Average (or mean value): The average value along the section.
- Standard deviation: A common measure of the dispersion. It shows how widely the data spread from the mean value.
- Coefficient of variation (CV): CV is a measure of the dispersion of probability distribution. It is the ratio of the standard deviation to the mean. It allows the user to compare the CV of populations that have different mean values. It is reported as a percentage.

| FWD-v12.1.xls  |                  |                  |       |         |            |           |                  |               |               |     |         |            |       |
|----------------|------------------|------------------|-------|---------|------------|-----------|------------------|---------------|---------------|-----|---------|------------|-------|
| Prediction     | Statistics       |                  |       | Details |            |           | Prediction       | Statistics    |               |     | Details |            |       |
|                | Average (psi/in) | Std Dev (psi/in) | CV    | Model   | Deflection | Noise     |                  | Average (psi) | Std Dev (psi) | CV  | Model   | Deflection | Noise |
| k <sub>s</sub> | 173              | 22               | 13%   | RGD-4   | 4          | 0         | E <sub>pcc</sub> | 5,020,752     | 622,546       | 12% | RGD-4   | 4          | 0     |
|                | 175              | 22               | 13%   | RGD-4   | 4          | 2         |                  | 5,067,013     | 569,653       | 11% | RGD-4   | 4          | 2     |
|                | 179              | 24               | 13%   | RGD-4   | 4          | 5         |                  | 4,900,213     | 610,821       | 12% | RGD-4   | 4          | 5     |
|                | 162              | 21               | 13%   | RGD-4   | 4          | 10        |                  | 5,346,606     | 669,888       | 13% | RGD-4   | 4          | 10    |
|                | 160              | 19               | 12%   | RGD-6   | 6          | 0         |                  | 5,698,906     | 898,348       | 16% | RGD-6   | 6          | 0     |
|                | 146              | 19               | 13%   | RGD-6   | 6          | 2         |                  | 6,304,443     | 1,340,237     | 21% | RGD-6   | 6          | 2     |
|                | 142              | 20               | 14%   | RGD-6   | 6          | 5         |                  | 6,406,350     | 1,369,370     | 21% | RGD-6   | 6          | 5     |
|                | 141              | 19               | 14%   | RGD-6   | 6          | 10        |                  | 6,537,182     | 1,478,261     | 23% | RGD-6   | 6          | 10    |
|                | 156              | 20               | 13%   | RGD-7   | 7          | 0         |                  | 5,937,959     | 1,020,649     | 17% | RGD-7   | 7          | 0     |
|                | 146              | 21               | 14%   | RGD-7   | 7          | 2         |                  | 6,670,139     | 1,552,222     | 23% | RGD-7   | 7          | 2     |
|                | 145              | 21               | 15%   | RGD-7   | 7          | 5         |                  | 6,649,939     | 1,561,347     | 23% | RGD-7   | 7          | 5     |
|                | 142              | 21               | 15%   | RGD-7   | 7          | 10        |                  | 6,612,993     | 1,544,330     | 23% | RGD-7   | 7          | 10    |
|                | 160              | 19               | 12%   | RGD-8   | 8          | 0         |                  | 5,677,559     | 866,172       | 15% | RGD-8   | 8          | 0     |
|                | 148              | 19               | 13%   | RGD-8   | 8          | 2         |                  | 6,372,195     | 1,269,669     | 20% | RGD-8   | 8          | 2     |
|                | 147              | 19               | 13%   | RGD-8   | 8          | 5         |                  | 6,269,710     | 1,293,671     | 21% | RGD-8   | 8          | 5     |
| 147            | 20               | 14%              | RGD-8 | 8       | 10         | 6,351,421 | 1,341,378        | 21%           | RGD-8         | 8   | 10      |            |       |

Note: k<sub>s</sub> predictions are limited to ranges between 50 and 1,000 psi/in. Back Note: E<sub>pcc</sub> predictions are limited to ranges between 1,000,000 and 15,000,000 psi.

| Prediction | Statistics   |              |    | Details |            |       | Prediction       | Statistics |         |    | Details |            |       |
|------------|--------------|--------------|----|---------|------------|-------|------------------|------------|---------|----|---------|------------|-------|
|            | Average (in) | Std Dev (in) | CV | Model   | Deflection | Noise |                  | Average    | Std Dev | CV | Model   | Deflection | Noise |
| RRS        | 35           | 2            | 5% | RGD-4   | 4          | 0     | σ <sub>pcc</sub> | 161        | 4       | 2% | RGD-4   | 4          | 0     |
|            | 38           | 2            | 5% | RGD-6   | 6          | 0     |                  | 164        | 4       | 2% | RGD-6   | 6          | 0     |
|            | 38           | 2            | 6% | RGD-7   | 7          | 0     |                  | 166        | 4       | 2% | RGD-7   | 7          | 0     |
|            | 38           | 2            | 5% | RGD-8   | 8          | 0     |                  | 164        | 4       | 2% | RGD-8   | 8          | 0     |

Note: RRS predictions are limited to ranges between 15 and 141 in. Note: PCC Stress predictions are limited to ranges between 20 and 400 psi.

Figure 102. Output statistics sheet

In summary, the following are some of the specific features of the ANN-based, user-friendly pavement structural analysis spreadsheet tool:

- A comprehensive pavement structural analysis tool incorporating all three common pavement types (flexible, rigid, and composite)
- Integration of all the ANN models developed as part of this research into a comprehensive unified framework
- Rapid backcalculation of pavement layer moduli and prediction of critical pavement responses from FWD data (100,000 deflection basins analyzed in less than a second)
- Useful for both project-level and network-level pavement structural evaluation
- Visualization of results through automatic plotting capability
- Commonly used Import/Export options for transporting data
- Automatic generation of output statistics

## SUMMARY AND CONCLUSIONS

Evaluating structural condition of existing, in-service pavements is a part of the routine maintenance and rehabilitation activities undertaken by the most DOTs. In the field, the pavement deflection profiles (or basins) gathered from the nondestructive FWD test data are typically used to evaluate pavement structural conditions. This kind of evaluation requires the use of a backcalculation-type structural analysis to determine pavement layer stiffness and, as a result, estimate a pavement's remaining life. Over the past decade, there has been an increased interest in a new class of computational intelligence system, ANNs, for use in geomechanical and pavement systems applications. ANNs have been found to be powerful and versatile computational tools for organizing and correlating information in ways that have proved useful for solving certain types of problems too complex, too poorly understood, or too resource-intensive to tackle using more traditional computational methods.

The overall objective of this research was to develop ANN models as a pavement evaluation toolbox for: (1) rapidly and accurately backcalculating field or in-service pavement layer properties; (2) predicting critical stress, strain, and deformation responses of these in-service pavements in real time from the measured FWD deflection data; and (3) incorporating these predicted critical pavement responses, such as tensile strain for asphalt concrete fatigue, directly into mechanistic-based pavement analysis and design methodologies with an emphasis on pavement performance prediction and extended pavement life design concepts. The research focused on developing ANN-based models for analyzing all three pavement systems: flexible, rigid, and composite.

Over 300 ANN models were developed for predicting pavement layer moduli and for predicting critical pavement responses from FWD data using solutions from state-of-the-art structural analysis programs (ILLI-PAVE, ISLAB2000, and DIPLOMAT). All successfully developed models were incorporated into a backcalculation toolbox developed using Microsoft Visual Basic and Excel. Using the field-validated, nondestructive pavement evaluation toolbox, it will be possible by city, county, and Iowa DOT engineers and pavement management teams to assess pavement condition, estimate remaining pavement life, and eventually help assess pavement rehabilitation strategies.

Overall, it was demonstrated that ANN-based models are capable of successfully predicting the pavement layer moduli and critical pavement response values using the FWD field deflection measurements. Field data used as case studies from LTPP and the Iowa DOT database showed that the ANN-based pavement layer prediction methodology is a step forward in backcalculation techniques. Such methodology will be an invaluable tool for pavement engineers in evaluating the structural condition of Iowa pavement systems.

The research findings demonstrated that the quality of FWD data is the most important issue in the backcalculation of the pavement layer parameters. The success of the developed ANN-based backcalculation models is directly related to the quality of the pavement surface deflection data. As shown in this research, the predicted layer moduli are very sensitive to the pavement layer thickness, especially in rigid pavements. Since the PCC layer thickness and pavement surface

deflections are the only input parameters in the developed ANN-based backcalculation models, even a small change in the assumed PCC layer thickness causes considerable differences in the backcalculated elastic moduli of the PCC layer.

The adoption of an ANN-based approach also resulted in a drastic reduction in computation time and a simplification of the complicated traditional layer backcalculation approaches. Rapid prediction ability of the ANN models provides a tremendous advantage to the pavement engineers by allowing them to nondestructively assess the condition of the transportation infrastructure systems in real time while the FWD testing takes place in the field. Elimination of selecting seed layer moduli with the integration of ANN-based backcalculation approach can be invaluable for the state and federal agencies in rapidly analyzing a large number of pavement deflection basins needed for routine deflection testing.

### **Benefits**

Currently, Iowa DOT engineers do not employ any preferable FWD backcalculation analysis technique. The results of this study will help for easily and rapidly analyzing the collected FWD deflection data by Iowa DOT engineers and technicians dealing with pavement and materials issues. This study demonstrated that properly trained ANN models are capable of backcalculating the pavement layer moduli and predicting the maximum stresses and strains with very low AAE of those obtained directly from finite element analyses. These error magnitudes are much smaller than the statistically formulated algorithms previously developed and currently used by some state agencies. Once validated, ANN models will provide more accurate and rapid (real-time) analyses of the collected FWD deflection data. The developed user-friendly software and the toolbox will be very helpful for assessing pavement condition, estimating remaining pavement life, and evaluating pavement rehabilitation alternatives. The developed tools will also help the Iowa DOT engineers in adopting the mechanistic-based pavement design procedures such as the MEPDG.

### **Implementation**

Because the research is specific to Iowa conditions, results will be implemented by county, city, and state highway agencies and contractors statewide as follows:

- It is expected that Iowa DOT engineers and technicians dealing with pavement and materials issues will adopt the proposed nondestructive pavement evaluation methodology for analyzing the FWD deflection data. Currently, Iowa DOT engineers do not employ any preferable FWD backcalculation analysis technique.
- Neural network-based structural models based on the state-of-the-art, stress-dependent, widely used, and validated finite element models (e.g., ILLI-PAVE for flexible and ISLAB2000 for rigid pavements) will provide realistic predictions of pavement layer moduli and pavement condition rating. Pavement management personnel at the Iowa DOT and Center for Transportation Research and Education will be able to make more reliable pavement condition predictions with the developed ANN models.

- ANN-based tools, models developed for directly predicting the critical pavement responses, will help the Iowa DOT engineers in implementing the mechanistic-based pavement design procedures such as the MEPDG. Pavement design engineers will also directly benefit from the results of this project in designing the new and rehabilitated pavement sections, in addition to analyzing the existing pavement sections.

## RECOMMENDATIONS

The quality of the FWD data is the most important issue in the backcalculation of the pavement layer parameters. The success of the developed ANN-based backcalculation models is directly related to the quality of the pavement surface deflection data.

Calibration of the equipment is very important to ensure accurate recording of deflection data. First, the weight should be dropped at least five times and relative differences in each loading should be checked prior to testing. Second, the deflection measurements for each sensor should be adjusted at least once a month or as specified by the manufacturer so they will produce the same deflection measurement within the precision limits of the sensors, as specified by the manufacturer.

As shown in this research, the predicted layer moduli are very sensitive to the pavement layer thickness, especially in rigid pavements. Because the PCC layer thickness and pavement surface deflections are the only input parameters in the developed ANN-based backcalculation models, even a small change in the assumed PCC layer thickness causes considerable differences in the backcalculated elastic moduli of the PCC layer. Also, because it is difficult to construct a long pavement section with a uniform slab thickness value during the backcalculation of the pavement parameters, it is assumed that pavement thickness is uniform for a given section and that it is the value taken from the project files. Therefore, to improve the  $E_{PCC}$  backcalculation, GPR readings can be taken along the test sections to determine the thickness of the layers at the FWD test points more accurately, as many recent studies have demonstrated.

Combined use of FWD and GPR testing is a very effective approach in evaluating the pavement condition. GPR provides more in-depth information on the thickness of the pavement sublayers, the layered structure of the subgrade/natural soil, and in determining depth to bedrock. GPR data also provide very useful information in detecting the voids and irregularities, or non-uniformities, under the pavement structures, which cause cracking, deformities, and roughness on the pavement surface.

For optimal results, FWD data should be collected early in the morning to reduce the curling effects in the backcalculation of the pavement parameters. In addition, ANN-based backcalculation models that include the outer sensor data (6-, 7-, and 8-Deflection) are recommended for the subgrade moduli backcalculations. However, 4-Deflection ANN models are recommended for the elastic moduli backcalculations for more realistic predictions.

## REFERENCES

- AASHTO T307-99, 2000, "Determining the resilient modulus of soils and aggregate materials." Standard Specifications for Transportation Materials and Methods of Sampling and Testing, 20th Edition, AASHTO, Washington D.C.
- Attoh-Okine, N.O. 1993. Using neural network to identify pavement structure based on radar output. Pacific Rim TransTech Conf. ASCE, NY, pp. 450-456.
- Barenberg, E. J., and K. A. Petros. *Evaluation of Concrete Pavements Using NDT Results*. Project IHR-512, University of Illinois at Urbana-Champaign and Illinois Department of Transportation, Report No. UILU-ENG-91-2006, 1991.
- Bayrak, B., Gopalakrishnan, K., and Ceylan, H. Neural Network-Based Backcalculation Models for Non-Destructive Evaluation of Rigid Airfield Pavement Systems, Accepted for Presentation and Publication at the 6th International DUT-Workshop on Fundamental Modeling of Design and Performance of Concrete Pavements, Old-Turnhout, Belgium, September 14-17, 2006.
- Brown, S.F., and Pappin, J.W., 1981, "Analysis of pavements with granular bases." In Transportation Research Record 810, TRB, National Research Council, Washington, D.C., pp. 17-23.
- Burmister, D.M. "The Theory of Stresses and Displacements in Layered Systems and Application to the Design of Airport Runways "Proceedings, Highway Research Board, Vol. 23, National Research Council, Washington D.C, 1943, pp. 126-144.
- Burmister, D.M. "The General Theory of Stresses and Displacements in Layered Systems, "Journal of Applied Physics, 1945, Vol. 16, No. 2, pp. 89-96; No.3 pp. 126-127; No.5, pp. 296-302.
- Ceylan, H., Tutumluer, E., and Barenberg, E. J. 1998. Artificial neural networks as design tools in concrete airfield pavement design. Proceedings of the 25th ASCE International Air Transportation Conference, Austin, Texas, USA, pp. 447-465.
- Ceylan, H., Tutumluer, E., and Barenberg, E.J. 1999a. Analysis of concrete airfield slabs serving the Boeing 777 aircraft using artificial neural networks. Journal of the Transportation Research Board, 1684: 110-117.
- Ceylan, H., Tutumluer, E., and Barenberg, E.J. 1999b. Artificial neural network analysis of concrete airfield pavements serving the Boeing B-777 aircraft. Transportation Research Record, 1684, Transportation Research Board, Washington, D.C., pp. 110-117.
- Ceylan, H., Tutumluer, E., and Barenberg, E.J. 2000. Effects of simultaneous temperature and gear loading on the response of concrete airfield pavements serving the Boeing 777 aircraft. Proceedings of the ASCE 26th International Air Transportation Conference, San Francisco, California, USA, pp. 25-44.

- Ceylan, H. 2002. Analysis and design of concrete pavement systems using artificial neural networks. Ph.D. Dissertation, University of Illinois at Urbana-Champaign, Department of Civil Engineering, Urbana, IL, USA, 256 pp.
- Ceylan, H., Guclu, A., Tutumluer, E., Thompson, M.R., and Gomez-Ramirez F. 2004a. Neural network-based structural models for rapid analysis of flexible pavements with unbound aggregate layers. In Proceedings of the 6th International Symposium on Pavements Unbound (UNBAR6), Nottingham, England, July 6-8, pp. 139-147.
- Ceylan, H. 2004b. Use of artificial neural networks for the analysis & design of concrete pavement systems. 5th International CROW-workshop on Fundamental Modeling of the design and performance of concrete pavements, Istanbul, Turkey, March 30-April 2.
- Ceylan, H. and Guclu, A. 2004c. Use of artificial neural networks for the analysis and design of concrete pavement systems serving the A380-800 aircraft. Intelligent Engineering Systems Through Artificial Neural Networks, ANNIE-2004, 14, pp. 665-670.
- Ceylan, H., Bayrak, M.B. and Guclu, A. 2005a. Use of neural networks to develop robust backcalculation algorithms for nondestructive evaluation of flexible pavement systems. Intelligent Engineering Systems Through Artificial Neural Networks, ANNIE-2005, 15, 731-740.
- Ceylan, H., Bayrak, M.B., Guclu, A., Tutumluer, E. 2005b. Forward and Backcalculation of Nonlinear Pavement Systems Using Neural Networks. In Proceedings of the 11th International Conference of the Association for Computer Methods and Advances in Geomechanics (IACMAG), Turin, Italy, June 19-24, 571-578.
- Ceylan, H., Guclu, A., Tutumluer, E., and Thompson, M.R. 2005c. Use of Artificial Neural Networks for Analyzing Full Depth Asphalt Pavements. International Journal of Pavement Engineering, 6 (3): 171-182.
- Ceylan, H., Gopalakrishnan, K. and Guclu, A. 2007. Advanced Approaches to Characterizing Nonlinear Pavement System Responses. Transportation Research Record: Journal of the Transportation Research Board, No. 2005, pp. 86-94.
- Chou, Y. T. *Structural Analysis Computer Programs for Rigid Multicomponent Pavement Structures with Discontinuities - WESLIQID and WESLAYER*. Technical Report GL-81-6, U.S. Army Engineer Waterways Experiment Station, May 1981.
- Darter, M.I., K.T. Hall, and C. Kuo. *Support Under Portland Cement Concrete Pavements*. NCHRP Report 372. Washington, DC: National Cooperative Highway Research Program, 1995.
- Duncan, J.M., Monismith, C.L., and Wilson, E.L. "Finite element analyses of pavements." In *Highway Research Record* No. 228, Highway Research Board, National Research Council, Washington D.C., 1968.

- European CEN Std EN 13286-7, 2003, “Unbound and hydraulically bound mixtures - Test methods – Part 7: Cyclic load triaxial test for unbound mixtures.” European Standard, European Committee for Standardization, European Union.
- FAA Report. *Use of Nondestructive Testing in the Evaluation of Airport Pavements*, FAA Advisory Circular No. 150/5370-11A, Office of Airport Safety and Standards, Federal Aviation Administration, 2004.
- Foxworthy, P. T., and M. I. Darter. ILLI-SLAB and FWD Deflection Basins for Characterization of Rigid Pavements. Nondestructive Testing of Pavements and Backcalculation of Moduli. *American Society for Testing and Materials*, 1989, pp. 368-386.
- Garg, N. E., Tutumluer, E., and M. R. Thompson. Structural Modelling Concepts for the Design of Airport Pavements for Heavy Aircraft. *Proceedings of the Fifth International Conference on the Bearing Capacity of Roads and Airfields*, Trondheim, Norway, 1998.
- Gomez-Achecar, M., and Thompson, M.R., 1986, “ILLI-PAVE based response algorithms for full depth asphalt concrete pavements.” In Transportation Research Record No. 1095, TRB, National Research Council, Washington D.C., pp. 11-18.
- Gomez-Ramirez, F., Thompson, M.R., and Bejarano, M., 2002, “ILLI-PAVE based flexible pavement design concepts for multiple wheel heavy gear load aircraft.” In Proceedings of the 9th International Conference on Asphalt Pavements, Copenhagen, Denmark.
- Gucunski, N., and Krstic, V. 1996. Backcalculation of pavement profiles from Spectral-Analysis-of-Surface-Waves test by neural networks using individual receiver spacing approach. Transportation Research Record, 1526, Transportation Research Board, Washington, D.C., pp. 6-13.
- Hall, K.T. (1991). Performance, Evaluation, and Rehabilitation of Asphalt-Overlaid Concrete Pavements. Thesis presented to the University of Illinois, at Urbana, IL, in partial fulfillment of the requirements for the degree of Doctor of Philosophy.
- Hall, K.T. (1992). “Backcalculation Solutions for Concrete Pavements,” technical memo prepared for SHRP Contract P-020, “Long-Term Pavement Performance Data Analysis.
- Hall, K.T., M.I. Darter, T.E. Hoerner, and L. Khazanovich. (1997). LTPP Data Analysis—Phase I: Validation of Guidelines for k-Value Selection and Concrete Pavement Performance Prediction. Technical Report FHWA-RD-96-198.
- Haykin, S. Neural networks: A comprehensive foundation. *Prentice-Hall, Inc.*, NJ, USA. 1999.
- Heiler, M., McNeil, S., and Garrett, J.J. 1995. Ground-penetrating radar for highway and bridge deck condition assessment and inventory. SPIE - The International Society for Optical Engineering, Nondestructive Evaluation of Aging Bridges and Highways, 2456, Oakland, CA, pp. 195-206.

- Hicks, R.G., and C.L. Monismith, 1971, "Factors influencing the resilient properties of granular materials." In Transportation Research Record No. 345, TRB, National Research Council, Washington D.C., pp. 15-31.
- Hoffman, M. S., and M. R. Thompson. Backcalculating Nonlinear Resilient Moduli from Deflection Data. *Transportation Research Record* 852, TRB, National Research Council, Washington, D.C., 1982, pp. 42-51.
- Huang, Y.H. A Computer Package for Structural Analysis of Concrete Pavements. *Proceedings, 3<sup>rd</sup> International Conference on Concrete Pavement Design and Rehabilitation*, Purdue University, 1985, pp.295-307.
- Ioannides, A. M. Dimensional Analysis in NDT Rigid Pavement Evaluation. *Journal of Transportation Engineering*, Vol.116, No. 1, 1990, pp.23-36.
- Ioannides, A.M. Concrete Pavement Backcalculation Using ILLI-BACK 3.0, Nondestructive Testing of Pavements and Backcalculation of Moduli. *American Society for Testing and Materials*, Vol. 2, 1994, pp.103-124.
- Ioannides, A. M., E. J. Barenberg, and J. A. Lary. Interpretation of Falling Weight Deflectometer Results Using Principals of Dimensional Analysis. *Proceedings, 4th International Conference on Concrete Pavement Design and Rehabilitation*, Purdue University, 1989, pp.231-247.
- Ioannides, A.M. and Khazanovich, L., "Analytical and Numerical Methods for Multi-Layered Concrete Pavements" *Proceedings, Third International Workshop on the Design and Rehabilitation of Concrete Pavements*, Krumbach, Austria, October, 1994.
- Ioannides, A.M., E.J. Barenberg, and J. A. Lary. Interpretation of Falling Weight Deflectometer Results Using Principals of Dimensional Analysis. *Proceedings, 4th International Conference on Concrete Pavement Design and Rehabilitation*, Purdue University, 1989, pp.231-247.
- Ioannides, A.M., Khazanovich, L., and Becque, J.L. Structural Evaluation of Base Layers in Concrete Pavement Systems. In *Transportation Research Record: Journal of the Transportation Research Board*, No. 1370, Washington, D.C., 1992, pp. 20-28.
- Irwin, L. H., Szenbenyi, T. *User's Guide to MODCOMP3 Version 3.2*, CLRP Report Number 91-4, Cornell University, Local Roads Program, Ithaca, NY, 1991.
- Irwin, L. H., *Instructional Guide for Back-Calculation and the Use of MODCOMP*, CLRP Publication No. 94-10, Cornell University, Local Roads Program, Ithaca, NY, 1994.
- Khazanovich, L. *Structural Analysis of Multi-Layered Concrete Pavement Systems*, Ph.D. dissertation, University of Illinois, Illinois, USA, 1994.

- Khazanovich, L., and Ioannides, A.M. 1995. DIPLOMAT: Analysis program for bituminous and concrete pavements. *Transportation Research Record*, 1482, Transportation Research Board, Washington, D.C., pp. 52-60.
- Khazanovich, L. and Roesler, J. 1997. DIPLOBACK: A neural networks-based backcalculation program for composite pavements. *Transportation Research Record*, 1570, Transportation Research Board, Washington, D.C., pp. 143-150.
- Khazanovich, L., Yu, H.T., Rao, S., Galasova, K., Shats, E., and Jones, R. *ISLAB2000 - Finite Element Analysis Program for Rigid and Composite Pavements*, User's Guide, ERES Consultants, A Division of Applied Research Associates, Champaign, Illinois, 2000.
- Kennedy J.C. Material Nonlinear and Time-Dependent Effects on Pavement Design for Heavyweight, Multi-Wheel Vehicles. *Proceedings of the First International symposium on 3D Finite Element for Pavement Analysis and Design*, 1998.
- Kim, Y. and Kim, Y.R. 1998. Prediction of layer moduli from FWD and surface wave measurements using artificial neural network. *Transportation Research Record*, 1639, Transportation Research Board, Washington, D.C., pp. 53-61.
- Lawrence, J. and Fredricson, J. (1993) *BrainMaker User's guide and Reference Manual 7th Edition*, California Scientific Software, Nevada City, CA.
- LeCun, Y., 1993, Efficient learning and second-order methods, a tutorial at NIPS 93, Denver.
- LTPP Standard Data Release 20*, Long-Term Pavement Performance (LTPP) program, Federal Highway Administration, Washington DC, 2005.
- Lytton, R.L. "Backcalculation of Pavement Layer Properties" *Nondestructive Testing of Pavements and Backcalculation of Moduli*" ASTM Testing and Materials, Philadelphia, pp. 7-38., 1989.
- Mallela, J., and K.P. George. Three-Dimensional Dynamic Response Model for Rigid Pavements. In *Transportation Research Record: Journal of the Transportation Research Board*, No. 1448, TRB, Washington, D.C., 1994.
- Mehrotra, K., Mohan, C.K., and Ranka, S. (1997). *Elements of Artificial Neural Networks*, MIT Press, Cambridge, MA.
- Meier, R.W. and Rix, G.J. 1994. Backcalculation of flexible pavement moduli using artificial neural network. *Transportation Research Record*, 1448, Transportation Research Board, Washington, D.C., pp. 75-82.
- Meier, R.W. and Rix, G.J. 1995. Backcalculation of flexible pavement moduli from dynamic deflection basins using artificial neural network. *Transportation Research Record*, 1473, Transportation Research Board, Washington, D.C., pp. 72-81.

- Meier, R.W., Alexander, D.R., and Freeman, R.B. 1997. Using artificial neural networks as a forward approach to backcalculation. *Transportation Research Record*, 1570, Transportation Research Board, Washington, D.C., pp. 126-133.
- NCHRP Report. *Guide for Mechanistic-Empirical Design of New and Rehabilitated Pavement Structures*, Appendix QQ: Structural Response Models for Rigid Pavements, 2003.
- PCS/Law Engineering, *SHRP's Layer Moduli Back-Calculation Procedure: Software Selection*, SHRP-P651, Washington, DC: Strategic Highway Research Program, National Academy of Science, 1993.
- Raad, L., and Figueroa, J.L., 1980, "Load response of transportation support systems." *Transportation Engineering Journal*, ASCE, Vol. 16, No. TE1.
- Rada, G., and Witzak, M.W., 1981, "Comprehensive evaluation of laboratory resilient moduli results for granular material." In *Transportation Research Record No. 810*, TRB, National Research Council, Washington D.C., pp. 23-33.
- Smith, K.D. et al. (1995). *Performance of Concrete Pavements Volume III—Improving Concrete Pavement Performance*. Final Report. Contract DTFH61-91-C-00053. McLean, VA: Federal Highway Administration.
- Smith, K. D., M. J. Wade, D. G. Peshkin, L. Khazanovich, H. T. Yu, and M. I. Dater. *Performance of Concrete Pavements, Volume II – Evaluation of In-Service Concrete Pavements*. Report No. FHWA-RD-95-110, ERES Consultants, Champaign, IL, 1996.
- Tabatabaie, A.M. 1977. Structural analysis of concrete pavement joints. PhD thesis, Univ. of Illinois at Urbana-Champaign, Urbana, IL, USA.
- Tabatabaie, A.M., and E.J. Barenberg. Finite Element Analysis of Jointed or Cracked Concrete Pavements. In *Transportation Research Record: No. 671*, TRB, 1978, pp. 11-18.
- Thompson, M.R., 1989, "ILLI-PAVE Based NDT Analysis Procedures," *Nondestructive Testing of Pavements and Backcalculation of Moduli*, ASTM STP 1026, A. J. Bush III and G. Y. Baladi, Eds., American Society for Testing and Materials, Philadelphia, pp. 487-501.
- Thompson, M.R., and Robnett, Q.L., 1979, "Resilient properties of subgrade soils." *Transportation Engineering Journal*. ASCE. Vol. 105, No. TE1.
- Thompson, M. R. and R. P. Elliot ILLI-PAVE Based Response Algorithms for Design of Conventional Flexible Pavements. *Transportation Research Record* 1043, TRB, National Research Council, Washington, D.C. 1985., pp.50-57.
- Thompson, M.R., 1992, "ILLI-PAVE based conventional flexible pavement design procedure." In *Proceedings of the 7th International Conference on Asphalt Pavements*, Nottingham, U.K.

- Ullidtz, P., “*ELCON: Evaluation of Layer Moduli and Overlay Design (ELMOD for Concrete)*”, Dynatest Engineering A/S, Denmark, 1987.
- Uzan, J., 1985, “Characterization of granular materials.” In Transportation Research Record No. 1022, TRB, National Research Council, Washington D.C., pp. 52-59.
- Uzan, J., Witzak, M.W., Scullion, T., and Lytton, R.L., 1992, “Development and validation of realistic pavement response models.” In Proceedings of the 7th International Conference on Asphalt Pavements, Nottingham, UK, Vol. 1, pp. 334-350.
- Yang, J., Lu, J.J., and Gunaratne, M., 2003, “Application of Neural Network Models for Forecasting of Pavement Crack Index and Pavement Condition Rating.” Report submitted to the Florida Department of Transportation.
- Van Cauwelaert, F. J., Alexander, D. R., White, T. D., and W. R. Barker. Multilayer elastic program for elastic program for backcalculating layer moduli in pavement evaluation. *Nondestructive Testing of Pavements and Backcalculation of Moduli*, ASTM STP 1026, Philadelphia, USA, 1989.
- Williams, T.P., and Gucunski, N. 1995. Neural networks for backcalculation of moduli from SASW test. *Journal of Computing in Civil Engineering*, ASCE, 9(1): 1-8.
- Winkler, E., *Die Lehre von der Elastizitt und Festigkeit (Theory of Elasticity and Strength)*, H. Dominicus, Prague, Czechoslovakia (in German), 1864.